AN INTRODUCTION TO LAGRANGIAN MECHANICS

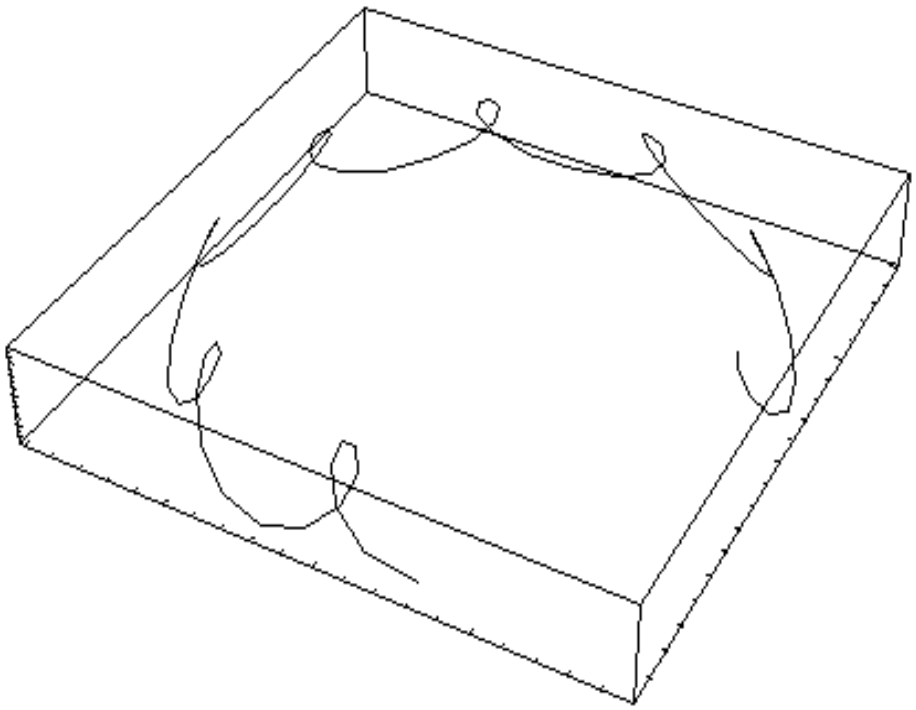

Alain J. Brizard

Department of Chemistry and Physics
Saint Michael's College, Colchester, VT 05439

July 7, 2007

Preface

The original purpose of the present lecture notes on Classical Mechanics was to supplement the standard undergraduate textbooks (such as Marion and Thorton's *Classical Dynamics of Particles and Systems*) normally used for an intermediate course in Classical Mechanics by inserting a more general and rigorous introduction to Lagrangian and Hamiltonian methods suitable for undergraduate physics students at sophomore and junior levels. The outcome of this effort is that the lecture notes are now meant to provide a self-consistent introduction to Classical Mechanics without the need of any additional material.

It is expected that students taking this course will have had a one-year calculus-based introductory physics course followed by a one-semester course in Modern Physics. Ideally, students should have completed their three-semester calculus sequence by the time they enroll in this course and, perhaps, have taken a course in ordinary differential equations. On the other hand, this course should be taken before a rigorous course in Quantum Mechanics in order to provide students with a sound historical perspective involving the connection between Classical Physics and Quantum Physics. Hence, the second semester of the sophomore year or the fall semester of the junior year provide a perfect niche for this course.

The structure of the lecture notes presented here is based on achieving several goals. As a first goal, I originally wanted to model these notes after the wonderful monograph of Landau and Lifschitz on *Mechanics*, which is often thought to be too concise for most undergraduate students. One of the many positive characteristics of Landau and Lifschitz's *Mechanics* is that Lagrangian mechanics is introduced in its first chapter and not in later chapters as is usually done in more standard textbooks used at the sophomore/junior undergraduate level. Consequently, Lagrangian mechanics becomes the centerpiece of the course and provides a continous thread throughout the text.

As a second goal, the lecture notes introduce several numerical investigations of dynamical equations appearing throughout the text. These numerical investigations present an interactive pedagogical approach, which should enable students to begin their own numerical investigations. As a third goal, an attempt was made to introduce relevant historical facts (whenever appropriate) about the pioneers of Classical Mechanics. Much of the historical information included in the Notes is taken from René Dugas (*History of Mechanics*, 1955), Wolfgang Yourgrau and Stanley Mandelstam (*Variational Principles in Dynamics and Quantum Theory*, 1968), or Cornelius Lanczos (*The Variational Principles of Mechanics*, 1970). In fact, from a pedagogical point of view, this historical perspective helps educating undergraduate students in establishing the deep connections between Classical and Quantum Mechanics, which are often ignored or even inverted (as can be observed when undergraduate students are surprised to hear that Hamiltonians have an independent classical existence). As a fourth and final goal, I wanted to keep the scope of these

notes limited to a one-semester course in contrast to standard textbooks, which often include an extensive review of Newtonian Mechanics as well as additional material such as Hamiltonian chaos.

The standard topics covered in these notes are listed in order as follows: Introduction to the Calculus of Variations (Chapter 1), Lagrangian Mechanics (Chapter 2), Hamiltonian Mechanics (Chapter 3), Motion in a Central Field (Chapter 4), Collisions and Scattering Theory (Chapter 5), Motion in a Non-Inertial Frame (Chapter 6), Rigid Body Motion (Chapter 7), Normal-Mode Analysis (Chapter 8), and Continuous Lagrangian Systems (Chapter 9). Each chapter contains a problem set with variable level of difficulty; sections identified with an asterisk may be omitted for a one-semester course. Lastly, in order to ensure a self-contained presentation, a summary of mathematical methods associated with linear algebra, and trigonometic and elliptic functions is presented in Appendix A. Appendix B presents a brief summary of the derivation of the Schrödinger equation based on the Lagrangian formalism developed by R. P. Feynman.

Several innovative topics not normally discussed in standard undergraduate textbooks are included throughout the notes. In Chapter 1, a complete discussion of Fermat's Principle of Least Time is presented, from which a generalization of Snell's Law for light refraction through a nonuniform medium is derived and the equations of geometric optics are obtained. We note that Fermat's Principle proves to be an ideal introduction to variational methods in the undergraduate physics curriculum since students are already familiar with Snell's Law of light refraction.

In Chapter 2, we establish the connection between Fermat's Principle and Maupertuis-Jacobi's Principle of Least Action. In particular, Jacobi's Principle introduces a geometric representation of single-particle dynamics that establishes a clear pre-relativistic connection between Geometry and Physics. Next, the nature of mechanical forces is discussed within the context of d'Alembert's Principle, which is based on a dynamical generalization of the Principle of Virtual Work. Lastly, the fundamental link between the energy-momentum conservation laws and the symmetries of the Lagrangian function is first discussed through Noether's Theorem and then Routh's procedure to eliminate ignorable coordinates is applied to a Lagrangian with symmetries.

In Chapter 3, the problem of charged-particle motion in an electromagnetic field is investigated by the Lagrangian method in the three-dimensional configuration space and the Hamiltonian method in the six-dimensional phase space. This important physical example presents a clear link between the two methods.

Contents

Chapter 1

Introduction to the Calculus of Variations

A wide range of equations in physics, from quantum field and superstring theories to general relativity, from fluid dynamics to plasma physics and condensed-matter theory, are derived from action (variational) principles. The purpose of this chapter is to introduce the methods of the Calculus of Variations that figure prominently in the formulation of action principles in physics.

1.1 Foundations of the Calculus of Variations

1.1.1 A Simple Minimization Problem

It is a well-known fact that the shortest distance between two points in Euclidean ("flat") space is calculated along a straight line joining the two points. Although this fact is intuitively obvious, we begin our discussion of the problem of minimizing certain integrals in mathematics and physics with a search for an explicit proof. In particular, we prove that the straight line $y_0(x) = mx$ yields a path of shortest distance between the two points $(0, 0)$ and $(1, m)$ on the (x, y)-plane as follows.

First, we consider the length integral

$$\mathcal{L}[y] \ = \int_0^1 \sqrt{1 + (y')^2}\, dx, \tag{1.1}$$

where $y' = y'(x)$ and the notation $\mathcal{L}[y]$ is used to denote the fact that the value of the integral (1.1) depends on the choice we make for the function $y(x)$ ($\mathcal{L}[y]$ is, thus, called a *functional* of y); we insist, however, that the function $y(x)$ satisfy the boundary conditions

$y(0) = 0$ and $y(1) = m$. Next, by introducing the modified function

$$y(x;\epsilon) \;=\; y_0(x) \;+\; \epsilon\,\delta y(x),$$

where $y_0(x) = mx$ and the variation function $\delta y(x)$ is required to satisfy the prescribed boundary conditions $\delta y(0) = 0 = \delta y(1)$, we define the modified length integral

$$\mathcal{L}[y_0 + \epsilon\,\delta y] \;= \int_0^1 \sqrt{1 + (m + \epsilon\,\delta y')^2}\,dx$$

as a function of ϵ and a functional of δy. We now show that the function $y_0(x) = mx$ minimizes the integral (1.1) by evaluating the following derivatives

$$\left(\frac{d}{d\epsilon}\mathcal{L}[y_0 + \epsilon\,\delta y]\right)_{\epsilon=0} \;=\; \frac{m}{\sqrt{1+m^2}} \int_0^1 \delta y'\,dx \;=\; \frac{m}{\sqrt{1+m^2}}\,[\,\delta y(1) - \delta y(0)] \;=\; 0,$$

and

$$\left(\frac{d^2}{d\epsilon^2}\mathcal{L}[y_0 + \epsilon\,\delta y]\right)_{\epsilon=0} \;=\; \int_0^1 \frac{(\delta y')^2}{(1+m^2)^{3/2}}\,dx \;>\; 0,$$

which holds for a fixed value of m and for all variations $\delta y(x)$ that satisfy the conditions $\delta y(0) = 0 = \delta y(1)$. Hence, we have shown that $y(x) = mx$ minimizes the length integral (1.1) since the first derivative (with respect to ϵ) vanishes at $\epsilon = 0$, while its second derivative is positive. We note, however, that our task was made easier by our knowledge of the actual minimizing function $y_0(x) = mx$; without this knowledge, we would be required to choose a trial function $y_0(x)$ and test for all variations $\delta y(x)$ that vanish at the integration boundaries.

Another way to tackle this minimization problem is to find a way to characterize the function $y_0(x)$ that minimizes the length integral (1.1), for *all* variations $\delta y(x)$, without actually solving for $y(x)$. For example, the characteristic property of a straight line $y(x)$ is that its second derivative vanishes for all values of x. The methods of the Calculus of Variations introduced in this Chapter present a mathematical procedure for transforming the problem of minimizing an integral to the problem of finding the solution to an ordinary differential equation for $y(x)$. The mathematical foundations of the Calculus of Variations were developed by Joseph-Louis Lagrange (1736-1813) and Leonhard Euler (1707-1783), who developed the mathematical method for finding curves that minimize (or maximize) certain integrals.

1.1.2 Methods of the Calculus of Variations

Euler's First Equation

The methods of the Calculus of Variations transform the problem of minimizing an integral of the form

$$\mathcal{F}[y] \;=\; \int_a^b F(y, y'; x)\,dx \tag{1.2}$$

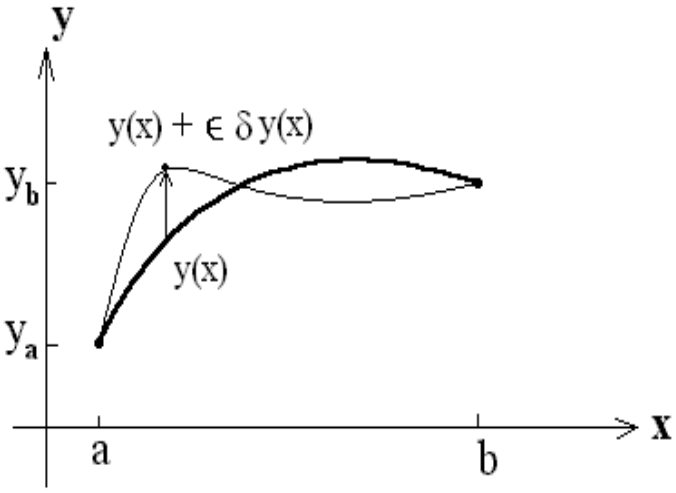

Figure 1.1: Virtual displacement

(with fixed boundary points a and b) into the solution of a differential equation for $y(x)$ expressed in terms of derivatives of the integrand $F(y, y'; x)$, assumed to be a smooth function of $y(x)$ and its first derivative $y'(x)$, with a possible explicit dependence on x.

The problem of minimizing the integral (1.2) will be treated in analogy with the problem of finding the minimum value of any (smooth) function $f(x)$, i.e., finding the value x_0 where

$$f'(x_0) \;=\; \lim_{\epsilon \to 0} \; \frac{1}{\epsilon} \left(f(x_0 + \epsilon) \;-\; f(x_0) \right) \;\equiv\; \frac{1}{h} \left(\frac{d}{d\epsilon} f(x_0 + \epsilon\, h) \right)_{\epsilon = 0} \;=\; 0,$$

where h is an arbitrary constant factor. First, we introduce the first-order *functional variation* $\delta\mathcal{F}[y; \delta y]$ defined as

$$\delta\mathcal{F}[y; \delta y] \;\equiv\; \left(\frac{d}{d\epsilon} \mathcal{F}[y + \epsilon\, \delta y] \right)_{\epsilon = 0} \;=\; \left[\; \frac{d}{d\epsilon} \left(\int_a^b F\left(y + \epsilon\, \delta y, y' + \epsilon\, \delta y', x\right) \; dx \right) \right]_{\epsilon = 0}, \quad (1.3)$$

where $\delta y(x)$ is an arbitrary smooth variation of the path $y(x)$ subject to the boundary conditions $\delta y(a) = 0 = \delta y(b)$, i.e., the end points of the path are not affected by the variation (see Figure 1.1). By performing the ϵ-derivatives in the functional variation (1.3), which involves partial derivatives of $F(y, y', x)$ with respect to y and y', we find

$$\delta\mathcal{F}[y; \delta y] \;=\; \int_a^b \left[\; \delta y(x) \, \frac{\partial F}{\partial y(x)} \;+\; \delta y'(x) \, \frac{\partial F}{\partial y'(x)} \; \right] \, dx,$$

which, when the second term is integrated by parts, becomes

$$\delta\mathcal{F}[y; \delta y] \;=\; \int_a^b \delta y \left[\; \frac{\partial F}{\partial y} \;-\; \frac{d}{dx} \left(\frac{\partial F}{\partial y'} \right) \; \right] dx \;+\; \left[\; \delta y_b \left(\frac{\partial F}{\partial y'} \right)_b \;-\; \delta y_a \left(\frac{\partial F}{\partial y'} \right)_a \; \right].$$

Here, since the variation $\delta y(x)$ vanishes at the integration boundaries ($\delta y_b = 0 = \delta y_a$), the last terms involving δy_b and δy_a vanish explicitly and we obtain

$$\delta\mathcal{F}[y;\delta y] \;=\; \int_a^b \delta y \left[\frac{\partial F}{\partial y} \;-\; \frac{d}{dx}\left(\frac{\partial F}{\partial y'}\right) \right] dx \;\equiv\; \int_a^b \delta y\, \frac{\delta\mathcal{F}}{\delta y}\, dx, \tag{1.4}$$

where $\delta\mathcal{F}/\delta y$ is called the *functional derivative* of $\mathcal{F}[y]$ with respect to the function y. The stationarity condition $\delta\mathcal{F}[y;\delta y] = 0$ for all variations δy yields Euler's First equation

$$\frac{d}{dx}\left(\frac{\partial F}{\partial y'}\right) \;\equiv\; y''\,\frac{\partial^2 F}{\partial y'\,\partial y'} \;+\; y'\,\frac{\partial^2 F}{\partial y\,\partial y'} \;+\; \frac{\partial^2 F}{\partial x\,\partial y'} \;=\; \frac{\partial F}{\partial y}, \tag{1.5}$$

representing a second-order ordinary differential equation for $y(x)$. According to the Calculus of Variations, the solution $y(x)$ to this ordinary differential equation, subject to the boundary conditions $y(a) = y_a$ and $y(b) = y_b$, yields a solution to the problem of minimizing the integral (1.2). Lastly, we note that Lagrange's variation operator δ, while analogous to the derivative operator d, commutes with the integral operator, i.e.,

$$\delta \int_a^b \; P(y(x))\, dx \;=\; \int_a^b \; P'(y(x))\, \delta y(x)\, dx,$$

for any smooth function P.

Extremal Values of an Integral

Euler's First Equation (1.5) results from the stationarity condition $\delta\mathcal{F}[y;\delta y] = 0$, which does not necessarily imply that the Euler path $y(x)$, in fact, minimizes the integral (1.2). To investigate whether the path $y(x)$ actually minimizes Eq. (1.2), we must evaluate the second-order functional variation

$$\delta^2\mathcal{F}[y;\delta y] \;\equiv\; \left(\frac{d^2}{d\epsilon^2}\mathcal{F}[y+\epsilon\,\delta y]\right)_{\epsilon=0}.$$

By following steps similar to the derivation of Eq. (1.4), the second-order variation is expressed as

$$\delta^2\mathcal{F}[y;\delta y] \;=\; \int_a^b \left\{ \delta y^2 \left[\frac{\partial^2 F}{\partial y^2} \;-\; \frac{d}{dx}\left(\frac{\partial^2 F}{\partial y \partial y'}\right) \right] \;+\; (\delta y')^2 \;\frac{\partial^2 F}{\partial (y')^2} \right\} dx. \tag{1.6}$$

The necessary and sufficient condition for a minimum is $\delta^2\mathcal{F} > 0$ and, thus, the sufficient conditions for a minimal integral are

$$\frac{\partial^2 F}{\partial y^2} \;-\; \frac{d}{dx}\left(\frac{\partial^2 F}{\partial y \partial y'}\right) \;>\; 0 \quad \text{and} \quad \frac{\partial^2 F}{(\partial y')^2} \;>\; 0, \tag{1.7}$$

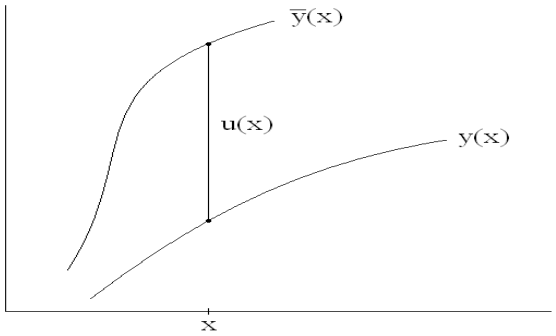

Figure 1.2: Jacobi deviation from two extremal curves

for all smooth variations $\delta y(x)$. For a small enough interval (a, b), the $(\delta y')^2$-term will normally dominate over the $(\delta y)^2$-term and the sufficient condition becomes $\partial^2 F/(\partial y')^2 > 0$.

Because variational problems often involve finding the minima or maxima of certain integrals, the methods of the Calculus of Variations enable us to find extermal solutions $y_0(x)$ for which the integral $\mathcal{F}[y]$ is stationary (i.e., $\delta\mathcal{F}[y_0] = 0$), without specifying whether the second-order variation is positive-definite (corresponding to a minimum), negative-definite (corresponding to a maximum), or with indefinite sign (i.e., when the coefficients of $(\delta y)^2$ and $(\delta y')^2$ have opposite signs).

Jacobi Equation*

Carl Gustav Jacobi (1804-1851) derived a useful differential equation describing the deviation $u(x) = \overline{y}(x) - y(x)$ between two extremal curves (see Figure 1.2) that solve Euler's First Equation (1.5) for a given function $F(x, y, y')$. Upon Taylor expanding Euler's First Equation (1.5) for $\overline{y} = y + u$ and keeping only linear terms in u (which is assumed to be small), we easily obtain the linear ordinary differential equation

$$\frac{d}{dx}\left(u'\,\frac{\partial^2 F}{(\partial y')^2} \;+\; u\,\frac{\partial^2 F}{\partial y \partial y'}\right) \;=\; u\,\frac{\partial^2 F}{\partial y^2} \;+\; u'\,\frac{\partial^2 F}{\partial y' \partial y}. \tag{1.8}$$

By performing the x-derivative on the second term on the left side, we obtain a partial cancellation with the second term on the right side and find the Jacobi equation

$$\frac{d}{dx}\left(\frac{\partial^2 F}{(\partial y')^2}\,\frac{du}{dx}\right) \;=\; u\,\left[\;\frac{\partial^2 F}{\partial y^2} \;-\; \frac{d}{dx}\left(\frac{\partial^2 F}{\partial y \partial y'}\right)\;\right]. \tag{1.9}$$

We can, thus, immediately see that the extremal properties (1.7) of the solutions of Euler's First Equation (1.5) are intimately connected to the behavior of the deviation $u(x)$ between two nearby extremal curves.

For example, if we simply assume that the coefficients in Jacobi's equation (1.9) are both positive (or both negative) constants $\pm\,\alpha^2$ and $\pm\,\beta^2$, respectively (i.e., the extremal curves are either minimal or maximal), then Jacobi's equation becomes $\alpha^2\,u'' = \beta^2\,u$, with exponential solutions $u(x) = a\,e^{\gamma\,x} + b\,e^{-\gamma\,x}$, where (a,b) are determined from initial conditions and $\gamma = \beta/\alpha$. On the other hand, if we assume that the coefficients are constants $\pm\,\alpha^2$ and $\mp\,\beta^2$ of opposite signs (i.e., the extremals are neither minimal nor maximal), then Jacobi's equation becomes $\alpha^2\,u'' = -\,\beta^2\,u$, with periodic solutions $u(x) = a\,\cos(\gamma\,x) + b\,\sin(\gamma\,x)$, where (a,b) are determined from initial conditions and $\gamma = \beta/\alpha$. The special case where the coefficient on the right side of Jacobi's equation (1.9) vanishes (i.e., F is independent of y) yields a differential equation for $u(x)$ whose solution is independent of the sign of the coefficient $\partial^2 F/\partial(y')^2$ (i.e., identical solutions are obtained for minimal and maximal curves).

We note that the differential equation (1.8) may be derived from the variational principle $\delta\,\int J(u,u')\,dx = 0$ as the Jacobi-Euler equation

$$\frac{d}{dx}\left(\frac{\partial J}{\partial u'}\right) \;=\; \frac{\partial J}{\partial u}, \tag{1.10}$$

where the Jacobi function $J(u,u';x)$ is defined as

$$\begin{aligned} J(u,u') \;&\equiv\; \frac{1}{2}\,\left(\frac{d^2}{d\epsilon^2}\;F(y+\epsilon\,u,y'+\epsilon\,u')\right)_{\epsilon=0} \\ &\equiv\; \frac{u^2}{2}\,\frac{\partial^2 F}{\partial y^2} \;+\; u\,u'\,\frac{\partial^2 F}{\partial y\partial y'} \;+\; \frac{u'^2}{2}\,\frac{\partial^2 F}{(\partial y')^2}. \end{aligned} \tag{1.11}$$

For example, for $F(y,y') = \sqrt{1+(y')^2} = \sqrt{1+m^2} \equiv \Lambda$, then $\partial^2 F/\partial y^2 = 0 = \partial^2 F/\partial y\partial y'$ and $\partial^2 F/\partial(y')^2 = \Lambda^{-3}$, and the Jacobi function becomes $J(u,u') = \frac{1}{2}\,\Lambda^{-3}(u')^2$. The Jacobi equation (1.9), therefore, becomes $(\Lambda^{-3}\,u')' = 0$, or $u'' = 0$, i.e., deviations diverge linearly.

Lastly, the second functional variation (1.6) can be combined with the Jacobi equation (1.9) to yield the expression

$$\delta^2\mathcal{F}[y;\delta y] \;=\; \int_a^b\;\frac{\partial^2 F}{(\partial y')^2}\left(\delta y' \;-\; \delta y\,\frac{u'}{u}\right)^2\,dx,$$

where $u(x)$ is a solution of the Jacobi equation (1.9). We note that the minimum condition $\delta^2\mathcal{F} > 0$ is now clearly associated with the condition $\partial^2 F/\partial(y')^2 > 0$. Furthermore, we note that the Jacobi equation describing space-time geodesic deviations plays a fundamental role in Einstein's Theory of General Relativity. We shall return to the Jacobi equation in Sec. 1.4 where we briefly discuss Fermat's Principle of Least Time and its applications to the general theory of geometric optics.

Euler's Second Equation

Under certain conditions ($\partial F/\partial x \equiv 0$), we may obtain a partial solution to Euler's First Equation (1.5). This partial solution is derived as follows. First, we write the exact x-derivative of $F(y, y'; x)$ as

$$\frac{dF}{dx} \;=\; \frac{\partial F}{\partial x} \;+\; y' \,\frac{\partial F}{\partial y} \;+\; y'' \,\frac{\partial F}{\partial y'},$$

and substitute Eq. (1.5) to combine the last two terms so that we obtain Euler's Second equation

$$\frac{d}{dx}\left(F \;-\; y' \,\frac{\partial F}{\partial y'}\right) \;=\; \frac{\partial F}{\partial x}. \tag{1.12}$$

This equation is especially useful when the integrand $F(y, y')$ in Eq. (1.2) is independent of x, for which Eq. (1.12) yields the solution

$$F(y, y') \;-\; y' \,\frac{\partial F}{\partial y'}(y, y') \;=\; \alpha, \tag{1.13}$$

where the constant α is determined from the condition $y(x_0) = y_0$ and $y'(x_0) = y'_0$. Here, Eq. (1.13) is a *partial* solution (in some sense) of Eq. (1.5), since we have reduced the derivative order from second-order derivative $y''(x)$ in Eq. (1.5) to first-order derivative $y'(x)$ in Eq. (1.13) on the solution $y(x)$. Hence, Euler's Second Equation has produced an equation of the form $G(y, y'; \alpha) = 0$, which can often be integrated by *quadrature* as we shall see later.

1.1.3 Path of Shortest Distance and Geodesic Equation

We now return to the problem of minimizing the length integral (1.1), with the integrand written as $F(y, y') = \sqrt{1 + (y')^2}$. Here, Euler's First Equation (1.5) yields

$$\frac{d}{dx}\left(\frac{\partial F}{\partial y'}\right) \;=\; \frac{y''}{[1 + (y')^2]^{3/2}} \;=\; \frac{\partial F}{\partial y} \;=\; 0,$$

so that the function $y(x)$ that minimizes the length integral (1.1) is the solution of the differential equation $y''(x) = 0$ subject to the boundary conditions $y(0) = 0$ and $y(1) = m$, i.e., $y(x) = m\,x$. Note that the integrand $F(y, y')$ also satisfies the sufficient minimum conditions (1.7) so that the path $y(x) = m\,x$ is indeed the path of shortest distance between two points on the plane.

Geodesic equation*

We generalize the problem of finding the path of shortest distance on the Euclidean plane (x, y) to the problem of finding *geodesic* paths in arbitrary geometry because it introduces

important geometric concepts in Classical Mechanics needed in later chapters. For this purpose, let us consider a path in space from point A to point B parametrized by the continuous parameter σ, i.e., $\mathbf{x}(\sigma)$ such that $\mathbf{x}(A) = \mathbf{x}_A$ and $\mathbf{x}(B) = \mathbf{x}_B$. The length integral from point A to B is

$$\mathcal{L}[\mathbf{x}] \;=\; \int_A^B \left(g_{ij}\, \frac{dx^i}{d\sigma}\, \frac{dx^j}{d\sigma} \right)^{1/2} d\sigma, \tag{1.14}$$

where the space metric g_{ij} is defined so that the squared infinitesimal length element is $ds^2 \equiv g_{ij}(\mathbf{x})\, dx^i\, dx^j$ (summation over repeated indices is implied throughout the text). Next, using the definition (1.3), the first-order variation $\delta\mathcal{L}[\mathbf{x}]$ is given as

$$\begin{aligned} \delta\mathcal{L}[\mathbf{x}] \;&=\; \frac{1}{2} \int_A^B \left[\frac{\partial g_{ij}}{\partial x^k}\, \delta x^k\, \frac{dx^i}{d\sigma}\, \frac{dx^j}{d\sigma} \;+\; 2\, g_{ij}\, \frac{d\delta x^i}{d\sigma}\, \frac{dx^j}{d\sigma} \right] \frac{d\sigma}{ds/d\sigma} \\ &=\; \frac{1}{2} \int_a^b \left[\frac{\partial g_{ij}}{\partial x^k}\, \delta x^k\, \frac{dx^i}{ds}\, \frac{dx^j}{ds} \;+\; 2\, g_{ij}\, \frac{d\delta x^i}{ds}\, \frac{dx^j}{ds} \right] ds, \end{aligned}$$

where $a = s(A)$ and $b = s(B)$ and we have performed a parametrization change: $\mathbf{x}(\sigma) \to \mathbf{x}(s)$. By integrating the second term by parts, we obtain

$$\begin{aligned} \delta\mathcal{L}[\mathbf{x}] \;&=\; -\int_a^b \left[\frac{d}{ds} \left(g_{ij}\, \frac{dx^j}{ds} \right) \;-\; \frac{1}{2}\, \frac{\partial g_{jk}}{\partial x^i}\, \frac{dx^j}{ds}\, \frac{dx^k}{ds} \right] \delta x^i\, ds \\ &=\; -\int_a^b \left[g_{ij}\, \frac{d^2x^j}{ds^2} \;+\; \left(\frac{\partial g_{ij}}{\partial x^k} \;-\; \frac{1}{2}\, \frac{\partial g_{jk}}{\partial x^i} \right) \frac{dx^j}{ds}\, \frac{dx^k}{ds} \right] \delta x^i\, ds. \end{aligned} \tag{1.15}$$

We now note that, using symmetry properties under interchange of the j-k indices, the second term in Eq. (1.15) can also be written as

$$\begin{aligned} \left(\frac{\partial g_{ij}}{\partial x^k} \;-\; \frac{1}{2}\, \frac{\partial g_{jk}}{\partial x^i} \right) \frac{dx^j}{ds}\, \frac{dx^k}{ds} \;&=\; \frac{1}{2} \left(\frac{\partial g_{ij}}{\partial x^k} \;+\; \frac{\partial g_{ik}}{\partial x^j} \;-\; \frac{\partial g_{jk}}{\partial x^i} \right) \frac{dx^j}{ds}\, \frac{dx^k}{ds} \\ &=\; \Gamma_{i|jk}\, \frac{dx^j}{ds}\, \frac{dx^k}{ds}, \end{aligned}$$

using the definition of the Christoffel symbol

$$\Gamma^{\ell}_{\;jk} \;=\; g^{\ell i}\, \Gamma_{i|jk} \;=\; \frac{g^{\ell i}}{2} \left(\frac{\partial g_{ij}}{\partial x^k} \;+\; \frac{\partial g_{ik}}{\partial x^j} \;-\; \frac{\partial g_{jk}}{\partial x^i} \right) \;\equiv\; \Gamma^{i}_{\;kj}, \tag{1.16}$$

where g^{ij} denotes a component of the inverse metric (i.e., $g^{ij}\, g_{jk} = \delta^i{}_k$). Hence, the first-order variation (1.15) can be expressed as

$$\delta\mathcal{L}[\mathbf{x}] \;=\; \int_a^b \left[\frac{d^2x^i}{ds^2} \;+\; \Gamma^{i}_{\;jk}\, \frac{dx^j}{ds}\, \frac{dx^k}{ds} \right] g_{i\ell}\, \delta x^{\ell}\, ds. \tag{1.17}$$

The stationarity condition $\delta\mathcal{L} = 0$ for arbitrary variations δx^ℓ yields an equation for the path $\mathbf{x}(s)$ of shortest distance known as the *geodesic* equation

$$\frac{d^2x^i}{ds^2} \;+\; \Gamma^i_{jk}\,\frac{dx^j}{ds}\,\frac{dx^k}{ds} \;=\; 0. \tag{1.18}$$

Returning to two-dimensional Euclidean geometry, where the components of the metric tensor are constants (either 0 or 1), the geodesic equations are $x''(s) = 0 = y''(s)$ which once again leads to a straight line.

Geodesic equation on a sphere

For example, geodesic curves on the surface of a sphere of radius R are expressed in terms of extremal curves of the length functional

$$\mathcal{L}[\varphi] \;=\; \int\, R\sqrt{1 \;+\; \sin^2\theta\,\left(\frac{d\varphi}{d\theta}\right)^2}\;d\theta \;\equiv\; R\,\int\,L(\varphi',\theta)\;d\theta, \tag{1.19}$$

where the azimuthal angle $\varphi(\theta)$ is an arbitrary function of the polar angle θ. Since the function $L(\varphi',\theta)$ in Eq. (1.19) is independent of the azimuthal angle φ, its corresponding Euler equation is

$$\frac{\partial L}{\partial\varphi'} \;=\; \frac{\sin^2\theta\;\varphi'}{\sqrt{1+\sin^2\theta\,(\varphi')^2}} \;=\; \sin\alpha,$$

where α is an arbitrary constant angle. Solving for φ' we find

$$\varphi'(\theta) \;=\; \frac{\sin\alpha}{\sin\theta\,\sqrt{\sin^2\theta-\sin^2\alpha}},$$

which can, thus, be integrated to give

$$\varphi \;-\; \beta \;=\; \int\,\frac{\sin\alpha\;d\theta}{\sin\theta\,\sqrt{\sin^2\theta-\sin^2\alpha}} \;=\; -\;\int\,\frac{\tan\alpha\;du}{\sqrt{1-u^2\;\tan^2\alpha}},$$

where β is another constant angle and we used the change of variable $u = \cot\theta$. A simple trigonometric substitution finally yields

$$\cos(\varphi-\beta) \;=\; \tan\alpha\;\cot\theta,$$

which describes a great circle on the surface of the sphere; you should check this for yourself by generating (using Maple or Mathematica) a three-dimensional parametric plot of the unit vector $\widehat{\mathsf{r}}(\varphi) = \sin\theta(\varphi)\,\widehat{\rho}(\varphi) + \cos\theta(\varphi)\,\widehat{\mathsf{z}}$.

1.2 Classical Variational Problems

The development of the Calculus of Variations led to the resolution of several classical optimization problems in mathematics and physics. In this section, we present two classical variational problems that were connected to its original development. First, in the Isoperimetric problem, we show how Lagrange modified Euler's formulation of the Calculus of Variations by allowing constraints to be imposed on the search for finding extremal values of certain integrals. Next, in the Brachistochrone problem, we show how the Calculus of Variations is used to find the path of *quickest* descent for a bead sliding along a frictionless wire under the action of gravity.

1.2.1 Isoperimetric Problem

Isoperimetric problems represent some of the earliest applications of the variational approach to solving mathematical optimization problems. Pappus (ca. 290-350) was among the first to recognize that among all the isoperimetric closed planar curves (i.e., closed curves that have the same perimeter length), the circle encloses the greatest area.[1] The variational formulation of the isoperimetric problem requires that we maximize the area integral $A = \int y(x)\,dx$ while keeping the perimeter length integral $L = \int \sqrt{1+(y')^2}\,dx$ constant.

The isoperimetric problem falls in a class of variational problems called *constrained* variational principles, where a certain functional $\int f(y,y',x)\,dx$ is to be optimized under the constraint that another functional $\int g(y,y',x)\,dx$ be held constant (say at value G). The constrained variational principle is then expressed in terms of the functional

$$\begin{aligned} \mathcal{F}_\lambda[y] &= \int f(y,y',x)\,dx \;+\; \lambda\left(G \;-\; \int g(y,y',x)\,dx\right) \\ &= \int \Big[\; f(y,y',x) \;-\; \lambda\, g(y,y',x) \;\Big]\; dx \;+\; \lambda G, \end{aligned} \tag{1.20}$$

where the parameter λ is called a Lagrange *multiplier*. Note that the functional $\mathcal{F}_\lambda[y]$ is chosen, on the one hand, so that the derivative

$$\frac{d\mathcal{F}_\lambda[y]}{d\lambda} \;=\; G \;-\; \int g(y,y',x)\,dx \;=\; 0$$

enforces the constraint for all curves $y(x)$. On the other hand, the stationarity condition $\delta\mathcal{F}_\lambda = 0$ for the functional (1.20) with respect to arbitrary variations $\delta y(x)$ (which vanish at the integration boundaries) yields Euler's First Equation:

$$\frac{d}{dx}\left(\frac{\partial f}{\partial y'} \;-\; \lambda\,\frac{\partial g}{\partial y'}\right) \;=\; \frac{\partial f}{\partial y} \;-\; \lambda\,\frac{\partial g}{\partial y}. \tag{1.21}$$

[1] Such results are normally described in terms of the so-called isoperimetric inequalities $4\pi A \le L^2$, where A denotes the area enclosed by a closed curve of perimeter length L; here, equality is satisfied by the circle.

Here, we assume that this second-order differential equation is to be solved subject to the conditions $y(x_0) = y_0$ and $y'(x_0) = 0$; the solution $y(x;\lambda)$ of Eq. (1.21) is, however, parametrized by the unknown Lagrange multiplier λ.

If the integrands $f(y, y')$ and $g(y, y')$ in Eq. (1.20) are both explicitly independent of x, then Euler's Second Equation (1.13) for the functional (1.20) becomes

$$\frac{d}{dx}\left[\left(f \;-\; y'\,\frac{\partial f}{\partial y'}\right) \;-\; \lambda\,\left(g \;-\; y'\,\frac{\partial g}{\partial y'}\right)\right] \;=\; 0. \tag{1.22}$$

By integrating this equation we obtain

$$\left(f \;-\; y'\,\frac{\partial f}{\partial y'}\right) \;-\; \lambda\,\left(g \;-\; y'\,\frac{\partial g}{\partial y'}\right) \;=\; 0,$$

where the constant of integration on the right is chosen from the conditions $y(x_0) = y_0$ and $y'(x_0) = 0$, so that the value of the constant Lagrange multiplier is now defined as

$$\lambda(x_0) \;=\; \frac{f(y_0, 0)}{g(y_0, 0)}.$$

Hence, the solution $y(x)$ of the constrained variational problem (1.20) is now uniquely determined.

We return to the isoperimetric problem now represented in terms of the constrained functional

$$\begin{aligned}\mathcal{A}_\lambda[y] \;&=\; \int\, y\,dx \;+\; \lambda\left(L \;-\; \int\,\sqrt{1+(y')^2}\,dx\right)\\ &=\; \int\,\left[\,y \;-\; \lambda\,\sqrt{1+(y')^2}\,\right]\,dx \;+\; \lambda\,L,\end{aligned} \tag{1.23}$$

where L denotes the value of the constant-length constraint. From Eq. (1.21), the stationarity of the functional (1.23) with respect to arbitrary variations $\delta y(x)$ yields

$$\frac{d}{dx}\left(-\,\frac{\lambda\,y'}{\sqrt{1+(y')^2}}\right) \;=\; 1,$$

which can be integrated to give

$$-\,\frac{\lambda\,y'}{\sqrt{1+(y')^2}} \;=\; x \;-\; x_0, \tag{1.24}$$

where x_0 denotes a constant of integration associated with the condition $y'(x_0) = 0$. Since the integrands $f(y, y') = y$ and $g(y, y') = \sqrt{1+(y')^2}$ are both explicitly independent of x, then Euler's Second Equation (1.22) applies, and we obtain

$$\frac{d}{dx}\left(y \;-\; \frac{\lambda}{\sqrt{1+(y')^2}}\right) \;=\; 0,$$

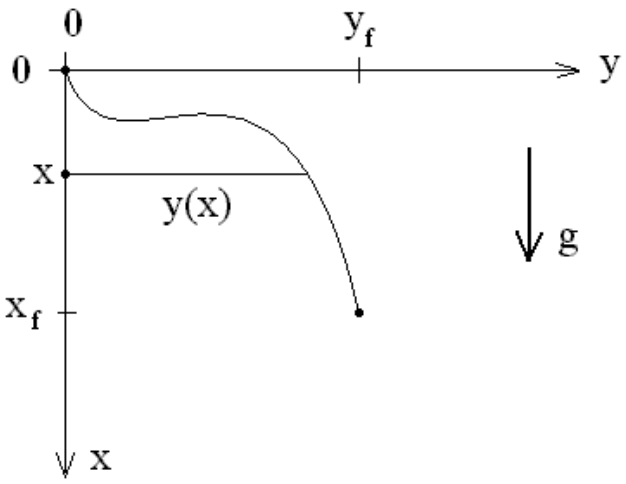

Figure 1.3: Brachistrochrone problem

which can be integrated to give

$$\frac{\lambda}{\sqrt{1+(y')^2}} \;=\; y. \tag{1.25}$$

Here, the constant of integration is chosen, with $y'(x_0) = 0$, so that $y(x_0) = \lambda$. By combining Eqs. (1.24) and (1.25), we obtain $y\,y' + (x - x_0) = 0$, which can lastly be integrated to give $y^2(x) = \lambda^2 - (x - x_0)^2$. We immediately recognize that the maximal isoperimetric curve $y(x)$ is a circle of radius $r = \lambda$ with perimeter length $L = 2\pi\,\lambda$ and maximal enclosed area $A = \pi\,\lambda^2 = L^2/4\pi$.

1.2.2 Brachistochrone Problem

The brachistochrone problem is a *least-time* variational problem, which was first solved in 1696 by Johann Bernoulli (1667-1748). The problem can be stated as follows. A bead is released from rest (at the origin in Figure 1.3) and slides down a frictionless wire that connects the origin to a given point (x_f, y_f). The question posed by the brachistochrone problem is to determine the shape $y(x)$ of the wire for which the frictionless descent of the bead under gravity takes the shortest amount of time.

Using the (x, y)-coordinates shown above, the speed of the bead after it has fallen a vertical distance x along the wire is $v = \sqrt{2g\,x}$ (where g denotes the gravitational acceleration) and, thus, the time integral

$$\mathcal{T}[y] \;=\; \int \frac{ds}{v} \;=\; \int_0^{x_f} \sqrt{\frac{1+(y')^2}{2\,gx}}\,dx \;=\; \int_0^{x_f} F(y, y', x)\,dx, \tag{1.26}$$

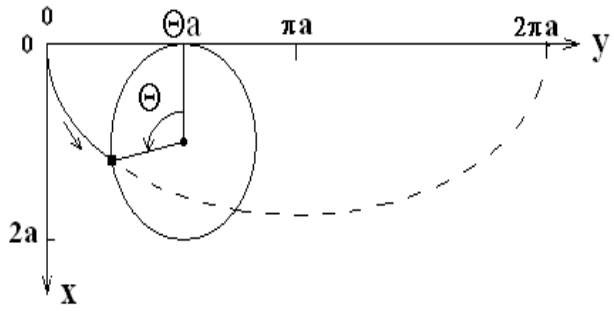

Figure 1.4: Brachistochrone solution

is a functional of the path $y(x)$. Note that, in the absence of friction, the bead's mass does not enter into the problem. Since the integrand of Eq. (1.26) is independent of the y-coordinate ($\partial F/\partial y = 0$), Euler's First Equation (1.5) simply yields

$$\frac{d}{dx}\left(\frac{\partial F}{\partial y'}\right) \;=\; 0 \quad \rightarrow \quad \frac{\partial F}{\partial y'} \;=\; \frac{y'}{\sqrt{2\,gx\;[1+(y')^2]}} \;=\; \alpha,$$

where α is a constant, which can be rewritten in terms of the scale length $\lambda = (2\alpha^2 g)^{-1}$ as

$$\frac{(y')^2}{1+(y')^2} \;=\; \frac{x}{\lambda}. \tag{1.27}$$

Integration by quadrature of Eq. (1.27) yields the integral solution

$$y(x) \;=\; \int_0^x \sqrt{\frac{s}{\lambda - s}}\, ds,$$

subject to the initial condition $y(x=0) = 0$. Using the trigonometric substitution (with $\lambda = 2a$)

$$s \;=\; 2a\,\sin^2(\theta/2) \;=\; a\,(1 \;-\; \cos\theta),$$

we obtain the parametric solution $x(\theta) = a\,(1-\cos\theta)$ and

$$y(\theta) \;=\; \int_0^\theta \sqrt{\frac{1-\cos\theta}{1+\cos\theta}}\; a\,\sin\theta\; d\theta \;=\; a\,\int_0^\theta (1-\cos\theta)\; d\theta \;=\; a\,(\theta \;-\; \sin\theta). \tag{1.28}$$

This solution yields a parametric representation of the *cycloid* (Figure 1.4) where the bead is placed on a rolling hoop of radius a.

1.3 Fermat's Principle of Least Time

Several *minimum* principles have been invoked throughout the history of Physics to explain the behavior of light and particles. In one of its earliest form, Hero of Alexandria (ca. 75

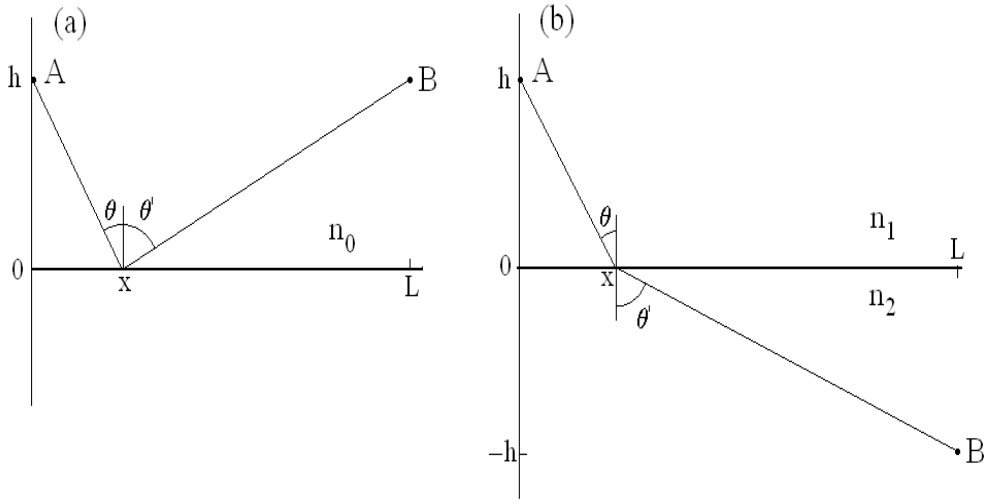

Figure 1.5: Reflection (a) and refraction (b) of light

AD) stated that *light travels in a straight line* and that light follows a path of shortest distance when it is reflected. In 1657, Pierre de Fermat (1601-1665) stated the Principle of *Least Time*, whereby light travels between two points along a path that minimizes the travel time, to explain Snell's Law (Willebrord Snell, 1591-1626) associated with light refraction in a stratified medium. Using the index of refraction $n_0 \geq 1$ of the uniform medium, the speed of light in the medium is expressed as $v_0 = c/n_0 \leq c$, where c is the speed of light in vacuum. This straight path is not only a path of shortest distance but also a path of least time.

The laws of reflection and refraction as light propagates in uniform media separated by sharp boundaries (see Figure 1.5) are easily formulated as minimization problems as follows. First, for the law of light reflection (as shown in Figure 1.5(a)), the time taken by light to go from point $A = (0, h)$ to point $B = (L, h)$ after being reflected at point $(x, 0)$ is given by

$$T_{AB}(x) \;=\; \frac{n_0}{c}\left[\,\sqrt{x^2+h^2} \;+\; \sqrt{(L-x)^2+h^2}\,\right],$$

where n_0 denotes the index of refraction of the medium. We easily evaluate the derivative of $T_{AB}(x)$ to find

$$T'_{AB}(x) \;=\; \frac{n_0}{c}\left[\,\frac{x}{\sqrt{x^2+h^2}} \;-\; \frac{(L-x)}{\sqrt{(L-x)^2+h^2}}\,\right] \;=\; \frac{n_0}{c}\Big(\sin\theta \;-\; \sin\theta'\Big),$$

where the angles θ and θ' are defined in Figure 1.5(a). Here, the law of reflection is expressed in terms of the extremum condition $T'_{AB}(x) = 0$, which implies that the path of least time is obtained when the reflected angle θ' is equal to the incidence angle θ (or $x = L/2$).

Next, the law of light refraction (as shown in Figure 1.5(b)) involving light travelling from point $A = (0, h)$ in one medium (with index of refraction n_1) to point $B = (L, -h)$ in another medium (with index of refraction n_2) is similarly expressed as a minimization problem based on the time function

$$T_{AB}(x) \;=\; \frac{1}{c}\left[\, n_1\,\sqrt{x^2+h^2} \;+\; n_2\,\sqrt{(L-x)^2+h^2}\,\right],$$

where definitions are found in Figure 1.5(b). Here, the extremum condition $T'_{AB}(x) = 0$ yields Snell's law

$$n_1\,\sin\theta \;=\; n_2\,\sin\theta'. \tag{1.29}$$

Note that Snell's law implies that the refracted light ray bends toward the medium with the largest index of refraction. In what follows, we generalize Snell's law to describe light refraction in a continuous nonuniform medium.

1.3.1 Light Propagation in a Nonuniform Medium

According to Fermat's Principle, light propagates in a nonuniform medium by travelling along a path that *minimizes* the travel time between an initial point A (where a light ray is launched) and a final point B (where the light ray is received). Hence, the time taken by a light ray following a path γ from point A to point B (parametrized by σ) is

$$\mathcal{T}[\mathbf{x}] \;=\; \int\, c^{-1}n(\mathbf{x})\,\left|\frac{d\mathbf{x}}{d\sigma}\right|\,d\sigma \;=\; c^{-1}\,\mathcal{L}_n[\mathbf{x}], \tag{1.30}$$

where $\mathcal{L}_n[\mathbf{x}]$ represents the length of the *optical* path taken by light as it travels in a medium with refractive index n and

$$\left|\frac{d\mathbf{x}}{d\sigma}\right| \;=\; \sqrt{\left(\frac{dx}{d\sigma}\right)^2 \;+\; \left(\frac{dy}{d\sigma}\right)^2 \;+\; \left(\frac{dz}{d\sigma}\right)^2}.$$

We now consider ray propagation in two dimensions (x, y), with the index of refraction $n(y)$, and return to general properties of ray propagation in Sec. 1.4.

For ray propagation in two dimensions (labeled x and y) in a medium with nonuniform refractive index $n(y)$, an arbitrary point $(x,\ y = y(x))$ along the light path $\mathbf{x}(\sigma)$ is parametrized by the x-coordinate [i.e., $\sigma = x$ in Eq. (1.30)], which starts at point $A = (a, y_a)$ and ends at point $B = (b, y_b)$ (see Figure 1.6). Along the path $y : x \mapsto y(x)$, the infinitesimal length element is $ds = \sqrt{1+(y')^2}\,dx$ and the optical length

$$\mathcal{L}_n[y] \;=\; \int_a^b\, n(y)\,\sqrt{1+(y')^2}\,dx \tag{1.31}$$

is a *functional* of y (i.e., changing the path y changes the value of the integral $\mathcal{L}_n[y]$).

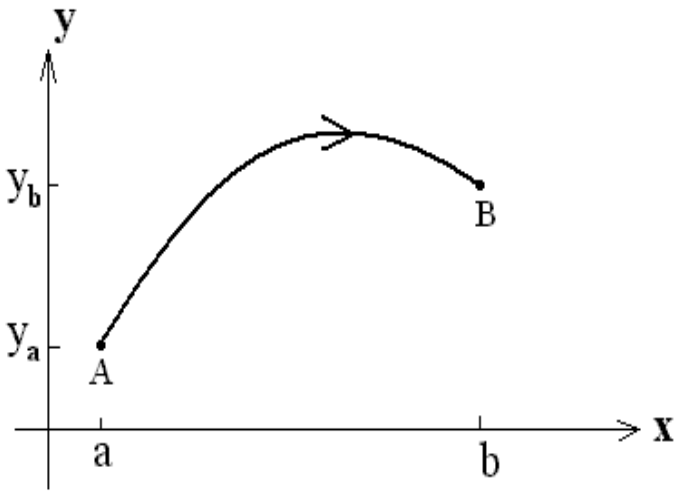

Figure 1.6: Light path in a nonuniform medium

We now apply the variational principle $\delta\mathcal{L}_n[y] = 0$ for the case where $F(y, y') = n(y)\sqrt{1 + (y')^2}$, from which we find

$$\frac{\partial F}{\partial y'} = \frac{n(y)\, y'}{\sqrt{1 + (y')^2}} \quad \text{and} \quad \frac{\partial F}{\partial y} = n'(y)\sqrt{1 + (y')^2},$$

so that Euler's First Equation (1.5) becomes

$$n(y)\, y'' = n'(y)\left[1 + (y')^2\right]. \tag{1.32}$$

Although the solution of this (nonlinear) second-order ordinary differential equation is difficult to obtain for general functions $n(y)$, we can nonetheless obtain a qualitative picture of its solution by noting that y'' has the same sign as $n'(y)$. Hence, when $n'(y) = 0$ for all y (i.e., the medium is spatially uniform), the solution $y'' = 0$ yields the straight line $y(x; \varphi_0) = \tan\varphi_0\ x$, where φ_0 denotes the initial launch angle (as measured from the horizontal axis). The case where $n'(y) > 0$ (or < 0), on the other hand, yields a light path which is concave upwards (or downwards) as will be shown below.

Note that the sufficient conditions (1.7) for the optical path are expressed as

$$\frac{\partial^2 F}{(\partial y')^2} = \frac{n}{[1 + (y')^2]^{3/2}} > 0,$$

which is satisfied for all refractive media, and

$$\frac{\partial^2 F}{\partial y^2} - \frac{d}{dx}\left(\frac{\partial^2 F}{\partial y \partial y'}\right) = n''\sqrt{1 + (y')^2} - \frac{d}{dx}\left(\frac{n'\, y'}{\sqrt{1 + (y')^2}}\right) = \frac{n^2}{F}\,\frac{d^2 \ln n}{dy^2},$$

whose sign is indefinite. Hence, the sufficient condition for a minimal optical length for light traveling in a nonuniform refractive medium is $d^2 \ln n/dy^2 > 0$; note, however, that only the stationarity of the optical path is physically meaningful and, thus, we shall not discuss the minimal properties of light paths in what follows.

Since the function $F(y, y') = n(y)\sqrt{1 + (y')^2}$ is explicitly independent of x, we find

$$F \; - \; y' \, \frac{\partial F}{\partial y'} \; = \; \frac{n(y)}{\sqrt{1 + (y')^2}} \; = \; \text{constant},$$

and, thus, the partial solution of Eq. (1.32) is

$$n(y) \; = \; \alpha \, \sqrt{1 + (y')^2}, \tag{1.33}$$

where α is a constant determined from the initial conditions of the light ray. We note that Eq. (1.33) states that as a light ray enters a region of increased (decreased) refractive index, the slope of its path also increases (decreases). In particular, by substituting Eq. (1.32) into Eq. (1.33), we find

$$\alpha^2 \, y'' \; = \; \frac{1}{2} \, \frac{dn^2(y)}{dy},$$

and, hence, the path of a light ray is concave upward (downward) where $n'(y)$ is positive (negative), as previously discussed. Eq. (1.33) can be integrated by *quadrature* to give the integral solution

$$x(y) \; = \; \int_0^y \frac{\alpha \, ds}{\sqrt{[n(s)]^2 \; - \; \alpha^2}}, \tag{1.34}$$

subject to the condition $x(y = 0) = 0$. From the explicit dependence of the index of refraction $n(y)$, one may be able to perform the integration in Eq. (1.34) to obtain $x(y)$ and, thus, obtain an explicit solution $y(x)$ by inverting $x(y)$.

1.3.2 Snell's Law

We now show that the partial solution (1.33) corresponds to Snell's Law for light refraction in a nonuniform medium. Consider a light ray travelling in the (x, y)-plane launched from the initial position $(0, 0)$ at an initial angle φ_0 (measured from the x-axis) so that $y'(0) = \tan\varphi_0$ is the slope at $x = 0$. The constant α is then simply determined from Eq. (1.33) as $\alpha = n_0 \, \cos\varphi_0$, where $n_0 = n(0)$ is the refractive index at $y(0) = 0$. Next, let $y'(x) = \tan\varphi(x)$ be the slope of the light ray at $(x, \, y(x))$, so that $\sqrt{1 + (y')^2} = \sec\varphi$ and Eq. (1.33) becomes $n(y) \cos\varphi = n_0 \cos\varphi_0$. Lastly, when we substitute the complementary angle $\theta = \pi/2 - \varphi$ (measured from the vertical y-axis), we obtain the *local* form of Snell's Law:

$$n[y(x)] \; \sin\theta(x) \; = \; n_0 \; \sin\theta_0, \tag{1.35}$$

properly generalized to include a light path in a nonuniform refractive medium. Note that Snell's Law (1.35) does not tell us anything about the actual light path $y(x)$; this solution must come from solving Eq. (1.34).

1.3.3 Application of Fermat's Principle

As an application of Fermat's Principle, we consider the propagation of a light ray in a medium with linear refractive index $n(y) = n_0\ (1 - \beta\, y)$ exhibiting a constant gradient $n'(y) = -\,n_0\,\beta$. Substituting this profile into the optical-path solution (1.34), we find

$$x(y) \;=\; \int_0^y \frac{\cos\varphi_0\; ds}{\sqrt{(1-\beta\, s)^2 - \cos^2\varphi_0}}. \tag{1.36}$$

Next, we use the trigonometric substitution

$$y(\varphi) \;=\; \frac{1}{\beta}\left(1 \;-\; \frac{\cos\varphi_0}{\cos\varphi}\right), \tag{1.37}$$

with $\varphi = \varphi_0$ at $(x, y) = (0, 0)$, so that Eq. (1.36) becomes

$$x(\varphi) \;=\; -\,\frac{\cos\varphi_0}{\beta}\;\ln\left(\frac{\sec\varphi + \tan\varphi}{\sec\varphi_0 + \tan\varphi_0}\right). \tag{1.38}$$

The *parametric* solution (1.37)-(1.38) for the optical path in a linear medium shows that the path reaches a maximum height $\overline{y} = y(0)$ at a distance $\overline{x} = x(0)$ when the *tangent* angle φ is zero:

$$\overline{x} \;=\; \frac{\cos\varphi_0}{\beta}\;\ln(\sec\varphi_0 + \tan\varphi_0) \quad \text{and} \quad \overline{y} \;=\; \frac{1-\cos\varphi_0}{\beta}.$$

Figure 1.7 shows a graph of the normalized solution $y(x;\beta)/\overline{y}(\beta)$ as a function of the normalized coordinate $x/\overline{x}(\beta)$ for $\varphi_0 = \pi/3$.

Lastly, we obtain an explicit solution $y(x)$ for the optical path by solving for $\sec\varphi$ as a function of x from Eq. (1.38):

$$\sec\varphi \;=\; \cosh\left[\frac{\beta\, x}{\cos\varphi_0} \;-\; \ln(\sec\varphi_0 + \tan\varphi_0)\right].$$

Substituting this equation into Eq. (1.37), we find the light path

$$y(x;\beta) \;=\; \frac{1}{\beta} \;-\; \frac{\cos\varphi_0}{\beta}\;\cosh\left[\frac{\beta\, x}{\cos\varphi_0} \;-\; \ln(\sec\varphi_0 + \tan\varphi_0)\right]. \tag{1.39}$$

We can check that, in the uniform case ($\beta = 0$), we recover the expected straight-line result $\lim_{\beta\to 0}\ y(x;\beta) = (\tan\varphi_0)\, x$.

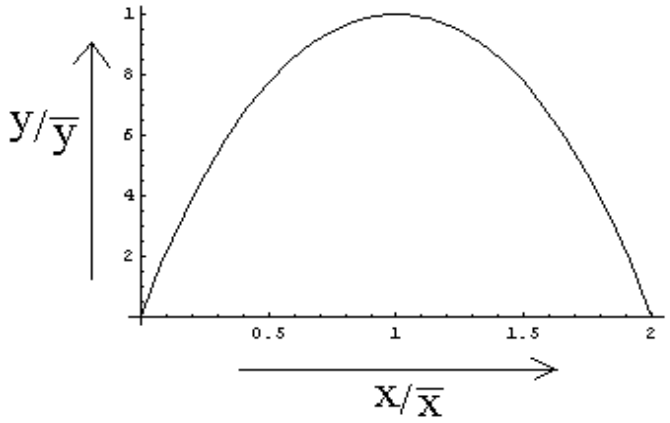

Figure 1.7: Light-path solution for a linear nonuniform medium

1.4 Geometric Formulation of Ray Optics*

1.4.1 Frenet-Serret Curvature of Light Path

We now return to the general formulation for light-ray propagation based on the time integral (1.30), where the integrand is

$$F\left(\mathbf{x},\, \frac{d\mathbf{x}}{d\sigma}\right) \;=\; n(\mathbf{x}) \;\left|\frac{d\mathbf{x}}{d\sigma}\right|,$$

and light rays are allowed to travel in a three-dimensional refractive medium with a general index of refraction $n(\mathbf{x})$. Euler's First equation in this case is

$$\frac{d}{d\sigma}\left(\frac{\partial F}{\partial(d\mathbf{x}/d\sigma)}\right) \;=\; \frac{\partial F}{\partial \mathbf{x}}, \tag{1.40}$$

where

$$\frac{\partial F}{\partial(d\mathbf{x}/d\sigma)} \;=\; \frac{n}{\Lambda}\,\frac{d\mathbf{x}}{d\sigma} \quad \text{and} \quad \frac{\partial F}{\partial \mathbf{x}} \;=\; \Lambda\,\nabla n,$$

with $\Lambda = |d\mathbf{x}/d\sigma|$. Euler's First Equation (1.40), therefore, becomes

$$\frac{d}{d\sigma}\left(\frac{n}{\Lambda}\,\frac{d\mathbf{x}}{d\sigma}\right) \;=\; \Lambda\,\nabla n. \tag{1.41}$$

Euler's Second Equation, on the other hand, states that

$$H(\sigma) \;\equiv\; F\left(\mathbf{x},\, \frac{d\mathbf{x}}{d\sigma}\right) \;-\; \frac{d\mathbf{x}}{d\sigma}\cdot\frac{\partial F}{\partial(d\mathbf{x}/d\sigma)} \;=\; 0$$

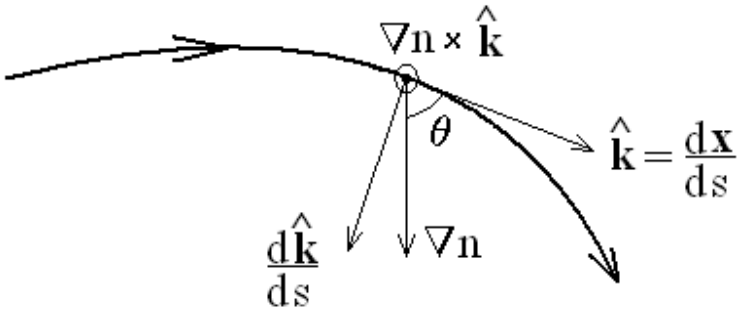

Figure 1.8: Light-path curvature and Frenet-Serret frame.

is a constant of motion. Note that, while Euler's Second Equation (1.33) was very useful in providing an explicit solution (Snell's Law) to finding the optical path in a nonuniform medium with index of refraction $n(y)$, it appears that Euler's Second Equation $H(\sigma) \equiv 0$ now reveals no information about the optical path. Where did the information go? To answer this question, we apply the Euler-Fermat equation (1.41) to the two-dimensional case where $\sigma = x$ and $\Lambda = \sqrt{1 + (y')^2}$ with $\nabla n = n'(y)\,\hat{\mathsf{y}}$. Hence, the Euler-Fermat equation (1.41) becomes

$$\frac{d}{dx}\left[\ \frac{n}{\Lambda}\ (\hat{\mathsf{x}} \ +\ y'\,\hat{\mathsf{y}})\ \right] \ =\ \Lambda\, n'\,\hat{\mathsf{y}},$$

from which we immediately conclude that Euler's Second Equation (1.33), $n = \alpha\,\Lambda$, now appears as a constant of the motion associated with a symmetry of the optical medium (i.e., the optical properties of the medium are invariant under translation along the x-axis). The association of symmetries with constants of the motion will later be discussed in terms of Noether's Theorem (see Sec. 2.5).

We now look at how the Euler-Fermat equation (1.41) can be simplified by an appropriate choice of parametrization. First, we can choose a ray parametrization such that $\Lambda = ds/d\sigma = n$, so that the Euler-Fermat equation (1.41) becomes $d^2\mathbf{x}/d\sigma^2 = n\,\nabla n = \frac{1}{2}\,\nabla n^2$ and, thus, the light ray is *accelerated* toward regions of higher index of refraction (see Figure 1.8). Next, by choosing the ray parametrization $d\sigma = ds$ (so that $\Lambda = 1$), we find that the ray *velocity* $d\mathbf{x}/ds = \hat{\mathsf{k}}$ is a unit vector which defines the direction of the wave vector $\mathbf{k}$. With this parametrization, the Euler-Fermat equation (1.41) is now replaced with the *light-curvature* equation

$$\frac{d\hat{\mathsf{k}}}{ds}\ =\ \hat{\mathsf{k}} \times \left(\nabla \ln n \times \hat{\mathsf{k}}\right)\ \equiv\ \kappa\,\hat{\mathsf{n}}, \tag{1.42}$$

where $\hat{\mathsf{n}}$ defines the principal normal unit vector and the *Frenet-Serret* curvature κ of the light path is $\kappa = |\nabla \ln n \times \hat{\mathsf{k}}|$ (see Appendix A). Note that for the one-dimensional problem discussed in Sec. 1.3.1, the curvature is $\kappa = |n'|/(n\,\Lambda) = |y''|/\Lambda^3$ in agreement with the Frenet-Serret curvature (see Appendix A).

Lastly, we introduce the general form of Snell's Law (1.35) as follows. First, we define the unit vector $\widehat{\mathsf{g}} = \nabla n/(|\nabla n|)$ to be pointing in the direction of increasing index of refraction and, after performing the cross-product of Eq. (1.41) with $\widehat{\mathsf{g}}$, we obtain the identity

$$\widehat{\mathsf{g}} \times \frac{d}{ds}\left(n\,\frac{d\mathbf{x}}{ds}\right) \;=\; \widehat{\mathsf{g}} \times \nabla n \;=\; 0.$$

Using this identity, we readily evaluate the s-derivative of $n\,\widehat{\mathsf{g}} \times \widehat{\mathsf{k}}$:

$$\frac{d}{ds}\left(\widehat{\mathsf{g}} \times n\,\frac{d\mathbf{x}}{ds}\right) \;=\; \frac{d\widehat{\mathsf{g}}}{ds} \times \left(n\,\frac{d\mathbf{x}}{ds}\right) \;=\; \frac{d\widehat{\mathsf{g}}}{ds} \times n\,\widehat{\mathsf{k}}.$$

Hence, if the unit vector $\widehat{\mathsf{g}}$ is constant along the path of a light ray (i.e., $d\widehat{\mathsf{g}}/ds = 0$), we then find the conservation law

$$\frac{d}{ds}\left(\widehat{\mathsf{g}} \times n\,\widehat{\mathsf{k}}\right) \;=\; 0, \tag{1.43}$$

which implies that the vector quantity $n\;\widehat{\mathsf{g}} \times \widehat{\mathsf{k}}$ is a constant along the light path. Note that, when a light ray progagates in two dimensions, this conservation law implies that the quantity $|\widehat{\mathsf{g}} \times n\;\widehat{\mathsf{k}}| = n \sin\theta$ is also a constant along the light path, where θ is the angle defined as $\cos\theta \equiv \widehat{\mathsf{g}} \cdot \widehat{\mathsf{k}}$. The conservation law (1.43), therefore, represents a generalization of Snell's Law (1.35).

1.4.2 Light Propagation in Spherical Geometry

By using the general ray-orbit equation (1.42), we can also show that for a spherically-symmetric nonuniform medium with index of refraction $n(r)$, the light-ray orbit $\mathbf{r}(s)$ satisfies the conservation law

$$\frac{d}{ds}\left(\mathbf{r} \times n(r)\,\frac{d\mathbf{r}}{ds}\right) \;=\; \mathbf{r} \times \frac{d}{ds}\left(n(r)\,\frac{d\mathbf{r}}{ds}\right) \;=\; \mathbf{r} \times \nabla n(r) \;=\; 0. \tag{1.44}$$

Here, we use the fact that the ray-orbit path is planar and, thus, we write

$$\mathbf{r} \times \frac{d\mathbf{r}}{ds} \;=\; r\,\sin\varphi\,\widehat{\mathsf{z}}, \tag{1.45}$$

where φ denotes the angle between the position vector $\mathbf{r}$ and the tangent vector $d\mathbf{r}/ds$ (see Figure 1.9). The conservation law (1.44) for ray orbits in a spherically-symmetric medium can, therefore, be expressed as $n(r)\,r\sin\varphi(r) = N\,a$, which is known as Bouguer's formula (Pierre Bouguer, 1698-1758), where N and a are constants (see Figure 1.9); note that the condition $n(r)\,r \geq N\,a$ must also be satisfied since $\sin\varphi(r) \leq 1$.

An explicit expression for the ray orbit $r(\theta)$ is obtained as follows. First, since $d\mathbf{r}/ds$ is a unit vector, we find

$$\frac{d\mathbf{r}}{ds} \;=\; \frac{d\theta}{ds}\left(r\,\widehat{\theta} \;+\; \frac{dr}{d\theta}\,\widehat{r}\right) \;=\; \frac{r\,\widehat{\theta} \;+\; (dr/d\theta)\,\widehat{r}}{\sqrt{r^2 \;+\; (dr/d\theta)^2}},$$

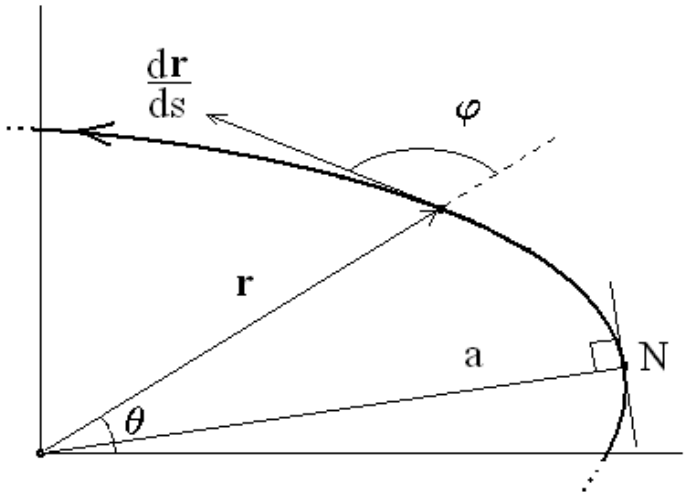

Figure 1.9: Light path in a nonuniform medium with spherical symmetry

so that

$$\frac{d\theta}{ds} \;=\; \frac{1}{\sqrt{r^2 \;+\; (dr/d\theta)^2}}$$

and Eq. (1.45) yields

$$\mathbf{r} \times \frac{d\mathbf{r}}{ds} \;=\; r\,\sin\varphi\,\hat{\mathsf{z}} \;=\; r^2\,\frac{d\theta}{ds}\,\hat{\mathsf{z}} \quad\rightarrow\quad \sin\varphi \;=\; \frac{r}{\sqrt{r^2 \;+\; (dr/d\theta)^2}} \;=\; \frac{Na}{nr},$$

where we made use of Bouguer's formula. Next, integration by quadrature yields

$$\frac{dr}{d\theta} \;=\; \frac{r}{Na}\,\sqrt{n(r)^2\,r^2 - N^2\,a^2} \quad\rightarrow\quad \theta(r) \;=\; N\,a\,\int_{r_0}^{r} \frac{d\rho}{\rho\,\sqrt{n^2(\rho)\,\rho^2 - N^2\,a^2}},$$

where we choose r_0 so that $\theta(r_0) = 0$. Lastly, a change of integration variable $\eta = Na/\rho$ yields

$$\theta(r) \;=\; \int_{Na/r}^{Na/r_0} \frac{d\eta}{\sqrt{\overline{n}^2(\eta) - \eta^2}}, \tag{1.46}$$

where $\overline{n}(\eta) \equiv n(Na/\eta)$. Hence, for a spherically-symmetric medium with index of refraction $n(r)$, we can compute the light-ray orbit $r(\theta)$ by inverting the integral (1.46) for $\theta(r)$.

Consider, for example, the spherically-symmetric refractive index $n(r) = n_0\,\sqrt{2 - (r/R)^2}$, where $n_0 = n(R)$ denotes the refractive index at $r = R$ (see Figure 1.10). Introducing the dimensional parameter $\epsilon = a/R$ and the transformation $\sigma = \eta^2$, Eq. (1.46) becomes

$$\theta(r) \;=\; \int_{Na/r}^{Na/r_0} \frac{\eta\,d\eta}{\sqrt{2n_0^2\,\eta^2 - n_0^2 N^2 \epsilon^2 - \eta^4}} \;=\; \frac{1}{2}\,\int_{(Na/r)^2}^{(Na/r_0)^2} \frac{d\sigma}{\sqrt{n_0^4\,\mathsf{e}^2 - (\sigma - n_0^2)^2}},$$

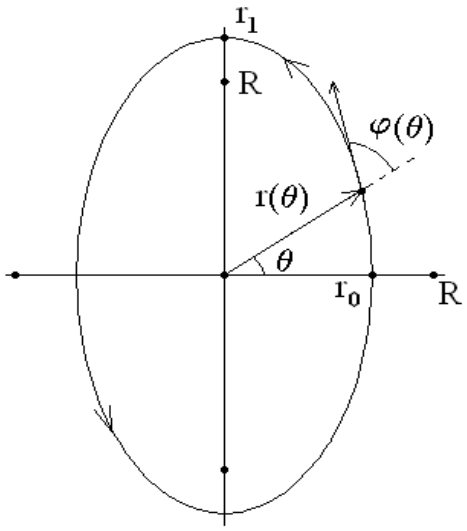

Figure 1.10: Elliptical light path in a spherically-symmetric refractive medium.

where $\mathsf{e} = \sqrt{1 - N^2\epsilon^2/n_0^2}$ (assuming that $n_0 > N\,\epsilon$). Next, using the trigonometric substitution $\sigma = n_0^2\,(1 + \mathsf{e}\,\cos\chi)$, we find $\theta(r) = \frac{1}{2}\,\chi(r)$ or

$$r^2(\theta) \;=\; \frac{r_0^2\,(1+\mathsf{e})}{1 \;+\; \mathsf{e}\,\cos 2\theta},$$

which represents an ellipse of major radius and minor radius $r_1 = R\,(1+\mathsf{e})^{1/2}$ and $r_0 = R\,(1-\mathsf{e})^{1/2}$, respectively. This example shows that, surprisingly, it is possible to trap light!

1.4.3 Geodesic Representation of Light Propagation

We now investigate the geodesic properties of light propagation in a nonuniform refractive medium. For this purpose, let us consider a path AB in space from point A to point B parametrized by the continuous parameter σ, i.e., $\mathbf{x}(\sigma)$ such that $\mathbf{x}(A) = \mathbf{x}_A$ and $\mathbf{x}(B) = \mathbf{x}_B$. The time taken by light in propagating from A to B is

$$\mathcal{T}[\mathbf{x}] \;=\; \int_A^B \frac{dt}{d\sigma}\,d\sigma \;=\; \int_A^B \frac{n}{c}\left(g_{ij}\,\frac{dx^i}{d\sigma}\,\frac{dx^j}{d\sigma}\right)^{1/2}\,d\sigma, \tag{1.47}$$

where $dt = n\,ds/c$ denotes the infinitesimal time interval taken by light in moving an infinitesimal distance ds in a medium with refractive index n and the space metric is denoted by g_{ij}. The geodesic properties of light propagation are investigated with the *vacuum* metric g_{ij} or the medium-modified metric $\overline{g}_{ij} = n^2\,g_{ij}$.

Vacuum-metric case

We begin with the vacuum-metric case and consider the light-curvature equation (1.42). First, we define the vacuum-metric tensor $g_{ij} = \mathsf{e}_i \cdot \mathsf{e}_j$ in terms of the basis vectors $(\mathsf{e}_1, \mathsf{e}_2, \mathsf{e}_3)$, so that the ray velocity is

$$\frac{d\mathbf{x}}{ds} \;=\; \frac{dx^i}{ds}\,\mathsf{e}_i.$$

Second, using the definition for the Christoffel symbol (1.16) and the relations

$$\frac{d\mathsf{e}_j}{ds} \;\equiv\; \Gamma^i_{jk}\,\frac{dx^k}{ds}\,\mathsf{e}_i,$$

we find

$$\frac{d\widehat{\mathsf{k}}}{ds} \;\equiv\; \frac{d^2\mathbf{x}}{ds^2} \;=\; \frac{d^2x^i}{ds^2}\,\mathsf{e}_i \;+\; \frac{dx^i}{ds}\,\frac{d\mathsf{e}_i}{ds} \;=\; \left(\frac{d^2x^i}{ds^2} \;+\; \Gamma^i_{jk}\,\frac{dx^j}{ds}\,\frac{dx^k}{ds}\right)\mathsf{e}_i.$$

By combining these relations, light-curvature equation (1.42) becomes

$$\frac{d^2x^i}{ds^2} \;+\; \Gamma^i_{jk}\,\frac{dx^j}{ds}\,\frac{dx^k}{ds} \;=\; \left(g^{ij} \;-\; \frac{dx^i}{ds}\,\frac{dx^j}{ds}\right)\frac{\partial \ln n}{\partial x^j}. \tag{1.48}$$

This equation shows that the path of a light ray departs from a vacuum geodesic line as a result of a refractive-index gradient projected along the tensor

$$h^{ij} \;\equiv\; g^{ij} \;-\; \frac{dx^i}{ds}\,\frac{dx^j}{ds}$$

which, by construction, is perpendicular to the ray velocity $d\mathbf{x}/ds$ (i.e., $h^{ij}\,dx_j/ds = 0$).

Medium-metric case

Next, we investigate the geodesic propagation of a light ray associated with the medium-modified (conformal) metric $\overline{g}_{ij} = n^2\,g_{ij}$, where $c^2dt^2 = n^2ds^2 = \overline{g}_{ij}\,dx^i dx^j$. The derivation follows a variational formulation similar to that found in Sec. 1.1.3. Hence, the first-order variation $\delta\mathcal{T}[\mathbf{x}]$ is expressed as

$$\delta\mathcal{T}[\mathbf{x}] \;=\; \int_{t_A}^{t_B}\left[\;\frac{d^2x^i}{dt^2} \;+\; \overline{\Gamma}^i_{jk}\,\frac{dx^j}{dt}\,\frac{dx^k}{dt}\;\right]\overline{g}_{i\ell}\,\delta x^\ell\,\frac{dt}{c^2}, \tag{1.49}$$

where the medium-modified Christoffel symbols $\overline{\Gamma}^i_{jk}$ include the effects of the gradient in the refractive index $n(\mathbf{x})$. We, therefore, find that the light path $\mathbf{x}(t)$ is a solution of the geodesic equation

$$\frac{d^2x^i}{dt^2} \;+\; \overline{\Gamma}^i_{jk}\,\frac{dx^j}{dt}\,\frac{dx^k}{dt} \;=\; 0, \tag{1.50}$$

which is also the path of least time for which $\delta\mathcal{T}[\mathbf{x}] = 0$.

Jacobi equation for light propagation

Lastly, we point out that the Jacobi equation for the deviation $\boldsymbol{\xi}(\sigma) = \overline{\mathbf{x}}(\sigma) - \mathbf{x}(\sigma)$ between two rays that satisfy the Euler-Fermat ray equation (1.41) can be obtained from the Jacobian function

$$\begin{aligned} J(\boldsymbol{\xi}, d\boldsymbol{\xi}/d\sigma) &\equiv \frac{1}{2}\left[\frac{d^2}{d\epsilon^2}\left(n(\mathbf{x}+\epsilon\,\boldsymbol{\xi})\left|\frac{d\mathbf{x}}{d\sigma}+\epsilon\,\frac{d\boldsymbol{\xi}}{d\sigma}\right|\right)\right]_{\epsilon=0} \\ &\equiv \frac{n}{2\Lambda^3}\left|\frac{d\boldsymbol{\xi}}{d\sigma}\times\frac{d\mathbf{x}}{d\sigma}\right|^2 + \frac{\boldsymbol{\xi}\cdot\nabla n}{\Lambda}\,\frac{d\boldsymbol{\xi}}{d\sigma}\cdot\frac{d\mathbf{x}}{d\sigma} + \frac{\Lambda}{2}\,\boldsymbol{\xi}\boldsymbol{\xi}:\nabla\nabla n, \end{aligned} \tag{1.51}$$

where the Euler-Fermat ray equation (1.41) was taken into account and the exact σ-derivative, which cancels out upon integration, is omitted. Hence, the Jacobi equation describing light-ray deviation is expressed as the Jacobi-Euler-Fermat equation

$$\frac{d}{d\sigma}\left(\frac{\partial J}{\partial(d\boldsymbol{\xi}/d\sigma)}\right) = \frac{\partial J}{\partial\boldsymbol{\xi}},$$

which yields

$$\begin{aligned} \frac{d}{d\sigma}\left[\frac{n}{\Lambda^3}\,\frac{d\mathbf{x}}{d\sigma}\times\left(\frac{d\boldsymbol{\xi}}{d\sigma}\times\frac{d\mathbf{x}}{d\sigma}\right)\right] &= \Lambda\,\boldsymbol{\xi}\cdot\nabla\nabla n\cdot\left(\mathbf{I} - \frac{1}{\Lambda^2}\,\frac{d\mathbf{x}}{d\sigma}\,\frac{d\mathbf{x}}{d\sigma}\right) \\ &+ \left[\frac{d\boldsymbol{\xi}}{d\sigma} - (\boldsymbol{\xi}\cdot\nabla\ln n)\,\frac{d\mathbf{x}}{d\sigma}\right]\times\left(\frac{\nabla n}{\Lambda}\times\frac{d\mathbf{x}}{d\sigma}\right). \end{aligned} \tag{1.52}$$

The Jacobi equation (1.52) describes the property of nearby rays to converge or diverge in a nonuniform refractive medium. Note, here, that the terms involving $\Lambda^{-1}\nabla n\times d\mathbf{x}/d\sigma$ in Eq. (1.52) can be written in terms of the Euler-Fermat ray equation (1.41) as

$$\frac{\nabla n}{\Lambda}\times\frac{d\mathbf{x}}{d\sigma} = \frac{1}{\Lambda^2}\,\frac{d}{d\sigma}\left(\frac{n}{\Lambda}\,\frac{d\mathbf{x}}{d\sigma}\right)\times\frac{d\mathbf{x}}{d\sigma} = \frac{n}{\Lambda^3}\left(\frac{d^2\mathbf{x}}{d\sigma^2}\times\frac{d\mathbf{x}}{d\sigma}\right),$$

which, thus, involve the Frenet-Serret ray curvature.

1.4.4 Eikonal Representation

The complementary picture of rays propagating in a nonuniform medium was proposed by Christiaan Huygens (1629-1695) in terms of wavefronts. Here, a wavefront is defined as the surface that is locally perpendicular to a ray. Hence, the index of refraction itself (for an isotropic medium) can be written as

$$n = |\nabla\mathcal{S}| = \frac{ck}{\omega} \quad \text{or} \quad \nabla\mathcal{S} = n\,\frac{d\mathbf{x}}{ds} = \frac{c\,\mathbf{k}}{\omega}, \tag{1.53}$$

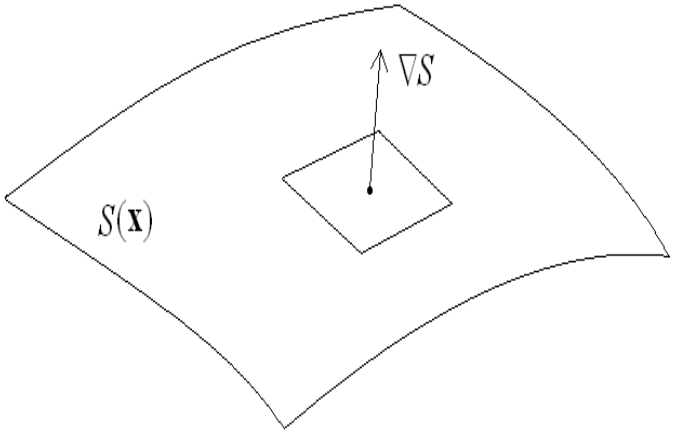

Figure 1.11: Eikonal surface.

where $\mathcal{S}$ is called the *eikonal* function (i.e., a wavefront is defined by the surface $\mathcal{S} =$ constant). To show that this definition is consistent with Eq. (1.42), we easily check that

$$\frac{d}{ds}\left(n\,\frac{d\mathbf{x}}{ds}\right) \;=\; \frac{d\nabla\mathcal{S}}{ds} \;=\; \nabla\left(\frac{d\mathcal{S}}{ds}\right) \;=\; \nabla n,$$

where $d\mathcal{S} = n\,ds$. This definition, therefore, implies that the wavevector $\mathbf{k}$ is curl-free.

$$\nabla\times\mathbf{k} \;=\; \nabla\times\nabla\left(\frac{\omega}{c}\,\mathcal{S}\right) \;\equiv\; 0, \tag{1.54}$$

where we used the fact that the frequency of a wave is unchanged by refraction. Hence, we find that $\nabla\times\widehat{\mathsf{k}} = \widehat{\mathsf{k}}\times\nabla\ln n$, from which we obtain the light-curvature equation (1.42).

A light wave is characterized by a polarization (unit) vector $\widehat{\mathsf{e}}$ that is tangent to the eikonal surface $\mathcal{S} =$ constant, i.e., $\widehat{\mathsf{e}}\cdot\nabla\mathcal{S} = 0$. We may, thus, write the polarization vector as

$$\widehat{\mathsf{e}} \;\equiv\; \cos\varphi\;\widehat{\mathsf{n}} \;+\; \sin\varphi\;\widehat{\mathsf{b}}, \tag{1.55}$$

where the normal and binormal unit vectors $\widehat{\mathsf{n}}$ and $\widehat{\mathsf{b}}$ are perpendicular to the wave-vector $\mathbf{k}$ of a light ray that crosses the eikonal surface. Using the Frenet-Serret equations $d\widehat{\mathsf{n}}/ds = \tau\,\widehat{\mathsf{b}} - \kappa\,\widehat{\mathsf{k}}$ and $d\widehat{\mathsf{b}}/ds = -\tau\,\widehat{\mathsf{n}}$, where κ and τ denote the curvature and torsion of the light ray, we find that the polarization vector satisfies the following evolution equation along a light ray:

$$\frac{d\widehat{\mathsf{e}}}{ds} \;=\; -\,\kappa\,\cos\varphi\;\widehat{\mathsf{k}} \;+\; \left(\frac{d\varphi}{ds} \;+\; \tau\right)\widehat{\mathsf{h}}, \tag{1.56}$$

where $\widehat{\mathsf{h}} \equiv \widehat{\mathsf{k}}\times\widehat{\mathsf{e}} = \partial\widehat{\mathsf{e}}/\partial\varphi$.

Note that, in the absence of sources and sinks, the light energy flux entering a finite volume bounded by a closed surface is equal to the light energy flux leaving the volume and, thus, the intensity of light I satisfies the conservation law

$$0 \;=\; \nabla\cdot\left(I\,\nabla\mathcal{S}\right) \;=\; I\,\nabla^2\mathcal{S} \;+\; \nabla\mathcal{S}\cdot\nabla I. \tag{1.57}$$

Using the definition $\nabla\mathcal{S}\cdot\nabla \equiv n\,\partial/\partial s$, we find the intensity *evolution* equation

$$\frac{\partial \ln I}{\partial s} \;=\; -\,n^{-1}\,\nabla^2\mathcal{S},$$

whose solution is expressed as

$$I \;=\; I_0\,\exp\left(-\int_0^s \nabla^2\mathcal{S}\,\frac{d\sigma}{n}\right), \tag{1.58}$$

where I_0 is the light intensity at position $s = 0$ along a ray. This equation, therefore, determines whether light intensity increases ($\nabla^2\mathcal{S} < 0$) or decreases ($\nabla^2\mathcal{S} > 0$) along a ray depending on the sign of $\nabla^2\mathcal{S}$. Lastly, in a refractive medium with spherical symmetry, with $\mathcal{S}'(r) = n(r)$ and $\widehat{\mathsf{k}} = \widehat{r}$, the conservation law (1.57) becomes

$$0 \;=\; \frac{1}{r^2}\,\frac{d}{dr}\left(r^2\,I\,n\right),$$

which implies that the light intensity satisfies the inverse-square law: $I(r)n(r)\,r^2 = I_0 n_0\,r_0^2$.

1.5 Problems

Problem 1

Find Euler's first and second equations following the extremization of the integral

$$\mathcal{F}[y] \;=\; \int_a^b \; F(y, y', y'')\; dx.$$

State whether an additional set of boundary conditions for $\delta y'(a)$ and $\delta y'(b)$ are necessary.

Problem 2

Find the curve joining two points (x_1, y_1) and (x_2, y_2) that yields a surface of revolution (about the x-axis) of minimum area by minimizing the integral

$$\mathcal{A}[y] \;=\; \int_{x_1}^{x_2} \; y\,\sqrt{1 + (y')^2}\; dx.$$

Problem 3

Show that the time required for a particle to move without friction to the minimum point of the cycloid solution of the Brachistochrone problem is $\pi\,\sqrt{a/g}$.

Problem 4

A thin rope of mass m (and uniform density) is attached to two vertical poles of height H separated by a horizontal distance D; the coordinates of the pole tops are set at $(\pm\, D/2,\; H)$. If the length L of the rope is greater than D, it will sag under the action of gravity and its lowest point (at its midpoint) will be at a height $y(x = 0) = y_0$. The shape of the rope, subject to the boundary conditions $y(\pm\, D/2) = H$, is obtained by minimizing the gravitational potential energy of the rope expressed in terms of the functional

$$\mathcal{U}[y] \;=\; \int_{D/2}^{-D/2} \; mg\, y\,\sqrt{1 + (y')^2}\; dx.$$

Show that the extremal curve $y(x)$ (known as the *catenary* curve) for this problem is

$$y(x) \;=\; c\,\cosh\left(\frac{x - b}{c}\right),$$

where $b = 0$ and $c = y_0$.

Problem 5

A light ray travels in a medium with refractive index

$$n(y) \;=\; n_0 \;\exp\,(-\beta\, y),$$

where n_0 is the refractive index at $y = 0$ and β is a positive constant.

(a) Use the results of the Principle of Least Time contained in the Notes distributed in class to show that the path of the light ray is expressed as

$$y(x;\beta) \;=\; \frac{1}{\beta}\;\ln\left[\;\frac{\cos(\beta\, x-\varphi_0)}{\cos\varphi_0}\;\right], \tag{1.59}$$

where the light ray is initially travelling upwards from $(x, y) = (0, 0)$ at an angle φ_0.

(b) Using the appropriate mathematical techniques, show that we recover the expected result $\lim_{\beta\to 0}\; y(x;\beta) = (\tan\varphi_0)\; x$ from Eq. (1.59).

(c) The light ray reaches a maximum height $\overline{y}$ at $x = \overline{x}(\beta)$, where $y'(\overline{x};\beta) = 0$. Find expressions for $\overline{x}$ and $\overline{y}(\beta) = y(\overline{x};\beta)$.

Problem 6

Consider the path associated with the index of refraction $n(y) = H/y$, where the height H is a constant and $0 < y < H\,\alpha^{-1} \equiv R$ to ensure that, according to Eq. (1.33), $n(y) > \alpha$. Show that the light path has the simple semi-circular form:

$$(R-x)^2 + y^2 \;=\; R^2 \quad\to\quad y(x) \;=\; \sqrt{x\,(2R-x)}.$$

Problem 7

Using the parametric solutions (1.37)-(1.38) of the optical path in a linear refractive medium, calculate the Frenet-Serret curvature coefficient

$$\kappa(\varphi) \;=\; \frac{|\mathbf{r}''(\varphi)\times\mathbf{r}'(\varphi)|}{|\mathbf{r}'(\varphi)|^3},$$

and show that it is equal to $|\widehat{\mathsf{k}}\times\nabla\ln n|$.

Problem 8

Assuming that the refractive index $n(z)$ in a nonuniform medium is a function of z only, derive the Euler-Fermat equations (1.42) for the components (α, β, γ) of the unit vector $\widehat{\mathsf{k}} = \alpha\,\widehat{\mathsf{x}} + \beta\,\widehat{\mathsf{y}} + \gamma\,\widehat{\mathsf{z}}$.

Problem 9

In Figure 1.10, show that the angle $\varphi(\theta)$ defined from the conservation law (1.44) is expressed as

$$\varphi(\theta) \;=\; \arcsin\left[\;\frac{1 \;+\; \mathsf{e}\,\cos 2\theta}{\sqrt{1+\mathsf{e}^2+2\,\mathsf{e}\,\cos 2\theta}}\;\right],$$

so that $\varphi = \frac{\pi}{2}$ at $\theta = 0$ and $\frac{\pi}{2}$, as expected for an ellipse.

Problem 10

Find the light-path trajectory $r(\theta)$ for a spherically-symmetric medium with index of refraction $n(r) = n_0\,(b/r)^2$, where b is an arbitrary constant and $n_0 = n(b)$.

Problem 11

Derive the Jacobi equation (1.52) for two-dimensional light propagation in a nonuniform medium with index of refraction $n(y)$. (*Hint*: choose $\sigma = x$) Compare your Jacobi equation with that obtained from Eq. (1.9).

Chapter 2

Lagrangian Mechanics

In this Chapter, we present four principles by which single-particle dynamics may be described. Here, each principle provides an algorithm by which dynamical equations are derived.

2.1 Maupertuis-Jacobi's Principle of Least Action

The publication of Fermat's Principle of Least Time in 1657 generated an intense controversy between Fermat and disciples of René Descartes (1596-1650) involving whether light travels slower (Fermat) or faster (Descartes) in a dense medium as compared to free space.

In 1740, Pierre Louis Moreau de Maupertuis (1698-1759) stated (without proof) that, in analogy with Fermat's Principle of Least Time for light, a particle of mass m under the influence of a force $\mathbf{F} = -\nabla U$ moves along a path which satisfies the Principle of *Least Action*: $\delta\mathcal{S} = 0$, where the action integral is defined as

$$\mathcal{S}[\mathbf{x}] \;=\; \int \mathbf{p}\cdot d\mathbf{x} \;=\; \int mv\, ds, \tag{2.1}$$

where $v = ds/dt$ denotes the magnitude of particle velocity, which can also be expressed as

$$v(s) \;=\; \sqrt{(2/m)\,[E - U(s)]}, \tag{2.2}$$

with the particle's kinetic energy $K = mv^2/2$ written in terms of its total energy E and its potential energy $U(s)$.

2.1.1 Maupertuis' principle

In 1744, Euler proved Maupertuis' Principle of Least Action $\delta \int mv\, ds = 0$ for particle motion in the (x, y)-plane as follows. For this purpose, we use the Frenet-Serret curvature

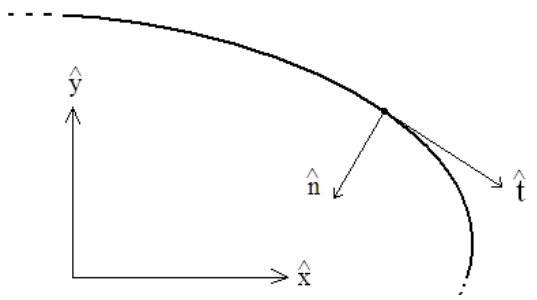

Figure 2.1: Frenet-Serret frame

formula for the path $y(x)$, where we define the tangent unit vector $\hat{\mathsf{t}}$ and the principal normal unit vector $\hat{\mathsf{n}}$ as

$$\hat{\mathsf{t}} \;=\; \frac{d\mathbf{x}}{ds} \;=\; \frac{\hat{\mathsf{x}} \,+\, y'\,\hat{\mathsf{y}}}{\sqrt{1+(y')^2}} \quad \text{and} \quad \hat{\mathsf{n}} \;=\; \frac{y'\,\hat{\mathsf{x}} \,-\, \hat{\mathsf{y}}}{\sqrt{1+(y')^2}} \;\equiv\; (-\hat{\mathsf{z}}) \times \hat{\mathsf{t}}, \tag{2.3}$$

where $y' = dy/dx$ and $ds = dx\,\sqrt{1+(y')^2}$. The Frenet-Serret formula for the curvature of a two-dimensional curve (see Appendix A) is

$$\frac{d\hat{\mathsf{t}}}{ds} \;=\; \frac{|y''|\,\hat{\mathsf{n}}}{[1+(y')^2]^{3/2}} \;=\; \kappa\,\hat{\mathsf{n}},$$

where the instantaneous radius of curvature ρ is defined as $\rho = \kappa^{-1}$ (see Figure 2.1). First, by using Newton's Second Law of Motion and the Energy conservation law, we find the relation

$$\mathbf{F} \;=\; mv\left(\frac{dv}{ds}\,\hat{\mathsf{t}} \,+\, v\,\frac{d\hat{\mathsf{t}}}{ds}\right) \;=\; \hat{\mathsf{t}}\left(\hat{\mathsf{t}}\cdot\nabla K\right) \,+\, mv^2\,\kappa\,\hat{\mathsf{n}} \;=\; \nabla K \tag{2.4}$$

between the unit vectors $\hat{\mathsf{t}}$ and $\hat{\mathsf{n}}$ associated with the path, the Frenet-Serret curvature κ, and the kinetic energy $K = \frac{1}{2}\,mv^2(x,y)$ of the particle. Note that Eq. (2.4) can be re-written as

$$\frac{d\hat{\mathsf{t}}}{ds} \;=\; \hat{\mathsf{t}}\times\left(\nabla \ln v \times \hat{\mathsf{t}}\right), \tag{2.5}$$

which hightlights a deep connection with Eq. (1.42) derived from Fermat's Principle of Least Time, where the index of refraction n is now replaced by the speed $v = \sqrt{(2/m)[E-U(s)]}$. Lastly, we point out that the type of dissipationless forces considered in Eq. (2.4) involves *active* forces (defined as forces that do work), as opposed to *passive* forces (defined as forces that do no work, such as constraint forces).

Next, the action integral (2.1) is expressed as

$$S \;=\; \int m\,v(x,y)\,\sqrt{1+(y')^2}\,dx \;=\; \int F(y,y';x)\,dx, \tag{2.6}$$

so that the Euler's First Equation (1.5) corresponding to Maupertuis' action integral (2.6), with

$$\frac{\partial F}{\partial y'} \;=\; \frac{mv\,y'}{\sqrt{1+(y')^2}} \quad \text{and} \quad \frac{\partial F}{\partial y} \;=\; m\,\sqrt{1+(y')^2}\,\frac{\partial v}{\partial y},$$

yields the Maupertuis-Euler equation

$$\frac{m\,v\,y''}{[1+(y')^2]^{3/2}} \;=\; \frac{m}{\sqrt{1+(y')^2}}\,\frac{\partial v}{\partial y} \;-\; \frac{m\,y'}{\sqrt{1+(y')^2}}\,\frac{\partial v}{\partial x} \;\equiv\; m\,\hat{\mathsf{n}}\cdot\nabla v, \tag{2.7}$$

which can also be expressed as $mv\,\kappa \,=\, m\,\hat{\mathsf{n}}\cdot\nabla v$. Using the relation $\mathbf{F} \,=\, \nabla K$ and the Frenet-Serret formulas (2.3), the Maupertuis-Euler equation (2.7) becomes

$$mv^2\,\kappa \;=\; \mathbf{F}\cdot\hat{\mathsf{n}},$$

from which we recover Newton's Second Law (2.4).

2.1.2 Jacobi's principle

Jacobi emphasized the connection between Fermat's Principle of Least Time (1.30) and Maupertuis' Principle of Least Action (2.1) by introducing a different form of the Principle of Least Action $\delta\mathcal{S} = 0$, where Jacobi's action integral is

$$\mathcal{S}[\mathbf{x}] \;=\; \int\,\sqrt{2m\,(E-U)}\,ds \;=\; 2\int K\,dt, \tag{2.8}$$

where particle momentum is written as $p = \sqrt{2m\,(E-U)}$. To obtain the second expression of Jacobi's action integral (2.8), Jacobi made use of the fact that, by introducing a path parameter τ such that $v = ds/dt = s'/t'$ (where a prime, here, denotes a τ-derivative), we find

$$K \;=\; \frac{m\,(s')^2}{2\,(t')^2} \;=\; E \;-\; U,$$

so that $2\,K\,t' = s'\,p$, and the second form of Jacobi's action integral results. Next, Jacobi used the Principle of Least Action (2.8) to establish the geometric foundations of particle mechanics. Here, the Euler-Jacobi equation resulting from Jacobi's Principle of Least Action is expressed as

$$\frac{d}{ds}\left(\sqrt{E-U}\,\frac{d\mathbf{x}}{ds}\right) \;=\; \nabla\sqrt{E-U}\,,$$

which is identical in form to the light-curvature equation (1.42), with the index of refraction n substituted with $\sqrt{E-U}$.

Note that the connection between Fermat's Principle of Least Time and Maupertuis-Jacobi's Principle of Least Action involves the relation $n = \gamma\,|\mathbf{p}|$, where γ is a constant.

This connection was later used by Prince Louis Victor Pierre Raymond de Broglie (1892-1987) to establish the relation $|\mathbf{p}| = \hbar|\mathbf{k}| = n\,(\hbar\omega/c)$ between the momentum of a particle and its wavenumber $|\mathbf{k}| = 2\pi/\lambda = n\,\omega/c$. Using de Broglie's relation $\mathbf{p} = \hbar\,\mathbf{k}$ between the particle momentum $\mathbf{p}$ and the wave vector $\mathbf{k}$, we note that

$$\frac{|\mathbf{p}|^2}{2m} \;=\; \frac{\hbar^2|\mathbf{k}|^2}{2m} \;\equiv\; \frac{\hbar^2}{2m}\,|\nabla\Theta|^2 \;=\; E \;-\; U, \tag{2.9}$$

where Θ is the dimensionless (eikonal) phase. Letting $\Theta = \ln\psi$, so that $\nabla\Theta = \nabla\ln\psi$, Eq. (2.9) becomes

$$\frac{\hbar^2}{2m}\,|\nabla\psi|^2 \;=\; (E \;-\; U)\;\psi^2.$$

Lastly, by taking its variation

$$\frac{\hbar^2}{m}\,\nabla\psi\cdot\nabla\delta\psi \;-\; \delta\psi\,(E \;-\; U)\;\psi \;=\; 0,$$

and integrating over space (upon integration by parts), we obtain

$$0 \;=\; \int_V \delta\psi\;\left[\;(E \;-\; U)\;\psi \;+\; \frac{\hbar^2}{2m}\,\nabla^2\psi\;\right]\,d^3x,$$

which yields (for arbitrary variations $\delta\psi$) the time-independent Schrödinger equation

$$-\,\frac{\hbar^2}{2m}\,\nabla^2\psi \;+\; U\,\psi \;=\; E\,\psi.$$

Further historical comments concerning the derivation of Schrödinger's equation can be found in Yougrau and Mandelstam's (*Variational Principles in Dynamics and Quantum Theory*, 1968).

2.2 D'Alembert's Principle

So far, we have studied the Maupertuis-Jacobi principles (2.1) and (2.8), which make use of the length variable s as the orbit parameter to describe particle motion. We now turn our attention to two principles that will provide a clear path toward the ultimate variational principle called Hamilton's Principle, from which equations of motion are derived in terms of generalized spatial coordinates.

First, within the context of Newtonian mechanics, we distinguish between two classes of forces, depending on whether a force is able to do work or not. In the first class, an *active* force $\mathbf{F}_w$ is involved in performing infinitesimal work $dW = \mathbf{F}_w\cdot d\mathbf{x}$ evaluated along the infinitesimal displacement $d\mathbf{x}$; the class of active forces includes conservative (e.g., gravity) and nonconservative (e.g., friction) forces. In the second class, a *passive* force (labeled $\mathbf{F}_0$) is defined as a force not involved in performing work, which includes constraint forces such as normal and tension forces. Here, the infinitesimal work performed by a passive force is $\mathbf{F}_0\cdot d\mathbf{x} = 0$ because the infinitesimal displacement $d\mathbf{x}$ is required to satisfy the constraints.

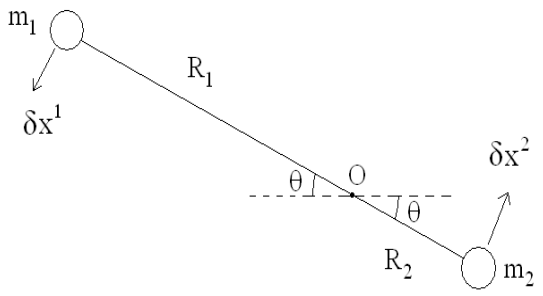

Figure 2.2: Static equilibrium of a lever

2.2.1 Principle of Virtual Work

The Principle of Virtual Work is one of the oldest principle in Physics that may find its origin in the work of Aristotle (384-322 B.C.) on the static equilibrium of levers. The Principle of Virtual Work was finally written in its current form in 1717 by Jean Bernoulli (1667-1748) and states that a system composed of N particles is in static equilibrium if the virtual work

$$\delta W \;=\; \sum_{i=1}^{N} \mathbf{F}_i \cdot \delta \mathbf{x}^i \;=\; 0 \tag{2.10}$$

for all virtual displacements $(\delta \mathbf{x}^1,\; ..., \delta \mathbf{x}^N)$ that satisfy physical constraints.

As an application of the Principle of Virtual Work (2.10), we consider the static equilibrium of a lever (see Figure 2.2) composed of two masses m_1 and m_2 placed on a massless rod at distances R_1 and R_2, respectively, from the fulcrum point O. Here, the only active forces acting on the masses are due to gravity: $\mathbf{F}_i = -\, m_i\, g\, \hat{\mathsf{y}}$, and the position vectors of m_1 and m_2 are

$$\mathbf{r}_1 \;=\; R_1\, (-\,\cos\theta\, \hat{\mathsf{x}} \;+\; \sin\theta\, \hat{\mathsf{y}}) \quad \text{and} \quad \mathbf{r}_2 \;=\; R_2\, (\cos\theta\, \hat{\mathsf{x}} \;-\; \sin\theta\, \hat{\mathsf{y}})\,,$$

respectively (see Fig. 2.2). By using the virtual displacements $\delta \mathbf{x}^i = \epsilon \hat{\mathsf{z}} \times \mathbf{r}_i$ (where ϵ is an infinitesimal angular displacement and the axis of rotation is directed along the z-axis), the Principle of Virtual Work (2.10) yields the following condition for static equilibrium:

$$0 \;=\; \epsilon \cos\theta\, (m_1 g\, R_1 \;-\; m_2 g\, R_2) \quad \rightarrow \quad m_1\, R_1 \;=\; m_2\, R_2.$$

Note that, although the static equilibrium of the lever is based on the concept of *torque* (moment of force) equilibrium, the Principle of Virtual Work shows that all static equilibria are encompassed by the Principle.

2.2.2 Lagrange's Equations from D'Alembert's Principle

It was Jean Le Rond d'Alembert (1717-1783) who generalized the Principle of Virtual Work (in 1742) by including the *accelerating* force $-\,m_i\,\ddot{\mathbf{x}}^i$ in the Principle of Virtual Work (2.10):

$$\sum_{i=1}^{N}\,\left(\mathbf{F}_i\;-\;m_i\,\frac{d^2\mathbf{x}^i}{dt^2}\right)\cdot\delta\mathbf{x}^i\;=\;0 \tag{2.11}$$

so that the equations of dynamics could be obtained from Eq. (2.11). Hence, d'Alembert's Principle, in effect, states that the work done by all active forces acting in a system is algebraically equal to the work done by all the acceleration forces (taken to be positive).

As a simple application of d'Alembert's Principle (2.11), we return to the lever problem (see Fig. 2.2), where we now assume $m_2\,R_2 > m_1\,R_1$. Here, the particle accelerations are

$$\ddot{\mathbf{x}}^i\;=\;-\,(\dot{\theta})^2\,\mathbf{r}_i\;-\;\ddot{\theta}\,\hat{\mathbf{z}}\times\mathbf{r}_i,$$

so that d'Alembert's Principle (2.11) yields (with $\delta\mathbf{x}^i=\epsilon\,\hat{\mathbf{z}}\times\mathbf{r}_i$)

$$0\;=\;\epsilon\Big[\;(m_1 g\,R_1\;-\;m_2 g\,R_2)\;\cos\theta\;+\;\left(m_1\,R_1^2\;+\;m_2\,R_2^2\right)\ddot{\theta}\;\Big].$$

Hence, according to d'Alembert's Principle, the angular acceleration $\ddot{\theta}$ of the unbalanced lever is

$$\ddot{\theta}\;=\;\frac{g\,\cos\theta}{I}\;(m_2\,R_2\;-\;m_1\,R_1)\,,$$

where $I=m_1R_1^2+m_2R_2^2$ denotes the moment of inertia of the lever as it rotates about the fulcrum point O. Thus, we see that rotational dynamics associated with unbalanced torques can be described in terms of d'Alembert's Principle.

The most historically significant application of d'Alembert's Principle (2.11), however, came from Lagrange who transformed it as follows. Consider, for simplicity, the following infinitesimal-work identity

$$0\;=\;\left(\mathbf{F}\;-\;m\,\frac{d^2\mathbf{x}}{dt^2}\right)\cdot\delta\mathbf{x}\;=\;\delta W\;-\;\frac{d}{dt}\left(m\,\frac{d\mathbf{x}}{dt}\cdot\delta\mathbf{x}\right)\;+\;m\,\frac{d\mathbf{x}}{dt}\cdot\frac{d\,\delta\mathbf{x}}{dt}, \tag{2.12}$$

where $\mathbf{F}$ denotes an active force applied to a particle of mass m so that $\delta W=\mathbf{F}\cdot\delta\mathbf{x}$ denotes the virtual work calculated along the virtual displacement $\delta\mathbf{x}$. We note that if the position vector $\mathbf{x}(q_1,...,q_k;t)$ is a time-dependent function of k *generalized* coordinates, then we find

$$\delta\mathbf{x}\;=\;\sum_{i=1}^{k}\,\frac{\partial\mathbf{x}}{\partial q_i}\,\delta q_i,$$

and

$$\mathbf{v}\;=\;\frac{d\mathbf{x}}{dt}\;=\;\frac{\partial\mathbf{x}}{\partial t}\;+\;\sum_{i=1}^{k}\,\frac{\partial\mathbf{x}}{\partial q_i}\,\dot{q}_i.$$

Next, we introduce the variation of the kinetic energy $K = mv^2/2$:

$$\delta K \;=\; m\,\frac{d\mathbf{x}}{dt}\cdot\frac{d\,\delta\mathbf{x}}{dt} \;=\; \sum_i\,\delta q_i\,\frac{\partial K}{\partial q_i},$$

since the virtual variation operator δ (introduced by Lagrange) commutes with the time derivative d/dt, and we introduce the generalized force

$$Q^i \;\equiv\; \mathbf{F}\cdot\frac{\partial\mathbf{x}}{\partial q_i},$$

so that $\delta W = \sum_i\,Q^i\,\delta q_i$. We shall also use the identity

$$m\,\frac{d^2\mathbf{x}}{dt^2}\cdot\frac{\partial\mathbf{x}}{\partial q_i} \;=\; \frac{d}{dt}\left(m\mathbf{v}\cdot\frac{\partial\mathbf{x}}{\partial q_i}\right) \;-\; m\mathbf{v}\cdot\frac{d}{dt}\left(\frac{\partial\mathbf{x}}{\partial q_i}\right),$$

with

$$\frac{d}{dt}\left(\frac{\partial\mathbf{x}}{\partial q_i}\right) \;\equiv\; \frac{\partial^2\mathbf{x}}{\partial t\,\partial q_i} \;+\; \dot q_j\,\frac{\partial^2\mathbf{x}}{\partial q_j\,\partial q_i} \;\equiv\; \frac{\partial\mathbf{v}}{\partial q_i},$$

and

$$\frac{\partial\mathbf{v}}{\partial\dot q_i} \;=\; \frac{\partial\mathbf{x}}{\partial q_i}.$$

Our first result derived from D'Alembert's Principle (2.12) is now expressed in terms of the generalized coordinates $(q_1, ..., q_k)$ as

$$0 \;=\; \sum_i\,\delta q_i\left[\;\frac{d}{dt}\left(\frac{\partial K}{\partial\dot q_i}\right) \;-\; \frac{\partial K}{\partial q_i} \;-\; Q^i\;\right].$$

Since this relation must hold for any variation δq_i $(i = 1, ..., k)$, we obtain Lagrange's equation

$$\frac{d}{dt}\left(\frac{\partial K}{\partial\dot q_i}\right) \;-\; \frac{\partial K}{\partial q_i} \;=\; Q^i, \tag{2.13}$$

where we note that the generalized force Q^i is associated with any active (conservative or nonconservative) force $\mathbf{F}$. Hence, for a *conservative* active force derivable from a single potential energy U (i.e., $\mathbf{F} = -\nabla U$), the ith-component of the generalized force is $Q^i = -\,\partial U/\partial q_i$, and Lagrange's equation (2.13) becomes

$$\frac{d}{dt}\left(\frac{\partial K}{\partial\dot q_i}\right) \;-\; \frac{\partial K}{\partial q_i} \;=\; -\,\frac{\partial U}{\partial q_i}. \tag{2.14}$$

We shall soon return to this important equation.

Our second result based on D'Alembert's Principle (2.12), now expressed as

$$\delta K \;+\; \delta W \;=\; \frac{d}{dt}\left(m\,\frac{d\mathbf{x}}{dt}\cdot\delta\mathbf{x}\right), \tag{2.15}$$

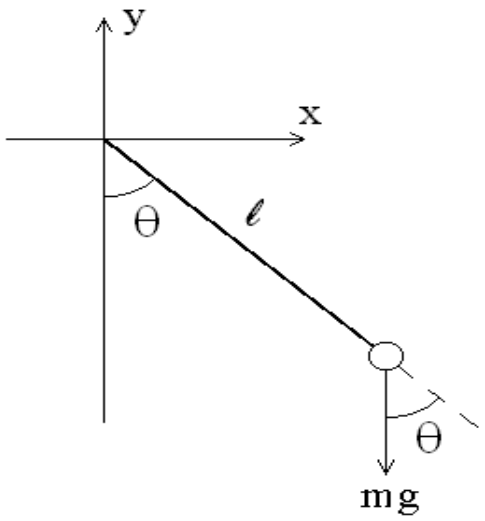

Figure 2.3: The two-dimensional pendulum problem.

is obtained as follows. For a *conservative* active force derivable from a single potential energy U (i.e., $\mathbf{F} = -\nabla U$), the virtual work is $\delta W = -\delta U$, so that time integration of Eq. (2.15) yields an important principle known as Hamilton's Principle

$$\int_{t_1}^{t_2} \Big(\delta K \; - \; \delta U \Big) \, dt \; \equiv \; \delta \int_{t_1}^{t_2} \; L \, dt \; = \; 0, \tag{2.16}$$

where $\delta \mathbf{x}$ vanishes at $t = t_1$ and t_2 and the function $L = K - U$, obtained by substracting the potential energy U from the kinetic energy K, is known as the Lagrangian function of the system.

2.3 Hamilton's Principle and Euler-Lagrange Equations

2.3.1 Constraint Forces

To illustrate Hamilton's Principle (2.16), we consider a pendulum composed of an object of mass m and a massless string of constant length ℓ in a constant gravitational field with acceleration g. We first investigate the motion of the pendulum as a dynamical problem in two dimensions with a single constraint (i.e., constant length) and later reduce this problem to a single dimension by carefully choosing a single generalized coordinate.

Using Cartesian coordinates (x, y) for the pendulum mass shown in Figure 2.3, the kinetic energy is $K = \frac{1}{2} m(\dot{x}^2 + \dot{y}^2)$ and the gravitational potential energy is $U = mg\, y$,

where the length of the pendulum string ℓ is *constrained* to be constant (i.e., $\ell^2 = x^2 + y^2$). Hence, the constrained action integral is expressed as

$$\mathcal{A}_\lambda[\mathbf{x}] \;=\; \int \Big[\; \frac{1}{2}\, m \left(\dot{x}^2 \;+\; \dot{y}^2\right) \;-\; mg\, y \;+\; \lambda \left(\ell \;-\; \sqrt{x^2 + y^2}\right) \Big]\; dt \;\equiv\; \int F(\mathbf{x}, \dot{\mathbf{x}}; \lambda)\, dt,$$

where λ represents a Lagrange multiplier used to enforce the constant-length constraint (see Sec. 1.2.1) so that, by definition, we find $\partial F / \partial \lambda = 0$ for all $\mathbf{x}$. Euler's equations for x and y, respectively, are

$$m\, \ddot{x} \;=\; -\, \lambda\, \frac{x}{\ell} \quad \text{and} \quad m\, \ddot{y} \;=\; -\, mg \;-\; \lambda\, \frac{y}{\ell},$$

so that, using the constant-length constraint, the Lagrange multiplier is defined by the relation

$$\lambda \;\equiv\; -\, \frac{m}{\ell}\, [\, g\, y \;+\; (x\, \ddot{x} \;+\; y\, \ddot{y})\,]\,. \tag{2.17}$$

Next, using the second time derivative of the constant-length constraint $\ell^2 = x^2 + y^2$, we obtain

$$x\, \ddot{x} \;+\; y\, \ddot{y} \;=\; -\, \left(\dot{x}^2 + \dot{y}^2\right),$$

so that Eq. (2.17) becomes

$$\lambda \;=\; \frac{m}{\ell}\, \left(\dot{x}^2 + \dot{y}^2\right) \;-\; mg\, \frac{y}{\ell}.$$

Hence, the physical interpretation of the Lagrange multiplier λ is given in terms of the tension force in the pendulum string, where the first term (quadratic in velocities) represents the centrifugal force while the second term represents the component of the gravitational force along the pendulum string.

It turns out that a constraint force in a dynamical system can most often be represented in terms of a constraint involving spatial coordinates. On the other hand, we shall now see that each constraint force can be eliminated from the dynamical problem by making use of new spatial coordinates that enforce the constraint. For example, in the case of the pendulum problem discussed above, we note that the constant-length constraint can be enforced by expressing the Cartesian coordinates $x = \ell\, \sin\theta$ and $y = -\, \ell\, \cos\theta$ in terms of the angle θ (see Figure 2.3).

2.3.2 Generalized Coordinates in Configuration Space

The *configuration* space of a mechanical system with constraints evolving in n-dimensional space, with spatial coordinates $\mathbf{x} = (x^1, x^2, ..., x^n)$, can sometimes be described in terms of *generalized* coordinates $\mathbf{q} = (q^1, q^2, ..., q^k)$ in a k-dimensional *configuration* space, with $k \leq n$. Each generalized coordinate is said to describe motion along a *degree of freedom* of the mechanical system.

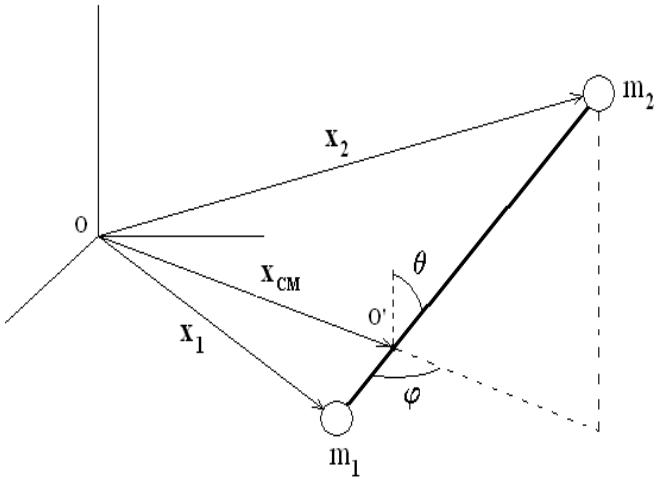

Figure 2.4: Configuration space

For example, consider a mechanical system composed of two particles (see Figure 2.4), with masses (m_1, m_2) and three-dimensional coordinate positions $(\mathbf{x}_1, \mathbf{x}_2)$, tied together with a massless rigid rod (so that the distance $|\mathbf{x}_1 - \mathbf{x}_2|$ is constant). The configuration of this two-particle system can be described in terms of the coordinates

$$\mathbf{x}_{CM} \equiv \frac{\sum_i m_i \mathbf{x}_i}{\sum_i m_i} = \frac{m_1 \mathbf{x}_1 + m_2 \mathbf{x}_2}{m_1 + m_2} \tag{2.18}$$

of the center-of-mass (CM) in the Laboratory frame (O) and the orientation of the rod in the CM frame (O') expressed in terms of the two angles (θ, φ). Hence, as a result of the existence of a single constraint $(\ell = |\mathbf{x}_1 - \mathbf{x}_2|)$, the generalized coordinates for this system are $(\mathbf{x}_{CM}; \theta, \varphi)$ and we have reduced the number of coordinates needed to describe the state of the system from six to five. Each generalized coordinate is said to describe dynamics along a *degree of freedom* of the mechanical system; for example, in the case of the two-particle system discussed above, the generalized coordinates $\mathbf{x}_{CM}$ describe the arbitrary translation of the center-of-mass while the generalized coordinates (θ, φ) describe arbitrary rotation about the center-of-mass.

Constraints are found to be of two different types refered to as *holonomic* and *non-holonomic* constraints. For example, the differential (kinematical) constraint equation $dq(\mathbf{r}) = \mathbf{B}(\mathbf{r}) \cdot d\mathbf{r}$ is said to be *holonomic* (or integrable) if the vector field $\mathbf{B}$ satisfies the integrability condition

$$0 = \nabla \times \mathbf{B}, \tag{2.19}$$

so that the function $q(\mathbf{r})$ can be explicitly constructed and, thus, the number of independent coordinates can be reduced by one. For example, consider the differential constraint

equation

$$dz \;=\; B_x(x,y)\,dx \;+\; B_y(x,y)\,dy,$$

where an infinitesimal change in the x and y coordinates produce an infinitesimal change in the z coordinate. This differential constraint equation is integrable if the components B_x and B_y satisfy the integrability condition $\partial B_x/\partial y = \partial B_y/\partial x$, which implies that there exists a function $f(x,y)$ such that $B_x = \partial f/\partial x$ and $B_y = \partial f/\partial y$. Hence, under this integrability condition, the differential constraint equation becomes $dz = df(x,y)$, which can be integrated to give $z = f(x,y)$ and, thus, the number of independent coordinates has been reduced from 3 to 2.

If the vector field $\mathbf{B}$ does not satisfy the integrability condition (2.19), however, the condition $dq(\mathbf{r}) = \mathbf{B}(\mathbf{r})\cdot d\mathbf{r}$ is said to be *non-holonomic*. An example of non-holonomic condition is the case of the rolling of a solid body on a surface. Moreover, we note that a kinematical condition is called *rheonomic* if it is time-dependent, otherwise it is called *scleronomic*.

In summary, the presence of holonomic constraints can always be treated by the introduction of generalized coordinates. The treatment of nonholonomic constraints, on the other hand, requires the addition of constraint forces on the right side of Lagrange's equation (2.13), which falls outside the scope of this introductory course.

2.3.3 Constrained Motion on a Surface

As an example of motion under an holonomic constraint, we consider the general problem associated with the motion of a particle constrained to move on a surface described by the relation $F(x,y,z) = 0$. First, since the velocity $d\mathbf{x}/dt$ of the particle along its trajectory must be perpendicular to the gradient ∇F, the displacement $d\mathbf{x}$ is required to satisfy the constraint condition $d\mathbf{x}\cdot\nabla F = 0$. Next, any point $\mathbf{x}$ on the surface $F(x,y,z) = 0$ may be parametrized by two *surface* coordinates (u,v) such that

$$\frac{\partial \mathbf{x}}{\partial u}(u,v)\cdot\nabla F \;=\; 0 \;=\; \frac{\partial \mathbf{x}}{\partial v}(u,v)\cdot\nabla F.$$

Hence, we may write

$$d\mathbf{x} \;=\; \frac{\partial \mathbf{x}}{\partial u}\,du \;+\; \frac{\partial \mathbf{x}}{\partial v}\,dv \quad\text{and}\quad \frac{\partial \mathbf{x}}{\partial u}\times\frac{\partial \mathbf{x}}{\partial v} \;=\; \mathcal{J}\,\nabla F,$$

where the function $\mathcal{J}$ depends on the surface coordinates (u,v). It is, thus, quite clear that the surface coordinates (u,v) are the generalized coordinates for this constrained motion.

For example, we consider the motion of a particle constrained to move on the surface of a cone of apex angle α (see Fig. 2.5). Here, the constraint is expressed as $F(x,y,z) = \sqrt{x^2+y^2} - z\,\tan\alpha = 0$ with $\nabla F = \widehat{\rho} - \tan\alpha\,\widehat{\mathsf{z}}$, where $\rho^2 = x^2+y^2$ and $\widehat{\rho} = (x\,\widehat{\mathsf{x}} + y\,\widehat{\mathsf{y}})/\rho$.

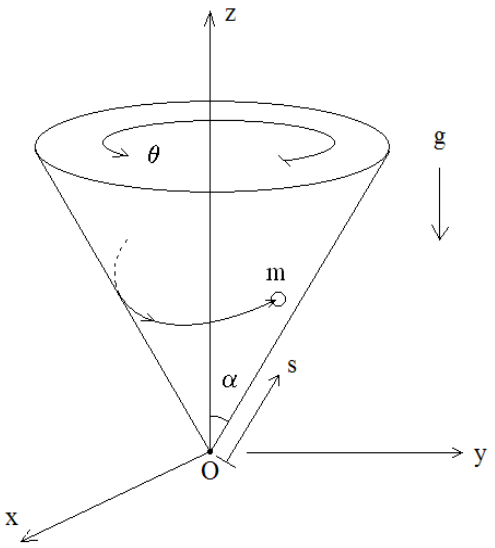

Figure 2.5: Motion on the surface of a cone

The surface coordinates can be chosen to be the polar angle θ and the function

$$s(x,y,z) \;=\; \sqrt{x^2+y^2+z^2} \;\equiv\; \sqrt{\rho^2+z^2},$$

which measures the distance from the apex of the cone (defining the origin), so that

$$\frac{\partial \mathbf{x}}{\partial \theta} \;=\; \rho\,\widehat{\theta} \;=\; \rho\,\widehat{\mathsf{z}}\times\widehat{\rho} \quad\text{and}\quad \frac{\partial \mathbf{x}}{\partial s} \;=\; \sin\alpha\;\widehat{\rho} \;+\; \cos\alpha\;\widehat{\mathsf{z}} \;=\; \widehat{s},$$

with

$$\frac{\partial \mathbf{x}}{\partial \theta}\times\frac{\partial \mathbf{x}}{\partial s} \;=\; \rho\;\cos\alpha\;\nabla F$$

and $\mathcal{J} = \rho\,\cos\alpha$. We shall return to this example in Sec. 2.5.4.

2.3.4 Euler-Lagrange Equations

Hamilton's principle (sometimes called THE Principle of Least Action) is expressed in terms of a function $L(\mathbf{q},\dot{\mathbf{q}};\,t)$ known as the *Lagrangian*, which appears in the *action* integral

$$\mathcal{S}[\mathbf{q}] \;=\; \int_{t_i}^{t_f}\; L(\mathbf{q},\dot{\mathbf{q}};\,t)\;dt, \tag{2.20}$$

where the action integral is a functional of the generalized coordinates $\mathbf{q}(t)$, providing a path from the initial point $\mathbf{q}_i = \mathbf{q}(t_i)$ to the final point $\mathbf{q}_f = \mathbf{q}(t_f)$. The stationarity of the action integral

$$0 \;=\; \delta\mathcal{S}[\mathbf{q};\delta\mathbf{q}] \;=\; \left(\frac{d}{d\epsilon}\mathcal{S}[\mathbf{q}+\epsilon\,\delta\mathbf{q}]\right)_{\epsilon=0} \;=\; \int_{t_i}^{t_f}\delta\mathbf{q}\cdot\left[\;\frac{\partial L}{\partial \mathbf{q}} \;-\; \frac{d}{dt}\left(\frac{\partial L}{\partial \dot{\mathbf{q}}}\right)\;\right]\;dt,$$

where the variation $\delta\mathbf{q}$ is assumed to vanish at the integration boundaries ($\delta\mathbf{q}_i = 0 = \delta\mathbf{q}_f$), yields the *Euler-Lagrange* equation for the generalized coordinate q^j ($j = 1, ..., k$):

$$\frac{d}{dt}\left(\frac{\partial L}{\partial \dot{q}^j}\right) \;=\; \frac{\partial L}{\partial q^j}. \tag{2.21}$$

The Lagrangian also satisfies the second Euler equation:

$$\frac{d}{dt}\left(L \;-\; \dot{\mathbf{q}}\cdot\frac{\partial L}{\partial \dot{\mathbf{q}}}\right) \;=\; \frac{\partial L}{\partial t}, \tag{2.22}$$

and thus, for time-independent Lagrangian systems ($\partial L/\partial t = 0$), we find that $L - \dot{\mathbf{q}}\cdot\partial L/\partial\dot{\mathbf{q}}$ is a conserved quantity whose interpretation will be discussed shortly.

Note that, according to d'Alembert's Principle (2.11), or Eq. (2.16), the form of the Lagrangian function $L(\mathbf{r}, \dot{\mathbf{r}}; t)$ is dictated by our requirement that Newton's Second Law $m\,\ddot{\mathbf{r}} = -\nabla U(\mathbf{r}, t)$, which describes the motion of a particle of mass m in a nonuniform (possibly time-dependent) potential $U(\mathbf{r}, t)$, be written in the Euler-Lagrange form (2.21). One easily obtains the form

$$L(\mathbf{r}, \dot{\mathbf{r}}; t) \;=\; \frac{m}{2}\,|\dot{\mathbf{r}}|^2 \;-\; U(\mathbf{r}, t), \tag{2.23}$$

for the Lagrangian of a particle of mass m, which is simply the kinetic energy of the particle **minus** its potential energy. The minus sign in Eq. (2.23) is important; not only does this form give us the correct equations of motion but, without the minus sign, energy would not be conserved. In fact, we note that Jacobi's action integral (2.8) can also be written as $A = \int[(K - U) + E]\,dt$, using the Energy conservation law $E = K + U$; hence, Energy conservation is the important connection between the Principles of Least Action of Maupertuis-Jacobi and Euler-Lagrange.

For a simple mechanical system, the Lagrangian function is obtained by computing the kinetic energy of the system and its potential energy and then construct Eq. (2.23). The construction of a Lagrangian function for a system of N particles, therefore, proceeds in four steps as follows.

• **Step I.** Define k generalized coordinates $\{q^1(t), ..., q^k(t)\}$ that represent the instantaneous *configuration* of the mechanical system of N particles at time t.

• **Step II.** For each particle, construct the position vector $\mathbf{r}_a(\mathbf{q}; t)$ in Cartesian coordinates and its associated velocity

$$\mathbf{v}_a(\mathbf{q}, \dot{\mathbf{q}}; t) \;=\; \frac{\partial \mathbf{r}_a}{\partial t} \;+\; \sum_{j=1}^{k} \dot{q}^j\,\frac{\partial \mathbf{r}_a}{\partial q^j}$$

for $a = 1, ..., N$.

• **Step III.** Construct the kinetic energy

$$K(\mathbf{q}, \dot{\mathbf{q}}; t) \;=\; \sum_a \; \frac{m_a}{2} \, |\mathbf{v}_a(\mathbf{q}, \dot{\mathbf{q}}; t)|^2$$

and the potential energy

$$U(\mathbf{q}; t) \;=\; \sum_a \; U(\mathbf{r}_a(\mathbf{q}; t), \, t)$$

for the system and combine them to obtain the Lagrangian

$$L(\mathbf{q}, \dot{\mathbf{q}}; t) \;=\; K(\mathbf{q}, \dot{\mathbf{q}}; t) \;-\; U(\mathbf{q}; t).$$

• **Step IV.** From the Lagrangian $L(\mathbf{q}, \dot{\mathbf{q}}; t)$, the Euler-Lagrange equations (2.21) are derived for each generalized coordinate q^j:

$$\sum_a \; \frac{d}{dt} \left(\frac{\partial \mathbf{r}_a}{\partial q^j} \cdot m_a \, \mathbf{v}_a \right) \;=\; \sum_a \left(m_a \, \mathbf{v}_a \cdot \frac{\partial \mathbf{v}_a}{\partial q^j} \;-\; \frac{\partial \mathbf{r}_a}{\partial q^j} \cdot \nabla_a U \right), \tag{2.24}$$

where we have used the identity $\partial \mathbf{v}_a / \partial \dot{q}^j = \partial \mathbf{r}_a / \partial q^j$.

Note that in the presence of k time-dependent constraints $\Phi^j(\mathbf{r}_1, ..., \mathbf{r}_n; t) = 0$ $(j = 1, ..., k)$ among n point particles, the Euler-Lagrange equation for the i^{th}-coordinate x^i_ℓ of the ℓ^{th}-particle is expressed as

$$\frac{d}{dt} \left(\frac{\partial L}{\partial \dot{x}^i_\ell} \right) \;-\; \frac{\partial L}{\partial x^i_\ell} \;=\; \sum_{j=1}^{k} \; \lambda_j(t) \; \frac{\partial \Phi^j}{\partial x^i_\ell},$$

where $\lambda_j(t)$ $(j = 1, ..., k)$ denote the Lagrange multipliers needed to impose the constraints.

2.3.5 Lagrangian Mechanics in Curvilinear Coordinates*

The Euler-Lagrange equation (2.24) can be framed within the context of Riemannian geometry as follows; Jacobi was the first to investigate the relation between particle dynamics and Riemannian geometry. The kinetic energy of a single particle of mass m, with generalized coordinates $\mathbf{q} = (q^1, ..., q^k)$, is expressed as

$$K \;=\; \frac{m}{2} \, |\mathbf{v}|^2 \;=\; \frac{m}{2} \, \frac{\partial \mathbf{r}}{\partial q^i} \cdot \frac{\partial \mathbf{r}}{\partial q^j} \, \dot{q}^i \, \dot{q}^j \;\equiv\; \frac{m}{2} \, g_{ij} \, \dot{q}^i \, \dot{q}^j,$$

where g_{ij} denotes the metric tensor on configuration space. When the particle moves in a potential $U(\mathbf{q})$, the Euler-Lagrange equation (2.24) becomes

$$\begin{aligned} \frac{d}{dt} \left(m \, g_{ij} \, \dot{q}^j \right) \;&=\; m \, g_{ij} \, \ddot{q}^j \;+\; \frac{m}{2} \left(\frac{\partial g_{ij}}{\partial q^k} \;+\; \frac{\partial g_{ik}}{\partial q^j} \right) \dot{q}^j \, \dot{q}^k \\ &=\; \frac{m}{2} \, \frac{\partial g_{jk}}{\partial q^i} \, \dot{q}^j \, \dot{q}^k \;-\; \frac{\partial U}{\partial q^i}, \end{aligned}$$

or

$$m\, g_{ij} \left(\frac{d^2 q^j}{dt^2} \; + \; \Gamma^j_{\;k\ell} \, \frac{dq^k}{dt} \, \frac{dq^\ell}{dt} \right) \; = \; - \, \frac{\partial U}{\partial q^i}, \tag{2.25}$$

where the Christoffel symbol (1.16) is defined as

$$\Gamma^j_{\;k\ell} \; \equiv \; \frac{g^{ij}}{2} \left(\frac{\partial g_{ik}}{\partial q^\ell} \; + \; \frac{\partial g_{i\ell}}{\partial q^k} \; - \; \frac{\partial g_{k\ell}}{\partial q^i} \right).$$

Thus, the concepts associated with Riemannian geometry that appear extensively in the theory of General Relativity have natural antecedents in classical Lagrangian mechanics.

2.4 Lagrangian Mechanics in Configuration Space

In this Section, we explore the Lagrangian formulation of several mechanical systems listed here in order of increasing complexity. As we proceed with our examples, we should realize how the Lagrangian formulation maintains its relative simplicity compared to the application of the more familiar Newton's method (Isaac Newton, 1643-1727) associated with the vectorial composition of forces. Here, all constraint forces are eliminated in terms of generalized coordinates and all active conservative forces are expressed in terms of suitable potential energies.

2.4.1 Example I: Pendulum

As a first example, we reconsider the pendulum (see Sec. 2.3.1) composed of an object of mass m and a massless string of constant length ℓ in a constant gravitational field with acceleration g. Although the motion of the pendulum is two-dimensional, a single generalized coordinate is needed to describe the configuration of the pendulum: the angle θ measured from the negative y-axis (see Figure 2.6). Here, the position of the object is given as

$$x(\theta) \; = \; \ell \, \sin\theta \quad \text{and} \quad y(\theta) \; = \; - \, \ell \, \cos\theta,$$

with associated velocity components

$$\dot{x}(\theta, \dot{\theta}) \; = \; \ell \, \dot{\theta} \, \cos\theta \quad \text{and} \quad \dot{y}(\theta, \dot{\theta}) \; = \; \ell \, \dot{\theta} \, \sin\theta.$$

Hence, the kinetic energy of the pendulum is

$$K \; = \; \frac{m}{2} \left(\dot{x}^2 \; + \; \dot{y}^2 \right) \; = \; \frac{m}{2} \, \ell^2 \dot{\theta}^2,$$

and choosing the zero potential energy point when $\theta = 0$ (see Figure 2.6), the gravitational potential energy is

$$U \; = \; mg\ell \, (1 - \cos\theta).$$

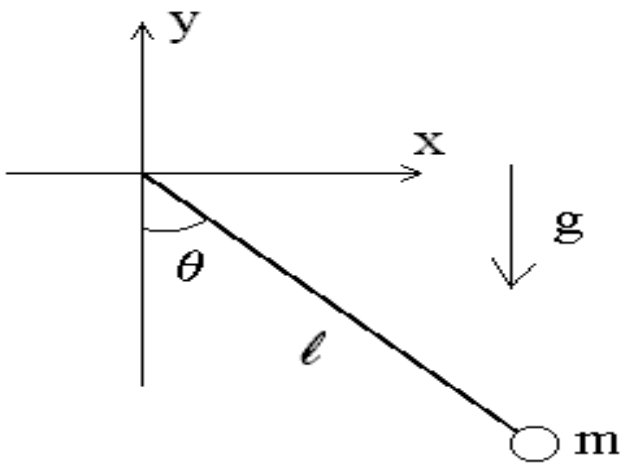

Figure 2.6: Generalized coordinates for the pendulum problem

The Lagrangian $L = K - U$ is, therefore, written as

$$L(\theta, \dot{\theta}) \;=\; \frac{m}{2}\,\ell^2\dot{\theta}^2 \;-\; mg\ell\,(1-\cos\theta),$$

and the Euler-Lagrange equation for θ is

$$\begin{aligned} \frac{\partial L}{\partial \dot{\theta}} \;=\; m\ell^2\,\dot{\theta} \;\;\rightarrow\;\; \frac{d}{dt}\left(\frac{\partial L}{\partial \dot{\theta}}\right) &= m\ell^2\,\ddot{\theta} \\ \frac{\partial L}{\partial \theta} &= -\,mg\ell\,\sin\theta \end{aligned}$$

or

$$\ddot{\theta} \;+\; \frac{g}{\ell}\,\sin\theta \;=\; 0. \tag{2.26}$$

The pendulum problem (2.26) is solved in the next Chapter through the use of the Energy method (a simplified version of the Hamiltonian method). Note that, whereas the tension in the pendulum string must be considered explicitly in the Newtonian method, the string tension is replaced by the constraint $\ell =$ constant in the Lagrangian method.

2.4.2 Example II: Bead on a Rotating Hoop

As a second example, we consider a bead of mass m sliding freely on a hoop of radius R rotating with angular velocity Ω in a constant gravitational field with acceleration g. Here, since the bead of the rotating hoop moves on the surface of a sphere of radius R, we use the generalized coordinates given by the two angles θ (measured from the negative z-axis)

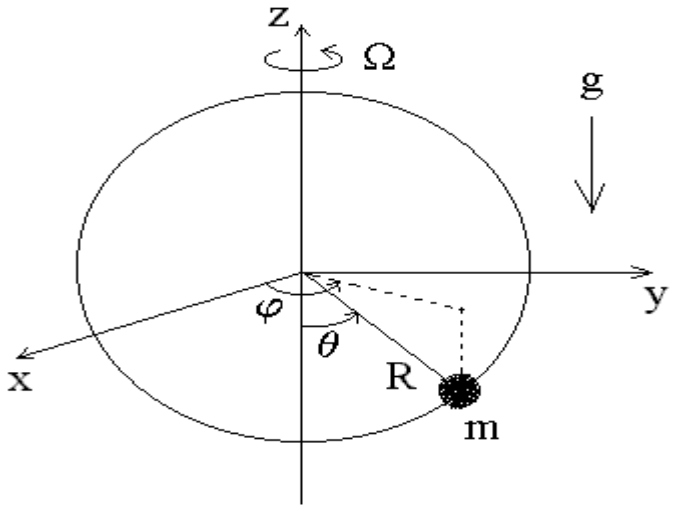

Figure 2.7: Generalized coordinates for the bead-on-a-rotating-hoop problem

and φ (measured from the positive x-axis), where $\dot{\varphi} = \Omega$. The position of the bead is given in terms of Cartesian coordinates as

$$\begin{aligned} x(\theta,t) &= R\,\sin\theta\,\cos(\varphi_0+\Omega t), \\ y(\theta,t) &= R\,\sin\theta\,\sin(\varphi_0+\Omega t), \\ z(\theta,t) &= -\,R\,\cos\theta, \end{aligned}$$

where $\varphi(t) = \varphi_0 + \Omega\,t$, and its associated Cartesian velocity components are

$$\begin{aligned} \dot{x}(\theta,\dot{\theta};t) &= R\left(\dot{\theta}\,\cos\theta\,\cos\varphi\,-\,\Omega\,\sin\theta\,\sin\varphi\right), \\ \dot{y}(\theta,\dot{\theta};t) &= R\left(\dot{\theta}\,\cos\theta\,\sin\varphi\,+\,\Omega\,\sin\theta\,\cos\varphi\right), \\ \dot{z}(\theta,\dot{\theta};t) &= R\,\dot{\theta}\,\sin\theta, \end{aligned}$$

so that the kinetic energy of the bead is

$$K(\theta,\dot{\theta}) \;=\; \frac{m}{2}\,|\mathbf{v}|^2 \;=\; \frac{m\,R^2}{2}\left(\dot{\theta}^2\;+\;\Omega^2\;\sin^2\theta\right).$$

The gravitational potential energy is

$$U(\theta) \;=\; mgR\,(1\;-\;\cos\theta),$$

where the zero-potential energy point is chosen at $\theta = 0$ (see Figure 2.7).

The Lagrangian $L = K - U$ is, therefore, written as

$$L(\theta,\dot{\theta}) \;=\; \frac{m\,R^2}{2}\left(\dot{\theta}^2\;+\;\Omega^2\;\sin^2\theta\right)\;-\;mgR\,(1-\cos\theta),$$

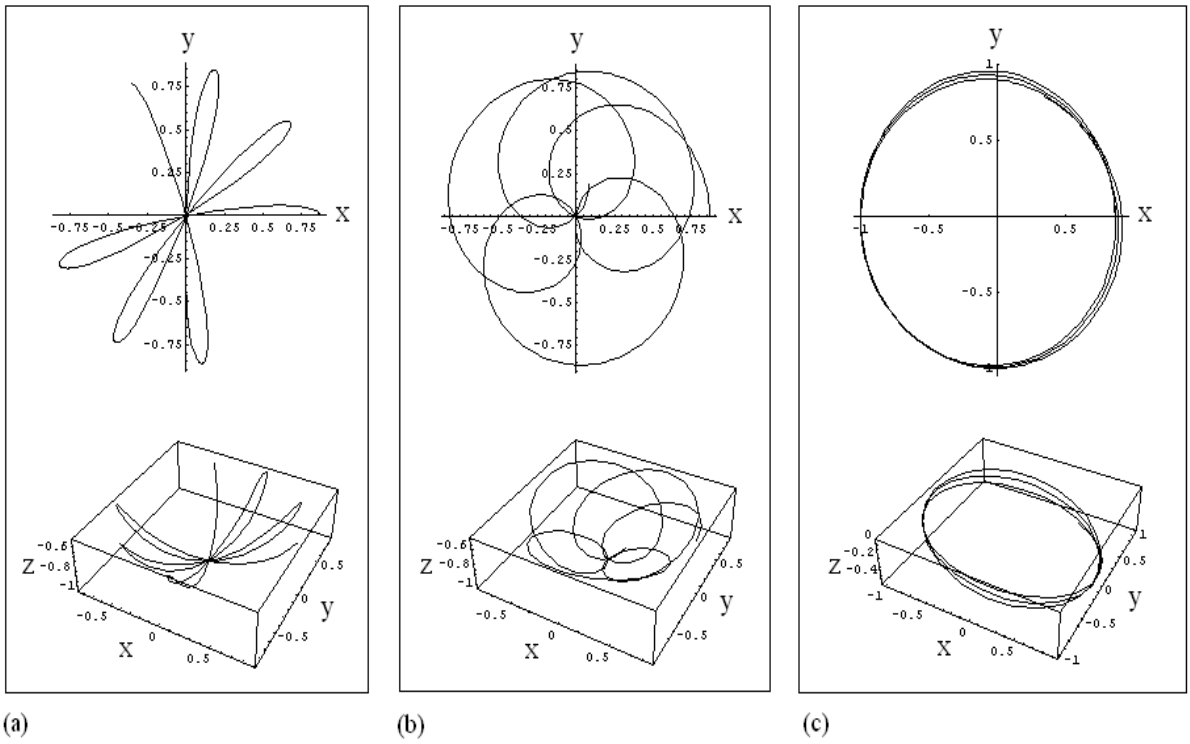

Figure 2.8: Numerical solutions for bead-on-a-rotating-hoop problem for $\theta_0 = \pi/3$ and $\dot{\theta}_0 = 0$ (with $\varphi_0 = 0$ and $R = 1$): (a) $\Omega^2 < g/R$; (b) $\Omega^2 = g/R$; and (c) $\Omega^2 > g/R$.

and the Euler-Lagrange equation for θ is

$$\begin{aligned} \frac{\partial L}{\partial \dot{\theta}} \;=\; mR^2\,\dot{\theta} \;\;\rightarrow\;\; \frac{d}{dt}\left(\frac{\partial L}{\partial \dot{\theta}}\right) &= mR^2\,\ddot{\theta} \\ \frac{\partial L}{\partial \theta} &= -\,mgR\,\sin\theta \\ &\quad +\; mR^2\Omega^2\,\cos\theta\,\sin\theta \end{aligned}$$

or

$$\ddot{\theta} \;+\; \sin\theta\left(\frac{g}{R} \;-\; \Omega^2\,\cos\theta\right) \;=\; 0$$

Note that the support (constraint) force provided by the hoop (necessary in the Newtonian method) is now replaced by the constraint $R =$ constant in the Lagrangian method. Furthermore, although the motion intrinsically takes place on the surface of a sphere of radius R, the azimuthal motion is completely determined by the equation $\varphi(t) = \varphi_0 + \Omega\,t$ and, thus, the motion of the bead takes place in one dimension.

Lastly, we note that this equation displays *bifurcation* behavior which is investigated in Chapter 8. For $\Omega^2 < g/R$, the equilibrium point $\theta = 0$ is stable while, for $\Omega^2 > g/R$, the equilibrium point $\theta = 0$ is now unstable and the new equilibrium point $\theta = \arccos(g/\Omega^2 R)$ is stable (see Figure 2.8).

2.4.3 Example III: Rotating Pendulum

As a third example, we consider a pendulum of mass m and length b attached to the edge of a disk of radius a rotating at angular velocity ω in a constant gravitational field with acceleration g. Placing the origin at the center of the disk, the coordinates of the pendulum mass are

$$\begin{aligned} x &= -\,a\,\sin\omega t \;+\; b\,\cos\theta \\ y &= a\,\cos\omega t \;+\; b\,\sin\theta \end{aligned}$$

so that the velocity components are

$$\begin{aligned} \dot{x} &= -\,a\omega\,\cos\omega t \;-\; b\,\dot{\theta}\,\sin\theta \\ \dot{y} &= -\,a\omega\,\sin\omega t \;+\; b\,\dot{\theta}\,\cos\theta \end{aligned}$$

and the squared velocity is

$$v^2 \;=\; a^2\omega^2 \;+\; b^2\dot{\theta}^2 \;+\; 2\,ab\,\omega\,\dot{\theta}\;\sin(\theta - \omega t).$$

Setting the zero potential energy at $x = 0$, the gravitational potential energy is

$$U \;=\; -\,mg\,x \;=\; mga\,\sin\omega t \;-\; mgb\,\cos\theta.$$

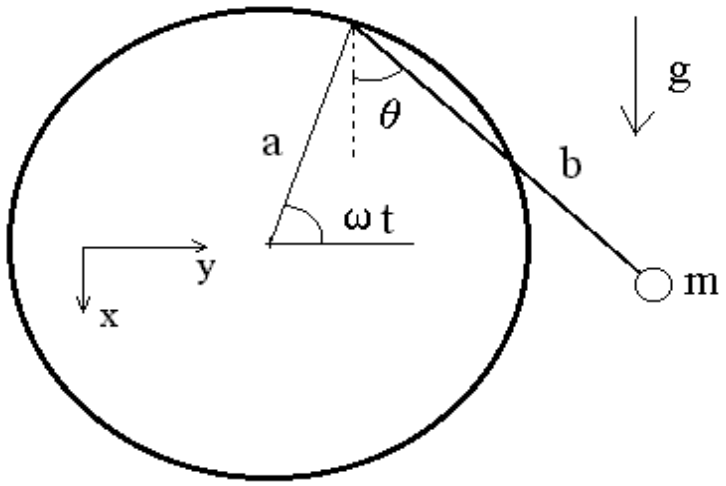

Figure 2.9: Generalized coordinates for the rotating-pendulum problem

The Lagrangian $L = K - U$ is, therefore, written as

$$\begin{aligned} L(\theta, \dot{\theta}; t) &= \frac{m}{2}\left[\, a^2\omega^2 \,+\, b^2\dot{\theta}^2 \,+\, 2\,ab\,\omega\,\dot{\theta}\,\sin(\theta - \omega t)\,\right] \\ &\quad -\, mga\,\sin\omega t \,+\, mgb\,\cos\theta, \end{aligned} \tag{2.27}$$

and the Euler-Lagrange equation for θ is

$$\begin{aligned} \frac{\partial L}{\partial \dot{\theta}} &= mb^2\,\dot{\theta} + m\,ab\,\omega\,\sin(\theta - \omega t) \;\;\rightarrow \\ \frac{d}{dt}\left(\frac{\partial L}{\partial \dot{\theta}}\right) &= mb^2\,\ddot{\theta} \,+\, m\,ab\,\omega\,(\dot{\theta} - \omega)\,\cos(\theta - \omega t) \end{aligned}$$

and

$$\frac{\partial L}{\partial \theta} = m\,ab\,\omega\,\dot{\theta}\,\cos(\theta - \omega t) \,-\, mg\,b\,\sin\theta$$

or

$$\ddot{\theta} \,+\, \frac{g}{b}\,\sin\theta \,-\, \frac{a}{b}\,\omega^2\,\cos(\theta - \omega t) \,=\, 0$$

We recover the standard equation of motion for the pendulum when a or ω vanish.

Note that the terms

$$\frac{m}{2}\,a^2\,\omega^2 \,-\, mga\,\sin\omega t$$

in the Lagrangian (2.27) play no role in determining the dynamics of the system. In fact, as can easily be shown, a Lagrangian L is always defined up to an exact time derivative,

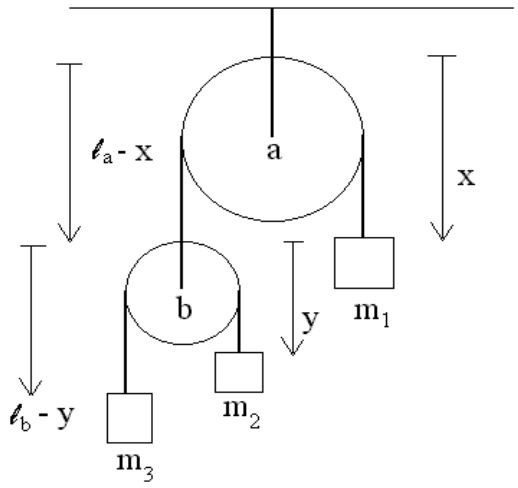

Figure 2.10: Generalized coordinates for the compound-Atwood problem

i.e., the Lagrangians L and $L' = L - df/dt$, where $f(\mathbf{q}, t)$ is an arbitrary function, lead to the same Euler-Lagrange equations (see Section 2.5). In the present case,

$$f(t) \;=\; [(m/2)\, a^2\omega^2]\, t + (mga/\omega)\;\cos\omega t$$

and thus this term can be omitted from the Lagrangian (2.27) without changing the equations of motion.

2.4.4 Example IV: Compound Atwood Machine

As a fourth (and penultimate) example, we consider a compound Atwood machine composed three masses (labeled m_1, m_2, and m_3) attached by two massless ropes through two massless pulleys in a constant gravitational field with acceleration g.

The two generalized coordinates for this system (see Figure 2.10) are the distance x of mass m_1 from the top of the first pulley and the distance y of mass m_2 from the top of the second pulley; here, the lengths ℓ_a and ℓ_b are constants. The coordinates and velocities of the three masses m_1, m_2, and m_3 are

$$\begin{aligned} x_1 \;&=\; x \;\;\rightarrow\;\; v_1 \;=\; \dot{x}, \\ x_2 \;=\; \ell_a \;-\; x \;+\; y \;\;&\rightarrow\;\; v_2 \;=\; \dot{y} - \dot{x}, \\ x_3 \;=\; \ell_a \;-\; x \;+\; \ell_b \;-\; y \;\;&\rightarrow\;\; v_3 \;=\; -\,\dot{x} - \dot{y}, \end{aligned}$$

respectively, so that the total kinetic energy is

$$K \;=\; \frac{m_1}{2}\,\dot{x}^2 \;+\; \frac{m_2}{2}\;(\dot{y} - \dot{x})^2 \;+\; \frac{m_3}{2}\;(\dot{x} + \dot{y})^2\,.$$

Placing the zero potential energy at the top of the first pulley, the total gravitational potential energy, on the other hand, can be written as

$$U \;=\; -\,g\,x\;\left(m_1 - m_2 - m_3\right) \;-\; g\,y\;\left(m_2 - m_3\right),$$

where constant terms were omitted. The Lagrangian $L = K - U$ is, therefore, written as

$$\begin{aligned} L(x,\dot{x},\,y,\dot{y}) \;&=\; \frac{m_1}{2}\,\dot{x}^2 \;+\; \frac{m_2}{2}\,\left(\dot{x}-\dot{y}\right)^2 \;+\; \frac{m_3}{2}\,\left(\dot{x}+\dot{y}\right)^2 \\ &\quad +\; g\,x\;\left(m_1 - m_2 - m_3\right) \;+\; g\,y\;\left(m_2 - m_3\right). \end{aligned}$$

The Euler-Lagrange equation for x is

$$\begin{aligned} \frac{\partial L}{\partial \dot{x}} \;&=\; \left(m_1 + m_2 + m_3\right)\dot{x} + \left(m_3 - m_2\right)\dot{y} \;\;\rightarrow \\ \frac{d}{dt}\left(\frac{\partial L}{\partial \dot{x}}\right) \;&=\; \left(m_1 + m_2 + m_3\right)\ddot{x} + \left(m_3 - m_2\right)\ddot{y} \\ \frac{\partial L}{\partial x} \;&=\; g\;\left(m_1 - m_2 - m_3\right) \end{aligned}$$

while the Euler-Lagrange equation for y is

$$\begin{aligned} \frac{\partial L}{\partial \dot{y}} \;&=\; \left(m_3 - m_2\right)\dot{x} \;+\; \left(m_2 + m_3\right)\dot{y} \;\;\rightarrow \\ \frac{d}{dt}\left(\frac{\partial L}{\partial \dot{y}}\right) \;&=\; \left(m_3 - m_2\right)\ddot{x} \;+\; \left(m_2 + m_3\right)\ddot{y} \\ \frac{\partial L}{\partial y} \;&=\; g\;\left(m_2 - m_3\right). \end{aligned}$$

We combine these two Euler-Lagrange equations

$$\left(m_1 + m_2 + m_3\right)\ddot{x} + \left(m_3 - m_2\right)\ddot{y} \;=\; g\;\left(m_1 - m_2 - m_3\right), \tag{2.28}$$

$$\left(m_3 - m_2\right)\ddot{x} \;+\; \left(m_2 + m_3\right)\ddot{y} \;=\; g\;\left(m_2 - m_3\right), \tag{2.29}$$

to describe the dynamical evolution of the Compound Atwood Machine. This set of equations can, in fact, be solved explicitly as

$$\ddot{x} \;=\; g\;\left(\frac{m_1\,m_+ \;-\; \left(m_+^2 - m_-^2\right)}{m_1\,m_+ \;+\; \left(m_+^2 - m_-^2\right)}\right) \quad \text{and} \quad \ddot{y} \;=\; g\;\left(\frac{2\,m_1\,m_-}{m_1\,m_+ \;+\; \left(m_+^2 - m_-^2\right)}\right),$$

where $m_\pm = m_2 \pm m_3$. Note also that, by using the energy conservation law $E = K + U$ it can be shown that the position z of the center of mass of the mechanical system (as measured from the top of the first pulley) satisfies the relation

$$Mg\,(z - z_0) \;=\; \frac{m_1}{2}\,\dot{x}^2 \;+\; \frac{m_2}{2}\,\left(\dot{y}-\dot{x}\right)^2 \;+\; \frac{m_3}{2}\,\left(\dot{x}+\dot{y}\right)^2 \;>\; 0, \tag{2.30}$$

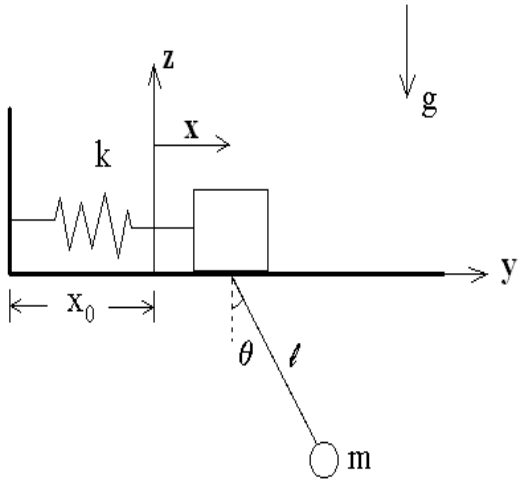

Figure 2.11: Generalized coordinates for the oscillating-pendulum problem

where $M = (m_1 + m_2 + m_3)$ denotes the total mass of the system and we have assumed that the system starts from rest (with its center of mass located at z_0). This important relation tells us that, as the masses start move ($\dot{x} \neq 0$ and $\dot{y} \neq 0$), the center of mass must fall: $z > z_0$.

Before proceeding to our next (and last) example, we introduce a convenient technique (henceforth known as *Freezing Degrees of Freedom*) for checking on the physical accuracy of any set of coupled Euler-Lagrange equations. Hence, for the Euler-Lagrange equation (2.28), we may freeze the degree of freedom associated with the y-coordinate (i.e., we set $\dot{y} = 0 = \ddot{y}$ or $m_- = 0$) to obtain $\ddot{x} = g\ (m_1 - m_+)/(m_1 + m_+)$, in agreement with the analysis of a *simple* Atwood machine composed of a mass m_1 on one side and a mass $m_+ = m_2 + m_3$ on the other side. Likewise, for the Euler-Lagrange equation (2.29), we may freeze the degree of freedom associated with the x-coordinate (i.e., we set $\dot{x} = 0 = \ddot{x}$ or $m_1 m_+ = m_+^2 - m_-^2$) to obtain $\ddot{y} = g\,(m_-/m_+)$, again in agreement with the analysis of a *simple* Atwood machine.

2.4.5 Example V: Pendulum with Oscillating Fulcrum

As a fifth and final example, we consider the case of a pendulum of mass m and length ℓ attached to a massless block which is attached to a fixed wall by a massless spring of constant k; of course, we assume that the massless block moves without friction on a set of rails. Here, we use the two generalized coordinates x and θ shown in Figure 2.11 and write the Cartesian coordinates (y, z) of the pendulum mass as $y = x + \ell \sin\theta$ and $z = -\ell \cos\theta$, with its associated velocity components $v_y = \dot{x} + \ell\dot{\theta} \cos\theta$ and $v_z = \ell\dot{\theta} \sin\theta$. The kinetic

energy of the pendulum is thus

$$K \;=\; \frac{m}{2}\left(v_y^2 \;+\; v_z^2\right) \;=\; \frac{m}{2}\left(\dot{x}^2 \;+\; \ell^2\dot{\theta}^2 \;+\; 2\,\ell\,\cos\theta\,\dot{x}\dot{\theta}\right).$$

The potential energy $U = U_k + U_g$ has two terms: one term $U_k = \frac{1}{2}\,kx^2$ associated with displacement of the spring away from its equilibrium position and one term $U_g = mgz$ associated with gravity. Hence, the Lagrangian for this system is

$$L(x,\theta,\dot{x},\dot{\theta}) \;=\; \frac{m}{2}\left(\dot{x}^2 \;+\; \ell^2\dot{\theta}^2 \;+\; 2\,\ell\,\cos\theta\,\dot{x}\dot{\theta}\right) \;-\; \frac{k}{2}\,x^2 \;+\; mg\ell\,\cos\theta.$$

The Euler-Lagrange equation for x is

$$\begin{aligned}
&\frac{\partial L}{\partial \dot{x}} \;=\; m\,\left(\dot{x} \;+\; \ell\,\cos\theta\,\dot{\theta}\right) \;\rightarrow\\
&\frac{d}{dt}\left(\frac{\partial L}{\partial \dot{x}}\right) \;=\; m\,\ddot{x} \;+\; m\ell\left(\ddot{\theta}\,\cos\theta \;-\; \dot{\theta}^2\,\sin\theta\right)\\
&\frac{\partial L}{\partial x} \;=\; -\,k\,x
\end{aligned}$$

while the Euler-Lagrange equation for θ is

$$\begin{aligned}
&\frac{\partial L}{\partial \dot{\theta}} \;=\; m\ell\left(\ell\,\dot{\theta} \;+\; \dot{x}\,\cos\theta\right) \;\rightarrow\\
&\frac{d}{dt}\left(\frac{\partial L}{\partial \dot{\theta}}\right) \;=\; m\ell^2\,\ddot{\theta} \;+\; m\ell\left(\ddot{x}\,\cos\theta \;-\; \dot{x}\dot{\theta}\,\sin\theta\right)\\
&\frac{\partial L}{\partial \theta} \;=\; -\,m\ell\,\dot{x}\dot{\theta}\,\sin\theta \;-\; mg\ell\,\sin\theta
\end{aligned}$$

or

$$m\,\ddot{x} \;+\; k\,x \;=\; m\ell\left(\dot{\theta}^2\,\sin\theta \;-\; \ddot{\theta}\,\cos\theta\right), \tag{2.31}$$

$$\ddot{\theta} \;+\; (g/\ell)\,\sin\theta \;=\; -\,(\ddot{x}/\ell)\,\cos\theta. \tag{2.32}$$

Here, we recover the dynamical equation for a block-and-spring harmonic oscillator from Eq. (2.31) by freezing the degree of freedom associated with the θ-coordinate (i.e., by setting $\dot{\theta} = 0 = \ddot{\theta}$) and the dynamical equation for the pendulum from Eq. (2.32) by freezing the degree of freedom associated with the x-coordinate (i.e., by setting $\dot{x} = 0 = \ddot{x}$). It is easy to see from this last example how powerful and yet simple the Lagrangian method is compared to the Newtonian method.

Numerical Box

By introducing the frequencies $\omega_k = \sqrt{k/m}$ and $\omega_g = \sqrt{g/\ell}$, with $\Omega \equiv \omega_k/\omega_g$ and $d/dt = \omega_g\, d/d\tau$, the coupled equations (2.31) and (2.32) are now expressed in dimensionless form as

$$\begin{aligned} s'' \,+\, \Omega^2\, s \;&=\; (\theta')^2\, \sin\theta \;-\; \theta''\, \cos\theta \\ \theta'' \,+\, \sin\theta \;&=\; -\, s''\, \cos\theta, \end{aligned}$$

where a prime denotes a derivative with respect to the dimensionless time $\tau = \omega_g t$ and $s = x/\ell$ denotes the dimensionless displacement of the spring. Note that these coupled equations now involve the single parameter Ω, where $\Omega \ll 1$ represents the weak-spring limit while $\Omega \gg 1$ represents the strong-spring limit.

2.5 Symmetries and Conservation Laws

We are sometimes faced with a Lagrangian function that is either independent of time, independent of a linear spatial coordinate, or independent of an angular spatial coordinate. The Noether theorem (Amalie Emmy Noether, 1882-1935) states that *for each symmetry of the Lagrangian there corresponds a conservation law (and vice versa).* When the Lagrangian L is invariant under a time translation, a space translation, or a spatial rotation, the conservation law involves energy, linear momentum, or angular momentum, respectively.

We begin our discussion with a general expression for the variation δL of the Lagrangian $L(\mathbf{q}, \dot{\mathbf{q}}, t)$:

$$\delta L \;=\; \delta\mathbf{q}\cdot\left[\,\frac{\partial L}{\partial \mathbf{q}} \;-\; \frac{d}{dt}\left(\frac{\partial L}{\partial \dot{\mathbf{q}}}\right)\,\right] \;+\; \frac{d}{dt}\left(\delta\mathbf{q}\cdot\frac{\partial L}{\partial \dot{\mathbf{q}}}\right),$$

obtained after re-arranging the term $\delta\dot{\mathbf{q}}\cdot\partial L/\partial\dot{\mathbf{q}}$. Next, we make use of the Euler-Lagrange equations for $\mathbf{q}$ (which enables us to drop the term $\delta\mathbf{q}\cdot[\cdots]$) and we find

$$\delta L \;=\; \frac{d}{dt}\left(\delta\mathbf{q}\cdot\frac{\partial L}{\partial \dot{\mathbf{q}}}\right). \tag{2.33}$$

Lastly, the variation δL can only be generated by a time translation δt, since

$$\begin{aligned} 0 \;=\; \delta\int L\, dt \;\;&=\;\; \int\left[\,\left(\delta L \;+\; \delta t\,\frac{\partial L}{\partial t}\right)dt \;+\; L\, d\delta t\,\right] \\ &=\;\; \int\left[\,\delta L \;-\; \delta t\left(\frac{dL}{dt} \;-\; \frac{\partial L}{\partial t}\right)\,\right]dt \end{aligned}$$

so that

$$\delta L \;=\; \delta t \left(\frac{dL}{dt} \;-\; \frac{\partial L}{\partial t} \right)$$

By combining this expression with Eq. (2.33), we find

$$\delta t \left(\frac{dL}{dt} \;-\; \frac{\partial L}{\partial t} \right) \;=\; \frac{d}{dt} \left(\delta \mathbf{q} \cdot \frac{\partial L}{\partial \dot{\mathbf{q}}} \right), \tag{2.34}$$

which we, henceforth, refer to as the Noether equation for finite-dimensional mechanical systems [see Eq. (9.10) in Chapter 9 for the infinite-dimensional case].

We now apply Noether's Theorem, based on the Noether equation (2.34), to investigate the connection between symmetries of the Lagrangian with conservation laws.

2.5.1 Energy Conservation Law

First, we consider time translations, $t \rightarrow t + \delta t$ and $\delta \mathbf{q} = \dot{\mathbf{q}}\, \delta t$, so that the Noether equation (2.34) becomes Euler's Second Equation for the Lagrangian:

$$-\, \frac{\partial L}{\partial t} \;=\; \frac{d}{dt} \left(\dot{\mathbf{q}} \cdot \frac{\partial L}{\partial \dot{\mathbf{q}}} \;-\; L \right).$$

Noether's Theorem states that if the Lagrangian is invariant under time translations, i.e., $\partial L / \partial t = 0$, then energy is conserved, $dE/dt = 0$, where

$$E \;=\; \dot{\mathbf{q}} \cdot \frac{\partial L}{\partial \dot{\mathbf{q}}} \;-\; L$$

defines the energy invariant.

2.5.2 Momentum Conservation Laws

Next, we consider invariance under spatial translations, $\mathbf{q} \rightarrow \mathbf{q} + \boldsymbol{\epsilon}$ (where $\delta \mathbf{q} = \boldsymbol{\epsilon}$ denotes a constant infinitesimal displacement and $\delta t = 0$), so that the Noether equation (2.34) yields the *linear* momentum conservation law

$$0 \;=\; \frac{d}{dt} \left(\frac{\partial L}{\partial \dot{\mathbf{q}}} \right) \;=\; \frac{d\mathbf{P}}{dt},$$

where $\mathbf{P}$ denotes the total linear momentum of the mechanical system. On the other hand, when the Lagrangian is invariant under spatial rotations, $\mathbf{q} \rightarrow \mathbf{q} + (\delta \boldsymbol{\varphi} \times \mathbf{q})$ (where $\delta \boldsymbol{\varphi} = \delta \varphi\, \widehat{\varphi}$ denotes a constant infinitesimal rotation about an axis along the $\widehat{\varphi}$-direction), the Noether equation (2.34) yields the *angular* momentum conservation law

$$0 \;=\; \frac{d}{dt} \left(\mathbf{q} \times \frac{\partial L}{\partial \dot{\mathbf{q}}} \right) \;=\; \frac{d\mathbf{L}}{dt},$$

where $\mathbf{L} = \mathbf{q} \times \mathbf{P}$ denotes the total angular momentum of the mechanical system.

2.5.3 Invariance Properties of a Lagrangian

Lastly, an important invariance property of the Lagrangian is related to the fact that the Euler-Lagrange equations themselves are invariant under the *gauge* transformation

$$L \;\rightarrow\; L \,+\, \frac{dF}{dt} \tag{2.35}$$

on the Lagrangian itself, where $F(\mathbf{q},t)$ is an arbitrary time-dependent function so that

$$\frac{dF(\mathbf{q},t)}{dt} \;=\; \frac{\partial F}{\partial t} \,+\, \sum_j \,\dot{q}^j\, \frac{\partial F}{\partial q^j}.$$

To investigate the invariance property (2.35), we call $L' = L + dF/dt$ the new Lagrangian and L the old Lagrangian, and consider the new Euler-Lagrange equations

$$\frac{d}{dt}\left(\frac{\partial L'}{\partial \dot{q}^i}\right) \;=\; \frac{\partial L'}{\partial q^i}.$$

We now express each term in terms of the old Lagrangian L and the function F. Let us begin with

$$\frac{\partial L'}{\partial \dot{q}^i} \;=\; \frac{\partial}{\partial \dot{q}^i}\left(L \,+\, \frac{\partial F}{\partial t} \,+\, \sum_j \,\dot{q}^j\, \frac{\partial F}{\partial q^j}\right) \;=\; \frac{\partial L}{\partial \dot{q}^i} \,+\, \frac{\partial F}{\partial q^i},$$

so that

$$\frac{d}{dt}\left(\frac{\partial L'}{\partial \dot{q}^i}\right) \;=\; \frac{d}{dt}\left(\frac{\partial L}{\partial \dot{q}^i}\right) \,+\, \frac{\partial^2 F}{\partial t \partial q^i} \,+\, \sum_k \,\dot{q}^k\, \frac{\partial^2 F}{\partial q^k \partial q^i}.$$

Next, we find

$$\frac{\partial L'}{\partial q^i} \;=\; \frac{\partial}{\partial q^i}\left(L \,+\, \frac{\partial F}{\partial t} \,+\, \sum_j \,\dot{q}^j\, \frac{\partial F}{\partial q^j}\right) \;=\; \frac{\partial L}{\partial q^i} \,+\, \frac{\partial^2 F}{\partial q^i \partial t} \,+\, \sum_j \,\dot{q}^j\, \frac{\partial^2 F}{\partial q^i \partial q^j}.$$

Using the symmetry properties

$$\dot{q}^j\, \frac{\partial^2 F}{\partial q^i \partial q^j} \;=\; \dot{q}^j\, \frac{\partial^2 F}{\partial q^j \partial q^i} \quad \text{and} \quad \frac{\partial^2 F}{\partial t \partial q^i} \;=\; \frac{\partial^2 F}{\partial q^i \partial t},$$

we easily verify that

$$\frac{d}{dt}\left(\frac{\partial L'}{\partial \dot{q}^i}\right) \,-\, \frac{\partial L'}{\partial q^i} \;=\; \frac{d}{dt}\left(\frac{\partial L}{\partial \dot{q}^i}\right) \,-\, \frac{\partial L}{\partial q^i} \;=\; 0.$$

Hence, since L and $L' = L + dF/dt$ lead to the same Euler-Lagrange equations, they are said to be equivalent.

Using this invariance property, for example, we note that the Lagrangian is also invariant under the Galilean velocity transformation $\mathbf{v} \to \mathbf{v} + \boldsymbol{\alpha}$, so that the Lagrangian variation

$$\delta L \;=\; \boldsymbol{\alpha} \cdot \left(\mathbf{v} \, \frac{\partial L}{\partial v^2} \right) \;\equiv\; \boldsymbol{\alpha} \cdot \frac{d\mathbf{x}}{dt} \, \frac{\partial L}{\partial v^2},$$

using the kinetic identity $\partial L / \partial v^2 = m/2$, can be written as an exact time derivative

$$\delta L \;=\; \frac{d}{dt} \left(\boldsymbol{\alpha} \cdot \frac{m}{2} \mathbf{x} \right) \;\equiv\; \frac{d \delta F}{dt}.$$

Hence, because Lagrangian mechanics is invariant under the *gauge* transformation (2.35), the Lagrangian L is said to be Galilean invariant.

2.5.4 Lagrangian Mechanics with Symmetries

As an example of Lagrangian mechanics with symmetries, we return to the motion of a particle of mass m constrained to move on the surface of a cone of apex angle α (such that $\sqrt{x^2 + y^2} = z \, \tan \alpha$) in the presence of a gravitational field (see Figure 2.5 and Sec. 2.3.3).

The Lagrangian for this constrained mechanical system is expressed in terms of the generalized coordinates (s, θ), where s denotes the distance from the cone's apex (labeled O in Figure 2.5) and θ is the standard polar angle in the (x, y)-plane. Hence, by combining the kinetic energy $K = \frac{1}{2} \, m (\dot{s}^2 + s^2 \, \dot{\theta}^2 \; \sin^2 \alpha)$ with the potential energy $U = mgz = mg \, s \; \cos \alpha$, we construct the Lagrangian

$$L(s, \theta; \dot{s}, \dot{\theta}) \;=\; \frac{1}{2} \, m \left(\dot{s}^2 + s^2 \, \dot{\theta}^2 \; \sin^2 \alpha \right) \;-\; mg \, s \; \cos \alpha. \tag{2.36}$$

Since the Lagrangian is independent of the polar angle θ, the canonical angular momentum

$$p_\theta \;=\; \frac{\partial L}{\partial \dot{\theta}} \;=\; m s^2 \, \dot{\theta} \; \sin^2 \alpha \tag{2.37}$$

is a constant of the motion (as predicted by Noether's Theorem). The Euler-Lagrange equation for s, on the other hand, is expressed as

$$\ddot{s} \;+\; g \; \cos \alpha \;=\; s \, \dot{\theta}^2 \; \sin^2 \alpha \;=\; \frac{p_\theta^2}{m^2 \, s^3 \sin^2 \alpha}, \tag{2.38}$$

where $g \, \cos \alpha$ denotes the component of the gravitational acceleration parallel to the surface of the cone. The right side of Eq. (2.38) involves s only after using $\dot{\theta} = p_\theta / (m \, s^2 \sin^2 \alpha)$, which follows from the conservation of angular momentum.

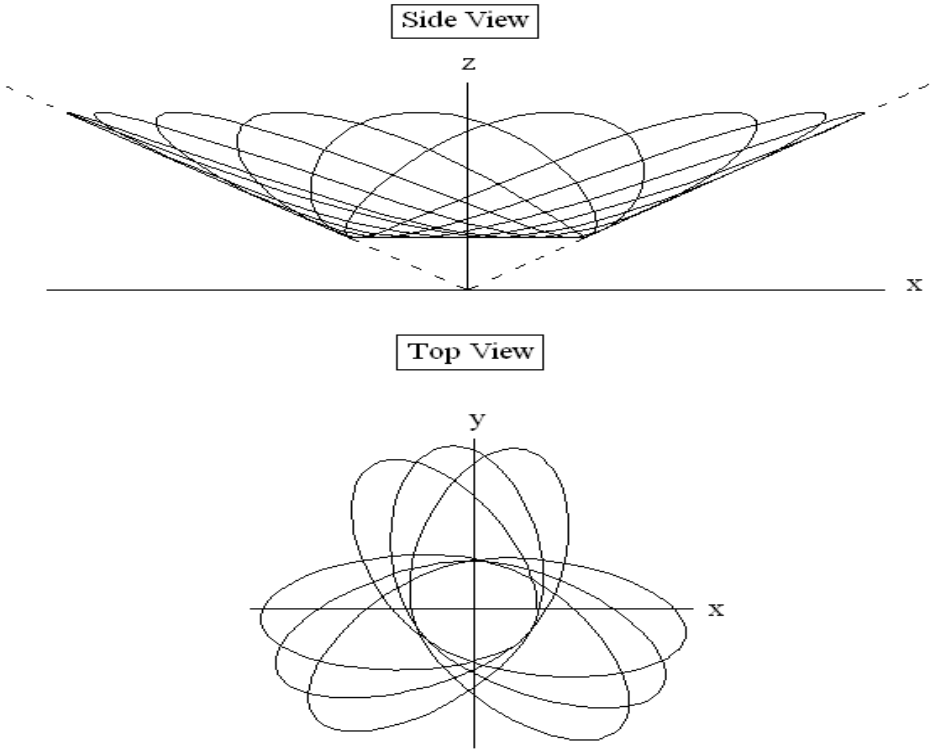

Figure 2.12: Particle orbits on the surface of a cone

Numerical Box

By introducing the frequency $\omega_g = \sqrt{(g/s_0)\cos\alpha}$, with $d/dt = \omega_g\, d/d\tau$, the dynamical equations (2.37) and (2.38) become

$$\sigma'' \;=\; -1 \;+\; \frac{1}{\sigma^3} \quad \text{and} \quad \theta' \;=\; \frac{1}{\sigma^2\,\sin\alpha},$$

where $\sigma \equiv s/s_0$, a prime denotes a derivative with respect to the dimensionless time $\tau = \omega_g t$, and

$$s_0 \;=\; \left(\frac{p_\theta^2}{m^2 g\,\sin^2\alpha\,\cos\alpha}\right)^{\frac{1}{3}}.$$

Figure 2.12 shows the results of the numerical integration of the dimensionless Euler-

Lagrange equations for $\theta(\tau)$ and $\sigma(\tau)$; see Numerical Box. The top figure in Figure 2.12 shows a projection of the path of the particle on the (x, z)-plane (side view), which clearly shows that the motion is periodic as the σ-coordinate oscillates between two finite values of σ. The bottom figure in Figure 2.12 shows a projection of the path of the particle on the (x, y)-plane (top view), which shows the slow precession motion in the θ-coordinate. In the next Chapter, we will show that the doubly-periodic motion of the particle moving on the surface of the inverted cone is a result of the conservation law of angular momentum and energy (since the Lagrangian system is also independent of time).

2.5.5 Routh's Procedure for Eliminating Ignorable Coordinates

Edward John Routh (1831-1907) introduced a simple procedure for eliminating ignorable degrees of freedom while introducing their corresponding conserved momenta. Consider, for example, two-dimensional motion on the (x, y)-plane represented by the Lagrangian $L(r;\, \dot{r}, \dot{\theta})$, where r and θ are the polar coordinates. Since the Lagrangian under consideration is independent of the angle θ, the canonical momentum $p_\theta = \partial L/\partial\dot{\theta}$ is conserved. Routh's procedure for deriving a *reduced* Lagrangian involves the construction of the *Routh-Lagrange* function (or Routhian) $R(r, \dot{r};\, p_\theta)$ defined as

$$R(r, \dot{r};\, p_\theta) \;=\; L(r;\, \dot{r}, \dot{\theta}) \;-\; p_\theta\, \dot{\theta}, \tag{2.39}$$

where $\dot{\theta}$ is expressed as a function of r and p_θ.

For example, for the constrained motion of a particle on the surface of a cone in the presence of gravity, the Lagrangian (2.36) can be reduced to the *Routh-Lagrange* (or Routhian) function

$$R(s, \dot{s}; p_\theta) \;=\; \frac{1}{2}\, m\dot{s}^2 \;-\; \left(mg\, s\, \cos\alpha \;+\; \frac{p_\theta^2}{2ms^2\, \sin^2\alpha}\right) \;=\; \frac{1}{2}\, m\dot{s}^2 \;-\; V(s), \tag{2.40}$$

and the equation of motion (2.38) can be expressed in Euler-Lagrange form

$$\frac{d}{ds}\left(\frac{\partial R}{\partial \dot{s}}\right) \;=\; \frac{\partial R}{\partial s} \quad\rightarrow\quad m\, \ddot{s} \;=\; -\, V'(s),$$

in terms of the effective potential

$$V(s) \;=\; mg\, s\, \cos\alpha \;+\; \frac{p_\theta^2}{2ms^2\, \sin^2\alpha}.$$

Here, the effective potential $V(s)$ has a single minimum at $s = s_0$, where

$$s_0 \;=\; \left(\frac{p_\theta^2}{m^2 g\, \sin^2\alpha\, \cos\alpha}\right)^{\frac{1}{3}}$$

and $V_0 \equiv V(s_0) = \frac{3}{2}\, mg\, s_0 \cos\alpha$.

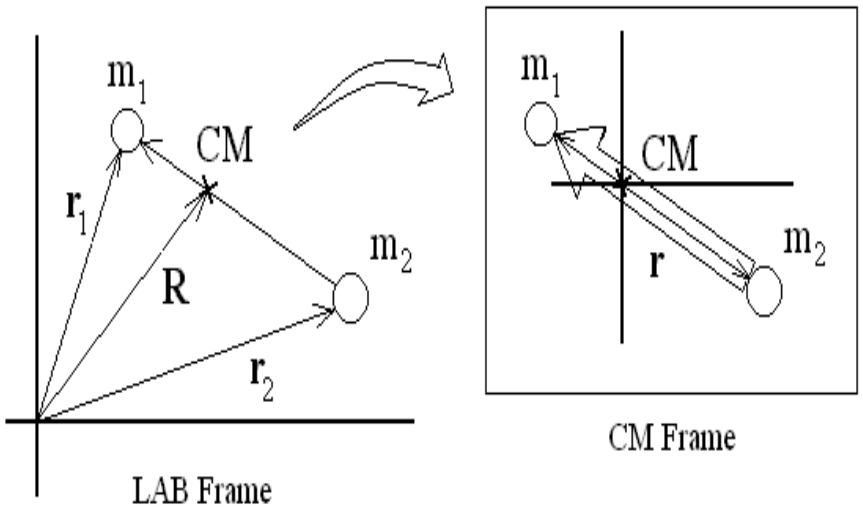

Figure 2.13: Center-of-Mass frame

2.6 Lagrangian Mechanics in the Center-of-Mass Frame

An important frame of reference associated with the dynamical description of the motion of interacting particles and rigid bodies is provided by the center-of-mass (CM) frame. The following discussion focuses on the Lagrangian for an isolated two-particle system expressed as

$$L \;=\; \frac{m_1}{2}\,|\dot{\mathbf{r}}_1|^2 \;+\; \frac{m_2}{2}\,|\dot{\mathbf{r}}_2|^2 \;-\; U(\mathbf{r}_1 - \mathbf{r}_2),$$

where $\mathbf{r}_1$ and $\mathbf{r}_2$ represent the positions of the particles of mass m_1 and m_2, respectively, and $U(\mathbf{r}_1,\, \mathbf{r}_2) = U(\mathbf{r}_1 - \mathbf{r}_2)$ is the potential energy for an isolated two-particle system (see Figure 2.13).

Let us now define the position $\mathbf{R}$ of the center of mass

$$\mathbf{R} \;=\; \frac{m_1\,\mathbf{r}_1 + m_2\,\mathbf{r}_2}{m_1 + m_2},$$

and define the relative inter-particle position vector $\mathbf{r} = \mathbf{r}_1 - \mathbf{r}_2$, so that the particle positions can be expressed as

$$\mathbf{r}_1 \;=\; \mathbf{R} \;+\; \frac{m_2}{M}\,\mathbf{r} \quad \text{and} \quad \mathbf{r}_2 \;=\; \mathbf{R} \;-\; \frac{m_1}{M}\,\mathbf{r},$$

where $M = m_1 + m_2$ is the total mass of the two-particle system (see Figure 2.13). The Lagrangian of the isolated two-particle system, thus, becomes

$$L \;=\; \frac{M}{2}\,|\dot{\mathbf{R}}|^2 \;+\; \frac{\mu}{2}\,|\dot{\mathbf{r}}|^2 \;-\; U(\mathbf{r}),$$

where

$$\mu \;=\; \frac{m_1\, m_2}{m_1 + m_2} \;=\; \left(\frac{1}{m_1} \;+\; \frac{1}{m_2}\right)^{-1}$$

denotes the *reduced* mass of the two-particle system. We note that the angular momentum of the two-particle system is expressed as

$$\mathbf{L} \;=\; \sum_a \mathbf{r}_a \times \mathbf{p}_a \;=\; \mathbf{R} \times \mathbf{P} \;+\; \mathbf{r} \times \mathbf{p}, \tag{2.41}$$

where the canonical momentum of the center-of-mass $\mathbf{P}$ and the canonical momentum $\mathbf{p}$ of the two-particle system in the CM frame are defined, respectively, as

$$\mathbf{P} \;=\; \frac{\partial L}{\partial \dot{\mathbf{R}}} \;=\; M\,\dot{\mathbf{R}} \quad \text{and} \quad \mathbf{p} \;=\; \frac{\partial L}{\partial \dot{\mathbf{r}}} \;=\; \mu \dot{\mathbf{r}}.$$

For an isolated system ($\partial L/\partial \mathbf{R} = 0$), the canonical momentum $\mathbf{P}$ of the center-of-mass is a constant of the motion. The CM reference frame is defined by the condition $\mathbf{R} = 0$, i.e., we move the origin of our coordinate system to the CM position.

In the CM frame, the Lagrangian for an isolated two-particle system is

$$L(\mathbf{r},\, \dot{\mathbf{r}}) \;=\; \frac{\mu}{2}\, |\dot{\mathbf{r}}|^2 \;-\; U(\mathbf{r}), \tag{2.42}$$

which describes the motion of a *fictitious* particle of mass μ at position $\mathbf{r}$, where the positions of the two *real* particles of masses m_1 and m_2 are

$$\mathbf{r}_1 \;=\; \frac{m_2}{M}\,\mathbf{r} \quad \text{and} \quad \mathbf{r}_2 \;=\; -\,\frac{m_1}{M}\,\mathbf{r}. \tag{2.43}$$

Hence, once the Euler-Lagrange equation for $\mathbf{r}$

$$\frac{d}{dt}\left(\frac{\partial L}{\partial \dot{\mathbf{r}}}\right) \;=\; \frac{\partial L}{\partial \mathbf{r}} \quad \rightarrow \quad \mu\, \ddot{\mathbf{r}} \;=\; -\,\nabla U(\mathbf{r})$$

is solved, the motion of the two particles in the CM frame is determined through Eqs. (2.43).

The angular momentum $\mathbf{L} = \mu\, \mathbf{r} \times \dot{\mathbf{r}}$ in the CM frame satisfies the evolution equation

$$\frac{d\mathbf{L}}{dt} \;=\; \mathbf{r} \times \mu \ddot{\mathbf{r}} \;=\; -\,\mathbf{r} \times \nabla U(\mathbf{r}). \tag{2.44}$$

Here, using spherical coordinates (r, θ, φ), we find

$$\frac{d\mathbf{L}}{dt} \;=\; -\,\widehat{\varphi}\,\frac{\partial U}{\partial \theta} \;+\; \frac{\widehat{\theta}}{\sin\theta}\,\frac{\partial U}{\partial \varphi}.$$

If motion is originally taking place on the (x, y)-plane (i.e., at $\theta = \pi/2$) and the potential $U(r, \varphi)$ is independent of the polar angle θ, then the angular momentum vector is $\mathbf{L} = \ell\, \widehat{\mathbf{z}}$ and its magnitude ℓ satisfies the evolution equation

$$\frac{d\ell}{dt} \;=\; -\,\frac{\partial U}{\partial \varphi}.$$

Hence, for motion in a potential $U(r)$ that depends only on the radial position r, the angular momentum remains along the z-axis $\mathbf{L} = \ell\,\hat{\mathsf{z}}$ represents an additional constant of motion. Motion in such potentials is refered to as motion in a *central-force* potential and will be studied in Chap. 4.

2.7 Problems

Problem 1

Consider a physical system composed of two blocks of mass m_1 and m_2 resting on incline planes placed at angles θ_1 and θ_2, respectively, as measured from the horizontal.

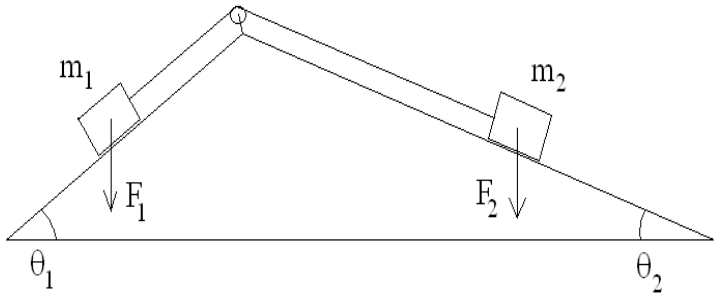

The only active forces acting on the blocks are due to gravity ($\mathbf{g} = -\,g\,\hat{\mathbf{y}}$): $\mathbf{F}_i = -\,m_i\,g\,\hat{\hat{y}}$ and, thus, the Principle of Virtual Work implies that the system is in static equilibrium if $0 = m_1 g\,\hat{\mathbf{y}}\cdot\delta\mathbf{x}^1 + m_2 g\,\hat{\mathbf{y}}\cdot\delta\mathbf{x}^2$. Find the virtual displacements $\delta\mathbf{x}^1$ and $\delta\mathbf{x}^2$ needed to show that, according to the Principle of Virtual Work, the condition for static equilibrium is $m_1\,\sin\theta_1 = m_2\,\sin\theta_2$.

Problem 2

A particle of mass m is constrained to slide down a curve $y = V(x)$ under the action of gravity without friction. Show that the Euler-Lagrange equation for this system yields the equation

$$\ddot{x} \;=\; -\,V'\,\left(g \;+\; \ddot{V}\right),$$

where $\dot{V} = \dot{x}\,V'$ and $\ddot{V} = (\dot{V})^{\cdot} = \ddot{x}\,V' + \dot{x}^2\,V''$.

Problem 3

Derive Eq. (2.30).

Problem 4

A bead (of mass m) slides without friction on a wire in the shape of a cycloid: $x(\theta) = a\,(\theta - \sin\theta)$ and $y(\theta) = a\,(1 + \cos\theta)$. (a) Find the Lagrangian $L(\theta, \dot{\theta})$ and derive the Euler-Lagrange equation for θ. (b) Find the equation of motion for $u = \cos(\theta/2)$.

Problem 5

A cart of mass M is placed on rails and attached to a wall with the help of a massless spring with constant k (as shown in the Figure below); the spring is in its equilibrium state when the cart is at a distance x_0 from the wall. A pendulum of mass m and length ℓ is attached to the cart (as shown).

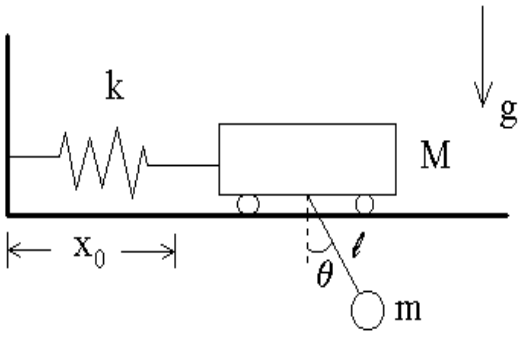

(a) Write the Lagrangian $L(x, \dot{x}, \theta, \dot{\theta})$ for the cart-pendulum system, where x denotes the position of the cart (as measured from a suitable origin) and θ denotes the angular position of the pendulum.

(b) From your Lagrangian, write the Euler-Lagrange equations for the generalized coordinates x and θ.

Problem 6

An Atwood machine is composed of two masses m and M attached by means of a massless rope into which a massless spring (with constant k) is inserted (as shown in the Figure below). When the spring is in a relaxed state, the spring-rope length is ℓ.

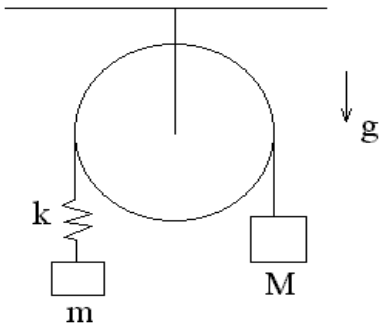

(a) Find suitable generalized coordinates to describe the motion of the two masses (allowing

for elongation or compression of the spring).

(b) Using these generalized coordinates, construct the Lagrangian and derive the appropriate Euler-Lagrange equations.

Chapter 3

Hamiltonian Mechanics

In the previous Chapter, the Lagrangian method was introduced as a powerful alternative to the Newtonian method for deriving equations of motion for complex mechanical systems. In the present Chapter, a complementary approach to the Lagrangian method, known as the Hamiltonian method, is presented. Although much of the Hamiltonian method is outside the scope of this course (e.g., the canonical and noncanonical Hamiltonian formulations of Classical Mechanics and the Hamiltonian formulation of Quantum Mechanics), a simplified version (the Energy method) is presented here as a practical method for *solving* the Euler-Lagrange equations by quadrature.

3.1 Canonical Hamilton's Equations

The k second-order Euler-Lagrange equations on configuration space $\mathbf{q} = (q^1, ..., q^k)$

$$\frac{d}{dt}\left(\frac{\partial L}{\partial \dot{q}^j}\right) \;=\; \frac{\partial L}{\partial q^j}, \tag{3.1}$$

can be written as $2k$ first-order differential equations, known as Hamilton's equations (William Rowan Hamilton, 1805-1865), on a $2k$-dimensional *phase* space with coordinates $\mathbf{z} = (q^1, ..., q^k;\; p_1, ..., p_k)$, where

$$p_j(\mathbf{q}, \dot{\mathbf{q}}; t) \;=\; \frac{\partial L}{\partial \dot{q}^j}(\mathbf{q}, \dot{\mathbf{q}}; t) \tag{3.2}$$

defines the j^{th}-component of the *canonical* momentum. In terms of these new coordinates, the Euler-Lagrange equations (3.1) are transformed into Hamilton's canonical equations

$$\frac{dq^j}{dt} \;=\; \frac{\partial H}{\partial p_j} \quad \text{and} \quad \frac{dp_j}{dt} \;=\; -\,\frac{\partial H}{\partial q^j}, \tag{3.3}$$

where the Hamiltonian function $H(\mathbf{q}, \mathbf{p}; t)$ is defined from the Lagrangian function $L(\mathbf{q}, \dot{\mathbf{q}}; t)$ by the Legendre transformation (Adrien-Marie Legendre, 1752-1833)

$$H(\mathbf{q}, \mathbf{p}; t) \;=\; \mathbf{p} \cdot \dot{\mathbf{q}}(\mathbf{q}, \mathbf{p}, t) \;-\; L[\mathbf{q}, \dot{\mathbf{q}}(\mathbf{q}, \mathbf{p}, t), t]. \tag{3.4}$$

We note that Hamilton's equations (3.3) can also be derived from a variational principle as follows. First, we use the inverse of the Legendre transformation

$$L(\mathbf{z}, \dot{\mathbf{z}}; t) \;=\; \mathbf{p} \cdot \dot{\mathbf{q}} - H(\mathbf{z}; t) \tag{3.5}$$

to obtain an expression for the Lagrangian function in phase space. Next, we calculate the first-variation of the action integral

$$\delta \int\, L(\mathbf{q}, \mathbf{p}; t)\, dt \;=\; \int \left[\, \delta \mathbf{p} \cdot \left(\dot{\mathbf{q}} \;-\; \frac{\partial H}{\partial \mathbf{p}} \right) \;+\; \left(\mathbf{p} \cdot \delta \dot{\mathbf{q}} \;-\; \delta \mathbf{q} \cdot \frac{\partial H}{\partial \mathbf{q}} \right) \,\right] \, dt,$$

where the variations δq^i and δp_i are now considered independent (and they are both assumed to vanish at the end points). Lastly, by integrating by parts the term $\mathbf{p} \cdot \delta \dot{\mathbf{q}}$, we find

$$\delta \int\, L(\mathbf{q}, \mathbf{p}; t)\, dt \;=\; \int \left[\, \delta \mathbf{p} \cdot \left(\dot{\mathbf{q}} \;-\; \frac{\partial H}{\partial \mathbf{p}} \right) \;-\; \delta \mathbf{q} \cdot \left(\dot{\mathbf{p}} \;+\; \frac{\partial H}{\partial \mathbf{q}} \right) \,\right] \, dt,$$

so that the Principle of Least Action $\int \delta L \, dt = 0$ now yields Hamilton's equations (3.3).

3.2 Legendre Transformation*

Before proceeding with the Hamiltonian formulation of particle dynamics, we investigate the conditions under which the Legendre transformation (3.4) is possible. It turns out that the condition under which the Legendre transformation can be used is associated with the condition under which the inversion of the relation $\mathbf{p}(\mathbf{r}, \dot{\mathbf{r}}, t) \rightarrow \dot{\mathbf{r}}(\mathbf{r}, \mathbf{p}, t)$ is possible. To simplify our discussion, we focus on motion in two dimensions (labeled x and y).

The general expression of the kinetic energy term of a Lagrangian with two degrees of freedom $L(x, \dot{x},\; y, \dot{y}) = K(x, \dot{x},\; y, \dot{y}) - U(x, y)$ is

$$K(x, \dot{x},\; y, \dot{y}) \;=\; \frac{\alpha}{2}\, \dot{x}^2 \;+\; \beta\, \dot{x}\, \dot{y} \;+\; \frac{\gamma}{2}\, \dot{y}^2 \;=\; \frac{1}{2}\, \dot{\mathbf{r}}^{\mathsf{T}} \;\cdot\; \mathsf{M} \;\cdot\; \dot{\mathbf{r}}, \tag{3.6}$$

where $\dot{\mathbf{r}}^{\top} = (\dot{x}, \dot{y})$ denotes the transpose of $\dot{\mathbf{r}}$ (see Appendix A for additional details concerning linear algebra) and the *mass* matrix M is

$$\mathsf{M} \;=\; \begin{pmatrix} \alpha & \beta \\ \\ \beta & \gamma \end{pmatrix}.$$

Here, the coefficients α, β, and γ may be function of x and/or y. The canonical momentum vector (3.2) is thus defined as

$$\mathbf{p} \;=\; \frac{\partial L}{\partial \dot{\mathbf{r}}} \;=\; \mathsf{M} \,\cdot\, \dot{\mathbf{r}} \;\;\rightarrow\;\; \begin{pmatrix} p_x \\ \\ p_y \end{pmatrix} \;=\; \begin{pmatrix} \alpha & \beta \\ \\ \beta & \gamma \end{pmatrix} \cdot \begin{pmatrix} \dot{x} \\ \\ \dot{y} \end{pmatrix}$$

or

$$\left.\begin{aligned} p_x &= \alpha\,\dot{x} \,+\, \beta\,\dot{y} \\ p_y &= \beta\,\dot{x} \,+\, \gamma\,\dot{y} \end{aligned}\right\}. \tag{3.7}$$

The Lagrangian is said to be *regular* if the matrix M is invertible, i.e., if its determinant

$$\Delta \;=\; \alpha\,\gamma \;-\; \beta^2 \;\neq\; 0.$$

In the case of a regular Lagrangian, we readily invert (3.7) to obtain

$$\dot{\mathbf{r}}(\mathbf{r},\mathbf{p},t) \;=\; \mathsf{M}^{-1} \,\cdot\, \mathbf{p} \;\;\rightarrow\;\; \begin{pmatrix} \dot{x} \\ \\ \dot{y} \end{pmatrix} \;=\; \frac{1}{\Delta} \begin{pmatrix} \gamma & -\,\beta \\ \\ -\,\beta & \alpha \end{pmatrix} \cdot \begin{pmatrix} p_x \\ \\ p_y \end{pmatrix}$$

or

$$\left.\begin{aligned} \dot{x} &= (\gamma\,p_x \;-\; \beta\,p_y)/\Delta \\ \dot{y} &= (\alpha\,p_y \;-\; \beta\,p_x)/\Delta \end{aligned}\right\}, \tag{3.8}$$

and the kinetic energy term becomes

$$K(x,p_x,\,y,p_y) \;=\; \frac{1}{2}\,\mathbf{p}^{\top} \,\cdot\, \mathsf{M}^{-1} \,\cdot\, \mathbf{p}.$$

Lastly, under the Legendre transformation, we find

$$\begin{aligned} H \;&=\; \mathbf{p}^{\top} \,\cdot\, \Big(\mathsf{M}^{-1} \,\cdot\, \mathbf{p}\Big) \;-\; \Big(\frac{1}{2}\,\mathbf{p}^{\top} \,\cdot\, \mathsf{M}^{-1} \,\cdot\, \mathbf{p} \;-\; U\Big) \\ &=\; \frac{1}{2}\,\mathbf{p}^{\top} \,\cdot\, \mathsf{M}^{-1} \,\cdot\, \mathbf{p} \;+\; U. \end{aligned}$$

Hence, we clearly see that the Legendre transformation is applicable only if the mass matrix M in the kinetic energy (3.6) is invertible.

Lastly, we note that the Legendre transformation is also used in other areas in physics such as Thermodynamics. Indeed, we begin with the First Law of Thermodynamics

$$dU(S,V) \;=\; T\,dS \;-\; P\,dV$$

expressed in terms of the internal energy function $U(S,V)$, where entropy S and volume V are the independent variables while temperature $T(S,V) = \partial U/\partial S$ and pressure $P(S,V) =$

$-\partial U/\partial V$ are dependent variables. It is possible, however, to choose other independent variables by defining new thermodynamic functions as shown in the Table below.

	Pressure P	Volume V	Temperature T	Entropy S
Pressure P	$\times$	$\times$	$G = H - T\,S$	$H = U + P\,V$
Volume V	$\times$	$\times$	$F = U - T\,S$	U
Temperature T	$G = H - T\,S$	$F = U - T\,S$	$\times$	$\times$
Entropy S	$H = U + P\,V$	U	$\times$	$\times$

For example, if we choose volume V and temperature T as independent variables, we introduce the Legendre transformation from the internal energy $U(S,V)$ to the Helmholtz free energy $F(V,T) = U - T\,S$, such that the First Law of Thermodynamics now becomes

$$dF(V,T) \;=\; dU \;-\; T\,dS \;-\; S\,dT \;=\; -\,P\,dV \;-\; S\,dT,$$

where pressure $P(V,T) = -\,\partial F/\partial V$ and entropy $S(V,T) = -\,\partial F/\partial T$ are dependent variables. Likewise, enthalpy $H(P,S) = U + P\,V$ and Gibbs free energy $G(T,P) = H - T\,S$ are introduced by Legendre transformations whenever one chooses (P,S) and (T,P), respectively, as independent variables.

3.3 Hamiltonian Optics and Wave-Particle Duality*

Historically, the Hamiltonian method was first introduced as a formulation of the dynamics of light rays. Consider the following *phase* integral

$$\Theta[\mathbf{z}] \;=\; \int_{t_1}^{t_2} \;[\;\mathbf{k}\cdot\dot{\mathbf{x}} \;-\; \omega(\mathbf{x},\mathbf{k};t)\;]\,dt, \tag{3.9}$$

where $\Theta[\mathbf{z}]$ is a functional of the light-path $\mathbf{z}(t) = (\mathbf{x}(t),\,\mathbf{k}(t))$ in *ray phase space*, expressed in terms of the instantaneous position $\mathbf{x}(t)$ of a light ray and its associated instantaneous wave vector $\mathbf{k}(t)$; here, the dispersion relation $\omega(\mathbf{x},\mathbf{k};t)$ is obtained as a root of the dispersion equation $\det \mathsf{D}(\mathbf{x},t;\,\mathbf{k},\omega) = 0$, and a dot denotes a total time derivative: $\dot{\mathbf{x}} = d\mathbf{x}/dt$.

Assuming that the phase integral $\Theta[\mathbf{z}]$ acquires a *minimal* value for a *physical* ray orbit $\mathbf{z}(t)$, henceforth called the Principle of *Phase Stationarity* $\delta\Theta = 0$, we can show that Euler's First Equation leads to *Hamilton's* ray equations:

$$\frac{d\mathbf{x}}{dt} \;=\; \frac{\partial\omega}{\partial\mathbf{k}} \quad\text{and}\quad \frac{d\mathbf{k}}{dt} \;=\; -\,\nabla\omega. \tag{3.10}$$

The first ray equation states that a ray travels at the *group* velocity while the second ray equation states that the wave vector $\mathbf{k}$ is refracted as the ray propagates in a non-uniform medium (see Chapter 1). Hence, the frequency function $\omega(\mathbf{x},\mathbf{k};t)$ is the Hamiltonian of ray dynamics in a nonuniform medium.

It was de Broglie who noted (as a graduate student well versed in Classical Mechanics) the similarities between Hamilton's equations (3.3) and (3.10), on the one hand, and the Maupertuis-Jacobi (2.1) and Euler-Lagrange (2.20) Principles of Least Action and Fermat's Principle of Least Time (1.30) and Principle of Phase Stationarity (3.9), on the other hand. By using the *quantum of action* $\hbar = h/2\pi$ defined in terms of Planck's constant h and Planck's energy hypothesis $E = \hbar\omega$, de Broglie suggested that a particle's momentum $\mathbf{p}$ be related to its wavevector $\mathbf{k}$ according to de Broglie's formula $\mathbf{p} = \hbar\,\mathbf{k}$ and introduced the wave-particle synthesis based on the identity $S[\mathbf{z}] = \hbar\,\Theta[\mathbf{z}]$ involving the action integral $S[\mathbf{z}]$ and the phase integral $\Theta[\mathbf{z}]$:

	Particle	Wave
phase space	$\mathbf{z} = (\mathbf{q}, \mathbf{p})$	$\mathbf{z} = (\mathbf{x}, \mathbf{k})$
Hamiltonian	$H(\mathbf{z})$	$\omega(\mathbf{z})$
Variational Principle I	Maupertuis − Jacobi	Fermat
Variational Principle II	Hamilton	Stationary − Phase

The final synthesis between Classical and Quantum Mechanics came from Richard Philips Feynman (1918-1988) who provided a derivation of Schroedinger's equation by associating the probability that a particle follow a particular path with the expression

$$\exp\left(\frac{i}{\hbar}\,S[\mathbf{z}]\right)$$

where $S[\mathbf{z}]$ denotes the action integral for the path (see Appendix B for a short derivation of Schroedinger's equation).

3.4 Particle Motion in an Electromagnetic Field*

Although the problem of the motion of a charged particle in an electromagnetic field is outside the scope of the present course, it represents a paradigm that beautifully illustrates the connection between Lagrangian and Hamiltonian mechanics and is well worth studying.

3.4.1 Euler-Lagrange Equations

The equations of motion for a charged particle of mass m and charge e moving in an electromagnetic field represented by the electric field $\mathbf{E}$ and magnetic field $\mathbf{B}$ are

$$\frac{d\mathbf{x}}{dt} = \mathbf{v} \tag{3.11}$$

$$\frac{d\mathbf{v}}{dt} = \frac{e}{m}\left(\mathbf{E} + \frac{d\mathbf{x}}{dt} \times \frac{\mathbf{B}}{c}\right), \tag{3.12}$$

where $\mathbf{x}$ denotes the position of the particle and $\mathbf{v}$ its velocity.[1]

By treating the coordinates $(\mathbf{x}, \mathbf{v})$ as generalized coordinates (i.e., $\delta\mathbf{v}$ is treated independently from $\delta\mathbf{x}$), we can show that the equations of motion (3.11) and (3.12) can be obtained as Euler-Lagrange equations from the Lagrangian (3.5)

$$L(\mathbf{x}, \dot{\mathbf{x}},\ \mathbf{v}, \dot{\mathbf{v}};\, t) \ =\ \left(m\,\mathbf{v}\ +\ \frac{e}{c}\,\mathbf{A}(\mathbf{x},t)\right)\cdot\dot{\mathbf{x}}\ -\ \left(e\,\Phi(\mathbf{x},t)\ +\ \frac{m}{2}\,|\mathbf{v}|^2\right), \tag{3.13}$$

where Φ and $\mathbf{A}$ are the electromagnetic potentials in terms of which electric and magnetic fields are defined

$$\mathbf{E}\ =\ -\,\nabla\Phi\ -\ \frac{1}{c}\,\frac{\partial\mathbf{A}}{\partial t}\ \text{ and }\ \mathbf{B}\ =\ \nabla\times\mathbf{A}. \tag{3.14}$$

Note that these expressions for $\mathbf{E}$ and $\mathbf{B}$ satisfy Faraday's law $\nabla\times\mathbf{E} = -\,c^{-1}\,\partial\mathbf{B}/\partial t$ and the divergenceless property $\nabla\cdot\mathbf{B} = 0$ of the magnetic field.

First, we look at the Euler-Lagrange equation for $\mathbf{x}$:

$$\frac{\partial L}{\partial\dot{\mathbf{x}}}\ =\ m\,\mathbf{v}\ +\ \frac{e}{c}\,\mathbf{A}\ \ \rightarrow\ \ \frac{d}{dt}\left(\frac{\partial L}{\partial\dot{\mathbf{x}}}\right)\ =\ m\,\dot{\mathbf{v}}\ +\ \frac{e}{c}\left(\frac{\partial\mathbf{A}}{\partial t}\ +\ \dot{\mathbf{x}}\cdot\nabla\mathbf{A}\right)$$

$$\frac{\partial L}{\partial\mathbf{x}}\ =\ \frac{e}{c}\,\nabla\mathbf{A}\cdot\dot{\mathbf{x}}\ -\ e\,\nabla\Phi,$$

which yields Eq. (3.12), since

$$m\,\dot{\mathbf{v}}\ =\ -\,e\left(\nabla\Phi\ +\ \frac{1}{c}\,\frac{\partial\mathbf{A}}{\partial t}\right)\ +\ \frac{e}{c}\,\dot{\mathbf{x}}\times\nabla\times\mathbf{A}\ =\ e\,\mathbf{E}\ +\ \frac{e}{c}\,\dot{\mathbf{x}}\times\mathbf{B}, \tag{3.15}$$

where the definitions (3.14) were used.

Next, we look at the Euler-Lagrange equation for $\mathbf{v}$:

$$\frac{\partial L}{\partial\dot{\mathbf{v}}}\ =\ 0\ \ \rightarrow\ \ \frac{d}{dt}\left(\frac{\partial L}{\partial\dot{\mathbf{v}}}\right)\ =\ 0\ =\ \frac{\partial L}{\partial\mathbf{v}}\ =\ m\,\dot{\mathbf{x}}\ -\ m\,\mathbf{v},$$

which yields Eq. (3.11). Because $\partial L/\partial\dot{\mathbf{v}} = 0$, we note that we could use Eq. (3.11) as a constraint which could be imposed *a priori* on the Lagrangian (3.13) to give

$$L(\mathbf{x}, \dot{\mathbf{x}};\, t)\ =\ \frac{m}{2}\ |\dot{\mathbf{x}}|^2\ +\ \frac{e}{c}\,\mathbf{A}(\mathbf{x},t)\cdot\dot{\mathbf{x}}\ -\ e\,\Phi(\mathbf{x},t). \tag{3.16}$$

The Euler-Lagrange equation for $\mathbf{x}$ in this case is identical to Eq. (3.15) with $\dot{\mathbf{v}} = \ddot{\mathbf{x}}$.

[1] Gaussian units are used whenever electromagnetic fields are involved.

3.4.2 Energy Conservation Law

We now show that the second Euler equation (i.e., the energy conservation law), expressed as

$$\frac{d}{dt}\left(L \,-\, \dot{\mathbf{x}}\cdot\frac{\partial L}{\partial \dot{\mathbf{x}}}\right) \,=\, \frac{\partial L}{\partial t},$$

is satisfied exactly by the Lagrangian (3.16) and the equations of motion (3.11) and (3.12). First, from the Lagrangian (3.16), we find

$$\begin{aligned}\frac{\partial L}{\partial t} \;&=\; \frac{e}{c}\,\frac{\partial \mathbf{A}}{\partial t}\cdot\mathbf{v} \,-\, e\,\frac{\partial \Phi}{\partial t}\\ L \,-\, \dot{\mathbf{x}}\cdot\frac{\partial L}{\partial \dot{\mathbf{x}}} \;&=\; L \,-\, \left(m\,\mathbf{v} \,+\, \frac{e}{c}\,\mathbf{A}\right)\cdot\mathbf{v}\\ &=\; -\left(\frac{m}{2}\,|\mathbf{v}|^2 \,+\, e\,\Phi\right).\end{aligned}$$

Next, we find

$$\frac{d}{dt}\left(L \,-\, \dot{\mathbf{x}}\cdot\frac{\partial L}{\partial \dot{\mathbf{x}}}\right) \,=\, -\,m\mathbf{v}\cdot\dot{\mathbf{v}} \,-\, e\left(\frac{\partial \Phi}{\partial t} \,+\, \mathbf{v}\cdot\nabla\Phi\right) \,=\, -e\,\frac{\partial}{\partial t}\left(\Phi \,-\, \frac{\mathbf{v}}{c}\cdot\mathbf{A}\right).$$

Using Eq. (3.11), we readily find $m\mathbf{v}\cdot\dot{\mathbf{v}} = e\,\mathbf{E}\cdot\mathbf{v}$ and thus

$$-\,e\,\mathbf{E}\cdot\mathbf{v} \,-\, e\left(\frac{\partial \Phi}{\partial t} \,+\, \mathbf{v}\cdot\nabla\Phi\right) \,=\, \frac{e}{c}\,\frac{\partial \mathbf{A}}{\partial t}\cdot\mathbf{v} \,-\, e\,\frac{\partial \Phi}{\partial t},$$

which is shown to be satisfied exactly by substituting the definition (3.14) for $\mathbf{E}$.

3.4.3 Gauge Invariance

The electric and magnetic fields defined in (3.14) are invariant under the gauge transformation

$$\Phi \;\rightarrow\; \Phi \,-\, \frac{1}{c}\,\frac{\partial \chi}{\partial t} \;\text{ and }\; \mathbf{A} \;\rightarrow\; \mathbf{A} \,+\, \nabla\chi, \tag{3.17}$$

where $\chi(\mathbf{x}, t)$ is an arbitrary scalar field. Although the equations of motion (3.11) and (3.12) are *manifestly* gauge invariant, the Lagrangian (3.16) is not manifestly gauge invariant since the electromagnetic potentials Φ and $\mathbf{A}$ appear explicitly. Under a gauge transformation (3.17), however, we find

$$L \;\rightarrow\; L \,+\, \frac{e}{c}\,\dot{\mathbf{x}}\cdot\nabla\chi \,-\, e\left(-\,\frac{1}{c}\,\frac{\partial \chi}{\partial t}\right) \,=\, L \,+\, \frac{d}{dt}\left(\frac{e}{c}\,\chi\right).$$

Since Lagrangian Mechanics is invariant under the transformation (2.35), we find that the Lagrangian (3.16) is invariant under a gauge transformation.

3.4.4 Canonical Hamilton's Equations

The canonical momentum $\mathbf{p}$ for a particle of mass m and charge e in an electromagnetic field is defined as

$$\mathbf{p}(\mathbf{x},\mathbf{v},t) \;=\; \frac{\partial L}{\partial \dot{\mathbf{x}}} \;=\; m\,\mathbf{v} \;+\; \frac{e}{c}\,\mathbf{A}(\mathbf{x},t). \tag{3.18}$$

The canonical Hamiltonian function $H(\mathbf{x},\mathbf{p},t)$ is now constructed through the Legendre transformation

$$\begin{aligned} H(\mathbf{x},\mathbf{p},t) \;&=\; \mathbf{p}\cdot\dot{\mathbf{x}}(\mathbf{x},\mathbf{p},t) \;-\; L[\mathbf{x},\dot{\mathbf{x}}(\mathbf{x},\mathbf{p},t),t] \\ &=\; e\,\Phi(\mathbf{x},t) \;+\; \frac{1}{2m}\left|\,\mathbf{p} \;-\; \frac{e}{c}\,\mathbf{A}(\mathbf{x},t)\,\right|^2, \end{aligned} \tag{3.19}$$

where $\mathbf{v}(\mathbf{x},\mathbf{p},t)$ was obtained by inverting $\mathbf{p}(\mathbf{x},\mathbf{v},t)$ from Eq. (3.18). Using the canonical Hamiltonian function (3.19), we immediately find

$$\begin{aligned} \dot{\mathbf{x}} \;&=\; \frac{\partial H}{\partial \mathbf{p}} \;=\; \frac{1}{m}\left(\mathbf{p} \;-\; \frac{e}{c}\,\mathbf{A}\right), \\ \dot{\mathbf{p}} \;&=\; -\,\frac{\partial H}{\partial \mathbf{x}} \;=\; -\,e\,\nabla\Phi \;-\; \frac{e}{c}\,\nabla\mathbf{A}\cdot\dot{\mathbf{x}}, \end{aligned}$$

from which we recover the equations of motion (3.11) and (3.12) once we use the definition (3.18) for the canonical momentum.

3.5 One-degree-of-freedom Hamiltonian Dynamics

In this Section, we investigate Hamiltonian dynamics with one degree of freedom in a time-independent potential. In particular, we show that such systems are always integrable (i.e., they can always be solved by quadrature).

The one degree-of-freedom Hamiltonian dynamics of a particle of mass m is based on the Hamiltonian

$$H(x,p) \;=\; \frac{p^2}{2m} \;+\; U(x), \tag{3.20}$$

where $p = m\dot{x}$ is the particle's momentum and $U(x)$ is the time-independent potential energy. The Hamilton's equations (3.3) for this Hamiltonian are

$$\frac{dx}{dt} \;=\; \frac{p}{m} \quad\text{and}\quad \frac{dp}{dt} \;=\; -\,\frac{dU(x)}{dx}. \tag{3.21}$$

Since the Hamiltonian (and Lagrangian) is time independent, the energy conservation law states that $H(x,p) = E$. In turn, this conservation law implies that the particle's velocity

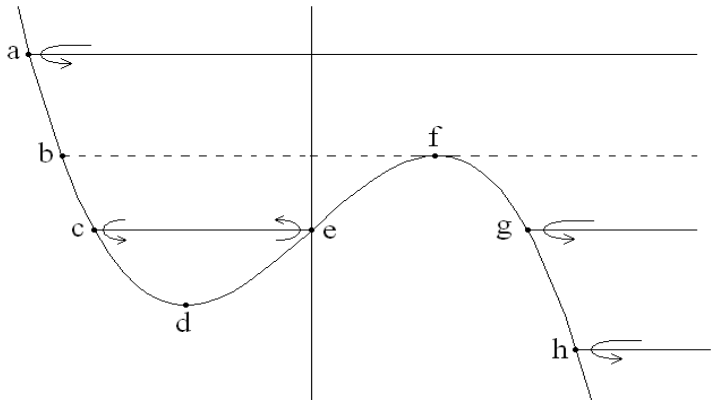

Figure 3.1: Bounded and unbounded energy levels in a cubic potential $U(x) = x - x^3/3$.

$\dot{x}$ can be expressed as

$$\dot{x}(x, E) \;=\; \pm\sqrt{\frac{2}{m}\,[E - U(x)]}, \tag{3.22}$$

where the sign of $\dot{x}$ is determined from the initial conditions.

It is immediately clear that physical motion is possible only if $E \geq U(x)$; points where $E = U(x)$ are known as *turning* points since the particle velocity $\dot{x}$ vanishes at these points. In Figure 3.1, which represents the dimensionless potential $U(x) = x - x^3/3$, each horizontal line corresponds to a constant energy value (called an energy *level*). For the top energy level, only one turning point (labeled a in Figure 3.1) exists and a particle coming from the right will be *reflected* at point a and return to large (positive) values of x; the motion in this case is said to be *unbounded* (see orbits I in Figure 3.2). As the energy value is lowered, two turning points (labeled b and f) appear and motion can either be *bounded* (between points b and f) or unbounded (if the initial position is to the right of point f); this energy level is known as a *separatrix* level since bounded and unbounded motions share one turning point (see orbits II and III in Figure 3.2). As energy is lowered below the separatrix level, three turning points (labeled c, e, and g) appear and, once again, motion can either be *bounded* (with turning points c and e) or unbounded if the initial position is to the right of point g (see orbits IV and V in Figure 3.2).[2] Lastly, we note that point d in Figure 3.1 is actually an equilibrium point (as is point f), where $\dot{x}$ and $\ddot{x}$ both vanish; only unbounded motion is allowed as energy is lowered below point d (e.g., point h) and the corresponding unbounded orbits are analogous to orbit V in Figure 3.2.

The dynamical solution $x(t; E)$ of the Hamilton's equations (3.21) is first expressed an

[2]Note: Quantum tunneling establishes a connection between the bounded and unbounded solutions.

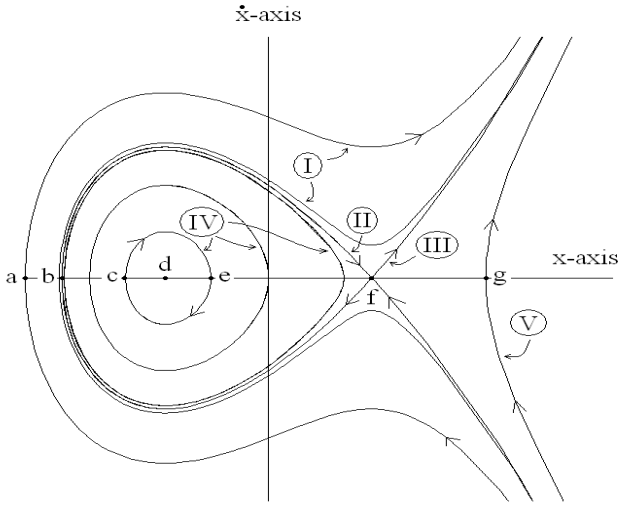

Figure 3.2: Bounded and unbounded orbits in the cubic potential shown in Figure 3.1: the orbits I correspond to the energy level with turning point a; the bounded orbit II and unbounded orbit III correspond to the separatrix energy level with turning points b and f; the bounded orbits IV correspond to the energy level with turning points c and e; and the unbounded orbit V corresponds to the energy level with turning point g.

integration by quadrature using Eq. (3.22) as

$$t(x;E) \;=\; \sqrt{\frac{m}{2}}\,\int_{x_0}^{x}\,\frac{ds}{\sqrt{E-U(s)}}, \tag{3.23}$$

where the particle's initial position x_0 is between the turning points $x_1 < x_2$ (allowing $x_2 \to \infty$) and we assume that $\dot{x}(0) > 0$. Next, inversion of the relation (3.23) yields the solution $x(t;E)$.

Lastly, for bounded motion in one dimension, the particle bounces back and forth between the two turning points x_1 and $x_2 > x_1$, and the period of oscillation $T(E)$ is a function of energy alone

$$T(E) \;=\; 2\,\int_{x_1}^{x_2}\,\frac{dx}{\dot{x}(x,E)} \;=\; \sqrt{2m}\,\int_{x_1}^{x_2}\,\frac{dx}{\sqrt{E-U(x)}}. \tag{3.24}$$

Thus, Eqs. (3.23) and (3.24) describe applications of the Energy Method in one dimension. We now look at a series of one-dimensional problems solvable by the Energy Method.

3.5.1 Simple Harmonic Oscillator

As a first example, we consider the case of a particle of mass m attached to a spring of constant k, for which the potential energy is $U(x) = \frac{1}{2}\,kx^2$. The motion of a particle with total energy E is always bounded, with turning points

$$x_{1,2}(E) \;=\; \pm\sqrt{2E/k} \;=\; \pm\, a.$$

We start with the solution (3.23) for $t(x;E)$ for the case of $x(0;E) = +a$, so that $\dot{x}(t;E) < 0$ for $t > 0$, and

$$t(x;E) \;=\; \sqrt{\frac{m}{k}}\,\int_x^a \frac{ds}{\sqrt{a^2-s^2}} \;=\; \sqrt{\frac{m}{k}}\,\arccos\left(\frac{x}{a}\right). \tag{3.25}$$

Inversion of this relation yields the well-known solution $x(t;E) = a\,\cos(\omega_0 t)$, where $\omega_0 = \sqrt{k/m}$. Next, using Eq. (3.24), we find the period of oscillation

$$T(E) \;=\; \frac{4}{\omega_0}\,\int_0^a \frac{dx}{\sqrt{a^2-x^2}} \;=\; \frac{2\pi}{\omega_0},$$

which turns out to be independent of energy E.

3.5.2 Pendulum

Our second example involves the case of the pendulum of length ℓ and mass m in a gravitational field g (see Sec. 2.4.1). The Hamiltonian in this case is

$$H \;=\; \frac{1}{2}\,m\ell^2\,\dot{\theta}^2 \;+\; mg\ell\,(1-\cos\theta).$$

The total energy of the pendulum is determined from its initial conditions $(\theta_0, \dot{\theta}_0)$:

$$E \;=\; \frac{1}{2}\,m\ell^2\,\dot{\theta}_0^2 \;+\; mg\ell\,(1-\cos\theta_0),$$

where the potential energy term is $mg\ell\,(1-\cos\theta) \le 2\,mg\ell$ and, thus, solutions of the pendulum problem are divided into three classes depending on the value of the total energy of the pendulum (see Figure 3.3): Class I (rotation) $E > 2\,mg\ell$, Class II (separatrix) $E = 2\,mg\ell$, and Class III (libration) $E < 2\,mg\ell$.

In the rotation class ($E > 2\,mg\ell$), the kinetic energy can never vanish and the pendulum keeps rotating either clockwise or counter-clockwise depending on the sign of $\dot{\theta}_0$. In the libration class ($E < 2\,mg\ell$), on the other hand, the kinetic energy vanishes at turning points easily determined by initial conditions if the pendulum starts from rest ($\dot{\theta}_0 = 0$) – in this case, the turning points are $\pm\,\theta_0$, where

$$\theta_0 \;=\; \arccos\left(1 \;-\; \frac{E}{mg\ell}\right).$$

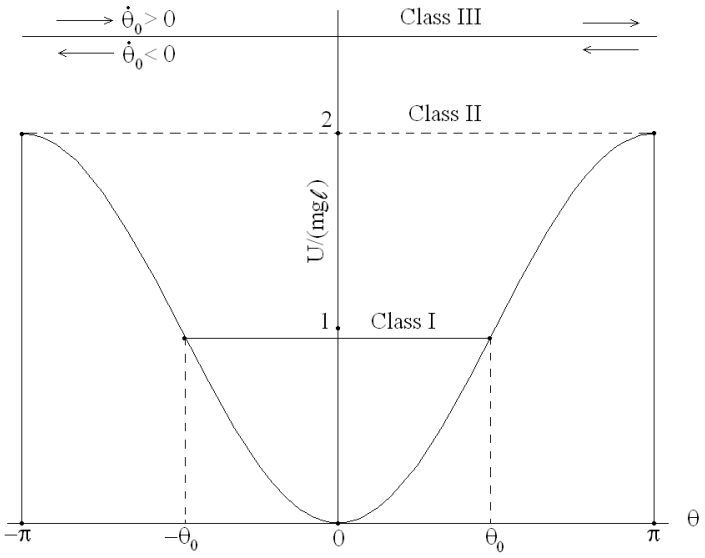

Figure 3.3: Normalized pendulum potential $U(\theta)/(mg\ell) = 1 - \cos\theta$.

In the separatrix class ($E = 2\,mg\ell$), the turning points are $\theta_0 = \pm\,\pi$. The numerical solution of the normalized pendulum equation $\ddot\theta + \sin\theta = 0$ subject to the initial condition θ_0 and $\dot\theta_0 = \pm\sqrt{2\,(\epsilon - 1 + \cos\theta_0)}$ yields the following curves (see Fig. 3.3). Here, the three classes I, II, and III are easily seen (with $\epsilon = 1 - \cos\theta_0$ and $\dot\theta_0 = 0$ for classes I and II and $\epsilon > 1 - \cos\theta_0$ for class III). Note that for rotations (class III), the pendulum slows down as it approaches $\theta = \pm\,\pi$ (the top part of the circle) and speeds up as it approaches $\theta = 0$ (the bottom part of the circle). In fact, since $\theta = \pi$ and $\theta = -\pi$ represent the same point in space, the lines AB and $A'B'$ in Figure 3.4 should be viewed as being identical (i.e., they should be glued together) and the geometry of the *phase space* for the pendulum problem is actually that of a cylinder.

Libration Class ($E < 2mg\ell$)

We now look at an explicit solution for pendulum librations (class I), where the angular velocity $\dot\theta$ is

$$\dot\theta(\theta; E) \;=\; \pm\,\omega_0\,\sqrt{2\,(\cos\theta - \cos\theta_0)} \;=\; \pm\,2\omega_0\,\sqrt{\sin^2(\theta_0/2) \;-\; \sin^2(\theta/2)}, \tag{3.26}$$

where $\omega_0 = \sqrt{g/\ell}$ denotes the characteristic angular frequency and, thus, $\pm\,\theta_0$ are the turning points for this problem. By making the substitution $\sin\theta/2 = k\,\sin\varphi$, where

$$k(E) \;=\; \sin[\,\theta_0(E)/2] \;=\; \sqrt{\frac{E}{2\,mg\ell}} \;<\; 1 \tag{3.27}$$

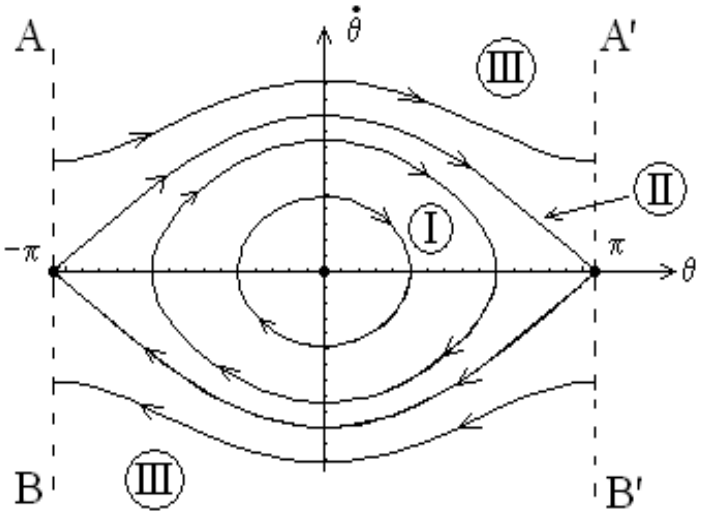

Figure 3.4: Phase space of the pendulum

and $\varphi = \pm\,\pi/2$ when $\theta = \pm\,\theta_0$, the libration solution of the pendulum problem is thus

$$\omega_0\, t(\theta; E) \;=\; \int_{\Theta(\theta;E)}^{\pi/2} \frac{d\varphi}{\sqrt{1 - k^2\,\sin^2\varphi}}, \tag{3.28}$$

where $\Theta(\theta; E) = \arcsin(k^{-1}\sin\theta/2)$. The inversion of this relation yields $\theta(t; E)$ expressed in terms of Jacobi elliptic functions (see Appendix A.3.2 for more details), while the period of oscillation is defined as

$$\begin{aligned} \omega_0\, T(E) \;&=\; 4\int_0^{\pi/2} \frac{d\varphi}{\sqrt{1 - k^2\,\sin^2\varphi}} \;=\; 4\int_0^{\pi/2} d\varphi \left(1 \,+\, \frac{k^2}{2}\,\sin^2\varphi \,+\, \cdots\right), \\ &=\; 2\pi\left(1 \,+\, \frac{k^2}{4} \,+\, \cdots\right) \;=\; 4\,K(k), \end{aligned} \tag{3.29}$$

where $K(k)$ denotes the complete elliptic integral of the first kind (see Figure 3.5 and Appendix A.3.2).

We note here that if $k \ll 1$ (or $\theta_0 \ll 1$) the libration period of a pendulum is nearly independent of energy, $T \simeq 2\pi/\omega_0$. However, we also note that as $E \to 2\,mg\ell$ ($k \to 1$ or $\theta_0 \to \pi$), the libration period of the pendulum becomes infinitely large, i.e., $T \to \infty$ in Eq. (3.29) (see Figure 3.5).

Separatrix Class ($E = 2mg\ell$)

In the separatrix case ($\theta_0 = \pi$), the pendulum equation (3.26) yields the *separatrix* equation $\dot\varphi = \omega_0\,\cos\varphi$, where $\varphi = \theta/2$. The separatrix solution is expressed in terms of the

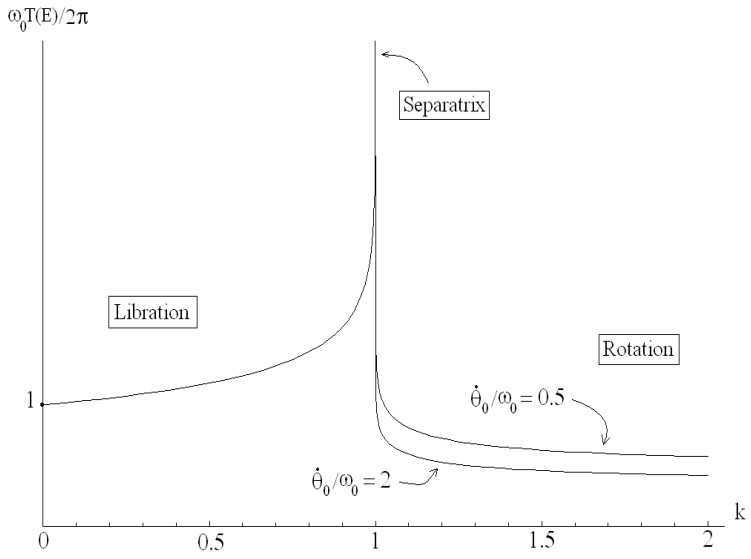

Figure 3.5: Normalized pendulum period $\omega_0\, T(E)/2\pi$ as a function of the normalized energy $k^2 = E/(2\, mg\ell)$ for Libration Class I ($k^2 < 1$) and Rotation Class III ($k^2 > 1$); note that, for the Separatrix Class II ($k^2 = 1$), the period is infinite.

transcendental equation

$$\sec\varphi(t) \;=\; \cosh(\omega_0 t + \gamma), \tag{3.30}$$

where $\cosh\gamma = \sec\varphi_0$ represents the initial condition. We again note that $\varphi \to \pi/2$ (or $\theta \to \pi$) only as $t \to \infty$. Separatrices are associated with turning points s_0 where $U'(s_0) = 0$ and $U''(s_0) < 0$, which are quite common in periodic dynamical systems as will be shown in Secs. 3.6 and 7.2.3.

Rotation Class ($E > 2mg\ell$)

The solution for rotations (class III) associated with the initial conditions $\theta_0 = \pm\pi$ and

$$\frac{1}{2}\,\dot\theta_0^2 \;=\; \omega_0^2\left(\frac{E}{mg\ell} \;-\; 2\right) \;=\; \frac{1}{2}\,\dot\theta^2 \;-\; \omega_0^2\,\Big(1 \;+\; \cos\theta\Big)\,,$$

or

$$\dot\theta \;=\; \pm\,\sqrt{\dot\theta_0^2 \;+\; 2\,\omega_0^2\,(1+\cos\theta)},$$

which shows that $\dot\theta$ does not vanish for rotations. We now write $\cos\theta = 1 - 2\,\sin^2(\theta/2)$ and define $\Omega_0^2 = \dot\theta_0^2 + 4\omega_0^2$, with so that

$$\dot\theta \;=\; \pm\,\Omega_0\,\sqrt{1 \;-\; k^{-2}\,\sin^2(\theta/2)},$$

where $k(E)$ is defined in Eq. (3.27). Hence, the solution for rotations is expressed as

$$\Omega_0\, t \;=\; \int_{-\pi}^{\theta} \frac{d\theta'}{\sqrt{1 \;-\; k^{-2}\, \sin^2(\theta'/2)}},$$

and the rotation period is defined as

$$\omega_0\, T(E) \;=\; \frac{4\,\omega_0}{\Omega_0} \int_0^{\pi/2} \frac{d\varphi}{\sqrt{1 \;-\; k^{-2}\, \sin^2\varphi}} \;=\; \frac{4\,\omega_0}{\Omega_0}\, K(k^{-1}).$$

Figure 3.5 shows the plot of the normalized pendulum period as a function of k^2 for the Libration Class I and Rotation Class III (two cases are shown: $\dot\theta_0/\omega_0 = 2$ and 0.5).

3.5.3 Constrained Motion on the Surface of a Cone

The constrained motion of a particle of mass m on a cone in the presence of gravity was shown in Sec. 2.5.4 to be doubly periodic in the generalized coordinates s and θ. The fact that the Lagrangian (2.36) is independent of time leads to the conservation law of energy

$$E \;=\; \frac{m}{2}\,\dot s^2 \;+\; \left(\frac{\ell^2}{2m\sin^2\alpha\, s^2} \;+\; mg\cos\alpha\, s\right) \;=\; \frac{m}{2}\,\dot s^2 \;+\; V(s), \tag{3.31}$$

where we have taken into account the conservation law of angular momentum $\ell = ms^2\sin^2\alpha\,\dot\theta$. The effective potential $V(s)$ has a single minimum $V_0 = \frac{3}{2}\, mgs_0\, \cos\alpha$ at

$$s_0 \;=\; \left(\frac{\ell^2}{m^2 g\, \sin^2\alpha\, \cos\alpha}\right)^{\frac{1}{3}},$$

and the only type of motion is bounded when $E > V_0$. The turning points for this problem are solutions of the cubic equation

$$\frac{3}{2}\,\epsilon \;=\; \frac{1}{2\sigma^2} \;+\; \sigma,$$

where $\epsilon = E/V_0$ and $\sigma = s/s_0$. Figure 3.6 shows the evolution of the three roots of this equation as the normalized energy parameter ϵ is varied. The three roots $(\sigma_0, \sigma_1, \sigma_2)$ satisfy the relations $\sigma_0\sigma_1\sigma_2 = -\frac{1}{2}$, $\sigma_0 + \sigma_1 + \sigma_2 = \frac{3}{2}\,\epsilon$, and $\sigma_1^{-1} + \sigma_2^{-1} + \sigma_0^{-1} = 0$. We see that one root (labeled σ_0) remains negative for all normalized energies ϵ; this root is unphysical since s must be positive (by definition). On the other hand, the other two roots (σ_1, σ_2), which are complex for $\epsilon < 1$ (i.e., for energies below the minumum of the effective potential energy V_0), become real at $\epsilon = 1$, where $\sigma_1 = \sigma_2$, and separate $(\sigma_1 < \sigma_2)$ for larger values of ϵ (in the limit $\epsilon \gg 1$, we find $\sigma_2 \simeq \frac{3}{2}\,\epsilon$ and $\sigma_1^{-1} \simeq -\,\sigma_0^{-1} \simeq \sqrt{3\epsilon}$). Lastly, the period of oscillation is determined by the definite integral

$$T(\epsilon) \;=\; 2\,\sqrt{\frac{s_0}{g\, \cos\alpha}} \int_{\sigma_1}^{\sigma_2} \frac{\sigma\; d\sigma}{\sqrt{3\epsilon\,\sigma^2 \;-\; 1 \;-\; 2\,\sigma^3}},$$

whose solution is expressed in terms of Weierstrass elliptic functions (see Appendix A.3.2).

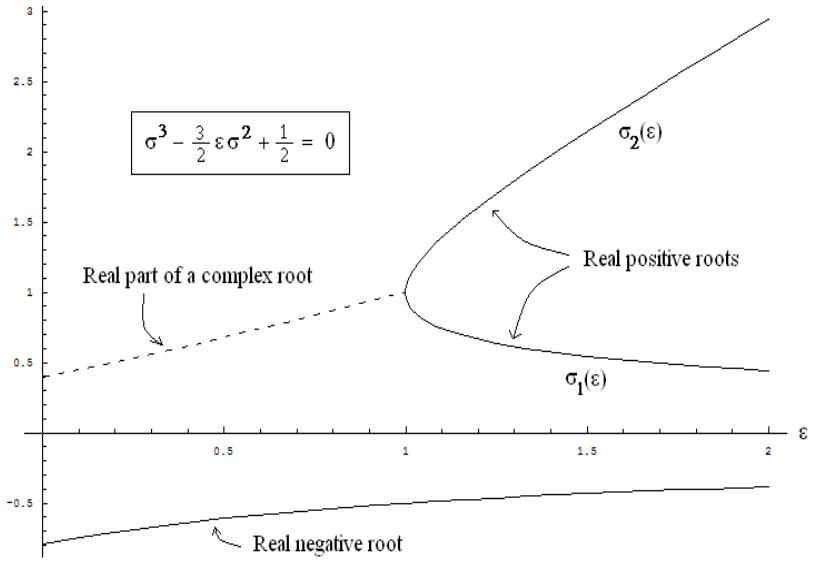

Figure 3.6: Roots of a cubic equation

3.6 Charged Spherical Pendulum in a Magnetic Field*

The following sophisticated example shows the power of the Hamiltonian method, where a system with three degrees of freedom is reduced to a system with one degree of freedom (which is, thus, integrable) as a result of the existence of two constants of motion: energy (the system is time independent) and azimuthal canonical momentum (the system is azimuthally symmetric).

A spherical pendulum of length ℓ and mass m carries a positive charge e and moves under the action of a constant gravitational field (with acceleration g) and a constant magnetic field B (see Figure 3.7). The position vector of the pendulum is $\mathbf{x} = \ell(\sin\theta\,\widehat{\rho} - \cos\theta\,\widehat{\mathsf{z}})$, and, thus, its velocity $\mathbf{v} = \dot{\mathbf{x}}$ is

$$\mathbf{v} \;=\; \ell\,\dot{\theta}\;(\cos\theta\,\widehat{\rho} \;+\; \sin\theta\,\widehat{\mathsf{z}}) \;+\; \ell\,\sin\theta\,\dot{\varphi}\,\widehat{\varphi},$$

and the kinetic energy of the pendulum is

$$K \;=\; \frac{m\,\ell^2}{2}\left(\dot{\theta}^2 \;+\; \sin^2\theta\,\dot{\varphi}^2\right).$$

3.6.1 Lagrangian and Routhian

Because the charged pendulum moves in a magnetic field $\mathbf{B} = -\,B\,\widehat{\mathsf{z}}$, we must include the magnetic term $\mathbf{v}\cdot e\mathbf{A}/c$ in the Lagrangian [see Eq. (3.16)]. Here, the vector potential $\mathbf{A}$

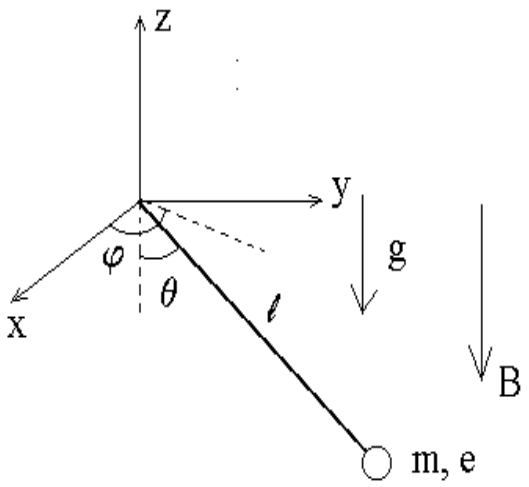

Figure 3.7: Charged pendulum in a magnetic field

must be evaluated at the position of the pendulum and is thus expressed as

$$\mathbf{A} \;=\; -\,\frac{B\ell}{2}\,\sin\theta\,\widehat{\varphi},$$

and, hence, we find

$$\frac{e}{c}\,\mathbf{A}\cdot\mathbf{v} \;=\; -\,\frac{eB\ell^2}{2c}\,\sin^2\theta\,\dot{\varphi}.$$

Note that this term is equivalent to a charged particle moving in the magnetic potential ($-\boldsymbol{\mu}\cdot\mathbf{B} = \mu_z\,B$), where

$$\boldsymbol{\mu} \;=\; \frac{e}{2mc}\,(\mathbf{x}\times\mathbf{v})$$

denotes the magnetic moment of a charge e moving about a magnetic field line. Lastly, the charged pendulum is under the influence of the gravitational potential $mg\ell\,(1-\cos\theta)$, so that by combining the various terms, the Lagrangian for the system is

$$L(\theta,\dot{\theta},\,\dot{\varphi}) \;=\; m\ell^2\left[\,\frac{\dot{\theta}^2}{2} \;+\; \sin^2\theta\left(\frac{\dot{\varphi}^2}{2} \;-\; \omega_L\,\dot{\varphi}\right)\,\right] \;-\; mg\ell\,(1-\cos\theta), \tag{3.32}$$

where the *Larmor* frequency ω_L is defined as $\omega_L = eB/2mc$. We note that, as a result of the azimuthal symmetry of the Lagrangian (3.32), the following Routh-Lagrange function $R(\theta,\dot{\theta};p_\varphi)$

$$R(\theta,\dot{\theta};p_\varphi) \;\equiv\; L \;-\; \dot{\varphi}\,\frac{\partial L}{\partial\dot{\varphi}} \;=\; \frac{m\ell^2}{2}\,\dot{\theta}^2 \;-\; V(\theta;p_\varphi)$$

may be constructed, where

$$V(\theta;p_\varphi) \;=\; mg\ell\,(1-\cos\theta) \;+\; \frac{1}{2m\ell^2\,\sin^2\theta}\left(p_\varphi \;+\; m\ell^2\omega_L\,\sin^2\theta\right)^2 \tag{3.33}$$

represents an *effective* potential under which the charged spherical pendulum moves.

3.6.2 Routh-Euler-Lagrange equations

The Routh-Euler-Lagrange equation for θ is expressed in terms of the effective potential (3.33) as

$$\frac{d}{dt}\left(\frac{\partial R}{\partial \dot\theta}\right) \;=\; \frac{\partial R}{\partial \theta} \quad\to\quad m\ell^2\,\ddot\theta \;=\; -\,\frac{\partial V}{\partial \theta},$$

which yields

$$\ddot\theta \;+\; \frac{g}{\ell}\,\sin\theta \;=\; \sin\theta\,\cos\theta\left[\,\left(\frac{p_\varphi}{m\ell^2\,\sin^2\theta}\right)^2 \;-\; \omega_L^2\,\right]. \tag{3.34}$$

Not surprisingly the integration of this second-order differential equation for θ is complex (see below). It turns out, however, that the Hamiltonian formalism gives us glimpses into the gobal structure of general solutions of this equation.

3.6.3 Hamiltonian

The Hamiltonian for the charged pendulum in a magnetic field is obtained through the Legendre transformation (3.4):

$$\begin{aligned} H \;&=\; \dot\theta\,\frac{\partial L}{\partial \dot\theta} \;+\; \dot\varphi\,\frac{\partial L}{\partial \dot\varphi} \;-\; L \\ &=\; \frac{p_\theta^2}{2m\ell^2} \;+\; \frac{1}{2m\ell^2\,\sin^2\theta}\left(p_\varphi \;+\; m\ell^2\omega_L\,\sin^2\theta\right)^2 \;+\; mg\ell\,(1-\cos\theta). \end{aligned} \tag{3.35}$$

The Hamilton's equations for (θ, p_θ) are

$$\begin{aligned} \dot\theta \;&=\; \frac{\partial H}{\partial p_\theta} \;=\; \frac{p_\theta}{m\ell^2} \\ \dot p_\theta \;&=\; -\,\frac{\partial H}{\partial \theta} \;=\; -\,mg\ell\,\sin\theta \;+\; m\ell^2\,\sin\theta\,\cos\theta\left[\,\left(\frac{p_\varphi}{m\ell^2\,\sin^2\theta}\right)^2 \;-\; \omega_L^2\,\right], \end{aligned}$$

while the Hamilton's equations for (φ, p_φ) are

$$\begin{aligned} \dot\varphi \;&=\; \frac{\partial H}{\partial p_\varphi} \;=\; \frac{p_\varphi}{m\ell^2\,\sin^2\theta} \;+\; \omega_L \\ \dot p_\varphi \;&=\; -\,\frac{\partial H}{\partial \varphi} \;=\; 0. \end{aligned}$$

It is readily seen that these Hamilton equations lead to the same equations as the Euler-Lagrange equations for θ and φ.

So what have we gained? It turns out that a most useful application of the Hamiltonian formalism resides in the use of the constants of the motion to plot Hamiltonian *orbits* in phase space. Indeed, for the problem considered here, a Hamiltonian orbit is expressed in the form $p_\theta(\theta;\ E, p_\varphi)$, i.e., each orbit is labeled by values of the two constants of motion E (the total energy) and p_φ the azimuthal canonical momentum (actually an angular momentum):

$$p_\theta \ = \ \pm \Big[\, 2\, m\ell^2 \, (E \ - \ mg\ell \ + \ mg\ell \, \cos\theta) \ - \ \frac{1}{\sin^2\theta} \Big(p_\varphi \ + \ m\ell^2 \, \sin^2\theta \, \omega_L \Big)^2 \, \Big]^{1/2} .$$

Hence, for charged pendulum of given mass m and charge e with a given Larmor frequency ω_L (and g), we can completely determine the motion of the system once initial conditions are known (from which E and p_φ can be calculated).

Numerical Box

By using the following dimensionless parameters $\Omega = \omega_L/\omega_g$ and $\alpha = p_\varphi/(m\ell^2\omega_g)$ (which can be positive or negative), we may write the effective potential (3.33) in dimensionless form $\overline{V}(\theta) = V(\theta)/(mg\ell)$ as

$$\overline{V}(\theta) \ = \ 1 \ - \ \cos\theta \ + \ \frac{1}{2} \Big(\frac{\alpha}{\sin\theta} \ + \ \Omega \ \sin\theta \Big)^2 .$$

The normalized Euler-Lagrange equations are

$$\varphi' \ = \ \Omega \ + \ \frac{\alpha}{\sin^2\theta} \quad \text{and} \quad \theta'' \ + \ \sin\theta \ = \ \sin\theta \, \cos\theta \left(\frac{\alpha^2}{\sin^4\theta} \ - \ \Omega^2 \right) \tag{3.36}$$

where $\tau = \omega_g t$ denotes the dimensionless time parameter and the dimensionless parameters are defined in terms of physical constants.

Figure 3.8 shows the dimensionless effective potential $\overline{V}(\theta)$ for $\alpha = 1$ and several values of the dimensionless parameter Ω. When Ω is below the *threshold* value $\Omega_{th} = 1.94204...$ (for $\alpha = 1$), the effective potential has a single local minimum (point a' in Figure 3.8). At threshold ($\Omega = \Omega_{th}$), an inflection point develops at point b'. Above this threshold ($\Omega > \Omega_{th}$), a local maximum (at point b) develops and two local minima (at points a and c) appear. Note that the local maximum at point b implies the existence of a separatrix solution, which separates the bounded motion in the lower well and the upper well.

Figures 3.9 show three-dimensional spherical projections (first row) and (x, y)-plane projections (second row) for three cases above threshold ($\Omega > \Omega_{th}$): motion in the lower

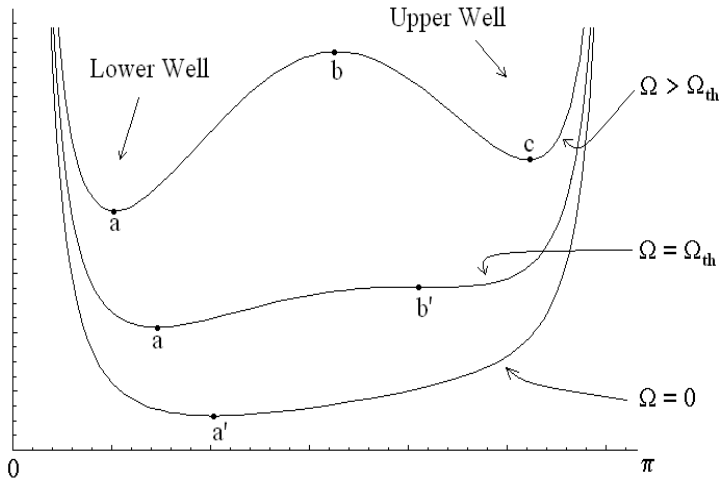

Figure 3.8: Effective potential of the charged pendulum in a magnetic field

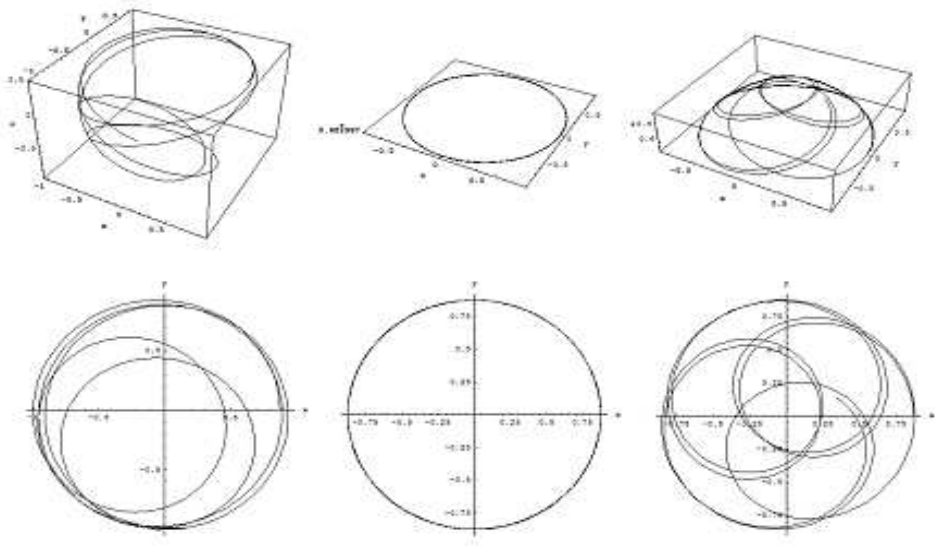

Figure 3.9: Orbits of the charged pendulum in a magnetic field.

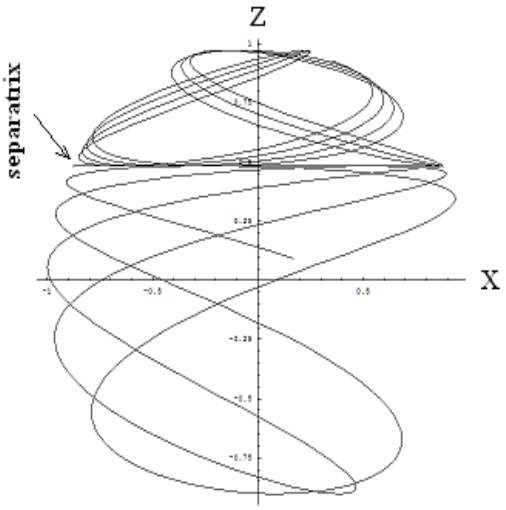

Figure 3.10: Orbit projections

well (left column), separatrix motion (center column), and motion in the upper well (right column). Figure 3.10 shows the (x, z)-plane projections for these three cases combined on the same graph. These Figures clearly show that a separatrix solution exists which separates motion in either the upper well or the lower well.

Note that the equation (3.36) for φ' does not change sign if $\alpha > -\Omega$, while its sign can change if $\alpha < -\Omega$ (or $p_\varphi < -m\ell^2\,\omega_L$). Figures 3.11 show the effect of changing $\alpha \to -\alpha$ by showing the graphs θ versus φ (first row), the (x, y)-plane projections (second row), and the (x, z)-plane projections (third row). One can clearly observe the wonderfully complex dynamics of the charged pendulum in a uniform magnetic field, which is explicitly characterized by the effective potential $V(\theta)$ given by Eq. (3.33).

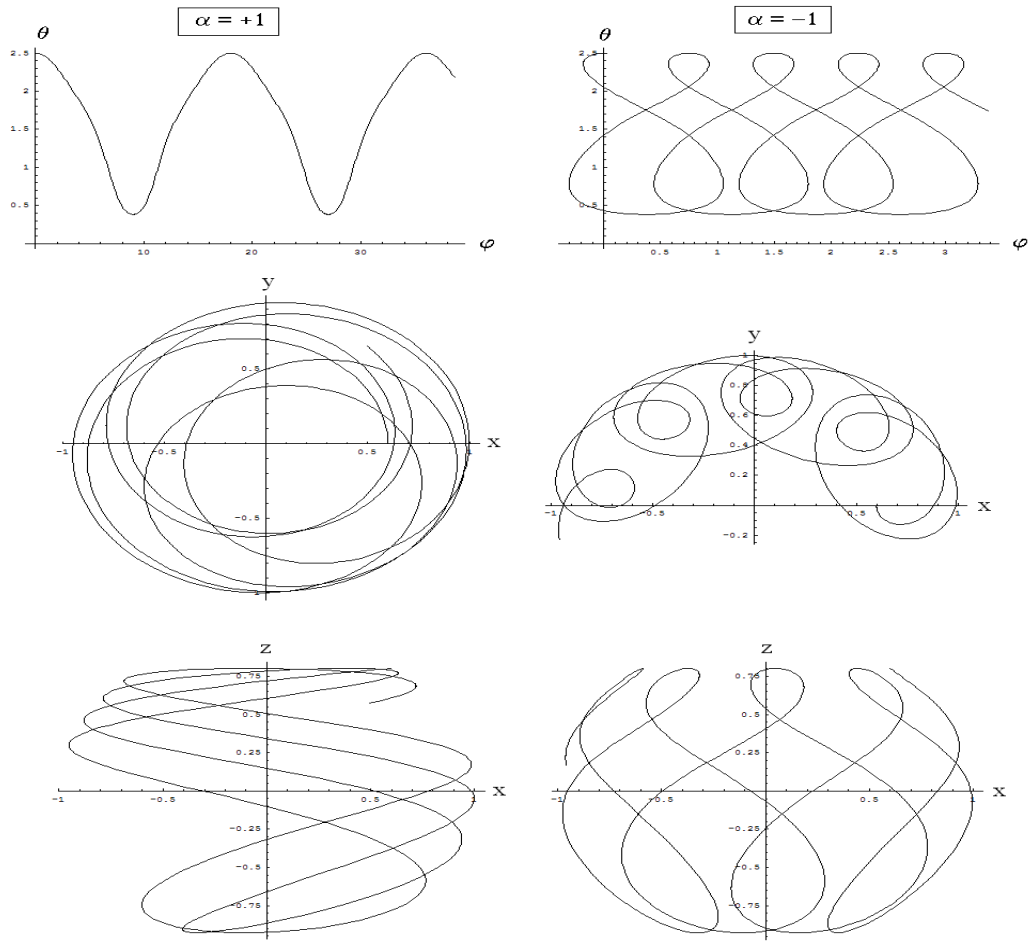

Figure 3.11: Retrograde motion

3.7 Problems

Problem 1

A particle of mass m and total energy E moves periodically in a one-dimensional potential given as

$$U(x) \;=\; F\,|x| \;=\; \begin{cases} F\,x & (x > 0) \\ \\ -\,F\,x & (x < 0) \end{cases}$$

where F is a positive constant.

(a) Find the turning points for this potential.

(b) Find the dynamical solution $x(t; E)$ for this potential by choosing a suitable initial condition.

(c) Find the period $T(E)$ for the motion.

Problem 2

A block of mass m rests on the inclined plane (with angle θ) of a triangular block of mass M as shown in the Figure below. Here, we consider the case where both blocks slide without friction (i.e., m slides on the inclined plane without friction and M slides without friction on the horizontal plane).

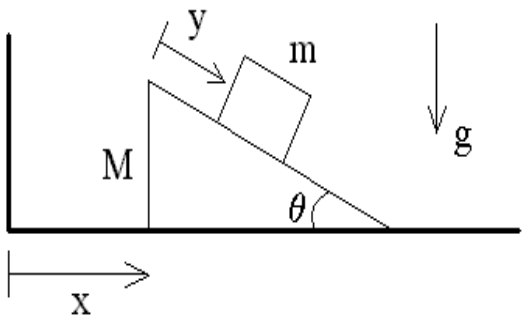

(a) Using the generalized coordinates (x, y) shown in the Figure above, construct the La-

grangian $L(x, \dot{x},\ y, \dot{y})$.

(b) Derive the Euler-Lagrange equations for x and y.

(c) Calculate the canonical momenta

$$p_x(x, \dot{x},\ y, \dot{y}) \ = \ \frac{\partial L}{\partial \dot{x}} \quad \text{and} \quad p_y(x, \dot{x},\ y, \dot{y}) \ = \ \frac{\partial L}{\partial \dot{y}},$$

and invert these expressions to find the functions $\dot{x}(x, p_x,\ y, p_y)$ and $\dot{y}(x, p_x,\ y, p_y)$.

(d) Calculate the Hamiltonian $H(x, p_x,\ y, p_y)$ for this system by using the Legendre transformation

$$H(x, p_x,\ y, p_y) \ = \ p_x\, \dot{x} \ + \ p_y\, \dot{y} \ - \ L(x, \dot{x},\ y, \dot{y}),$$

where the functions $\dot{x}(x, p_x,\ y, p_y)$ and $\dot{y}(x, p_x,\ y, p_y)$ are used.

(e) Find which of the two momenta found in Part (c) is a constant of the motion and discuss why it is so. If the two blocks start from rest, what is the value of this constant of motion?

Problem 3

Consider all possible orbits of a unit-mass particle moving in the dimensionless potential $U(x) = 1 - x^2/2 + x^4/16$. Here, orbits are solutions of the equation of motion $\ddot{x} = -\,U'(x)$ and the dimensionless energy equation is $E = \dot{x}^2/2 + U(x)$.

(a) Draw the potential $U(x)$ and identify all possible unbounded and bounded orbits (with their respective energy ranges).

(b) For each orbit found in part (a), find the turning point(s) for each energy level.

(c) Sketch the phase portrait $(x, \dot{x})$ showing all orbits (including the separatrix orbit).

(d) Show that the separatrix orbit (with initial conditions $x_0 = \sqrt{8}$ and $\dot{x}_0 = 0$) is expressed as $x(t) = \sqrt{8}\,\mathrm{sech}(t)$ by solving the integral

$$t(x) \ = \ \int_x^{\sqrt{8}} \frac{ds}{\sqrt{s^2\ (1 - s^2/8)}}.$$

(*Hint: use the hyperbolic trigonometric substitution* $s = \sqrt{8}\,\mathrm{sech}\,\xi$.)

(e) Write a numerical code to solve the second-order ordinary differential equation $\ddot{x} = x - x^3/4$ by choosing appropriate initial conditions needed to obtain all the possible orbits.

Problem 4

When a particle (of mass m) moving under the potential $U(x)$ is perturbed by the potential $\delta U(x)$, its period (3.24) is changed by a small amount defined as

$$\delta T \;=\; -\,\sqrt{2m}\,\frac{\partial}{\partial E}\left[\,\int_{x_1}^{x_2}\;\frac{\delta U(x)\,dx}{\sqrt{E-U(x)}}\,\right],$$

where $x_{1,2}$ are the turning points of the unperturbed problem. Calculate the change in the period of a particle moving in the quadratic potential $U(x) = m\omega^2\,x^2/2$ introduced by the perturbation potential $\delta U(x) = \epsilon\,x^4$. Here, ω denotes the unperturbed frequency, the particle is trapped in the region $-a \le x \le a$, and ϵ is a constant that satisfies the condition $\epsilon \ll m\omega^2/(2a^2)$.

Chapter 4

Motion in a Central-Force Field

4.1 Motion in a Central-Force Field

A particle moves under the influence of a central-force field $\mathbf{F}(\mathbf{r}) = F(r)\,\hat{\mathbf{r}}(\theta,\varphi)$ if the force on the particle is independent of the angular position (θ,φ) of the particle about the center of force and depends only on its distance r from the center of force. Here, the magnitude $F(r)$ (which is positive for a repulsive force and negative for an attractive force) is defined in terms of the central potential $U(r)$ as $F(r) = -\,U'(r)$. Note that, for a central-force potential $U(r)$, the angular momentum $\mathbf{L} = \ell\,\hat{\mathsf{z}}$ in the CM frame is a constant of the motion since $\mathbf{r} \times \nabla U(r) = 0$.

4.1.1 Lagrangian Formalism

The motion of two particles in an isolated system takes place on a two-dimensional plane, which we, henceforth, take to be the (x,y)-plane and, hence, the constant angular momentum is $\mathbf{L} = \ell\,\hat{\mathsf{z}}$. When these particles move in a central-force field, the center-of-mass Lagrangian is simply

$$L \;=\; \frac{\mu}{2}\left(\dot{r}^2 \;+\; r^2\,\dot{\theta}^2\right) \;-\; U(r), \tag{4.1}$$

where μ denotes the reduced mass for the two-particle system and polar coordinates (r,θ) are most conveniently used, with $x = r\,\cos\theta$ and $y = r\,\sin\theta$. Since the potential U is independent of θ, the canonical angular momentum

$$p_\theta \;=\; \frac{\partial L}{\partial \dot{\theta}} \;=\; \mu\,r^2\,\dot{\theta} \;\equiv\; \ell \tag{4.2}$$

is a constant of motion (labeled ℓ). The Euler-Lagrange equation for r, therefore, becomes the radial force equation

$$\mu\left(\ddot{r} \;-\; r\,\dot{\theta}^2\right) \;=\; \mu\,\ddot{r} \;-\; \frac{\ell^2}{\mu\,r^3} \;=\; F(r) \;\equiv\; -\,U'(r). \tag{4.3}$$

In this description, the planar orbit is parametrized by time, i.e., once $r(t)$ and $\theta(t)$ are obtained, a path $r(\theta)$ onto the plane is defined.

Since $\dot{\theta} = \ell/\mu r^2$ does not change sign on its path along the orbit (as a result of the conservation of angular momentum), we may replace $\dot{r}$ and $\ddot{r}$ with $r'(\theta)$ and $r''(\theta)$ as follows. First, we begin with

$$\dot{r} \;=\; \dot{\theta}\,r' \;=\; \frac{\ell\,r'}{\mu\,r^2} \;=\; -\,\frac{\ell}{\mu}\left(\frac{1}{r}\right)' \;=\; -\,(\ell/\mu)\,s',$$

where we use the conservation of angular momentum and define the new dependent variable $s(\theta) = 1/r(\theta)$. Next, we write $\ddot{r} = -\,(\ell/\mu)\,\dot{\theta}\,s'' = -\,(\ell/\mu)^2\,s^2\,s''$, so that the radial force equation (4.3) becomes

$$s'' \;+\; s \;=\; -\,\frac{\mu}{\ell^2\,s^2}\,F(1/s) \;\equiv\; -\,\frac{d\overline{U}(s)}{ds}, \tag{4.4}$$

where

$$\overline{U}(s) \;=\; \frac{\mu}{\ell^2}\,U(1/s) \tag{4.5}$$

denotes the normalized central potential expressed as a function of s.

Note that the form of the potential $U(r)$ can be calculated from the function $s(\theta) = 1/r(\theta)$. For example, consider the particle trajectory described in terms of the function $r(\theta) = r_0\,\sec(\alpha\,\theta)$, where r_0 and α are constants. The radial equation (4.4) then becomes

$$s'' \;+\; s \;=\; -\,\left(\alpha^2 \;-\; 1\right)\,s \;=\; -\,\frac{d\overline{U}(s)}{ds},$$

and thus

$$\overline{U}(s) \;=\; \frac{1}{2}\,\left(\alpha^2 \;-\; 1\right)\,s^2 \quad\rightarrow\quad U(r) \;=\; \frac{\ell^2}{2\mu\,r^2}\left(\alpha^2 \;-\; 1\right).$$

We note here that, as expected, the central potential is either repulsive for $\alpha > 1$ or attractive for $\alpha < 1$ (see Figure 4.1). Note also that the function $\theta(t)$ is determined from the relation

$$\dot{\theta} \;=\; \frac{\ell}{\mu r^2(\theta)} \quad\rightarrow\quad t(\theta) \;=\; \frac{\mu}{\ell}\,\int_0^\theta\,r^2(\phi)\,d\phi.$$

Hence, we find

$$t(\theta) \;=\; \frac{\mu r_0^2}{\alpha\ell}\,\int_0^{\alpha\theta}\,\sec^2\phi\,d\phi \;=\; \frac{\mu r_0^2}{\alpha\ell}\,\tan(\alpha\theta) \quad\rightarrow\quad r(t) \;=\; r_0\,\sqrt{1 \;+\; \left(\frac{\alpha\ell\,t}{\mu r_0^2}\right)^2}$$

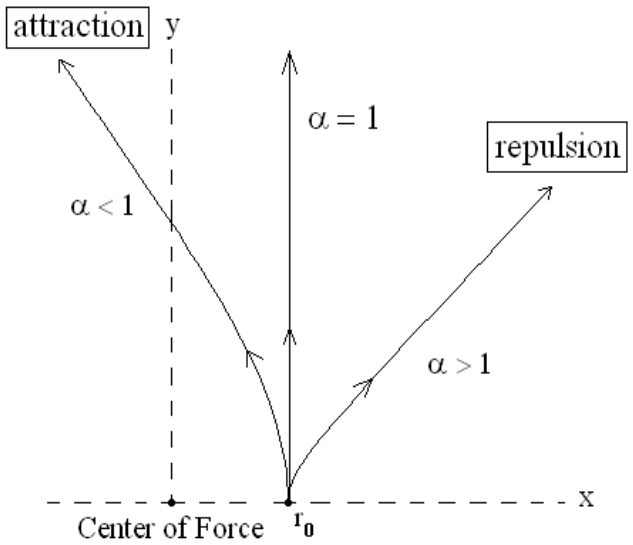

Figure 4.1: Repulsive ($\alpha > 1$) and attractive ($\alpha < 1$) orbits for the central-force potential $U(r) = (\ell^2/2\mu)\,(\alpha^2 - 1)\,r^{-2}$.

and the total energy

$$E \;=\; \frac{\alpha^2\,\ell^2}{2\mu r_0^2},$$

is determined from the initial conditions $r(0) = r_0$ and $\dot{r}(0) = 0$.

4.1.2 Hamiltonian Formalism

The Hamiltonian for the central-force problem (4.1) is

$$H \;=\; \frac{p_r^2}{2\mu} \;+\; \frac{\ell^2}{2\,\mu\,r^2} \;+\; U(r),$$

where $p_r = \mu\,\dot{r}$ is the radial canonical momentum and ℓ is the conserved angular momentum. Since energy is also conserved, we solve the energy equation

$$E \;=\; \frac{\mu\,\dot{r}^2}{2} \;+\; \frac{\ell^2}{2\,\mu\,r^2} \;+\; U(r)$$

for $\dot{r}(r; E, \ell)$ as

$$\dot{r} \;=\; \pm\sqrt{\frac{2}{\mu}\,[\,E \;-\; V(r)\,]}, \tag{4.6}$$

where

$$V(r) \;=\; \frac{\ell^2}{2\,\mu\,r^2} \;+\; U(r) \tag{4.7}$$

is the *effective* potential for central-force problems and the sign $\pm$ in Eq. (4.6) depends on initial conditions. Hence, Eq. (4.6) yields the integral solution

$$t(r; E, \ell) \;=\; \pm \int \frac{dr}{\sqrt{(2/\mu)\;[E - V(r)]}}. \tag{4.8}$$

We can also the energy equation

$$\mu E/\ell^2 \;=\; \frac{s'^2}{2} \;+\; \frac{s^2}{2} \;+\; \overline{U}(s), \tag{4.9}$$

to obtain

$$s'(\theta) \;=\; \pm \sqrt{\epsilon - 2\,\overline{U}(s) \;-\; s^2}, \tag{4.10}$$

where the normalized energy ϵ is defined as

$$\epsilon \;=\; \frac{2\mu\, E}{\ell^2}. \tag{4.11}$$

Hence, for a given central-force potential $U(r)$, we can solve for $r(\theta) = 1/s(\theta)$ by integrating

$$\theta(s) \;=\; -\int_{s_0}^{s} \frac{d\sigma}{\sqrt{\epsilon - 2\,\overline{U}(\sigma) \;-\; \sigma^2}}, \tag{4.12}$$

where s_0 defines $\theta(s_0) = 0$, and performing the inversion $\theta(s) \rightarrow s(\theta) = 1/r(\theta)$.

4.1.3 Turning Points

Eq. (4.10) yields the following energy equation

$$E \;=\; \frac{\mu}{2}\,\dot{r}^2 \;+\; \frac{\ell^2}{2\mu\, r^2} \;+\; U(r) \;=\; \frac{\ell^2}{2\mu}\left[\;(s')^2 \;+\; s^2 \;+\; 2\,\overline{U}(s)\;\right],$$

where $s' = -\,\mu\dot{r}/\ell$. *Turning* points are those special values of r_n (or s_n) $(n = 1, 2, ...)$ for which

$$E \;=\; U(r_n) \;+\; \frac{\ell^2}{2\mu\, r_n^2} \;=\; \frac{\ell^2}{\mu}\left[\;\overline{U}(s_n) \;+\; \frac{s_n^2}{2}\;\right],$$

i.e., $\dot{r}$ (or s') vanishes at these points. If two non-vanishing turning points $r_2 < r_1 < \infty$ (or $0 < s_1 < s_2$) exist, the motion is said to be *bounded* in the interval $r_2 < r < r_1$ (or $s_1 < s < s_2$), otherwise the motion is *unbounded*. If the motion is bounded, the angular period $\Delta\theta$ is defined as

$$\Delta\theta(s) \;=\; 2\int_{s_1}^{s_2} \frac{ds}{\sqrt{\epsilon - 2\,\overline{U}(s) \;-\; s^2}}. \tag{4.13}$$

Here, the bounded orbit is *closed* only if $\Delta\theta$ is a rational multiple of 2π.

4.2 Homogeneous Central Potentials*

An important class of central potentials is provided by homogeneous potentials that satisfy the condition $U(\lambda\,\mathbf{r}) = \lambda^n\,U(\mathbf{r})$, where λ denotes a rescaling parameter and n denotes the *order* of the homogeneous potential.

4.2.1 The Virial Theorem

The Virial Theorem is an important theorem in Celestial Mechanics and Astrophysics. We begin with the time derivative of the quantity $S = \sum_i\ \mathbf{p}_i \cdot \mathbf{r}_i$:

$$\frac{dS}{dt}\ =\ \sum_i \left(\frac{d\mathbf{p}_i}{dt}\cdot\mathbf{r}_i\ +\ \mathbf{p}_i\cdot\frac{d\mathbf{r}_i}{dt}\right), \tag{4.14}$$

where the summation is over all particles in a mechanical system under the influence of a self-interaction potential

$$U\ =\ \frac{1}{2}\ \sum_{i,\,j\neq i} U(\mathbf{r}_i - \mathbf{r}_j).$$

We note, however, that since Q itself can be written as a time derivative

$$S\ =\ \sum_i\ m_i\,\frac{d\mathbf{r}_i}{dt}\cdot\mathbf{r}_i\ =\ \frac{d}{dt}\left(\frac{1}{2}\ \sum_i\ m_i\ |\mathbf{r}_i|^2\right)\ =\ \frac{1}{2}\ \frac{d\mathcal{I}}{dt},$$

where $\mathcal{I}$ denotes the *moment of inertia* of the system and that, using Hamilton's equations

$$\frac{d\mathbf{r}_i}{dt}\ =\ \frac{\mathbf{p}_i}{m_i}\quad\text{and}\quad\frac{d\mathbf{p}_i}{dt}\ =\ -\ \sum_{j\neq i}\ \nabla_i\,U(\mathbf{r}_i - \mathbf{r}_j),$$

Eq. (4.14) can also be written as

$$\frac{1}{2}\ \frac{d^2\mathcal{I}}{dt^2}\ =\ \sum_i \left(\frac{|\mathbf{p}_i|^2}{m_i}\ -\ \mathbf{r}_i\cdot\sum_{j\neq i}\ \nabla_i U_{ij}\right)\ =\ 2\ K\ -\ \sum_{i,\,j\neq i}\ \mathbf{r}_i\cdot\nabla_i U_{ij}, \tag{4.15}$$

where K denotes the kinetic energy of the mechanical system. Next, using Newton's Third Law, we write

$$\sum_{i,\,j\neq i}\ \mathbf{r}_i\cdot\nabla_i U_{ij}\ =\ \frac{1}{2}\ \sum_{i,\,j\neq i}\ (\mathbf{r}_i - \mathbf{r}_j)\cdot\nabla U(\mathbf{r}_i - \mathbf{r}_j),$$

and, for a homogeneous central potential of order n, we find $\mathbf{r}\cdot\nabla U(\mathbf{r}) = n\,U(\mathbf{r})$, so that

$$\frac{1}{2}\ \sum_{i,\,j\neq i}\ (\mathbf{r}_i - \mathbf{r}_j)\cdot\nabla U(\mathbf{r}_i - \mathbf{r}_j)\ =\ n\,U.$$

Hence, Eq. (4.15) becomes the *virial of Clausius* (Rudolph Clausius, 1822-1888)

$$\frac{1}{2}\,\frac{d^2\mathcal{I}}{dt^2} \;=\; 2\,K \;-\; n\,U. \tag{4.16}$$

If we now assume that the mechanical system under consideration is periodic in time, then the time average (denoted $\langle\cdots\rangle$) of Eq. (4.16) yields the Virial Theorem

$$\langle K\rangle \;=\; \frac{n}{2}\,\langle U\rangle, \tag{4.17}$$

so that the time-average of the total energy of the mechanical system, $E = K + U$, is expressed as

$$E \;=\; \begin{cases} (1+n/2)\,\langle U\rangle \\ \\ (1+2/n)\,\langle K\rangle \end{cases}$$

since $\langle E\rangle = E$. For example, for the Kepler problem ($n = -1$), we find

$$E \;=\; \frac{1}{2}\langle U\rangle \;=\; -\,\langle K\rangle \;<\; 0, \tag{4.18}$$

which means that the total energy of a bounded Keplerian orbit is negative (see Sec. 4.3.1).

4.2.2 General Properties of Homogeneous Potentials

We now investigate the dynamical properties of orbits in homogeneous central potentials of the form $U(r) = (k/n)\,r^n$ ($n \neq -2$), where k denotes a positive constant. Note that the central force $\mathbf{F} = -\nabla U = -\,k\,r^{n-1}\,\hat{\mathsf{r}}$ is attractive if $k > 0$.

First, the effective potential (4.7) has an extremum at a distance $r_0 = 1/s_0$ defined as

$$r_0^{n+2} \;=\; \frac{\ell^2}{k\mu} \;=\; \frac{1}{s_0^{n+2}}.$$

It is simple to show that this extremum is a maximum if $n < -2$ or a minimum if $n > -2$; we shall, henceforth, focus our attention on the latter case, where the minimum in the effective potential is

$$V_0 \;=\; V(r_0) \;=\; \left(1 \;+\; \frac{n}{2}\right)\frac{k}{n}\,r_0^n \;=\; \left(1 \;+\; \frac{n}{2}\right)U_0.$$

In the vicinity of this minimum, we can certainly find periodic orbits with turning points ($r_2 = 1/s_2 < r_1 = 1/s_1$) that satisfy the condition $E = V(r)$.

Next, the radial equation (4.4) is written in terms of the potential $\overline{U}(s) = (\mu/\ell^2)\,U(1/s)$ as

$$s'' \;+\; s \;=\; -\,\frac{d\overline{U}}{ds} \;=\; \frac{s_0^{n+2}}{s^{n+1}},$$

and its solution is given as

$$\theta(s) \;=\; \int_s^{s_2} \frac{d\sigma}{\sqrt{\epsilon - (2/n)\, s_0^{n+2}/\sigma^n \;-\; \sigma^2}}, \tag{4.19}$$

where s_2 denotes the upper turning point in the s-coordinate. The solution (4.19) can be expressed in terms of closed analytic expressions obtained by trigonometric substitution only for $n = -1$ or $n = 2$ (when $\epsilon \neq 0$), which we now study in detail below (the cases $n = -3$ and -4, for example, are solved in terms of elliptic functions as is briefly discussed in Appendix A).

4.3 Kepler Problem

In this Section, we solve the Kepler problem where the central potential $U(r) = -\,k/r$ is homogeneous with order $n = -1$ and k is a positive constant. The Virial Theorem (4.17), therefore, implies that periodic solutions of the Kepler problem have negative total energies $E = -\,\langle K\rangle = (1/2)\,\langle U\rangle$.

We now turn to the general solution of the Kepler problem

$$\mu\,\ddot{r} \;=\; \frac{\ell^2}{\mu\, r^3} \;-\; \frac{k}{r^2} \quad \text{and} \quad \dot{\theta} \;=\; \frac{\ell}{\mu\, r^2},$$

whose orbits are either periodic or aperiodic (see Figure 4.2). To obtain an analytic solution $r(\theta)$ for the Kepler problem, as expressed by the radial force equation (4.4), we use the normalized central potential $\overline{U}(s) \;=\; -\,s_0 s$, where $s_0 \;=\; \mu k/\ell^2$, and Eq. (4.4) becomes $s'' + s = s_0$. Next, the turning points for the Kepler problem are solutions of the quadratic equation

$$s^2 \;-\; 2\, s_0\; s \;-\; \epsilon \;=\; 0,$$

which can be written as $s_{1,2} = s_0 \pm \sqrt{s_0^2 + \epsilon}$:

$$s_1 \;=\; s_0\,(1 - \mathsf{e}) \quad \text{and} \quad s_2 \;=\; s_0\,(1 + \mathsf{e}),$$

where the eccentricity is defined as

$$\mathsf{e} \;=\; \sqrt{1 + \epsilon/s_0^2} \;=\; \sqrt{1 \;+\; 2\; E\ell^2/\mu k^2}.$$

We clearly see from the Figure 4.2 that the effective potential

$$V(r) \;=\; \frac{\ell^2}{2\mu\, r^2} \;-\; \frac{k}{r}$$

for the Kepler problem has a single minimum at $r_0 = \ell^2/(k\mu)$ and that $V_0 = -\,k/(2r_0)$. We note that motion is bounded (i.e., orbits are periodic) when $E_0 = -\,k/(2r_0) \leq E < 0$ $(0 \leq \mathsf{e} < 1)$, and the motion is unbounded (i.e., orbits are aperiodic) when $E \geq 0$ $(\mathsf{e} \geq 1)$ (see Figure 4.2).

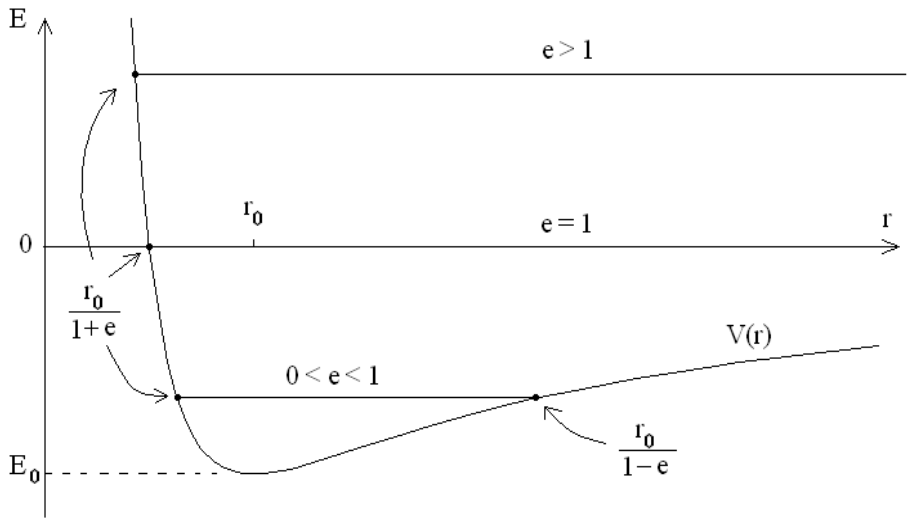

Figure 4.2: Effective potential for the Kepler problem

4.3.1 Bounded Keplerian Orbits

We look at the bounded case ($\epsilon < 0$ or $\mathsf{e} < 1$) first. We define $\theta(s_2) = 0$, so that for the Kepler problem, Eq. (4.12) becomes

$$\theta(s) \;=\; -\int_{s_0\,(1+\mathsf{e})}^{s} \frac{d\sigma}{\sqrt{s_0^2\mathsf{e}^2 - (\sigma - s_0)^2}}, \tag{4.20}$$

which can easily be integrated to yield (see Appendix A)

$$\theta(s) \;=\; \arccos\left(\frac{s - s_0}{s_0\,\mathsf{e}}\right),$$

and we easily verify that $\Delta\theta = 2\pi$, i.e., the bounded orbits of the Kepler problem are closed. This equation can be inverted to yield

$$s(\theta) \;=\; s_0\,(1 \;+\; \mathsf{e}\,\cos\theta), \tag{4.21}$$

where we readily check that this solution also satisfies the radial force equation (4.4).

Kepler's First Law

The solution for $r(\theta)$ is now trivially obtained from $s(\theta)$ as

$$r(\theta) \;=\; \frac{r_0}{1 \;+\; \mathsf{e}\,\cos\theta}, \tag{4.22}$$

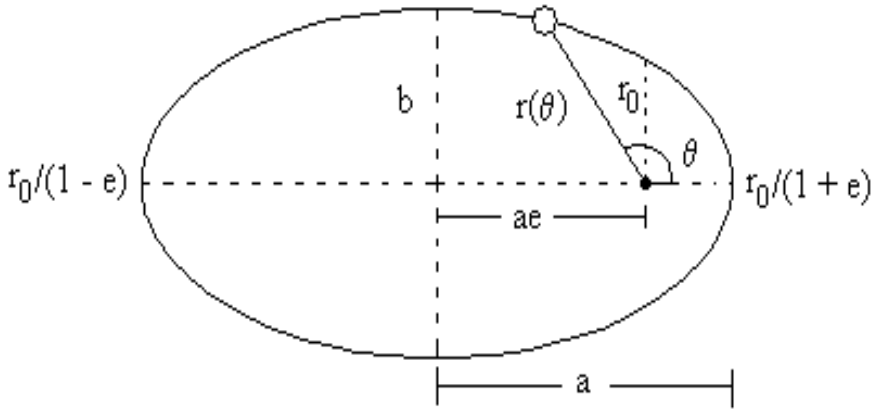

Figure 4.3: Elliptical orbit for the Kepler problem

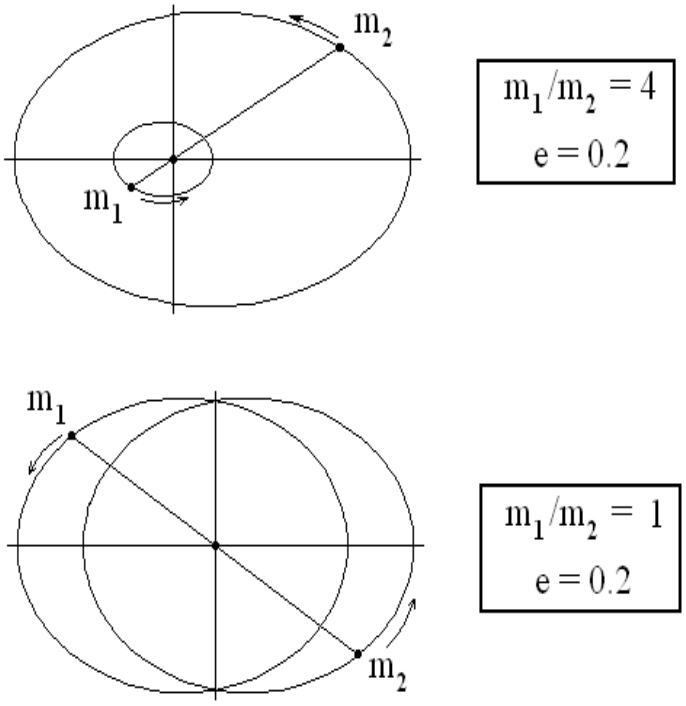

Figure 4.4: Keplerian two-body orbit

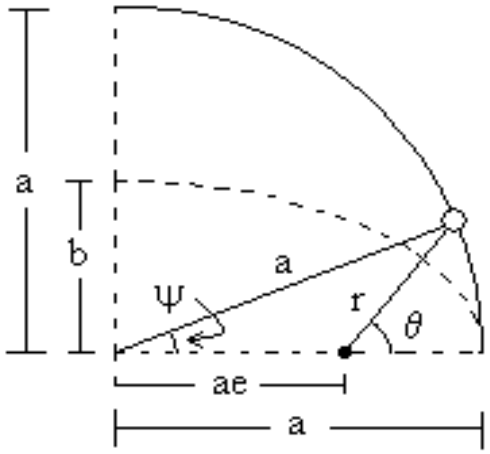

Figure 4.5: Eccentric anomaly

where $r_0 = 1/s_0$ denotes the position of the minimum of the *effective* potential $V'(r_0) = 0$.

Eq. (4.22) generates an ellipse of semi-major axis

$$2\,a \;=\; \frac{r_0}{1+\mathsf{e}} + \frac{r_0}{1-\mathsf{e}} \;\;\rightarrow\;\; a \;=\; \frac{r_0}{1-\mathsf{e}^2} \;=\; \sqrt{\frac{k}{2\,|E|}}$$

and semi-minor axis $b = a\sqrt{1-\mathsf{e}^2} = \sqrt{\ell^2/(2\mu\,|E|)}$ and, therefore, yields Kepler's First Law. When we plot the positions of the two objects (of mass m_1 and m_2, respectively) by using Kepler's first law (4.22), with the positions $\mathbf{r}_1$ and $\mathbf{r}_2$ determined by Eqs. (2.43), we obtain Figure 4.4. It is interesting to note that by detecting the small wobble motion of a distant star (with mass m_2), it has been possible to discover extra-solar planets (with masses $m_1 < m_2$).

Note that by using the eccentric anomaly angle ψ (see Figure 4.5), we find $a\cos\psi = a\,\mathsf{e} + r\cos\theta$ from which we obtain $\cos\psi = (\mathsf{e}+\cos\theta)/(1+\mathsf{e}\cos\theta)$ or $\cos\theta = (\cos\psi - \mathsf{e})/(1-\mathsf{e}\cos\psi)$. By substituting this last expression into Kepler's First Law (4.22), we obtain $r(\psi) = a\,(1 - e\,\cos\psi)$.

Kepler's Second Law

Using Eq. (4.2), we find

$$dt \;=\; \frac{\mu}{\ell}\,r^2\,d\theta \;=\; \frac{2\mu}{\ell}\,dA(\theta),$$

where $dA(\theta) = (\int r\, dr)\, d\theta = \frac{1}{2}\,[r(\theta)]^2\, d\theta$ denotes an infinitesimal area swept by $d\theta$ at radius $r(\theta)$. When integrated, this relation yields Kepler's Second law

$$\Delta t \;=\; \frac{2\mu}{\ell}\,\Delta A, \tag{4.23}$$

i.e., equal areas ΔA are swept in equal times Δt since μ and ℓ are constants.

Kepler's Third Law

The orbital period T of a bound system is defined as

$$T \;=\; \int_0^{2\pi} \frac{d\theta}{\dot\theta} \;=\; \frac{\mu}{\ell}\int_0^{2\pi} r^2\, d\theta \;=\; \frac{2\mu}{\ell}\,A \;=\; \frac{2\pi\,\mu}{\ell}\,a\,b$$

where $A = \pi\, ab$ denotes the area of an ellipse with semi-major axis a and semi-minor axis b; here, we used the identity

$$\int_0^{2\pi} \frac{d\theta}{(1+\mathsf{e}\,\cos\theta)^2} \;=\; \frac{2\pi}{(1-\mathsf{e}^2)^{3/2}}.$$

Using the expressions for a and b found above, we find

$$T \;=\; \frac{2\pi\,\mu}{\ell}\;\cdot\;\frac{k}{2|E|}\;\cdot\;\sqrt{\frac{\ell^2}{2\mu\,|E|}} \;=\; 2\pi\,\sqrt{\frac{\mu\,k^2}{(2\,|E|)^3}}.$$

If we now substitute the expression for $a = k/2|E|$ and square both sides of this equation, we obtain Kepler's Third Law

$$T^2 \;=\; \frac{(2\pi)^2\mu}{k}\,a^3. \tag{4.24}$$

In Newtonian gravitational theory, where $k/\mu = G\,(m_1 + m_2)$, we find that, although Kepler's Third Law states that T^2/a^3 is a constant for all planets in the solar system, which is only an approximation that holds for $m_1 \gg m_2$ (true for all solar planets).

4.3.2 Unbounded Keplerian Orbits

We now look at the case where the total energy is positive or zero (i.e., $\mathsf{e} \geq 1$). Eq. (4.22) yields $r\,(1+\mathsf{e}\,\cos\theta) = r_0$ or the hyperbola equation

$$\left(\sqrt{\mathsf{e}^2-1}\;x \;-\; \frac{\mathsf{e}\,r_0}{\sqrt{\mathsf{e}^2-1}}\right)^2 \;-\; y^2 \;=\; \frac{r_0^2}{\mathsf{e}^2-1}.$$

For $\mathsf{e} = 1$, the particle orbit is a parabola $x = (r_0^2 - y^2)/2r_0$, with distance of closest approach at $x(0) = r_0/2$.

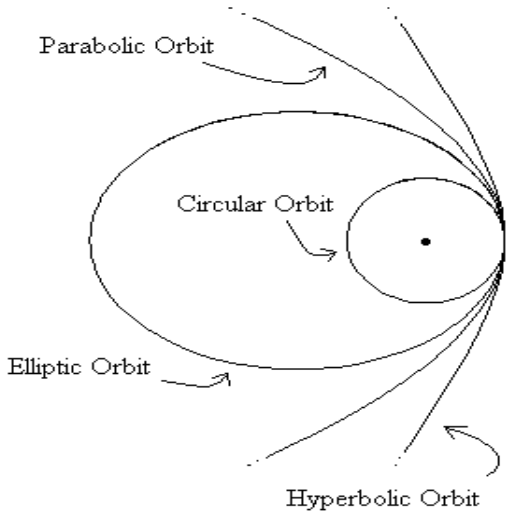

Figure 4.6: Bounded and unbounded orbits for the Kepler problem

4.3.3 Laplace-Runge-Lenz Vector*

Since the orientation of the unperturbed Keplerian ellipse is constant (i.e., it does not precess), it turns out there exists a third constant of the motion for the Kepler problem (in addition to energy and angular momentum); we note, however, that only two of these three invariants are independent.

Let us now investigate this additional constant of the motion for the Kepler problem. First, we consider the time derivative of the vector $\mathbf{p} \times \mathbf{L}$, where the linear momentum $\mathbf{p}$ and angular momentum $\mathbf{L}$ are

$$\mathbf{p} \;=\; \mu \left(\dot{r}\, \widehat{r} \;+\; r\dot{\theta}\, \widehat{\theta} \right) \quad \text{and} \quad \mathbf{L} \;=\; \ell\, \widehat{z} \;=\; \mu r^2 \dot{\theta}\, \widehat{z}.$$

The time derivative of the linear momentum is $\dot{\mathbf{p}} = -\nabla U(r) = -U'(r)\, \widehat{r}$ while the angular momentum $\mathbf{L} = \mathbf{r} \times \mathbf{p}$ is itself a constant of the motion so that

$$\begin{aligned} \frac{d}{dt}\left(\mathbf{p} \times \mathbf{L}\right) \;&=\; \frac{d\mathbf{p}}{dt} \times \mathbf{L} \;=\; -\,\mu\, \nabla U \times \left(\mathbf{r} \times \dot{\mathbf{r}}\right) \\ &=\; -\,\mu \dot{\mathbf{r}} \cdot \nabla U\; \mathbf{r} \;+\; \mu \mathbf{r} \cdot \nabla U\; \dot{\mathbf{r}}. \end{aligned}$$

By re-arranging some terms (and using $\dot{\mathbf{r}} \cdot \nabla U = dU/dt$ for time-independent potentials), we find

$$\frac{d}{dt}\left(\mathbf{p} \times \mathbf{L}\right) \;=\; -\,\frac{d}{dt}\left(\mu\, U\; \mathbf{r}\right) \;+\; \mu \left(\mathbf{r} \cdot \nabla U \;+\; U\right) \dot{\mathbf{r}},$$

or

$$\frac{d\mathbf{A}}{dt} \;=\; \mu \left(\mathbf{r} \cdot \nabla U \;+\; U\right) \dot{\mathbf{r}}, \tag{4.25}$$

where the Laplace-Runge-Lenz (LRL) vector is defined as

$$\mathbf{A} \;=\; \mathbf{p}\times\mathbf{L} \;+\; \mu\, U(r)\;\mathbf{r}. \tag{4.26}$$

We immediately note that the LRL vector (4.26) is a constant of the motion if the potential $U(r)$ satisfies the condition

$$\mathbf{r}\cdot\nabla U(r) \;+\; U(r) \;=\; \frac{d(r\,U)}{dr} \;=\; 0.$$

For the Kepler problem, with $U(r) = -\,k/r$, the vector (4.26) becomes

$$\mathbf{A} \;=\; \mathbf{p}\times\mathbf{L} \;-\; k\mu\,\widehat{r} \;=\; \left(\frac{\ell^2}{r} \;-\; k\mu\right)\widehat{r} \;-\; \ell\,\mu\dot{r}\;\widehat{\theta}, \tag{4.27}$$

which is a constant of the motion since $\mathbf{r}\cdot\nabla U = -\,U$.

Since the vector $\mathbf{A}$ is constant in both magnitude and direction, its magnitude is a constant

$$|\mathbf{A}|^2 \;=\; 2\mu\,\ell^2\left(\frac{p^2}{2\mu} \;+\; U\right) \;+\; k^2\mu^2 \;=\; k^2\mu^2\left(1 \;+\; \frac{2\ell^2 E}{\mu k^2}\right) \;=\; k^2\mu^2\mathsf{e}^2.$$

Here, we choose its direction to be along the x-axis ($\mathbf{A} = k\mu\mathsf{e}\,\widehat{\mathbf{x}}$) and its constant amplitude ($|\mathbf{A}| = k\mu\mathsf{e}$) is determined at the distance of closest approach $r_{min} = r_0/(1+\mathsf{e})$. We can easily show that

$$\left(\frac{\ell^2}{r} \;-\; k\,\mu\right) \;=\; \mathbf{A}\cdot\widehat{r} \;\equiv\; (k\mu\,\mathsf{e})\,\cos\theta$$

leads to the Kepler solution

$$r(\theta) \;=\; \frac{r_0}{1+\mathsf{e}\,\cos\theta},$$

where $r_0 = \ell^2/k\mu$ and the orbit's eccentricity is $\mathsf{e} = |\mathbf{A}|/k\mu$.

Note that if the Keplerian orbital motion is perturbed by the introduction of an additional potential term $\delta U(r)$, we find

$$\frac{d\mathbf{A}}{dt} \;=\; (\delta U \;+\; \mathbf{r}\cdot\nabla\delta U)\;\mathbf{p},$$

where $\mathbf{A} = \mathbf{A}_0 + \mu\,\delta U\,\mathbf{r}$ and, thus, we obtain the cross product (to lowest order in δU)

$$\mathbf{A}_0\times\frac{d\mathbf{A}}{dt} \;=\; (\delta U \;+\; \mathbf{r}\cdot\nabla\delta U)\;\left(p^2 \;+\; \mu\,U\right)\;\mathbf{L},$$

where $U = -\,k/r$ is the unperturbed Kepler potential. Next, using the expression for the unperturbed total energy

$$E \;=\; \frac{p^2}{2\mu} \;+\; U \;=\; -\,\frac{k}{2a},$$

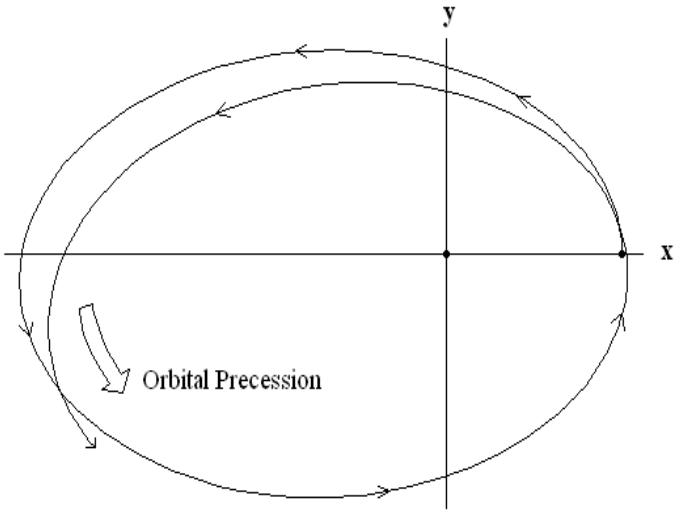

Figure 4.7: Perturbed Kepler problem

we define the precession frequency

$$\begin{aligned}\omega_{\rm p}(\theta) \;&=\; \widehat{\mathsf{z}}\cdot\frac{\mathbf{A}_0}{|\mathbf{A}_0|^2}\times\frac{d\mathbf{A}}{dt} \;=\; (\delta U \;+\; \mathbf{r}\cdot\nabla\delta U)\;\frac{\ell\,\mu}{(\mu k\mathsf{e})^2}\;(2\,E\;-\;U)\\ &=\; (\delta U \;+\; \mathbf{r}\cdot\nabla\delta U)\;\frac{\ell\mu k}{(\mu k\mathsf{e})^2}\;\left(\frac{1}{r}\;-\;\frac{1}{a}\right).\end{aligned}$$

Hence, using $a = r_0/(1-\mathsf{e}^2)$, the precession frequency is

$$\omega_{\rm p}(\theta) \;=\; \frac{1}{\ell}\;\Big(1\;+\;\mathsf{e}^{-1}\,\cos\theta\Big)\,(\delta U\;+\;\mathbf{r}\cdot\nabla\delta U)\,.$$

and the net precession shift $\delta\theta$ of the Keplerian orbit over one unperturbed period is

$$\delta\theta \;=\; \int_0^{2\pi}\;\omega_{\rm p}(\theta)\;\frac{d\theta}{\dot\theta} \;=\; \int_0^{2\pi}\;\left(\frac{1+\mathsf{e}^{-1}\,\cos\theta}{1+\mathsf{e}\,\cos\theta}\right)\;\left[\;r\;\frac{d}{dr}\left(\frac{r\;\delta U}{k}\right)\;\right]_{r=r(\theta)}\;d\theta.$$

For example, if $\delta U = -\,\epsilon/r^2$, then $r\;d(r\delta U/k)/dr = \epsilon/kr$ and the net precession shift is

$$\delta\theta \;=\; \frac{\epsilon}{kr_0}\;\int_0^{2\pi}\;\Big(1+\mathsf{e}^{-1}\,\cos\theta\Big)\;d\theta \;=\; 2\pi\;\frac{\epsilon}{kr_0}.$$

Figure 4.7 shows the numerical solution of the perturbed Kepler problem for the case where $\epsilon \simeq kr_0/16$.

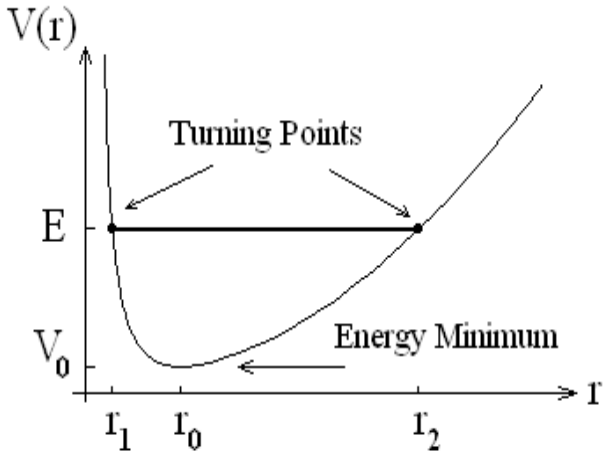

Figure 4.8: Effective potential for the isotropic simple harmonic oscillator problem

4.4 Isotropic Simple Harmonic Oscillator

As a second example of a central potential with closed bounded orbits, we now investigate the case when the central potential is of the form

$$U(r) \;=\; \frac{k}{2}\, r^2 \quad \rightarrow \quad \overline{U}(s) \;=\; \frac{\mu k}{2\ell^2\; s^2}. \tag{4.28}$$

The turning points for this problem are expressed as

$$r_1 \;=\; r_0 \left(\frac{1-\mathsf{e}}{1+\mathsf{e}}\right)^{\frac{1}{4}} \;=\; \frac{1}{s_1} \quad \text{and} \quad r_2 \;=\; r_0 \left(\frac{1+\mathsf{e}}{1-\mathsf{e}}\right)^{\frac{1}{4}} \;=\; \frac{1}{s_2},$$

where $r_0 = \sqrt{r_1\, r_2} = (\ell^2/\mu k)^{1/4} = 1/s_0$ is the radial position at which the effective potential has a minimum, i.e., $V'(r_0) = 0$ and $V_0 = V(r_0) = k\, r_0^2$ and

$$\mathsf{e} \;=\; \sqrt{1 \;-\; \left(\frac{k r_0^2}{E}\right)^2} \;=\; \sqrt{1 \;-\; \left(\frac{V_0}{E}\right)^2}.$$

Here, we see from Figure 4.8 that orbits are always bounded for $E > V_0$ (and thus $0 \le \mathsf{e} \le 1$). Next, using the change of coordinate $q = s^2$ in Eq. (4.12), we obtain

$$\theta \;=\; \frac{-1}{2} \int_{q_2}^{q} \frac{dq}{\sqrt{\varepsilon\, q \;-\; q_0^2 \;-\; q^2}}, \tag{4.29}$$

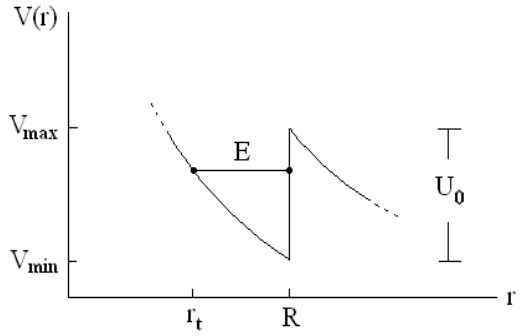

Figure 4.9: Effective potential for the internal hard sphere

where $q_2 = (1+\mathsf{e})\,\varepsilon/2$ and $q_0 = s_0^2$. We now substitute $q(\varphi) = (1+\mathsf{e}\,\cos\varphi)\,\varepsilon/2$ in Eq. (4.29) to obtain

$$\theta \;=\; \frac{1}{2}\;\arccos\left[\;\frac{1}{\mathsf{e}}\left(\frac{2\,q}{\varepsilon}-1\right)\;\right],$$

and we easily verify that $\Delta\theta = \pi$ and bounded orbits are closed. This equation can now be inverted to give

$$r(\theta) \;=\; \frac{r_0\;(1-\mathsf{e}^2)^{1/4}}{\sqrt{1+\mathsf{e}\,\cos 2\theta}}, \tag{4.30}$$

which describes the ellipse $x^2/b^2 + y^2/a^2 = 1$, with semi-major axis $a = r_2$ and semi-minor axis $b = r_1$. Note that this solution $x^2/b^2 + y^2/a^2 = 1$ may be obtained from the Cartesian representation for the Lagrangian $L = \frac{1}{2}\,\mu\,(\dot{x}^2+\dot{y}^2) - \frac{1}{2}\,k\,(x^2+y^2)$, which yields the solutions $x(t) = b\,\cos\omega t$ and $y(t) = a\,\sin\omega t$, where the constants a and b are determined from the conservation laws $E = \frac{1}{2}\,\mu\omega^2\,(a^2+b^2)$ and $\ell = \mu\omega\,a\,b$.

Lastly, the area of the ellipse is $A = \pi\,ab = \pi\,r_0^2$ while the *physical* period is

$$T(E,\ell) \;=\; \int_0^{2\pi}\;\frac{d\theta}{\dot{\theta}} \;=\; \frac{2\mu\,A}{\ell} \;=\; 2\pi\,\sqrt{\frac{\mu}{k}};$$

note that the *radial* period is $T/2$ since $\Delta\theta = \pi$. We, therefore, find that the period of an isotropic simple harmonic oscillator is independent of the constants of the motion E and ℓ, in analogy with the one-dimensional case.

4.5 Internal Reflection inside a Well

As a last example of bounded motion associated with a central-force potential, we consider the constant central potential

$$U(r) \;=\; \begin{cases} -\,U_0 & (r<R) \\ \\ 0 & (r>R) \end{cases}$$

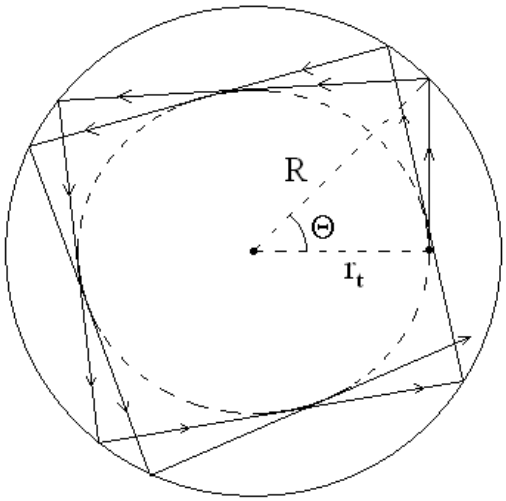

Figure 4.10: Internal reflections inside a hard sphere

where U_0 is a constant and R denotes the radius of a sphere. The effective potential $V(r) = \ell^2/(2\mu r^2) + U(r)$ associated with this potential is shown in Figure 4.9. Orbits are unbounded when $E > V_{\max} = \ell^2/(2\mu R^2)$. For energy values

$$V_{\min} \;=\; \frac{\ell^2}{2\mu R^2} - U_0 \;<\; E \;<\; V_{\max} \;=\; \frac{\ell^2}{2\mu R^2},$$

on the other hand, Figure 4.9 shows that bounded motion is possible, with turning points

$$r_1 \;=\; r_t \;=\; \sqrt{\frac{\ell^2}{2\mu\,(E+U_0)}} \quad \text{and} \quad r_2 \;=\; R.$$

When $E = V_{\min}$, the left turning point reaches its maximum value $r_t = R$ while it reaches its minimum value $r_t/R = (1 + U_0/E)^{-\frac{1}{2}} < 1$ when $E = V_{\max}$.

Assuming that the particle starts at $r = r_t$ at $\theta = 0$, the particle orbit is found by integration by quadrature as

$$\theta(s) \;=\; \int_s^{s_t} \frac{d\sigma}{\sqrt{s_t^2 - \sigma^2}},$$

where $s_t = 1/r_t$, which is easily integrated to yield

$$\theta(s) \;=\; \arccos\left(\frac{s}{s_t}\right) \quad \rightarrow \quad r(\theta) \;=\; r_t\,\sec\theta \;\; (\text{for} \;\; \theta \le \Theta),$$

where the maximum angle Θ defines the angle at which the particle hits the turning point R, i.e., $r(\Theta) = R$ and

$$\Theta \;=\; \arccos\left(\sqrt{\frac{\ell^2}{2\mu R^2\,(E+U_0)}}\right).$$

Subsequent motion of the particle involves an infinite sequence of *internal reflections* as shown in Figure 4.10. The case where $E > \ell^2/2\mu R^2$ involves a single turning point and is discussed in Sec. 5.6.2.

4.6 Problems

Problem 1

Consider a comet moving in a parabolic orbit in the plane of the Earth's orbit. If the distance of closest approach of the comet to the sun is $\beta\, r_E$, where r_E is the radius of the Earth's (assumed) circular orbit and where $\beta < 1$, show that the time the comet spends within the orbit of the Earth is given by $\sqrt{2\,(1-\beta)}\,(1+2\,\beta)\;\times\;1\ \text{year}/(3\,\pi)$.

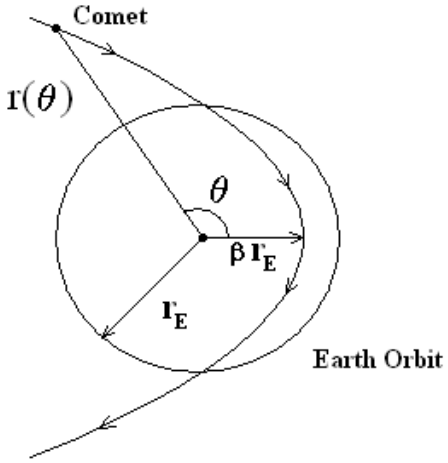

Problem 2

Find the effective potential $V(r) = U(r) + \ell^2/2\mu r^2$ that allows a particle to move in a spiral orbit given by $r = k\,\theta^2$, where k is a constant. Once this potential is determined, find the energy level corresponding to this unbounded orbit and solve for $r(t)$ and $\theta(t)$.

Problem 3

Consider the perturbed Kepler problem in which a particle of mass m, energy $E < 0$, and angular momentum ℓ is moving in the central-force potential

$$U(r) \;=\; -\,\frac{k}{r} \;+\; \frac{\alpha}{r^2},$$

where the perturbation potential α/r^2 is considered small in the sense that the dimensionless parameter $\epsilon = 2m\alpha/\ell^2 \ll 1$ is small.

(a) Show that the energy equation for this problem can be written using $s = 1/r$ as

$$E \;=\; \frac{\ell^2}{2m}\left[\,(s')^2 \;+\; \gamma^2\,s^2 \;-\; 2\,s_0 s\,\right],$$

where $s_0 = mk/\ell^2$ and $\gamma^2 = 1 + \epsilon$.

(b) Show that the turning points are

$$s_1 = \frac{s_0}{\gamma^2}\,(1 - \mathsf{e}) \quad \text{and} \quad s_2 = \frac{s_0}{\gamma^2}\,(1 + \mathsf{e}),$$

where $\mathsf{e} = \sqrt{1 + 2\,\gamma^2 \ell^2 E/mk^2}$.

(c) By solving the integral

$$\theta(s) \;=\; -\int_{s_2}^{s} \frac{d\sigma}{\sqrt{(2mE/\ell^2) + 2\,s_0\sigma - \gamma^2\,\sigma^2}},$$

where $\theta(s_2) = 0$, show that

$$r(\theta) \;=\; \frac{\gamma^2\,r_0}{1 \;+\; \mathsf{e}\,\cos(\gamma\theta)},$$

where $r_0 = 1/s_0$.

Problem 4

A Keplerian elliptical orbit, described by the relation $r(\theta) = r_0/(1 + \mathsf{e}\,\cos\theta)$, undergoes a precession motion when perturbed by the perturbation potential $\delta U(r)$, with precession frequency

$$\omega_{\rm p}(\theta) \;=\; \hat{\mathsf{z}} \cdot \frac{d\mathbf{A}}{dt} \times \frac{\mathbf{A}}{|\mathbf{A}|^2} \;=\; -\,\frac{1}{\ell}\,\Big(1 \;+\; \mathsf{e}^{-1}\,\cos\theta\Big)\,(\delta U \;+\; \mathbf{r} \cdot \nabla \delta U)$$

where $\mathbf{A} = \mathbf{p} \times \mathbf{L} - \mu k\,\hat{\mathsf{r}}$ denotes the Laplace-Runge-Lenz vector for the unperturbed Kepler problem.

Show that the net precession shift $\delta\theta$ of the Keplerian orbit over one unperturbed period is

$$\delta\theta \;=\; \int_0^{2\pi} \omega_{\rm p}(\theta)\,\frac{d\theta}{\dot\theta} \;=\; -\,6\pi\,\frac{\alpha}{kr_0^2}.$$

if the perturbation potential is $\delta U(r) = -\,\alpha/r^3$, where α is a constant.

Problem 5

In Kepler's work, angles are refered to as *anomalies*. In the Figure below, an ellipse (with eccentricity $\mathsf{e} < 1$) of semi-major axis a and semi-minor axis b is inscribed by a circle of radius a. Here, the lengths of the segments $\overline{CQ}$, $\overline{CS}$, $\overline{SR}$, and $\overline{RQ}$ are, respectively, a, $a\,\mathsf{e}$, $r(\theta)\,\cos\theta$, and $a\,\sin\psi$.

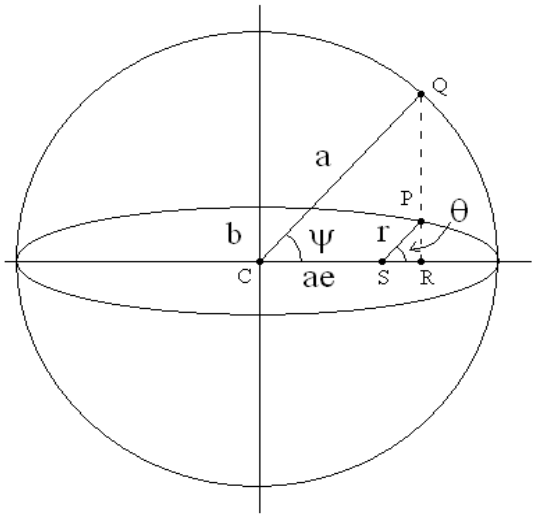

Show that the orbit of the planet (at point P) is described in terms of the *eccentric anomaly* ψ as

$$r(\psi) \;=\; a\,(1 - \mathsf{e}\,\cos\psi),$$

and the *true* anomaly θ is defined in terms of ψ as

$$\cos\theta(\psi) \;=\; \left(\frac{\cos\psi \;-\; \mathsf{e}}{1 - \mathsf{e}\,\cos\psi}\right).$$

Chapter 5

Collisions and Scattering Theory

In the previous Chapter, we investigated two types of orbits (bounded and unbounded) for two-particle systems evolving under the influence of a central potential. In the present Chapter, we focus our attention on unbounded orbits within the context of *elastic* collision theory. In this context, a collision between two interacting particles involves a three-step process: Step I – two particles are initially infinitely far apart (in which case, the energy of each particle is assumed to be strictly kinetic); Step II – as the two particles approach each other, their interacting potential (repulsive or attractive) causes them to reach a distance of closest approach; and Step III – the two particles then move progressively farther apart (eventually reaching a point where the energy of each particle is once again strictly kinetic).

These three steps form the foundations of Collision *Kinematics* and Collision *Dynamics*. The topic of Collision Kinematics, which describes the collision in terms of the conservation laws of momentum and energy, deals with Steps I and III; here, the incoming particles define the initial state of the two-particle system while the outgoing particles define the final state. The topic of Collision Dynamics, on the other hand, deals with Step II, in which the particular nature of the interaction is taken into account.

5.1 Two-Particle Collisions in the LAB Frame

Consider the collision of two particles (labeled 1 and 2) of masses m_1 and m_2, respectively. Let us denote the velocities of particles 1 and 2 *before* the collision as $\mathbf{u}_1$ and $\mathbf{u}_2$, respectively, while the velocities *after* the collision are denoted $\mathbf{v}_1$ and $\mathbf{v}_2$. Furthermore, the particle momenta before and after the collision are denoted $\mathbf{p}$ and $\mathbf{q}$, respectively.

To simplify the analysis, we define the laboratory (LAB) frame to correspond to the reference frame in which m_2 is at rest (i.e., $\mathbf{u}_2 = 0$); in this collision scenario, m_1 acts as the *projectile* particle and m_2 is the *target* particle. We now write the velocities $\mathbf{u}_1$, $\mathbf{v}_1$, and

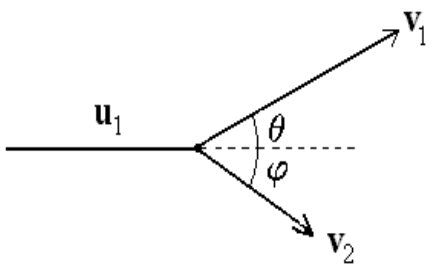

Figure 5.1: Collision kinematics in the LAB frame

$\mathbf{v}_2$ as

$$\left.\begin{array}{rcl} \mathbf{u}_1 &=& u\,\widehat{\mathbf{x}} \\ \mathbf{v}_1 &=& v_1\,(\cos\theta\,\widehat{\mathbf{x}}\,+\,\sin\theta\,\widehat{\mathbf{y}}) \\ \mathbf{v}_2 &=& v_2\,(\cos\varphi\,\widehat{\mathbf{x}}\,-\,\sin\varphi\,\widehat{\mathbf{y}}) \end{array}\right\}, \tag{5.1}$$

where the *deflection* angle θ and the *recoil* angle φ are defined in Figure 5.1. The conservation laws of momentum and energy

$$m_1\mathbf{u}_1 \;=\; m_1\mathbf{v}_1 \,+\, m_2\mathbf{v}_2 \quad\text{and}\quad \frac{m_1}{2}\,u^2 \;=\; \frac{m_1}{2}\,|\mathbf{v}_1|^2 \,+\, \frac{m_2}{2}\,|\mathbf{v}_2|^2$$

can be written in terms of the mass ratio $\alpha = m_1/m_2$ of the projectile mass to the target mass as

$$\alpha\,(u \,-\, v_1\,\cos\theta) \;=\; v_2\,\cos\varphi, \tag{5.2}$$

$$\alpha\,v_1\,\sin\theta \;=\; v_2\,\sin\varphi, \tag{5.3}$$

$$\alpha\,(u^2 \,-\, v_1^2) \;=\; v_2^2. \tag{5.4}$$

Since the **three** equations (5.2)-(5.4) are expressed in terms of **four** unknown quantities $(v_1, \theta,\ v_2, \varphi)$, for given incident velocity u and mass ratio α, we must choose one post-collision coordinate as an independent variable. Here, we choose the recoil angle φ of the target particle, and proceed with finding expressions for $v_1(u, \varphi; \alpha)$, $v_2(u, \varphi; \alpha)$ and $\theta(u, \varphi; \alpha)$; other choices lead to similar formulas (see problem 1).

First, adding the square of the mometum components (5.2) and (5.3), we obtain

$$\alpha^2\,v_1^2 \;=\; \alpha^2\,u^2 \;-\; 2\,\alpha\,uv_2\,\cos\varphi \;+\; v_2^2. \tag{5.5}$$

Next, using the energy equation (5.4), we find

$$\alpha^2\,v_1^2 \;=\; \alpha\,\left(\alpha\,u^2 \;-\; v_2^2\right) \;=\; \alpha^2\,u^2 \;-\; \alpha\,v_2^2, \tag{5.6}$$

so that these two equations combine to give

$$v_2(u, \varphi; \alpha) \;=\; 2\left(\frac{\alpha}{1+\alpha}\right)u\,\cos\varphi. \tag{5.7}$$

Once $v_2(u, \varphi; \alpha)$ is known and after substituting Eq. (5.7) into Eq. (5.6), we find

$$v_1(u, \varphi; \alpha) \;=\; u \sqrt{1 \;-\; 4\,\frac{\mu}{M}\,\cos^2\varphi}\,, \tag{5.8}$$

where $\mu/M = \alpha/(1+\alpha)^2$ is the ratio of the reduced mass μ and the total mass M.

Lastly, we take the ratio of the momentum components (5.2) and (5.3) in order to eliminate the unknown v_1 and find

$$\tan\theta \;=\; \frac{v_2\,\sin\varphi}{\alpha\,u \;-\; v_2\,\cos\varphi}.$$

If we substitute Eq. (5.7), we easily obtain

$$\tan\theta \;=\; \frac{2\,\sin\varphi\,\cos\varphi}{1 \;+\; \alpha \;-\; 2\,\cos^2\varphi},$$

or

$$\theta(\varphi; \alpha) \;=\; \arctan\left(\frac{\sin 2\varphi}{\alpha \;-\; \cos 2\varphi}\right). \tag{5.9}$$

In the limit $\alpha = 1$ (i.e., a collision involving identical particles), we find $v_2 = u\cos\varphi$ and $v_1 = u\sin\varphi$ from Eqs. (5.7) and (5.8), respectively, and

$$\tan\theta \;=\; \cot\varphi \quad\rightarrow\quad \varphi \;=\; \frac{\pi}{2} \;-\; \theta,$$

from Eq. (5.9) so that the angular sum $\theta + \varphi$ for like-particle collisions is always 90^o (for $\varphi \neq 0$).

We summarize by stating that, after the collision, the momenta $\mathbf{q}_1$ and $\mathbf{q}_2$ in the LAB frame (where m_2 is initially at rest) are

$$\begin{aligned}
\mathbf{q}_1 \;&=\; p\left[1 \;-\; \frac{4\,\alpha}{(1+\alpha)^2}\,\cos^2\varphi\right]^{1/2}\,(\cos\theta\,\hat{\mathbf{x}} \;+\; \sin\theta\,\hat{\mathbf{y}}) \\
\mathbf{q}_2 \;&=\; \frac{2p\,\cos\varphi}{1+\alpha}\,(\cos\varphi\,\hat{\mathbf{x}} \;-\; \sin\varphi\,\hat{\mathbf{y}})
\end{aligned}$$

where $\mathbf{p}_1 = p\,\hat{\mathbf{x}}$ is the initial momentum of particle 1. We note that these expressions for the particle momenta after the collision satisfy the law of conservation of (kinetic) energy in addition to the law of conservation of momentum.

5.2 Two-Particle Collisions in the CM Frame

In the center-of-mass (CM) frame, the elastic collision between particles 1 and 2 is described quite simply; the CM velocities and momenta are, henceforth, denoted with a prime. Before

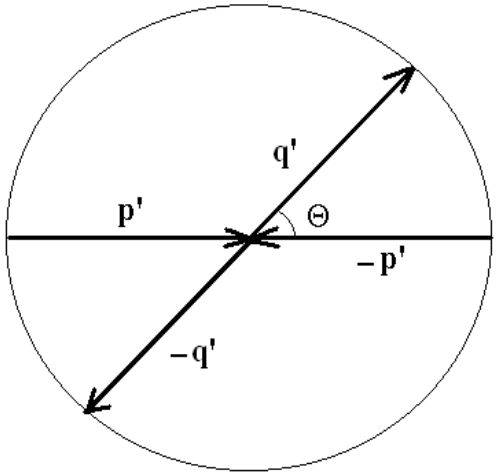

Figure 5.2: Collision kinematics in the CM frame

the collision, the momenta of particles 1 and 2 are equal in magnitude but with opposite directions

$$\mathbf{p}'_1 \;=\; \mu\, u\, \hat{\mathbf{x}} \;=\; -\,\mathbf{p}'_2,$$

where μ is the reduced mass of the two-particle system. After the collision (see Figure 5.2), conservation of energy-momentum dictates that

$$\mathbf{q}'_1 \;=\; \mu\, u\;(\cos\Theta\,\hat{\mathbf{x}} \;+\; \sin\Theta\,\hat{\mathbf{y}}) \;=\; -\,\mathbf{q}'_2,$$

where Θ is the scattering angle in the CM frame and $\mu\, u = p/(1+\alpha)$. Thus the particle velocities after the collision in the CM frame are

$$\mathbf{v}'_1 \;=\; \frac{\mathbf{q}'_1}{m_1} \;=\; \frac{u}{1+\alpha}\;(\cos\Theta\,\hat{\mathbf{x}} \;+\; \sin\Theta\,\hat{\mathbf{y}}) \quad \text{and} \quad \mathbf{v}'_2 \;=\; \frac{\mathbf{q}'_2}{m_2} \;=\; -\,\alpha\,\mathbf{v}'_1.$$

It is quite clear, thus, that the initial and final kinematic states lie on the same circle in CM momentum space and the single variable defining the outgoing two-particle state is represented by the CM scattering angle Θ.

5.3 Connection between the CM and LAB Frames

We now establish the connection between the momenta $\mathbf{q}_1$ and $\mathbf{q}_2$ in the LAB frame and the momenta $\mathbf{q}'_1$ and $\mathbf{q}'_2$ in the CM frame. First, we denote the velocity of the CM as

$$\mathbf{w} \;=\; \frac{m_1\,\mathbf{u}_1 + m_2\,\mathbf{u}_2}{m_1 + m_2} \;=\; \frac{\alpha\, u}{1+\alpha}\,\hat{\mathbf{x}},$$

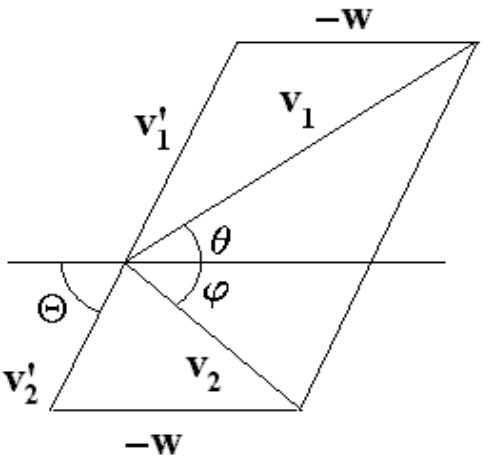

Figure 5.3: CM collision geometry

so that $w = |\mathbf{w}| = \alpha\, u/(1+\alpha)$ and $|\mathbf{v}_2'| = w = \alpha\, |\mathbf{v}_1'|$.

The connection between $\mathbf{v}_1'$ and $\mathbf{v}_1$ is expressed as

$$\mathbf{v}_1' \;=\; \mathbf{v}_1 \;-\; \mathbf{w} \quad\rightarrow\quad \left\{\begin{array}{lcl} v_1\,\cos\theta &=& w\,(1+\alpha^{-1}\,\cos\Theta) \\ \\ v_1\,\sin\theta &=& w\,\alpha^{-1}\,\sin\Theta \end{array}\right.$$

so that

$$\tan\theta \;=\; \frac{\sin\Theta}{\alpha+\cos\Theta}, \tag{5.10}$$

and

$$v_1 \;=\; v_1'\,\sqrt{1 \;+\; \alpha^2 \;+\; 2\,\alpha\,\cos\Theta},$$

where $v_1' = u/(1+\alpha)$. Likewise, the connection between $\mathbf{v}_2'$ and $\mathbf{v}_2$ is expressed as

$$\mathbf{v}_2' \;=\; \mathbf{v}_2 \;-\; \mathbf{w} \quad\rightarrow\quad \left\{\begin{array}{lcl} v_2\,\cos\varphi &=& w\,(1-\cos\Theta) \\ \\ v_2\,\sin\varphi &=& w\,\sin\Theta \end{array}\right.$$

so that

$$\tan\varphi \;=\; \frac{\sin\Theta}{1-\cos\Theta} \;=\; \cot\frac{\Theta}{2} \quad\rightarrow\quad \varphi \;=\; \frac{1}{2}\,(\pi \;-\; \Theta),$$

and

$$v_2 \;=\; 2\,v_2'\,\sin\frac{\Theta}{2},$$

where $v_2' = \alpha\, u/(1+\alpha) = w$.

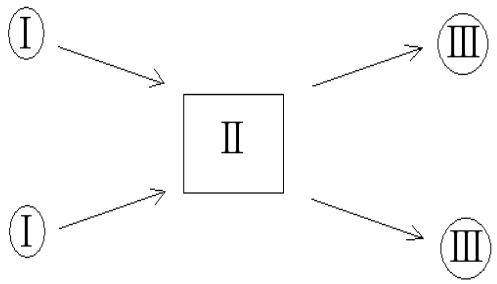

Figure 5.4: Collision kinematics and dynamics

5.4 Scattering Cross Sections

In the previous Section, we investigated the connection between the initial and final kinematic states of an elastic collision described by Steps I and III, respectively, introduced earlier. Here, the initial kinematic state is described in terms of the speed u of the projectile particle in the Laboratory frame (assuming that the target particle is at rest), while the final kinematic state is described in terms of the velocity coordinates for the deflected projectile particle (v_1, θ) and the recoiled target particle (v_2, φ). In the present Section, we shall investigate Step II, namely, how the distance of closest approach influences the deflection angles (θ, φ) in the LAB frame and the deflection angle Θ in the CM frame.

5.4.1 Definitions

First, we consider for simplicity the case of a projectile particle of mass m being deflected by a repulsive central-force potential $U(r) > 0$ whose center is at rest at the origin (or $\alpha = 0$). As the projectile particle approaches from the right (at $r = \infty$ and $\theta = 0$) moving with speed u, it is progressively deflected until it reaches a minimum radius ρ at $\theta = \chi$ after which the projectile particle moves away from the repulsion center until it reaches $r = \infty$ at a deflection angle $\theta = \Theta$ and again moving with speed u. From Figure 5.5, we can see that the scattering process is symmetric about the line of closest approach (i.e., $2\chi = \pi - \Theta$, where Θ is the CM deflection angle). The angle of closest approach

$$\chi \;=\; \frac{1}{2}\,(\pi - \Theta) \tag{5.11}$$

is a function of the distance of closest approach ρ, the total energy E, and the angular momentum ℓ. The distance ρ is, of course, a turning point ($\dot{r} = 0$) and is the only root of the equation

$$E \;=\; U(\rho) \;+\; \frac{\ell^2}{2m\,\rho^2}, \tag{5.12}$$

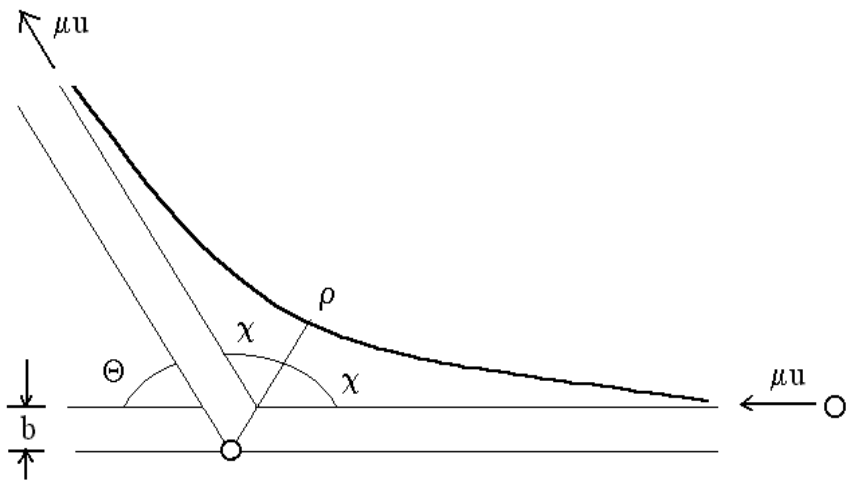

Figure 5.5: Scattering geometry

where $E = m\,u^2/2$ is the total initial energy of the projectile particle.

The path of the projectile particle in Figure 5.5 is labeled by the *impact parameter* b (the distance of closest approach in the non-interacting case: $U = 0$) and a simple calculation (using $\mathbf{r} \times \mathbf{v} = bu\,\hat{\mathbf{z}}$) shows that the angular momentum is

$$\ell \;=\; mu\,b \;=\; \sqrt{2m\,E}\;b. \tag{5.13}$$

It is, thus, quite clear that ρ is a function of $E \equiv \ell^2/(2m\,b^2)$, m, and b. Hence, the angle χ is defined in terms of the standard integral

$$\chi \;=\; \int_\rho^\infty \frac{(\ell/r^2)\;dr}{\sqrt{2m\,[E - U(r)] \;-\; (\ell^2/r^2)}} \;=\; \int_0^{b/\rho} \frac{dx}{\sqrt{1 \;-\; x^2 \;-\; b^2\,\overline{U}(x/b)}}. \tag{5.14}$$

Once an expression $\Theta(b)$ is obtained from Eq. (5.14), we may invert it to obtain $b(\Theta)$.

5.4.2 Scattering Cross Sections in CM and LAB Frames

We are now ready to discuss the *likelyhood* of the outcome of a collision by introducing the concept of differential cross section $\sigma'(\Theta)$ in the CM frame. The infinitesimal cross section $d\sigma'$ in the CM frame is defined in terms of $b(\Theta)$ as $d\sigma'(\Theta) = \pi\,db^2(\Theta)$. Physically, $d\sigma/d\Sigma$ measures the ratio of the number of incident particles per unit time scattered into a solid angle $d\Omega$ to the incident flux

Using Eqs. (5.11) and (5.14), the differential cross section in the CM frame is defined

as

$$\sigma'(\Theta) \;=\; \frac{d\sigma'}{2\pi\,\sin\Theta\,d\Theta} \;=\; \frac{b(\Theta)}{\sin\Theta}\,\left|\frac{db(\Theta)}{d\Theta}\right|, \tag{5.15}$$

and the total cross section is, thus, defined as

$$\sigma_T \;=\; 2\pi\,\int_0^{\pi}\,\sigma'(\Theta)\,\sin\Theta\,d\Theta.$$

We note that, in Eq. (5.15), the quantity $db/d\Theta$ is often negative and, thus, we must take its absolute value to ensure that $\sigma'(\Theta)$ is positive.

The differential cross section can also be written in the LAB frame in terms of the deflection angle θ as

$$\sigma(\theta) \;=\; \frac{d\sigma}{2\pi\,\sin\theta\,d\theta} \;=\; \frac{b(\theta)}{\sin\theta}\,\left|\frac{db(\theta)}{d\theta}\right|. \tag{5.16}$$

Since the infinitesimal cross section $d\sigma = d\sigma'$ is the same in both frames (i.e., the likelyhood of a collision should not depend on the choice of a frame of reference), we find

$$\sigma(\theta)\,\sin\theta\,d\theta \;=\; \sigma'(\Theta)\,\sin\Theta\,d\Theta,$$

from which we obtain

$$\sigma(\theta) \;=\; \sigma'(\Theta)\,\frac{\sin\Theta}{\sin\theta}\,\frac{d\Theta}{d\theta}, \tag{5.17}$$

or

$$\sigma'(\Theta) \;=\; \sigma(\theta)\,\frac{\sin\theta}{\sin\Theta}\,\frac{d\theta}{d\Theta}. \tag{5.18}$$

Eq. (5.17) yields an expression for the differential cross section in the LAB frame $\sigma(\theta)$ once the differential cross section in the CM frame $\sigma'(\Theta)$ and an explicit formula for $\Theta(\theta)$ are

known. Eq. (5.18) represents the inverse transformation $\sigma(\theta) \rightarrow \sigma'(\Theta)$. We point out that, whereas the CM differential cross section $\sigma'(\Theta)$ is naturally associated with theoretical calculations, the LAB differential cross section $\sigma(\theta)$ is naturally associated with experimental measurements. Hence, the transformation (5.17) is used to translate a theoretical prediction into an observable experimental cross section, while the transformation (5.18) is used to translate experimental measurements into a format suitable for theoretical analysis.

We note that these transformations rely on finding relations between the LAB deflection angle θ and the CM deflection angle Θ given by Eq. (5.10), which can be converted into

$$\sin(\Theta-\theta) \;=\; \alpha\,\sin\theta. \tag{5.19}$$

For example, using these relations, we now show how to obtain an expression for Eq. (5.17) by using Eqs. (5.10) and (5.19). First, we use Eq. (5.19) to obtain

$$\frac{d\Theta}{d\theta} \;=\; \frac{\alpha\,\cos\theta \;+\; \cos(\Theta-\theta)}{\cos(\Theta-\theta)}, \tag{5.20}$$

where

$$\cos(\Theta - \theta) \;=\; \sqrt{1 \;-\; \alpha^2\,\sin^2\theta}\;\;.$$

Next, using Eq. (5.10), we show that

$$\frac{\sin\Theta}{\sin\theta} \;=\; \frac{\alpha + \cos\Theta}{\cos\theta} \;=\; \frac{\alpha \;+\; [\cos(\Theta-\theta)\,\cos\theta \;-\; \overbrace{\sin(\Theta-\theta)}^{=\,\alpha\,\sin\theta}\,\sin\theta]}{\cos\theta}$$

$$=\; \frac{\alpha\,(1-\sin^2\theta) \;+\; \cos(\Theta-\theta)\,\cos\theta}{\cos\theta} \;=\; \alpha\,\cos\theta \;+\; \sqrt{1 \;-\; \alpha^2\,\sin^2\theta}\;\;. \quad (5.21)$$

Thus by combining Eqs. (5.20) and (5.21), we find

$$\frac{\sin\Theta}{\sin\theta}\,\frac{d\Theta}{d\theta} \;=\; \frac{[\alpha\,\cos\theta \;+\; \sqrt{1 \;-\; \alpha^2\,\sin^2\theta}]^2}{\sqrt{1 \;-\; \alpha^2\,\sin^2\theta}} \;=\; 2\,\alpha\,\cos\theta \;+\; \frac{1+\alpha^2\,\cos 2\theta}{\sqrt{1 \;-\; \alpha^2\,\sin^2\theta}}, \quad (5.22)$$

which is valid for $\alpha < 1$. Lastly, noting from Eq. (5.19), that the CM deflection angle is defined as

$$\Theta(\theta) \;=\; \theta \;+\; \arcsin(\,\alpha\,\sin\theta\,),$$

the transformation $\sigma'(\Theta) \rightarrow \sigma(\theta)$ is now complete. Similar manipulations yield the transformation $\sigma(\theta) \rightarrow \sigma'(\Theta)$. We note that the LAB-frame cross section $\sigma(\theta)$ are generally difficult to obtain for arbitrary mass ratio $\alpha = m_1/m_2$.

5.5 Rutherford Scattering

As an explicit example of the scattering formalism developed in this Chapter, we investigate the scattering of a charged particle of mass m_1 and charge q_1 by another charged particle of mass $m_2 \gg m_1$ and charge q_2 such that $q_1\,q_2 > 0$ and $\mu \simeq m_1$. This situation leads to the two particles experiencing a repulsive central force with potential

$$U(r) \;=\; \frac{k}{r},$$

where $k = q_1 q_2/(4\pi\,\varepsilon_0) > 0$.

The turning-point equation in this case is

$$E \;=\; E\,\frac{b^2}{\rho^2} \;+\; \frac{k}{\rho},$$

whose solution is the distance of closest approach

$$\rho \;=\; r_0 \;+\; \sqrt{r_0^2 + b^2} \;=\; b\left(\epsilon \;+\; \sqrt{1+\epsilon^2}\right), \quad (5.23)$$

where $2\,r_0 = k/E$ is the distance of closest approach for a *head-on* collision (for which the impact parameter b is zero) and $\epsilon = r_0/b$; note, here, that the second solution $r_0 - \sqrt{r_0^2 + b^2}$ to the turning-point equation is negative and, therefore, is not allowed. The problem of the electrostatic repulsive interaction between a positively-charged alpha particle (i.e., the nucleus of a helium atom) and positively-charged nucleus of a gold atom was first studied by Rutherford and the scattering cross section for this problem is known as the Rutherford cross section.

The angle χ at which the distance of closest approach is reached is calculated from Eq. (5.14) as

$$\chi \;=\; \int_0^{b/\rho} \frac{dx}{\sqrt{1 \;-\; x^2 \;-\; 2\,\epsilon\,x}} \;=\; \int_0^{b/\rho} \frac{dx}{\sqrt{(1+\epsilon^2) \;-\; (x+\epsilon)^2}}, \tag{5.24}$$

where

$$\frac{b}{\rho} \;=\; \frac{1}{\epsilon + \sqrt{1+\epsilon^2}} \;=\; -\,\epsilon \;+\; \sqrt{1+\epsilon^2}.$$

Making use of the trigonometric substitution $x = -\,\epsilon + \sqrt{1+\epsilon^2}\,\cos\psi$, we find that

$$\chi \;=\; \arccos\left(\frac{\epsilon}{\sqrt{1+\epsilon^2}}\right) \quad\rightarrow\quad \epsilon \;=\; \cot\chi,$$

which becomes

$$\frac{b}{r_0} \;=\; \tan\chi. \tag{5.25}$$

Using the relation (5.11), we now find

$$b(\Theta) \;=\; r_0\;\cot\frac{\Theta}{2}, \tag{5.26}$$

and thus $db(\Theta)/d\Theta = -\,(r_0/2)\;\csc^2(\Theta/2)$. The CM Rutherford cross section is

$$\sigma'(\Theta) \;=\; \frac{b(\Theta)}{\sin\Theta}\;\left|\frac{db(\Theta)}{d\Theta}\right| \;=\; \frac{r_0^2}{4\;\sin^4(\Theta/2)},$$

or

$$\sigma'(\Theta) \;=\; \left(\frac{k}{4E\;\sin^2(\Theta/2)}\right)^2. \tag{5.27}$$

Note that the Rutherford scattering cross section (5.27) does not depend on the sign of k and is thus valid for both repulsive and attractive interactions. Moreover, we note (see Figure 5.6) that the Rutherford scattering cross section becomes very large in the forward direction $\Theta \rightarrow 0$ (where $\sigma' \rightarrow \Theta^{-4}$) while the differential cross section as $\Theta \rightarrow \pi$ behaves as $\sigma' \rightarrow (k/4E)^2$.

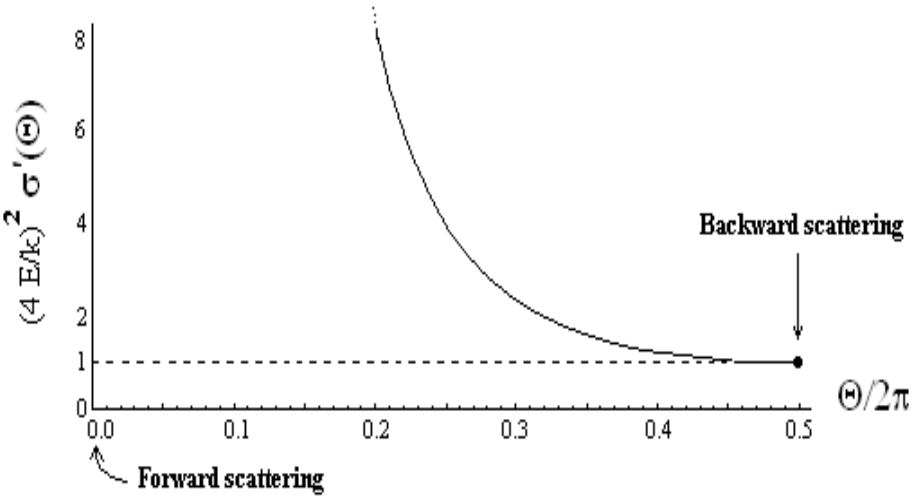

Figure 5.6: Rutherford scattering cross-section

5.6 Hard-Sphere and Soft-Sphere Scattering

Explicit calculations of differential cross sections tend to be very complex for general central potentials and, therefore, prove unsuitable for an undergraduate introductory course in Classical Mechanics. In the present Section, we consider two simple central potentials associated with a uniform central potential $U(r) \neq 0$ confined to a spherical region ($r < R$).

5.6.1 Hard-Sphere Scattering

We begin by considering the collision of a point-like particle of mass m_1 with a hard sphere of mass m_2 and radius R. In this particular case, the central potential for the hard sphere is

$$U(r) \;=\; \begin{cases} \infty & (\text{for } \; r < R) \\ \\ 0 & (\text{for } \; r > R) \end{cases}$$

and the collision is shown in Figure 5.7. From Figure 5.7, we see that the impact parameter is

$$b \;=\; R \, \sin\chi, \tag{5.28}$$

where χ is the angle of incidence. The angle of reflection η is different from the angle of incidence χ for the case of arbitrary mass ratio $\alpha = m_1/m_2$. To show this, we decompose the velocities in terms of components perpendicular and tangential to the surface of the sphere at the point of impact, i.e., we respectively find

$$\alpha \, u \, \cos\chi \;\; = \;\; v_2 \; - \; \alpha \, v_1 \, \cos\eta$$

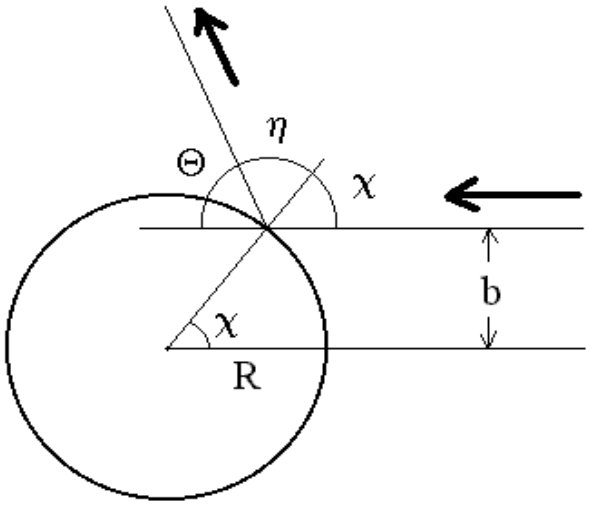

Figure 5.7: Hard-sphere scattering geometry

$$\alpha\, u\, \sin\chi \;=\; \alpha\, v_1\, \sin\eta.$$

From these expressions we obtain

$$\tan\eta \;=\; \frac{\alpha\, u\, \sin\chi}{v_2 - \alpha\, u\, \cos\chi}.$$

From Figure 5.7, we also find the deflection angle $\theta = \pi - (\chi + \eta)$ and the recoil angle $\varphi = \chi$ and thus, according to Chap. 5,

$$v_2 \;=\; \left(\frac{2\,\alpha}{1+\alpha}\right) u\, \cos\chi,$$

and thus

$$\tan\eta \;=\; \left(\frac{1+\alpha}{1-\alpha}\right) \tan\chi. \tag{5.29}$$

We, therefore, easily see that $\eta = \chi$ (the standard form of the Law of Reflection) only if $\alpha = 0$ (i.e., the target particle is infinitely massive).

In the CM frame, the collision is symmetric with a deflection angle $\chi = \frac{1}{2}(\pi - \Theta)$, so that

$$b \;=\; R\, \sin\chi \;=\; R\, \cos\frac{\Theta}{2}.$$

The scattering cross section in the CM frame is

$$\sigma'(\Theta) \;=\; \frac{b(\Theta)}{\sin\Theta} \left|\frac{db(\Theta)}{d\Theta}\right| \;=\; \frac{R\, \cos(\Theta/2)}{\sin\Theta} \;\cdot\; \left|-\frac{R}{2}\, \sin(\Theta/2)\right| \;=\; \frac{R^2}{4}, \tag{5.30}$$

and the total cross section is

$$\sigma_T \;=\; 2\pi \int_0^{\pi} \sigma'(\Theta)\, \sin\Theta \, d\Theta \;=\; \pi\, R^2, \tag{5.31}$$

i.e., the total cross section for the problem of hard-sphere collision is equal to the effective area of the sphere.

The scattering cross section in the LAB frame can also be obtained for the case $\alpha < 1$ using Eqs. (5.17) and (5.22) as

$$\sigma(\theta) \;=\; \frac{R^2}{4} \left(2\,\alpha \;\cos\theta \;+\; \frac{1 + \alpha^2 \;\cos 2\theta}{\sqrt{1 \;-\; \alpha^2 \;\sin^2\theta}} \right), \tag{5.32}$$

for $\alpha = m_1/m_2 < 1$. The integration of this formula must yield the total cross section

$$\sigma_T \;=\; 2\pi \int_0^{\pi} \sigma(\theta)\, \sin\theta \, d\theta,$$

where $\theta_{max} = \pi$ for $\alpha < 1$.

5.6.2 Soft-Sphere Scattering

We now consider the scattering of a particle subjected to the attractive potential considered in Sec. 4.5

$$U(r) \;=\; \begin{cases} -\,U_0 & (\text{for } \; r < R) \\ \\ 0 & \text{for } \; r > R \end{cases} \tag{5.33}$$

where the constant U_0 denotes the depth of the attractive potential well and $E > \ell^2/2\mu R^2$ involves a single turning point. We denote β the angle at which the incoming particle enters the *soft-sphere* potential (see Figure 5.8), and thus the impact parameter b of the incoming particle is $b = R\,\sin\beta$. The particle enters the soft-sphere potential region ($r < R$) and reaches a distance of closest approach ρ, defined from the turning-point condition

$$E \;=\; -\,U_0 \;+\; E\,\frac{b^2}{\rho^2} \quad \rightarrow \quad \rho \;=\; \frac{b}{\sqrt{1 + U_0/E}} \;=\; \frac{R}{n}\;\sin\beta,$$

where $n = \sqrt{1 + U_0/E}$ denotes the *index of refraction* of the soft-sphere potential region. From Figure 5.8, we note that an optical analogy helps us determine that, through Snell's law, we find

$$\sin\beta \;=\; n\;\sin\left(\beta \;-\; \frac{\Theta}{2}\right), \tag{5.34}$$

where the *transmission* angle α is given in terms of the *incident* angle β and the CM scattering angle $-\,\Theta$ as $\Theta = 2\,(\beta - \alpha)$.

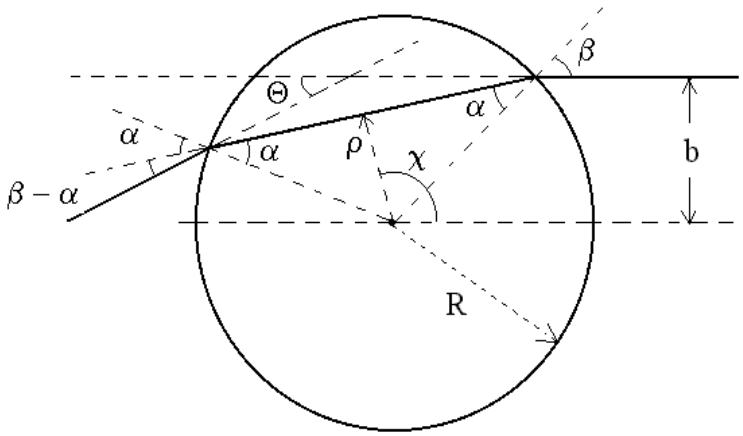

Figure 5.8: Soft-sphere scattering geometry

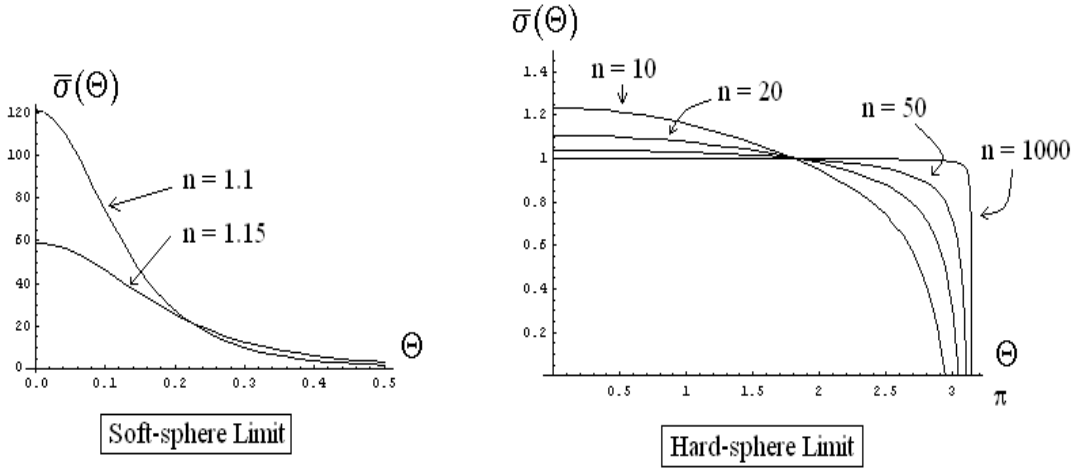

Figure 5.9: Soft-sphere scattering cross-section in the soft-sphere limit ($n \to 1$) and the hard-sphere limit ($n \gg 1$); here, note that $\overline{\sigma}(0) = n^2/(n-1)^2$.

The distance of closest approach is reached at an angle χ is determined as

$$\begin{aligned}\chi &= \beta + \int_\rho^R \frac{b\,dr}{r\sqrt{n^2r^2-b^2}} \\ &= \beta + \arccos\left(\frac{b}{nR}\right) - \underbrace{\arccos\left(\frac{b}{n\rho}\right)}_{=0} \\ &= \beta + \arccos\left(\frac{b}{nR}\right) = \frac{1}{2}(\pi+\Theta),\end{aligned} \tag{5.35}$$

and, thus, the impact parameter $b(\Theta)$ can be expressed as

$$b(\Theta) = nR\sin\left(\beta(b) - \frac{\Theta}{2}\right) \quad\rightarrow\quad b(\Theta) = \frac{nR\,\sin(\Theta/2)}{\sqrt{1+n^2-2n\,\cos(\Theta/2)}}, \tag{5.36}$$

and its derivative with respect to Θ yields

$$\frac{db}{d\Theta} = \frac{nR}{2}\,\frac{[n\,\cos(\Theta/2)-1]\,[n-\cos(\Theta/2)]}{[1+n^2-2n\,\cos(\Theta/2)]^{3/2}},$$

and the scattering cross section in the CM frame is

$$\sigma'(\Theta) = \frac{b(\Theta)}{\sin\Theta}\left|\frac{db(\Theta)}{d\Theta}\right| = \frac{n^2R^2}{4}\,\frac{|[n\,\cos(\Theta/2)-1]\,[n-\cos(\Theta/2)]|}{\cos(\Theta/2)\,[1+n^2-2n\,\cos(\Theta/2)]^2}.$$

Note that, on the one hand, when $\beta=0$, we find $\chi=\pi/2$ and $\Theta_{\rm min}=0$, while on the other hand, when $\beta=\pi/2$, we find $b=R$ and

$$1 = n\,\sin\left(\frac{\pi}{2}-\frac{\Theta_{\rm max}}{2}\right) = n\,\cos(\Theta_{\rm max}/2) \quad\rightarrow\quad \Theta_{\rm max} = 2\,\arccos\left(n^{-1}\right).$$

Moreover, when $\Theta=\Theta_{\rm max}$, we find that $db/d\Theta$ vanishes and, therefore, the differential cross section vanishes $\sigma'(\Theta_{\rm max})=0$, while at $\Theta=0$, we find $\sigma'(0)=[n/(n-1)]^2\,(R^2/4)$.

Figure 5.9 shows the soft-sphere scattering cross section $\overline{\sigma}(\Theta)$ (normalized to the hard-sphere cross section $R^2/4$) as a function of Θ for four cases: $n=(1.1,1.15)$ in the *soft-sphere limit* ($n\rightarrow 1$) and $n=(10,20,50,1000)$ in the *hard-sphere limit* ($n\rightarrow\infty$). We clearly see the strong forward-scattering behavior as $n\rightarrow 1$ (or $U_0\rightarrow 0$) in the soft-sphere limit and the hard-sphere limit $\overline{\sigma}\rightarrow 1$ as $n\rightarrow\infty$. We note that the total scattering cross section (using the substitution $x=n\,\cos\Theta/2$)

$$\sigma_T = 2\pi\int_0^{\Theta_{\rm max}}\sigma'(\Theta)\,\sin\Theta\,d\Theta = 2\pi\,R^2\int_1^n\frac{(x-1)\,(n^2-x)\,dx}{(1\,+\,n^2\,-\,2x)^2} = \pi\,R^2$$

is independent of the index of refraction n and equals the hard-sphere total cross section (5.31).

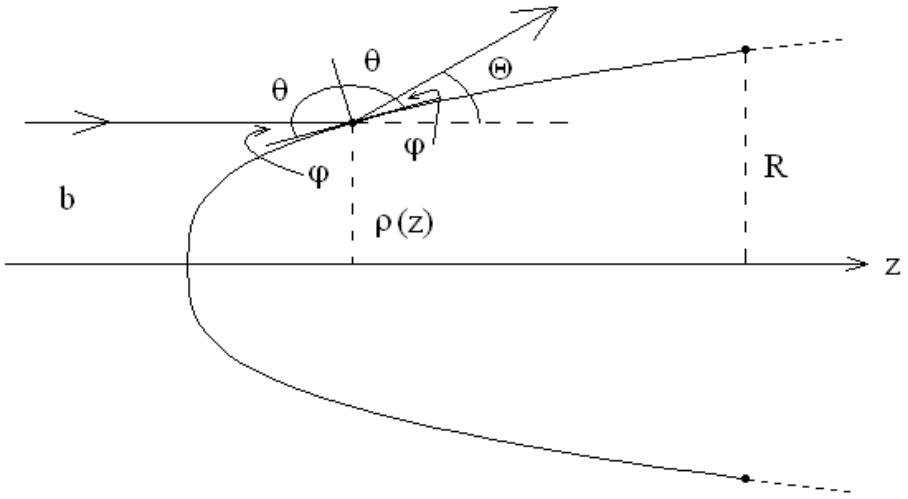

Figure 5.10: Scattering by a hard surface $\rho(z)$.

The opposite case of a repulsive soft-sphere potential, where $-U_0$ is replaced with U_0 in Eq. (5.33), is treated by replacing $n = (1 + U_0/E)^{\frac{1}{2}}$ with $n = (1 - U_0/E)^{-\frac{1}{2}}$ and Eq. (5.36) is replaced with

$$b(\Theta) \;=\; n^{-1}\, R\, \sin\left(\beta(b) \;+\; \frac{\Theta}{2}\right) \quad \rightarrow \quad b(\Theta) \;=\; \frac{R\, \sin(\Theta/2)}{\sqrt{1 + n^2 - 2n\, \cos(\Theta/2)}}, \tag{5.37}$$

while Snell's law (5.34) is replaced with

$$\sin\left(\beta \;+\; \frac{\Theta}{2}\right) \;=\; n\; \sin\beta.$$

5.7 Elastic Scattering by a Hard Surface

We generalize the hard-sphere scattering problem by considering scattering by a smooth hard surface $\rho(z)$ with maximal radial extent R (see Figure 5.10). Here, a particle of mass m, initially traveling along the z-axis with velocity u with an impact parameter b, collides with the hard surface and is scattered with deflection angle Θ. The particle hits the surface at a distance $b = \rho(z)$ from its axis of symmetry and the angle of incidence $\theta = \pi/2 - \varphi$ (measured from the normal to the surface) is defined in terms of the complementary angle φ, where $\cos\varphi = [1 + (\rho')^2]^{-1/2}$. Since the deflection angle Θ is defined in terms of φ as $\Theta = \pi - 2\,\theta = 2\,\varphi$, we find

$$\tan\varphi \;=\; \rho'(z) \;=\; \tan\frac{\Theta}{2}. \tag{5.38}$$

By using the identity $b(\Theta) = \rho(z)$, we can solve for $z(\Theta)$ [or $\Theta(z)$], we can now calculate the differential cross-section (5.15).

First, we use the identity

$$\frac{db}{d\Theta} \;=\; \rho' \,\frac{dz}{d\Theta} \;=\; \rho' \,\left(\frac{d\Theta}{dz}\right)^{-1},$$

where $\Theta(z) = 2\,\arctan(\rho')$ yields

$$\frac{d\Theta}{dz} \;=\; \frac{2\,\rho''}{[1+(\rho')^2]},$$

and, hence,

$$\left|\frac{db}{d\Theta}\right| \;=\; \frac{\rho'}{2\,|\rho''|}\,\left[1+(\rho')^2\right].$$

Lastly, using

$$\sin\Theta \;=\; 2\,\cos\varphi\,\sin\varphi \;=\; \frac{2\,\rho'}{[1+(\rho')^2]},$$

we find the differential scattering cross-section

$$\sigma(\Theta(z)) \;=\; \frac{\rho}{4\,|\rho''|}\,\left[1+(\rho')^2\right]^2 \;\equiv\; \left(\frac{\rho}{4\,\kappa}\right)\,\sec\frac{\Theta}{2}, \tag{5.39}$$

where $\kappa \equiv |\rho''|/[1+(\rho')^2]^{3/2}$ denotes the Frenet-Serret curvature of the curve $\rho(z)$ in the (ρ, z)-plane.

For example, we revisit the hard-sphere scattering problem studied in Sec. 5.6.1, with $\rho(z) = \sqrt{R^2 - z^2}$ for $-R \leq z \leq 0$. Here, the Frenet-Serret curvature is $\kappa = 1/R$ and

$$z \;=\; -\,\rho\,\tan\frac{\Theta}{2} \;\;\rightarrow\;\; \rho \;=\; R\,\cos\frac{\Theta}{2},$$

so that the differential cross-section (5.39) yields the standard hard-sphere result (5.30):

$$\sigma(\Theta(z)) \;=\; \left(\frac{R^2}{4}\,\cos\frac{\Theta}{2}\right)\,\sec\frac{\Theta}{2} \;=\; \frac{R^2}{4}.$$

Lastly, elastic scattering by hard surface $\rho(z) = C\,\sqrt{z}$, where C is a constant, yields the Rutherford formula

$$\sigma \;=\; \frac{C^4}{16\,\sin^4\frac{\Theta}{2}},$$

where $z = \frac{1}{4}\,C^2\,\cot^2\frac{\Theta}{2}$.

5.8 Problems

Problem 1

(a) Using the conservation laws of energy and momentum, solve for $v_1(u, \theta; \beta)$, where $\beta = m_2/m_1$ and

$$\begin{aligned} \mathbf{u}_1 &= u\,\widehat{\mathbf{x}} \\ \mathbf{v}_1 &= v_1\,(\cos\theta\,\widehat{\mathbf{x}} + \sin\theta\,\widehat{\mathbf{y}}) \\ \mathbf{v}_2 &= v_2\,(\cos\varphi\,\widehat{\mathbf{x}} - \sin\varphi\,\widehat{\mathbf{y}}) \end{aligned}$$

(b) Discuss the number of physical solutions for $v_1(u, \theta; \beta)$ for $\beta < 1$ and $\beta > 1$.

(c) For $\beta < 1$, show that physical solutions for $v_1(u, \theta; \beta)$ exist for $\theta < \arcsin(\beta) = \theta_{max}$.

Problem 2

Show that the momentum transfer $\Delta\mathbf{p}_1' = \mathbf{q}_1' - \mathbf{p}_1'$ of the projectile particle in the CM frame has a magnitude

$$|\Delta\mathbf{p}_1'| = 2\,\mu u\,\sin\frac{\Theta}{2},$$

where μ, u, and Θ are the reduced mass, initial projectile LAB speed, and CM scattering angle, respectively.

Problem 3

Show that the differential cross section $\sigma'(\Theta)$ for the elastic scattering of a particle of mass m from the repulsive central-force potential $U(r) = k/r^2$ with a fixed force-center at $r = 0$ (or an infinitely massive target particle) is

$$\sigma'(\Theta) = \frac{2\pi^2\,k}{m\,u^2}\,\frac{(\pi - \Theta)}{[\Theta\,(2\pi - \Theta)]^2\,\sin\Theta},$$

where u is the speed of the incoming projectile particle at $r = \infty$.

$$\textit{Hint}: \quad \textit{Show that} \quad b(\Theta) = \frac{r_0\,(\pi - \Theta)}{\sqrt{2\pi\,\Theta - \Theta^2}}, \quad \textit{where} \quad r_0^2 = \frac{2\,k}{m\,u^2}.$$

Problem 4

By using the relations $\tan\theta = \sin\Theta/(\alpha + \cos\Theta)$ and/or $\sin(\Theta - \theta) = \alpha\,\sin\theta$, where $\alpha = m_1/m_2$, show that the relation between the differential cross section in the CM frame,

$\sigma'(\Theta)$, and the differential cross section in the LAB frame, $\sigma(\theta)$, is

$$\sigma'(\Theta) \;=\; \sigma(\theta) \;\cdot\; \frac{1+\alpha\,\cos\Theta}{(1+2\,\alpha\,\cos\Theta+\alpha^2)^{3/2}}.$$

Problem 5

Consider the scattering of a particle of mass m by the localized repulsive central potential

$$U(r) \;=\; \begin{cases} -\,kr^2/2 & r \;\le\; R \\ \\ 0 & r \;>\; R \end{cases}$$

where the radius R denotes the range of the interaction.

(a) Show that for a particle of energy $E > 0$ moving towards the center of attraction with impact parameter $b = R\,\sin\beta$, the distance of closest approach ρ for this problem is

$$\rho \;=\; \sqrt{\frac{E}{k}\,(\mathsf{e}-1)}, \quad \text{where} \quad \mathsf{e} \;=\; \sqrt{1 \;+\; \frac{2\,kb^2}{E}}$$

(b) Show that the angle χ at closest approach is

$$\begin{aligned} \chi \;&=\; \beta \;+\; \int_\rho^R \frac{(b/r^2)\,dr}{\sqrt{1-b^2/r^2+kr^2/2E}} \\ &=\; \beta \;+\; \frac{1}{2}\,\arccos\left(\frac{2\,\sin^2\beta-1}{\mathsf{e}}\right) \end{aligned}$$

(c) Using the relation $\chi = \frac{1}{2}\,(\pi+\Theta)$ between χ and the CM scattering angle Θ, show that

$$\mathsf{e} \;=\; \frac{\cos 2\beta}{\cos(2\beta-\Theta)} \;<\; 1.$$

Problem 6

Consider elastic scattering by a hard ellipsoid $\rho(z) = \rho_0\,\sqrt{1-(z/z_0)^2}$ $(-\,z_0 \le z \le 0)$, where $\rho_0 = z_0\,\sqrt{1-\mathsf{e}^2} \le z_0$ and $0 \le \mathsf{e} < 1$ denotes the eccentricity of the ellipse in the (ρ, z)-plane.

(a) Show that the differential scattering cross-section is expressed as

$$\sigma(\Theta) \;=\; \frac{\rho_0^2\,(1-\mathsf{e}^2)}{4\,(1-\mathsf{e}^2\,\cos^2\frac{\Theta}{2})}.$$

(b) Show that the total cross-section σ_T is

$$\sigma_T \;=\; 2\pi\,\int_0^\pi\,\sigma(\Theta)\,\sin\Theta\,d\Theta \;=\; \pi\,\rho_0^2\left[\,\left(\frac{1}{\mathsf{e}^2}\;-\;1\right)\,\ln\left(\frac{1}{1-\mathsf{e}^2}\right)\,\right].$$

(c) Show that we recover the hard-sphere result $\sigma_T = \pi\,\rho_0^2$ in the limit $\mathsf{e} \to 0$.

Chapter 6

Motion in a Non-Inertial Frame

A reference frame is said to be an *inertial* frame if the motion of particles in that frame is subject only to physical forces (i.e., forces are derivable from a physical potential U such that $m\,\ddot{\mathbf{x}} = -\nabla U$). The Principle of Galilean Relativity (Sec. 2.5.3) states that the laws of physics are the same in all inertial frames and that all reference frames moving at constant velocity with respect to an inertial frame are also inertial frames. Hence, physical accelerations are identical in all inertial frames.

In contrast, a reference frame is said to be *non-inertial* if the motion of particles in that frame of reference violates the Principle of Galilean Relativity. Such non-inertial frames include all rotating frames and accelerated reference frames.

6.1 Time Derivatives in Fixed and Rotating Frames

To investigate the relationship between inertial and non-inertial frames, we consider the time derivative of an arbitrary vector $\mathbf{A}(t)$ in two reference frames. The first reference frame is called the *fixed* (inertial) frame and is expressed in terms of the Cartesian coordinates $\mathbf{r}' = (x', y', z')$. The second reference frame is called the *rotating* (non-inertial) frame and is expressed in terms of the Cartesian coordinates $\mathbf{r} = (x, y, z)$. In Figure 6.1, the rotating frame shares the same origin as the fixed frame (we relax this condition later) and the rotation angular velocity $\boldsymbol{\omega}$ of the rotating frame (with respect to the fixed frame) has components $(\omega_x, \omega_y, \omega_z)$.

Since observations can also be made in a rotating frame of reference, we decompose the vector $\mathbf{A}$ in terms of components A_i in the rotating frame (with unit vectors $\hat{\mathbf{x}}^i$). Thus, $\mathbf{A} = A_i\,\hat{\mathbf{x}}^i$ (using the summation rule) and the time derivative of $\mathbf{A}$ as observed in the fixed frame is

$$\frac{d\mathbf{A}}{dt} \;=\; \frac{dA_i}{dt}\,\hat{\mathbf{x}}^i \;+\; A_i\,\frac{d\hat{\mathbf{x}}^i}{dt}. \tag{6.1}$$

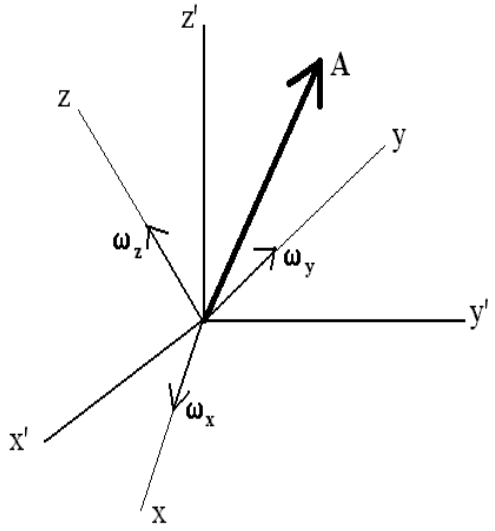

Figure 6.1: Rotating and fixed frames

The interpretation of the first term is that of the time derivative of $\mathbf{A}$ as observed in the rotating frame (where the unit vectors $\hat{\mathrm{x}}^i$ are constant) while the second term involves the time-dependence of the relation between the fixed and rotating frames. We now express $d\hat{\mathrm{x}}^i/dt$ as a vector in the rotating frame as

$$\frac{d\hat{\mathrm{x}}^i}{dt} \;=\; \boldsymbol{\omega} \times \hat{\mathrm{x}}^i, \tag{6.2}$$

where $\boldsymbol{\omega}$ denotes the angular velocity of the rotating frame. Hence, the second term in Eq. (6.1) becomes

$$A_i \frac{d\hat{\mathrm{x}}^i}{dt} \;=\; \boldsymbol{\omega} \times \mathbf{A}. \tag{6.3}$$

The time derivative of an arbitrary rotating-frame vector $\mathbf{A}$ in a fixed frame is, therefore, expressed as

$$\left(\frac{d\mathbf{A}}{dt}\right)_f \;=\; \left(\frac{d\mathbf{A}}{dt}\right)_r \;+\; \boldsymbol{\omega} \times \mathbf{A}, \tag{6.4}$$

where $(d/dt)_f$ denotes the time derivative as observed in the fixed (f) frame while $(d/dt)_r$ denotes the time derivative as observed in the rotating (r) frame. An important application of this formula relates to the time derivative of the rotation angular velocity $\boldsymbol{\omega}$ itself. One can easily see that

$$\left(\frac{d\boldsymbol{\omega}}{dt}\right)_f \;=\; \dot{\boldsymbol{\omega}} \;=\; \left(\frac{d\boldsymbol{\omega}}{dt}\right)_r,$$

since the second term in Eq. (6.4) vanishes for $\mathbf{A} = \boldsymbol{\omega}$; the time derivative of $\boldsymbol{\omega}$ is, therefore, the same in both frames of reference and is denoted $\dot{\boldsymbol{\omega}}$ in what follows.

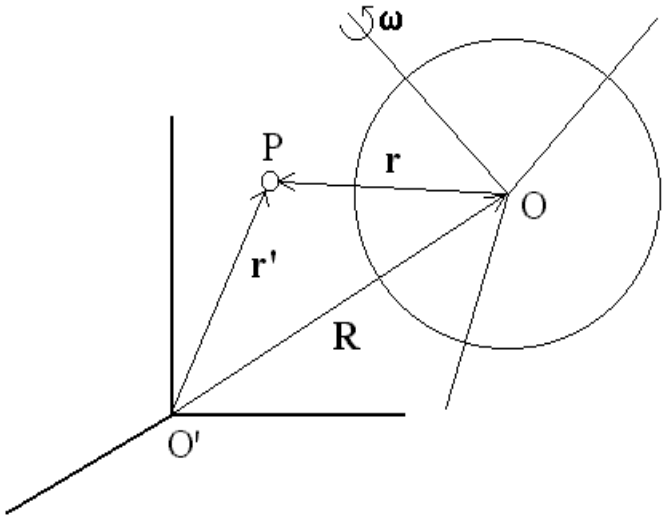

Figure 6.2: General rotating frame

6.2 Accelerations in Rotating Frames

We now consider the general case of a rotating frame and fixed frame being related by translation and rotation. In Figure 6.2, the position of a point P according to the fixed frame of reference is labeled $\mathbf{r}'$, while the position of the same point according to the rotating frame of reference is labeled $\mathbf{r}$, and

$$\mathbf{r}' \;=\; \mathbf{R} \;+\; \mathbf{r}, \tag{6.5}$$

where $\mathbf{R}$ denotes the position of the origin of the rotating frame (e.g., the center of mass) according to the fixed frame. Since the velocity of the point P involves the rate of change of position, we must now be careful in defining which time-derivative operator, $(d/dt)_f$ or $(d/dt)_r$, is used.

The velocities of point P as observed in the fixed and rotating frames are defined as

$$\mathbf{v}_f \;=\; \left(\frac{d\mathbf{r}'}{dt}\right)_f \quad \text{and} \quad \mathbf{v}_r \;=\; \left(\frac{d\mathbf{r}}{dt}\right)_r, \tag{6.6}$$

respectively. Using Eq. (6.4), the relation between the fixed-frame and rotating-frame velocities is expressed as

$$\mathbf{v}_f \;=\; \left(\frac{d\mathbf{R}}{dt}\right)_f \;+\; \left(\frac{d\mathbf{r}}{dt}\right)_f \;=\; \mathbf{V} \;+\; \mathbf{v}_r \;+\; \boldsymbol{\omega}\times\mathbf{r}, \tag{6.7}$$

where $\mathbf{V} = (d\mathbf{R}/dt)_f$ denotes the translation velocity of the rotating-frame origin (as observed in the fixed frame).

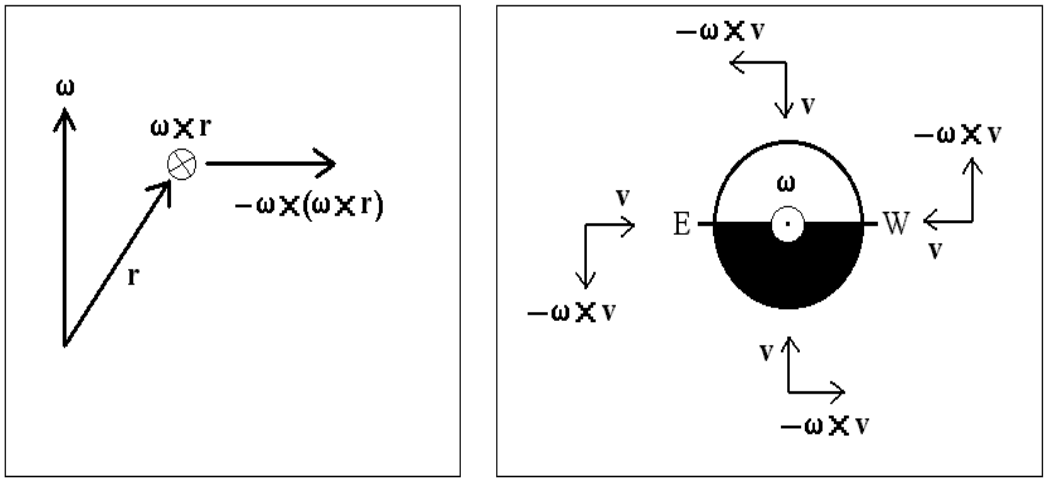

Figure 6.3: Centrifugal and Coriolis accelerations in a rotating frame of reference.

Using Eq. (6.7), we are now in a position to evaluate expressions for the acceleration of point P as observed in the fixed and rotating frames of reference

$$\mathbf{a}_f \;=\; \left(\frac{d\mathbf{v}_f}{dt}\right)_f \quad \text{and} \quad \mathbf{a}_r \;=\; \left(\frac{d\mathbf{v}_r}{dt}\right)_r, \tag{6.8}$$

respectively. Hence, using Eq. (6.7), we find

$$\begin{aligned}\mathbf{a}_f \;&=\; \left(\frac{d\mathbf{V}}{dt}\right)_f + \left(\frac{d\mathbf{v}_r}{dt}\right)_f + \left(\frac{d\boldsymbol{\omega}}{dt}\right)_f \times \mathbf{r} + \boldsymbol{\omega} \times \left(\frac{d\mathbf{r}}{dt}\right)_f \\ &=\; \mathbf{A} + (\mathbf{a}_r + \boldsymbol{\omega} \times \mathbf{v}_r) + \dot{\boldsymbol{\omega}} \times \mathbf{r} + \boldsymbol{\omega} \times (\mathbf{v}_r + \boldsymbol{\omega} \times \mathbf{r}),\end{aligned}$$

or

$$\mathbf{a}_f \;=\; \mathbf{A} + \mathbf{a}_r + 2\,\boldsymbol{\omega} \times \mathbf{v}_r + \dot{\boldsymbol{\omega}} \times \mathbf{r} + \boldsymbol{\omega} \times (\boldsymbol{\omega} \times \mathbf{r}), \tag{6.9}$$

where $\mathbf{A} = (d\mathbf{V}/dt)_f$ denotes the translational acceleration of the rotating-frame origin (as observed in the fixed frame of reference). We can now write an expression for the acceleration of point P as observed in the rotating frame as

$$\mathbf{a}_r \;=\; \mathbf{a}_f \;-\; \mathbf{A} \;-\; \boldsymbol{\omega} \times (\boldsymbol{\omega} \times \mathbf{r}) \;-\; 2\,\boldsymbol{\omega} \times \mathbf{v}_r \;-\; \dot{\boldsymbol{\omega}} \times \mathbf{r}, \tag{6.10}$$

which represents the sum of the net *inertial* acceleration $(\mathbf{a}_f - \mathbf{A})$, the centrifugal acceleration $-\,\boldsymbol{\omega} \times (\boldsymbol{\omega} \times \mathbf{r})$ and the *Coriolis* acceleration $-\,2\boldsymbol{\omega} \times \mathbf{v}_r$ (see Figures 6.3) and an angular acceleration term $-\,\dot{\boldsymbol{\omega}} \times \mathbf{r}$ which depends explicitly on the time dependence of the rotation angular velocity $\boldsymbol{\omega}$. The centrifugal acceleration (which is directed outwardly from the rotation axis) represents a familiar *non-inertial* effect in physics. A less familiar

non-inertial effect is the Coriolis acceleration discovered in 1831 by Gaspard Gustave de Coriolis (1792-1843). Figure 6.3 shows that an object *falling* inwardly also experiences an *eastward* acceleration.

6.3 Lagrangian Formulation of Non-Inertial Motion

We can recover the expression (6.10) for the acceleration in a rotating (non-inertial) frame from a Lagrangian formulation as follows. The Lagrangian for a particle of mass m moving in a non-inertial rotating frame (with its origin coinciding with the fixed-frame origin) in the presence of the potential $U(\mathbf{r})$ is expressed as

$$L(\mathbf{r}, \dot{\mathbf{r}}) \;=\; \frac{m}{2} \left| \dot{\mathbf{r}} \;+\; \boldsymbol{\omega} \times \mathbf{r} \right|^2 \;-\; U(\mathbf{r}), \tag{6.11}$$

where $\boldsymbol{\omega}$ is the angular velocity vector and we use the formula

$$\left| \dot{\mathbf{r}} \;+\; \boldsymbol{\omega} \times \mathbf{r} \right|^2 \;=\; \left| \dot{\mathbf{r}} \right|^2 \;+\; 2\, \boldsymbol{\omega} \cdot (\mathbf{r} \times \dot{\mathbf{r}}) \;+\; \left[\, \omega^2\, r^2 \;-\; (\boldsymbol{\omega} \cdot \mathbf{r})^2 \,\right].$$

Using the Lagrangian (6.11), we now derive the general Euler-Lagrange equation for $\mathbf{r}$. First, we derive an expression for the canonical momentum

$$\mathbf{p} \;=\; \frac{\partial L}{\partial \dot{\mathbf{r}}} \;=\; m\, (\dot{\mathbf{r}} \;+\; \boldsymbol{\omega} \times \mathbf{r})\,, \tag{6.12}$$

and

$$\frac{d}{dt} \left(\frac{\partial L}{\partial \dot{\mathbf{r}}} \right) \;=\; m\, (\ddot{\mathbf{r}} \;+\; \dot{\boldsymbol{\omega}} \times \mathbf{r} \;+\; \boldsymbol{\omega} \times \dot{\mathbf{r}})\,.$$

Next, we derive the partial derivative

$$\frac{\partial L}{\partial \mathbf{r}} \;=\; -\, \nabla U(\mathbf{r}) \;-\; m\, [\, \boldsymbol{\omega} \times \dot{\mathbf{r}} \;+\; \boldsymbol{\omega} \times (\boldsymbol{\omega} \times \mathbf{r})\,]\,,$$

so that the Euler-Lagrange equations are

$$m\, \ddot{\mathbf{r}} \;=\; -\, \nabla U(\mathbf{r}) \;-\; m\, [\, \dot{\boldsymbol{\omega}} \times \mathbf{r} \;+\; 2\, \boldsymbol{\omega} \times \dot{\mathbf{r}} \;+\; \boldsymbol{\omega} \times (\boldsymbol{\omega} \times \mathbf{r})\,]\,. \tag{6.13}$$

Here, the potential energy term generates the fixed-frame acceleration, $-\nabla U = m\, \mathbf{a}_f$, and thus the Euler-Lagrange equation (6.13) yields Eq. (6.10).

6.4 Motion Relative to Earth

We can now apply these non-inertial expressions to the important case of the fixed frame of reference having its origin at the center of Earth (point O' in Figure 6.4) and the rotating

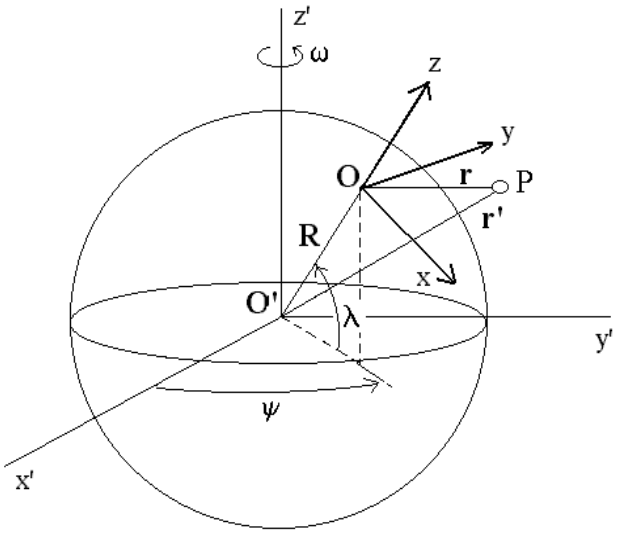

Figure 6.4: Earth frame

frame of reference having its origin at latitude λ and longitude ψ (point O in Figure 6.4). We note that the rotation of the Earth is now represented as $\dot{\psi} = \omega$ and that $\dot{\boldsymbol{\omega}} = 0$.

We arrange the (x, y, z) axis of the rotating frame so that the z-axis is a continuation of the position vector $\mathbf{R}$ of the rotating-frame origin, i.e., $\mathbf{R} = R\,\hat{\mathsf{z}}$ in the rotating frame (where $R = 6378$ km is the radius of a *spherical* Earth). When expressed in terms of the fixed-frame latitude angle λ and the azimuthal angle ψ, the unit vector $\hat{\mathsf{z}}$ is

$$\hat{\mathsf{z}} \;=\; \cos\lambda\;(\cos\psi\,\hat{\mathsf{x}}' \;+\; \sin\psi\,\hat{\mathsf{y}}') \;+\; \sin\lambda\,\hat{\mathsf{z}}',$$

i.e., $\hat{\mathsf{z}}$ points upward. Likewise, we choose the x-axis to be tangent to a *great circle* passing through the North and South poles, so that

$$\hat{\mathsf{x}} \;=\; \sin\lambda\;(\cos\psi\,\hat{\mathsf{x}}' \;+\; \sin\psi\,\hat{\mathsf{y}}') \;-\; \cos\lambda\,\hat{\mathsf{z}}',$$

i.e., $\hat{\mathsf{x}}$ points southward. Lastly, the y-axis is chosen such that

$$\hat{\mathsf{y}} \;=\; \hat{\mathsf{z}} \times \hat{\mathsf{x}} \;=\; -\sin\psi\,\hat{\mathsf{x}}' \;+\; \cos\psi\,\hat{\mathsf{y}}',$$

i.e., $\hat{\mathsf{y}}$ points eastward.

We now consider the acceleration of a point P as observed in the rotating frame O by writing Eq. (6.10) as

$$\frac{d^2\mathbf{r}}{dt^2} \;=\; \mathbf{g}_0 \;-\; \ddot{\mathbf{R}}_f \;-\; \boldsymbol{\omega} \times (\boldsymbol{\omega} \times \mathbf{r}) \;-\; 2\,\boldsymbol{\omega} \times \frac{d\mathbf{r}}{dt}. \tag{6.14}$$

The first term represents the *pure* gravitational acceleration due to the graviational pull of the Earth on point P (as observed in the fixed frame located at Earth's center)

$$\mathbf{g}_0 \;=\; -\,\frac{G\,M}{|\mathbf{r}'|^3}\,\mathbf{r}',$$

where $\mathbf{r}' = \mathbf{R} + \mathbf{r}$ is the position of point P in the fixed frame and $\mathbf{r}$ is the location of P in the rotating frame. When expressed in terms of rotating-frame spherical coordinates (r, θ, φ):

$$\mathbf{r} \;=\; r\,[\,\sin\theta\;(\cos\varphi\,\hat{\mathsf{x}} \;+\; \sin\varphi\,\hat{\mathsf{y}})\;+\;\cos\theta\,\hat{\mathsf{z}}\,]\,,$$

the fixed-frame position $\mathbf{r}'$ is written as

$$\mathbf{r}' \;=\; (R + r\,\cos\theta)\,\hat{\mathsf{z}} \;+\; r\,\sin\theta\;(\cos\varphi\,\hat{\mathsf{x}} + \sin\varphi\,\hat{\mathsf{y}})\,,$$

and thus

$$|\mathbf{r}'|^3 \;=\; \left(R^2 \;+\; 2\,R\,r\,\cos\theta \;+\; r^2\right)^{3/2}.$$

The pure gravitational acceleration is, therefore, expressed in the rotating frame of the Earth as

$$\mathbf{g}_0 \;=\; -\,g_0\,\left[\;\frac{(1+\epsilon\,\cos\theta)\,\hat{\mathsf{z}} \;+\; \epsilon\,\sin\theta\,(\cos\varphi\,\hat{\mathsf{x}} + \sin\varphi\,\hat{\mathsf{y}})}{(1 + 2\,\epsilon\,\cos\theta \;+\; \epsilon^2)^{3/2}}\;\right], \tag{6.15}$$

where $g_0 = GM/R^2 = 9.789$ m/s^2 and $\epsilon = r/R \ll 1$.

The angular velocity in the fixed frame is $\boldsymbol{\omega} = \omega\,\hat{\mathsf{z}}'$, where

$$\omega \;=\; \frac{2\pi \text{ rad}}{24 \;\times\; 3600 \text{ sec}} \;=\; 7.27 \;\times\; 10^{-5} \;\text{ rad/s}$$

is the rotation speed of Earth about its axis. In the rotating frame, we find

$$\boldsymbol{\omega} \;=\; \omega\;(\sin\lambda\,\hat{\mathsf{z}} \;-\; \cos\lambda\,\hat{\mathsf{x}})\,. \tag{6.16}$$

Because the position vector $\mathbf{R}$ rotates with the origin of the rotating frame, its time derivatives yield

$$\begin{aligned}
\dot{\mathbf{R}}_f \;&=\; \boldsymbol{\omega}\times\mathbf{R} \;=\; (\omega\,R\,\cos\lambda)\;\hat{\mathsf{y}},\\
\ddot{\mathbf{R}}_f \;&=\; \boldsymbol{\omega}\times\dot{\mathbf{R}}_f \;=\; \boldsymbol{\omega}\times(\boldsymbol{\omega}\times\mathbf{R}) \;=\; -\,\omega^2\,R\,\cos\lambda\;(\cos\lambda\,\hat{\mathsf{z}} \;+\; \sin\lambda\,\hat{\mathsf{x}})\,,
\end{aligned}$$

and thus the centrifugal acceleration due to $\mathbf{R}$ is

$$-\,\ddot{\mathbf{R}}_f \;=\; -\,\boldsymbol{\omega}\times(\boldsymbol{\omega}\times\mathbf{R}) \;=\; \alpha\,g_0\;\cos\lambda\,(\cos\lambda\,\hat{\mathsf{z}} \;+\; \sin\lambda\,\hat{\mathsf{x}})\,, \tag{6.17}$$

where $\omega^2 R = 0.0337$ m/s^2 can be expressed in terms of the *pure* gravitational acceleration g_0 as $\omega^2 R = \alpha\,g_0$, where $\alpha = 3.4 \;\times\; 10^{-3}$ is the normalized centrifugal acceleration. We now define the physical gravitational acceleration as

$$\begin{aligned}
\mathbf{g} \;&=\; \mathbf{g}_0 \;-\; \boldsymbol{\omega}\times(\boldsymbol{\omega}\times\mathbf{R})\\
&=\; g_0\left[\,-\,\left(1 \;-\; \alpha\,\cos^2\lambda\right)\hat{\mathsf{z}} \;+\; (\alpha\;\cos\lambda\,\sin\lambda)\;\hat{\mathsf{x}}\,\right],
\end{aligned} \tag{6.18}$$

where terms of order $\epsilon = r/R$ have been neglected. For example, a plumb line experiences a small angular deviation $\delta(\lambda)$ (southward) from the true vertical given as

$$\tan\delta(\lambda) \;=\; \frac{g_x}{|g_z|} \;=\; \frac{\alpha\;\sin 2\lambda}{(2-\alpha) + \alpha\;\cos 2\lambda}.$$

This function exhibits a maximum at a latitude $\overline{\lambda}$ defined as $\cos 2\overline{\lambda} = -\alpha/(2-\alpha)$, so that

$$\tan\overline{\delta} \;=\; \frac{\alpha\,\sin 2\overline{\lambda}}{(2-\alpha)+\alpha\,\cos 2\overline{\lambda}} \;=\; \frac{\alpha}{2\sqrt{1-\alpha}} \;\simeq\; 1.7\times 10^{-3},$$

or

$$\overline{\delta} \;\simeq\; 5.86\ \text{arcmin} \quad \text{at} \quad \overline{\lambda} \;\simeq\; \left(\frac{\pi}{4} \;+\; \frac{\alpha}{4}\right)\ \text{rad} \;=\; 45.05^o.$$

We now return to Eq. (6.14), which is written to lowest order in ϵ and α as

$$\frac{d^2\mathbf{r}}{dt^2} \;=\; -\,g\,\widehat{\mathsf{z}} \;-\; 2\,\boldsymbol{\omega}\times\frac{d\mathbf{r}}{dt}, \tag{6.19}$$

where

$$\boldsymbol{\omega}\times\frac{d\mathbf{r}}{dt} \;=\; \omega\,[\,(\dot{x}\,\sin\lambda \;+\; \dot{z}\,\cos\lambda)\,\widehat{\mathsf{y}} \;-\; \dot{y}\,(\sin\lambda\,\widehat{\mathsf{x}} \;+\; \cos\lambda\,\widehat{\mathsf{z}})\,]\,.$$

Thus, we find the three components of Eq. (6.19) written explicitly as

$$\left.\begin{array}{rcl} \ddot{x} &=& 2\,\omega\,\sin\lambda\,\dot{y} \\ \ddot{y} &=& -\,2\,\omega\,(\sin\lambda\,\dot{x} \;+\; \cos\lambda\,\dot{z}) \\ \ddot{z} &=& -\,g \;+\; 2\,\omega\,\cos\lambda\,\dot{y} \end{array}\right\}. \tag{6.20}$$

A first integration of Eq. (6.20) yields

$$\left.\begin{array}{rcl} \dot{x} &=& 2\,\omega\,\sin\lambda\,y \;+\; C_x \\ \dot{y} &=& -\,2\,\omega\,(\sin\lambda\,x \;+\; \cos\lambda\,z) \;+\; C_y \\ \dot{z} &=& -\,g\,t \;+\; 2\,\omega\,\cos\lambda\,y \;+\; C_z \end{array}\right\}, \tag{6.21}$$

where (C_x, C_y, C_z) are constants defined from initial conditions (x_0, y_0, z_0) and $(\dot{x}_0, \dot{y}_0, \dot{z}_0)$:

$$\left.\begin{array}{rcl} C_x &=& \dot{x}_0 \;-\; 2\,\omega\,\sin\lambda\,y_0 \\ C_y &=& \dot{y}_0 \;+\; 2\,\omega\,(\sin\lambda\,x_0 \;+\; \cos\lambda\,z_0) \\ C_z &=& \dot{z}_0 \;-\; 2\,\omega\,\cos\lambda\,y_0 \end{array}\right\}. \tag{6.22}$$

A second integration of Eq. (6.21) yields

$$\begin{aligned} x(t) &= x_0 \;+\; C_x\,t \;+\; 2\,\omega\,\sin\lambda\,\int_0^t y\,dt, \\ y(t) &= y_0 \;+\; C_y\,t \;-\; 2\,\omega\,\sin\lambda\,\int_0^t x\,dt \;-\; 2\,\omega\,\cos\lambda\,\int_0^t z\,dt, \\ z(t) &= z_0 \;+\; C_z\,t \;-\; \frac{1}{2}\,g\,t^2 \;+\; 2\,\omega\,\cos\lambda\,\int_0^t y\,dt, \end{aligned}$$

which can also be rewritten as

$$\left.\begin{array}{rcl} x(t) &=& x_0 \;+\; C_x\,t \;+\; \delta x(t) \\ y(t) &=& y_0 \;+\; C_y\,t \;+\; \delta y(t) \\ z(t) &=& z_0 \;+\; C_z\,t \;-\; \frac{1}{2}\,g\,t^2 \;+\; \delta z(t) \end{array}\right\}, \tag{6.23}$$

where the Coriolis *drifts* are

$$\delta x(t) \;=\; 2\,\omega\,\sin\lambda\Big(\;y_0\,t\;+\;\frac{1}{2}\,C_y\,t^2\;+\;\int_0^t\;\delta y\,dt\;\Big) \tag{6.24}$$

$$\begin{aligned}\delta y(t) \;=\;& -\,2\,\omega\,\sin\lambda\;\Big(\;x_0\,t\;+\;\frac{1}{2}\,C_x\,t^2\;+\;\int_0^t\;\delta x\,dt\;\Big)\\ & -\;2\,\omega\,\cos\lambda\Big(\;z_0\,t\;+\;\frac{1}{2}\,C_z\,t^2\;-\;\frac{1}{6}\,g\,t^3\;+\;\int_0^t\;\delta z\,dt\;\Big)\end{aligned} \tag{6.25}$$

$$\delta z(t) \;=\; 2\,\omega\,\cos\lambda\Big(\;y_0\,t\;+\;\frac{1}{2}\,C_y\,t^2\;+\;\int_0^t\;\delta y\,dt\;\Big)\,. \tag{6.26}$$

Note that each Coriolis drift can be expressed as an infinite series in powers of ω and that all Coriolis effects vanish when $\omega = 0$.

6.4.1 Free-Fall Problem Revisited

As an example of the importance of Coriolis effects in describing motion relative to Earth, we consider the simple *free-fall* problem, where

$$(x_0, y_0, z_0) \;=\; (0, 0, h) \quad\text{and}\quad (\dot{x}_0, \dot{y}_0, \dot{z}_0) \;=\; (0, 0, 0),$$

so that the constants (6.22) are

$$C_x \;=\; 0 \;=\; C_z \quad\text{and}\quad C_y \;=\; 2\,\omega\,h\,\cos\lambda.$$

Substituting these constants into Eqs. (6.23) and keeping only terms up to first order in ω, we find

$$x(t) \;=\; 0, \tag{6.27}$$

$$y(t) \;=\; \frac{1}{3}\,gt^3\,\omega\,\cos\lambda, \tag{6.28}$$

$$z(t) \;=\; h\;-\;\frac{1}{2}\,gt^2. \tag{6.29}$$

Hence, a free-falling object starting from rest touches the ground $z(T) = 0$ after a time $T = \sqrt{2h/g}$ after which time the object has drifted eastward by a distance of

$$y(T) \;=\; \frac{1}{3}\,gT^3\,\omega\,\cos\lambda \;=\; \frac{\omega\,\cos\lambda}{3}\,\sqrt{\frac{8h^3}{g}},$$

which is maximum at the equator. At a height of 100 m and latitude 45^o, for example, we find an eastward drift of 1.55 cm.

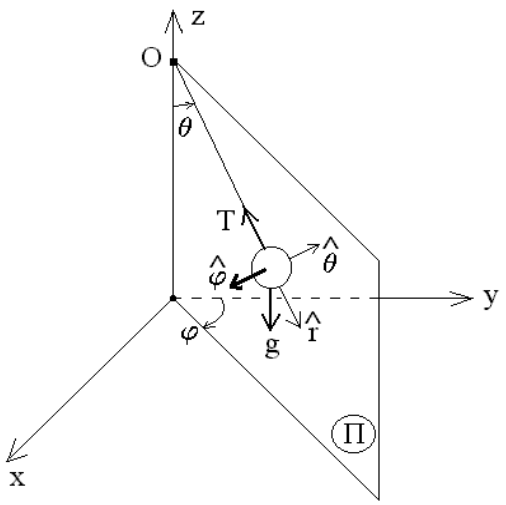

Figure 6.5: Foucault pendulum

6.4.2 Foucault Pendulum

In 1851, Jean Bernard Léon Foucault (1819-1868) was able to demonstrate, in a classic experiment demonstrating Earth's rotation, the role played by Coriolis effects in his investigations of the motion of a pendulum (of length $\ell$and mass m) in the rotating frame of the Earth. His analysis showed that, because of the Coriolis acceleration associated with the rotation of the Earth, the motion of the pendulum exhibits a precession motion whose period depends on the latitude at which the pendulum is located.

The equation of motion for the pendulum is given as

$$\ddot{\mathbf{r}} \;=\; \mathbf{a}_f \;-\; 2\,\boldsymbol{\omega}\times\dot{\mathbf{r}}, \tag{6.30}$$

where $\mathbf{a}_f = \mathbf{g}+\mathbf{T}/m$ is the net fixed-frame acceleration of the pendulum expressed in terms of the gravitational acceleration $\mathbf{g}$ and the string tension $\mathbf{T}$ (see Figure 6.5). Note that the vectors $\mathbf{g}$ and $\mathbf{T}$ span a plane Π in which the pendulum moves in the absence of the Coriolis acceleration $-\,2\boldsymbol{\omega}\times\dot{\mathbf{r}}$. Using spherical coordinates (r,θ,φ) in the rotating frame and placing the origin O of the pendulum system at its pivot point (see Figure 6.5), the position of the pendulum bob is

$$\mathbf{r} \;=\; \ell\;[\,\sin\theta\,(\sin\varphi\,\hat{\mathsf{x}} \;+\; \cos\varphi\,\hat{\mathsf{y}}) \;-\; \cos\theta\,\hat{\mathsf{z}}\,] \;=\; \ell\,\hat{r}(\theta,\varphi). \tag{6.31}$$

From this definition, we construct the unit vectors $\widehat{\theta}$ and $\widehat{\varphi}$ as

$$\frac{\partial\widehat{r}}{\partial\theta} \;=\; \widehat{\theta}, \quad \frac{\partial\widehat{r}}{\partial\varphi} \;=\; \sin\theta\,\widehat{\varphi}, \quad \text{and} \quad \frac{\partial\widehat{\theta}}{\partial\varphi} \;=\; \cos\theta\,\widehat{\varphi}. \tag{6.32}$$

Note that, whereas the unit vectors $\widehat{r}$ and $\widehat{\theta}$ lie on the plane Π, the unit vector $\widehat{\varphi}$ is perpendicular to it and, thus, the equation of motion of the pendulum *perpendicular* to the plane Π is

$$\ddot{\mathbf{r}} \cdot \widehat{\varphi} \;=\; -\,2\;(\boldsymbol{\omega} \times \dot{\mathbf{r}}) \cdot \widehat{\varphi}. \tag{6.33}$$

The pendulum velocity is obtained from Eq. (6.31) as

$$\dot{\mathbf{r}} \;=\; \ell \left(\dot{\theta}\, \widehat{\theta} \;+\; \dot{\varphi}\, \sin\theta\, \widehat{\varphi} \right), \tag{6.34}$$

so that the azimuthal component of the Coriolis acceleration is

$$-\,2\;(\boldsymbol{\omega} \times \dot{\mathbf{r}}) \cdot \widehat{\varphi} \;=\; 2\,\ell\omega\,\dot{\theta}\,(\sin\lambda\,\cos\theta \;+\; \cos\lambda\,\sin\theta\,\sin\varphi)\,.$$

If the length ℓ of the pendulum is large, the angular deviation θ of the pendulum can be small enough that $\sin\theta \ll 1$ and $\cos\theta \simeq 1$ and, thus, the azimuthal component of the Coriolis acceleration is approximately

$$-\,2\;(\boldsymbol{\omega} \times \dot{\mathbf{r}}) \cdot \widehat{\varphi} \;\simeq\; 2\,\ell\,(\omega\,\sin\lambda)\;\dot{\theta}. \tag{6.35}$$

Next, the azimuthal component of the pendulum acceleration is

$$\ddot{\mathbf{r}} \cdot \widehat{\varphi} \;=\; \ell \left(\ddot{\varphi}\;\sin\theta \;+\; 2\,\dot{\theta}\,\dot{\varphi}\;\cos\theta \right),$$

which for small angular deviations ($\theta \ll 1$) yields

$$\ddot{\mathbf{r}} \cdot \widehat{\varphi} \;\simeq\; 2\,\ell\;(\dot{\varphi})\;\dot{\theta}. \tag{6.36}$$

By combining these expressions into Eq. (6.33), we obtain an expression for the precession angular frequency of the Foucault pendulum

$$\dot{\varphi} \;=\; \omega\;\sin\lambda \tag{6.37}$$

as a function of latitude λ. As expected, the precession motion is clockwise in the Northern Hemisphere and reaches a maximum at the North Pole ($\lambda = 90^o$). Note that the precession period of the Foucault pendulum is $(1\ \text{day}/\sin\lambda)$ so that the period is 1.41 days at a latitude of 45^o or 2 days at a latitude of 30^o.

The more traditional approach to describing the precession motion of the Foucault pendulum makes use of Cartesian coordinates (x, y, z). The motion of the Foucault pendulum in the (x, y)-plane is described in terms of Eqs. (6.30) as

$$\left.\begin{array}{rcl} \ddot{x} \;+\; \omega_0^2\, x &=& 2\,\omega\sin\lambda\;\dot{y} \\ \ddot{y} \;+\; \omega_0^2\, y &=& -\,2\,\omega\sin\lambda\;\dot{x} \end{array}\right\}, \tag{6.38}$$

where $\omega_0^2 = T/m\ell \simeq g/\ell$ and $\dot{z} \simeq 0$ if ℓ is very large. Figure 6.6 shows the numerical solution of Eqs. (6.38) for the Foucault pendulum starting from rest at $(x_0, y_0) = (0, 1)$ with $2\,(\omega/\omega_0)\,\sin\lambda = 0.05$ at $\lambda = 45^o$. The left figure in Figure 6.6 shows the short time

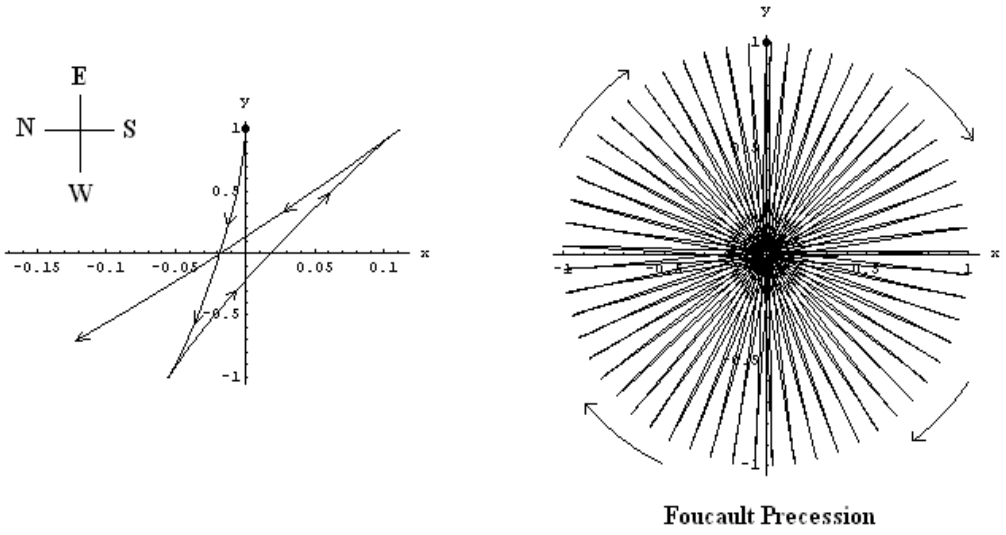

Figure 6.6: Numerical solution of the Foucault pendulum

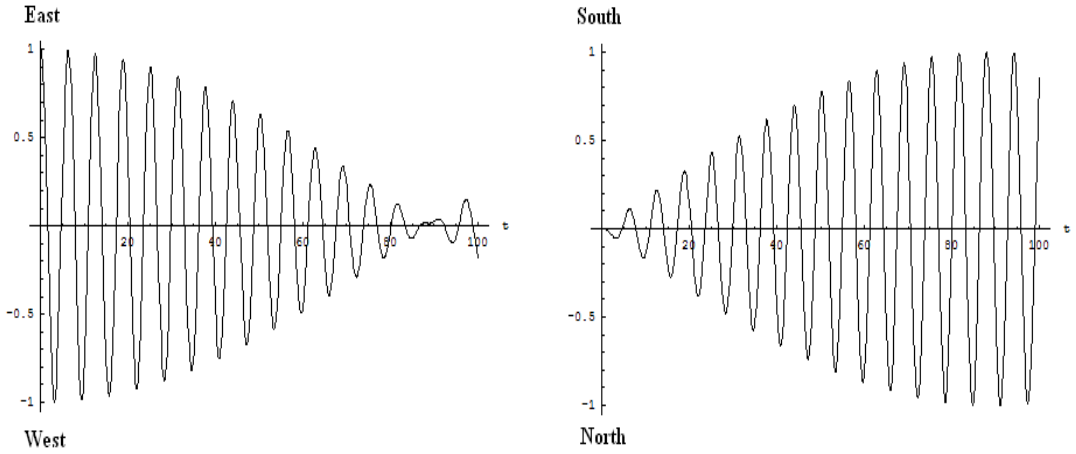

Figure 6.7: Projection of the Foucault pendulum along East-West and North-South directions.

behavior (note the different x and y scales) while the right figure in Figure 6.6 shows the complete Foucault precession. Figure 6.7 shows that, over a finite period of time, the pendulum motion progressively moves from the East-West axis to the North-South axis. We now define the complex-valued function

$$q \;=\; y + i\,x \;=\; \ell\,\sin\theta\,e^{i\varphi}, \tag{6.39}$$

so that Eq. (6.38) becomes

$$\ddot{q} \;+\; \omega_0^2\,q \;-\; 2i\,\omega\sin\lambda\,\dot{q} \;=\; 0.$$

Next, we insert the eigenfunction $q(t) = \rho\,\exp(i\Omega t)$ into this equation and find that the solution for the eigenfrequency Ω is

$$\Omega \;=\; \omega\,\sin\lambda \;\pm\; \sqrt{\omega^2\,\sin^2\lambda \;+\; \omega_0^2},$$

so that the eigenfunction is

$$q \;=\; \rho\,e^{i\omega\,\sin\lambda\,t}\;\sin\left(\sqrt{\omega^2\,\sin^2\lambda \;+\; \omega_0^2}\;t\right).$$

By comparing this solution with Eq. (6.39), we finally find

$$\rho\;\sin\left(\sqrt{\omega^2\,\sin^2\lambda \;+\; \omega_0^2}\;t\right) \;=\; \ell\;\sin\theta \;\simeq\; \ell\;\theta(t),$$

and

$$\varphi(t) \;=\; (\omega\;\sin\lambda)\;t,$$

from which we recover the Foucault pendulum precession frequency (6.37).

6.5 Problems

Problem 1

(a) Consider the case involving motion on the (x, y)-plane perpendicular to the angular velocity vector $\boldsymbol{\omega} = \omega\,\hat{\mathbf{z}}$ with the potential energy

$$U(\mathbf{r}) \;=\; \frac{1}{2}\,k\,\left(x^2 \;+\; y^2\right).$$

Using the Euler-Lagrange equations (6.13), derive the equations of motion for x and y.

(b) By using the equations of motion derived in Part (a), show that the canonical angular momentum $\ell = \hat{\mathbf{z}}\cdot(\mathbf{r}\times\mathbf{p})$ is a constant of the motion.

Problem 2

If a particle is projected vertically upward to a height h above a point on the Earth's surface at a northern latitude λ, show that it strikes the ground at a point

$$\frac{4\omega}{3}\;\cos\lambda\,\sqrt{\frac{8\,h^3}{g}}$$

to the west. (Neglect air resistance, and consider only small vertical heights.)

Problem 3

For the potential

$$U(\mathbf{r},\dot{\mathbf{r}}) \;=\; V(r) \;+\; \boldsymbol{\sigma}\cdot\mathbf{r}\times\dot{\mathbf{r}},$$

where $V(r)$ denotes an arbitrary central potential and $\boldsymbol{\sigma}$ denotes an arbitrary constant vector, derive the Euler-Lagrange equations of motion in terms of spherical coordinates.

Problem 4

The Lagrangian for the Foucault-pendulum equations (6.38) is

$$L(x,y;\dot{x},\dot{y}) \;=\; \frac{1}{2}\,\left(\dot{x}^2+\dot{y}^2\right) \;-\; \frac{\omega_0^2}{2}\,\left(x^2+y^2\right) \;+\; \omega\,\sin\lambda\;\left(x\,\dot{y}-\dot{x}\,y\right).$$

(a) By using the polar transformation $x(t) = \rho(t)\,\cos\varphi(t)$ and $y(t) = \rho(t)\,\sin\varphi(t)$, derive the new Lagrangian $L(\rho;\dot{\rho},\dot{\varphi})$.

(b) Since the new Lagrangian $L(\rho;\dot{\rho},\dot{\varphi})$ is independent of φ, derive an expression for the conserved momentum p_φ and find the Routhian $R(\rho,\dot{\rho};p_\varphi)$ and the Routh-Euler-Lagrangian equation for ρ.

Chapter 7

Rigid Body Motion

7.1 Inertia Tensor

7.1.1 Discrete Particle Distribution

We begin our description of rigid body motion by considering the case of a rigid *discrete* particle distribution in which the inter-particle distances are constant. The position of each particle α as measured from a *fixed* laboratory (LAB) frame is

$$\mathbf{r}'_\alpha \;=\; \mathbf{R} \;+\; \mathbf{r}_\alpha,$$

where $\mathbf{R}$ is the position of the center of mass (CM) in the LAB and $\mathbf{r}_\alpha$ is the position of the particle in the CM frame. The velocity of particle α in the LAB frame is

$$\mathbf{v}'_\alpha \;=\; \mathbf{V} \;+\; \boldsymbol{\omega} \times \mathbf{r}_\alpha, \tag{7.1}$$

where $\boldsymbol{\omega}$ is the angular velocity vector associated with the rotation of the particle distribution about an axis of rotation which passes through the CM and $\mathbf{V}$ is the CM velocity in the LAB frame. The total linear momentum in the LAB frame is equal to the momentum of the center of mass since

$$\mathbf{P}' \;=\; \sum_\alpha m_\alpha \mathbf{v}'_\alpha \;=\; M\,\mathbf{V} \;+\; \boldsymbol{\omega} \times \left(\sum_\alpha m_\alpha \mathbf{r}_\alpha \right) \;=\; M\,\mathbf{V},$$

where we have used the definition of the total mass of the particle distribution

$$M \;=\; \sum_\alpha m_\alpha \quad \text{and} \quad \sum_\alpha m_\alpha \mathbf{r}_\alpha \;=\; 0. \tag{7.2}$$

Hence, the total momentum of a rigid body in its CM frame is zero. The total angular momentum in the LAB frame, however, is expressed as

$$\mathbf{L}' \;=\; \sum_\alpha m_\alpha\, \mathbf{r}'_\alpha \times \mathbf{v}'_\alpha \;=\; M\,\mathbf{R} \times \mathbf{V} \;+\; \sum_\alpha m_\alpha\, \mathbf{r}_\alpha \times (\boldsymbol{\omega} \times \mathbf{r}_\alpha)\,, \tag{7.3}$$

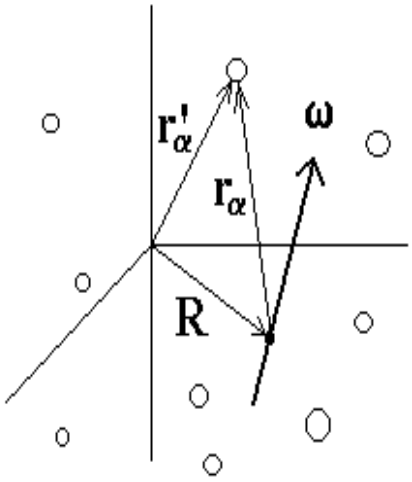

Figure 7.1: Discrete distribution of mass

where we have used the identities (7.2).

The kinetic energy of particle α (with mass m_α) in the LAB frame is

$$K'_\alpha \;=\; \frac{m_\alpha}{2}\,|\mathbf{v}'_\alpha|^2 \;=\; \frac{m_\alpha}{2}\left(|\mathbf{V}|^2 \;+\; 2\,\mathbf{V}\cdot\boldsymbol{\omega}\times\mathbf{r}_\alpha \;+\; |\boldsymbol{\omega}\times\mathbf{r}_\alpha|^2\right),$$

and thus, using the identities (7.2), the total kinetic energy $K' = \sum_\alpha K'_\alpha$ of the particle distribution is

$$K' \;=\; \frac{M}{2}\,|\mathbf{V}|^2 \;+\; \frac{1}{2}\left\{\,\omega^2\left(\sum_\alpha\, m_\alpha\, r_\alpha^2\right) \;-\; \boldsymbol{\omega}\boldsymbol{\omega} \;:\; \left(\sum_\alpha\, m_\alpha\,\mathbf{r}_\alpha\mathbf{r}_\alpha\right)\right\}. \tag{7.4}$$

Looking at Eqs. (7.3) and (7.4), we now introduce the *inertia tensor* of the particle distribution

$$\mathbf{I} \;=\; \sum_\alpha\, m_\alpha\left(r_\alpha^2\,\underline{\mathbf{1}} \;-\; \mathbf{r}_\alpha\,\mathbf{r}_\alpha\right), \tag{7.5}$$

where $\underline{\mathbf{1}}$ denotes the unit tensor (i.e., in Cartesian coordinates, $\underline{\mathbf{1}} = \hat{\mathsf{x}}\hat{\mathsf{x}} + \hat{\mathsf{y}}\hat{\mathsf{y}} + \hat{\mathsf{z}}\hat{\mathsf{z}}$). The inertia tensor can also be represented as a matrix

$$\mathbf{I} \;=\; \begin{pmatrix} \sum_\alpha\, m_\alpha\,(y_\alpha^2+z_\alpha^2) & -\sum_\alpha\, m_\alpha\,(x_\alpha y_\alpha) & -\sum_\alpha\, m_\alpha\,(x_\alpha z_\alpha) \\ -\sum_\alpha\, m_\alpha\,(y_\alpha x_\alpha) & \sum_\alpha\, m_\alpha\,(x_\alpha^2+z_\alpha^2) & -\sum_\alpha\, m_\alpha\,(y_\alpha z_\alpha) \\ -\sum_\alpha\, m_\alpha\,(z_\alpha x_\alpha) & -\sum_\alpha\, m_\alpha\,(z_\alpha y_\alpha) & \sum_\alpha\, m_\alpha\,(x_\alpha^2+y_\alpha^2) \end{pmatrix}, \tag{7.6}$$

where the symmetry property of the inertia tensor ($I^{ji} = I^{ij}$) is readily apparent. In terms of the inertia tensor (7.5), the angular momentum of a rigid body in the CM frame and its

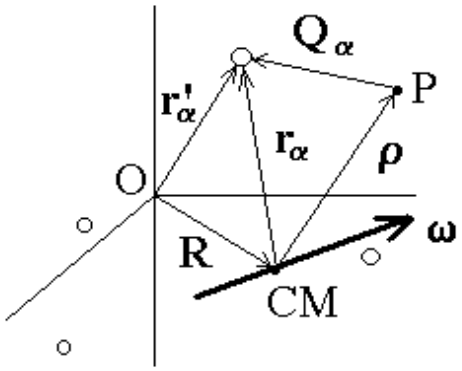

Figure 7.2: Parallel-axes theorem

rotational kinetic energy are

$$\mathbf{L} \;=\; \mathbf{I}\cdot\boldsymbol{\omega} \quad \text{and} \quad K_{rot} \;=\; \frac{1}{2}\,\boldsymbol{\omega}\cdot\mathbf{I}\cdot\boldsymbol{\omega}. \tag{7.7}$$

7.1.2 Parallel-Axes Theorem

A translation of the origin from which the inertia tensor is calculated leads to a different inertia tensor. Let $\mathbf{Q}_\alpha$ denote the position of particle α in a new frame of reference (with its origin located at point P in Figure 7.2) and let $\boldsymbol{\rho} = \mathbf{r}_\alpha - \mathbf{Q}_\alpha$ is the displacement from point CM to point P. The new inertia tensor

$$\mathbf{J} \;=\; \sum_\alpha m_\alpha \left(Q_\alpha^2\,\underline{\mathbf{1}} \;-\; \mathbf{Q}_\alpha\,\mathbf{Q}_\alpha\right)$$

can be expressed as

$$\begin{aligned}\mathbf{J} \;=\; & \sum_\alpha m_\alpha \left(\rho^2\,\underline{\mathbf{1}} \;-\; \boldsymbol{\rho}\,\boldsymbol{\rho}\right) \;+\; \sum_\alpha m_\alpha \left(r_\alpha^2\,\underline{\mathbf{1}} \;-\; \mathbf{r}_\alpha\,\mathbf{r}_\alpha\right) \\ & -\; \left\{\boldsymbol{\rho}\cdot\left(\sum_\alpha m_\alpha\,\mathbf{r}_\alpha\right)\right\}\underline{\mathbf{1}} \;+\; \left\{\boldsymbol{\rho}\,\left(\sum_\alpha m_\alpha\,\mathbf{r}_\alpha\right) \;+\; \left(\sum_\alpha m_\alpha\,\mathbf{r}_\alpha\right)\,\boldsymbol{\rho}\right\}.\end{aligned}$$

Since $M = \sum_\alpha m_\alpha$ and $\sum_\alpha m_\alpha \mathbf{r}_\alpha = 0$, we find

$$\mathbf{J} \;=\; M\,\left(\rho^2\,\underline{\mathbf{1}} \;-\; \boldsymbol{\rho}\,\boldsymbol{\rho}\right) \;+\; \mathbf{I}_{CM}. \tag{7.8}$$

Hence, once the inertia tensor $\mathbf{I}_{CM}$ is calculated in the CM frame, it can be calculated anywhere else. Eq. (7.8) is known as the Parallel-Axes Theorem.

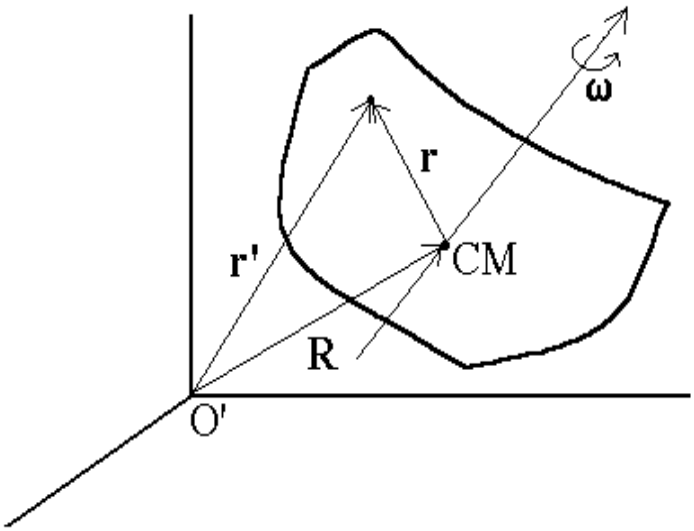

Figure 7.3: Continuous distribution of mass

7.1.3 Continuous Particle Distribution

For a continuous particle distribution the inertia tensor (7.5) becomes

$$\mathbf{I} \;=\; \int \, dm \, \left(r^2 \, \underline{\mathbf{1}} \;-\; \mathbf{r}\mathbf{r} \right), \tag{7.9}$$

where $dm(\mathbf{r}) \;=\; \rho(\mathbf{r})\, d^3r$ is the infinitesimal mass element at point $\mathbf{r}$, with mass density $\rho(\mathbf{r})$.

Consider, for example, the case of a uniform cube of mass M and volume b^3, with $dm = (M/b^3)\, dx\, dy\, dz$. The inertia tensor (7.9) in the LAB frame (with the origin placed at one of its corners) has the components

$$J^{11} \;=\; \frac{M}{b^3} \int_0^b dx \int_0^b dy \int_0^b dz \;\cdot\; \left(y^2 + z^2 \right) \;=\; \frac{2}{3}\, M\, b^2 \;=\; J^{22} \;=\; J^{33} \tag{7.10}$$

$$J^{12} \;=\; -\, \frac{M}{b^3} \int_0^b dx \int_0^b dy \int_0^b dz \;\cdot\; x\, y \;=\; -\, \frac{1}{4}\, M\, b^2 \;=\; J^{23} \;=\; J^{31} \tag{7.11}$$

and thus the inertia matrix for the cube is

$$\mathbf{J} \;=\; \frac{M\, b^2}{12} \begin{pmatrix} 8 & -3 & -3 \\ -3 & 8 & -3 \\ -3 & -3 & 8 \end{pmatrix}. \tag{7.12}$$

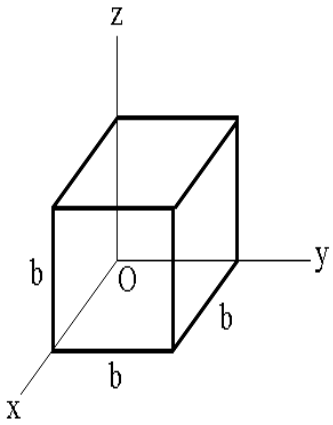

Figure 7.4: Cube

On the other hand, the inertia tensor calculated in the CM frame has the components

$$I^{11} \;=\; \frac{M}{b^3}\int_{-\,b/2}^{b/2} dx \int_{-\,b/2}^{b/2} dy \int_{-\,b/2}^{b/2} dz \;\cdot\; \left(y^2+z^2\right) \;=\; \frac{1}{6}\,M\,b^2 \;=\; I^{22} \;=\; I^{33} \tag{7.13}$$

$$I^{12} \;=\; -\,\frac{M}{b^3}\int_{-\,b/2}^{b/2} dx \int_{-\,b/2}^{b/2} dy \int_{-\,b/2}^{b/2} dz \;\cdot\; x\,y \;=\; 0 \;=\; I^{23} \;=\; I^{31} \tag{7.14}$$

and thus the CM inertia matrix for the cube is

$$\mathbf{I} \;=\; \frac{M\,b^2}{6}\begin{pmatrix} 1 & 0 & 0 \\ 0 & 1 & 0 \\ 0 & 0 & 1 \end{pmatrix}. \tag{7.15}$$

The displacement vector $\boldsymbol{\rho}$ from the CM point to the corner O is given as

$$\boldsymbol{\rho} = -\,\frac{b}{2}\,\left(\hat{\mathsf{x}}+\hat{\mathsf{y}}+\hat{\mathsf{z}}\right),$$

so that $\rho^2 = 3b^2/4$. By using the Parallel-Axis Theorem (7.8), the inertia tensor

$$M\,\left(\rho^2\,\underline{\mathbf{1}} \;-\; \boldsymbol{\rho}\,\boldsymbol{\rho}\right) \;=\; \frac{M\,b^2}{4}\begin{pmatrix} 2 & -1 & -1 \\ -1 & 2 & -1 \\ -1 & -1 & 2 \end{pmatrix}$$

when added to the CM inertia tensor (7.15), yields the inertia tensor (7.12)

7.1.4 Principal Axes of Inertia

In general, the CM inertia tensor $\mathbf{I}$ can be made into a *diagonal* tensor with components given by the eigenvalues I_1, I_2, and I_3 of the inertia tensor. These components (known as principal moments of inertia) are the three roots of the cubic polynomial

$$I^3 \;-\; \mathrm{Tr}(\mathbf{I})\, I^2 \;+\; \mathrm{Ad}(\mathbf{I})\, I \;-\; \mathrm{Det}(\mathbf{I}) \;=\; 0, \tag{7.16}$$

obtained from $\mathrm{Det}(\mathbf{I} - I\,\underline{\mathbf{1}}) = 0$, with coefficients

$$\begin{aligned}
\mathrm{Tr}(\mathbf{I}) &= I^{11} \;+\; I^{22} \;+\; I^{33}, \\
\mathrm{Ad}(\mathbf{I}) &= \mathrm{ad}_{11} \;+\; \mathrm{ad}_{22} \;+\; \mathrm{ad}_{33}, \\
\mathrm{Det}(\mathbf{I}) &= I^{11}\,\mathrm{ad}_{11} \;-\; I^{12}\,\mathrm{ad}_{12} \;+\; I^{13}\,\mathrm{ad}_{13},
\end{aligned}$$

where ad_{ij} is the determinant of the two-by-two matrix obtained from $\mathbf{I}$ by removing the i^{th}-row and j^{th}-column from the inertia matrix $\mathbf{I}$.

Each principal moment of inertia I_i represents the moment of inertia calculated about the principal axis of inertia with unit vector $\hat{\mathsf{e}}_i$. The unit vectors $(\hat{\mathsf{e}}_1, \hat{\mathsf{e}}_2, \hat{\mathsf{e}}_3)$ form a new frame of reference known as the *Body* frame. The unit vectors $(\hat{\mathsf{e}}_1, \hat{\mathsf{e}}_2, \hat{\mathsf{e}}_3)$ are related by a sequence of rotations to the Cartesian CM unit vectors $(\hat{\mathsf{x}}^1, \hat{\mathsf{x}}^2, \hat{\mathsf{x}}^3)$ by the relation

$$\hat{\mathsf{e}}_i \;=\; R_{ij}\,\hat{\mathsf{x}}^j, \tag{7.17}$$

where R_{ij} are components of the rotation matrix R. By denoting as $\mathbf{I}'$ the diagonal inertia tensor calculated in the *body* frame of reference (along the principal axes), we find

$$\mathbf{I}' \;=\; \mathsf{R}\cdot\mathbf{I}\cdot\mathsf{R}^{\mathrm{T}} \;=\; \begin{pmatrix} I_1 & 0 & 0 \\ 0 & I_2 & 0 \\ 0 & 0 & I_3 \end{pmatrix}, \tag{7.18}$$

where R^{T} denotes the transpose of R, i.e., $(\mathsf{R}^{\mathrm{T}})_{ij} = R_{ji}$. In the body frame, the inertia tensor is, therefore, expressed in dyadic form as

$$\mathbf{I}' \;=\; I_1\,\hat{\mathsf{e}}_1\,\hat{\mathsf{e}}_1 \;+\; I_2\,\hat{\mathsf{e}}_2\,\hat{\mathsf{e}}_2 \;+\; I_3\,\hat{\mathsf{e}}_3\,\hat{\mathsf{e}}_3, \tag{7.19}$$

and the rotational kinetic energy (7.7) is

$$K'_{rot} \;=\; \frac{1}{2}\,\boldsymbol{\omega}\cdot\mathbf{I}'\cdot\boldsymbol{\omega} \;=\; \frac{1}{2}\left(I_1\,\omega_1^2 \;+\; I_2\,\omega_2^2 \;+\; I_3\,\omega_3^2\right). \tag{7.20}$$

Note that general rotation matrices have the form

$$\mathsf{R}_n(\alpha) \;=\; \hat{\mathsf{n}}\,\hat{\mathsf{n}} \;+\; \cos\alpha\,(\underline{\mathbf{1}} \;-\; \hat{\mathsf{n}}\,\hat{\mathsf{n}}) \;+\; \sin\alpha\;\hat{\mathsf{n}}\times\underline{\mathbf{1}}, \tag{7.21}$$

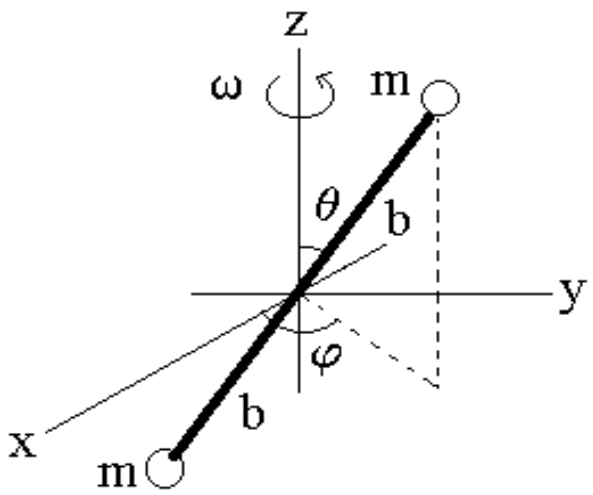

Figure 7.5: Dumbbell

where the unit vector $\hat{\mathsf{n}}$ defines the axis of rotation about which an angular rotation of angle α is performed according to the right-hand-rule.

A rigid body can be classified into one of three different categories. First, a rigid body can be said to be a *spherical top* if its three principal moments of inertia are equal ($I_1 = I_2 = I_3$), i.e., the three roots of the cubic polynomial (7.16) are triply degenerate. Next, a rigid body can be said to be a *symmetric top* if two of its principal moments of inertia are equal ($I_1 = I_2 \neq I_3$), i.e., I_3 is a single root and $I_1 = I_2$ are doubly-degenerate roots of the cubic polynomial (7.16). Lastly, when the three roots ($I_1 \neq I_2 \neq I_3$) are all single roots of the cubic polynomial (7.16), a rigid body is said to be an *asymmetric top*.

Before proceeding further, we consider the example of a dumbbell composed of two equal point masses m placed at the ends of a massless rod of total length $2\,b$ and rotating about the z-axis with angular frequency ω. Here, the positions of the two masses are expressed as

$$\mathbf{r}_\pm \;=\; \pm\, b\,[\sin\theta\,(\cos\varphi\,\hat{\mathsf{x}} \;+\; \sin\varphi\,\hat{\mathsf{y}}) \;+\; \cos\theta\,\hat{\mathsf{z}}\,]\,,$$

so that the CM inertia tensor is

$$\mathbf{I} \;=\; 2\,m\,b^2 \begin{pmatrix} 1-\cos^2\varphi\,\sin^2\theta & -\cos\varphi\,\sin\varphi\,\sin^2\theta & -\cos\varphi\,\cos\theta\,\sin\theta \\ -\cos\varphi\,\sin\varphi\,\sin^2\theta & 1-\sin^2\varphi\,\sin^2\theta & -\sin\varphi\,\cos\theta\,\sin\theta \\ -\cos\varphi\,\cos\theta\,\sin\theta & -\sin\varphi\,\cos\theta\,\sin\theta & 1-\cos^2\theta \end{pmatrix}. \quad (7.22)$$

After some tedious algebra, we find $\mathrm{Tr}(\mathbf{I}) = 4\,mb^2$, $\mathrm{Ad}(\mathbf{I}) = (2\,mb^2)^2$, and $\mathrm{Det}(\mathbf{I}) = 0$, and thus the cubic polynomial (7.16) has the single root $I_3 = 0$ and the double root $I_1 = I_2 = 2\,mb^2$, which makes the dumbbell a symmetric top.

The root $I_3 = 0$ clearly indicates that one of the three principal axes is the axis of symmetry of the dumbbell ($\widehat{\mathsf{e}}_3 = \widehat{r}$). The other two principal axes are located on the plane perpendicular to the symmetry axis (i.e., $\widehat{\mathsf{e}}_1 = \widehat{\theta}$ and $\widehat{\mathsf{e}}_2 = \widehat{\varphi}$). From these choices, we easily recover the rotation matrix

$$\mathsf{R} \;=\; \mathsf{R}_2(-\theta) \;\cdot\; \mathsf{R}_3(\varphi) \;=\; \begin{pmatrix} \cos\varphi\,\cos\theta & \sin\varphi\,\cos\theta & -\sin\theta \\ -\sin\varphi & \cos\varphi & 0 \\ \cos\varphi\,\sin\theta & \sin\varphi\,\sin\theta & \cos\theta \end{pmatrix},$$

so that, using the spherical coordinates (r, θ, φ), we find

$$\begin{aligned} \widehat{\mathsf{e}}_1 &= \cos\theta\;(\cos\varphi\,\widehat{\mathsf{x}} + \sin\varphi\,\widehat{\mathsf{y}}) \;-\; \sin\theta\,\widehat{\mathsf{z}} \;=\; \widehat{\theta}, \\ \widehat{\mathsf{e}}_2 &= -\;\sin\varphi\,\widehat{\mathsf{x}} \;+\; \cos\varphi\,\widehat{\mathsf{y}} \;=\; \widehat{\varphi}, \\ \widehat{\mathsf{e}}_3 &= \sin\theta\;(\cos\varphi\,\widehat{\mathsf{x}} + \sin\varphi\,\widehat{\mathsf{y}}) \;+\; \cos\theta\,\widehat{\mathsf{z}} \;=\; \widehat{r}. \end{aligned}$$

Indeed, the principal moment of inertia about the $\widehat{r}$-axis is zero, while the principal moments of inertia about the perpendicular $\widehat{\theta}$- and $\widehat{\varphi}$-axes are equally given as $2\,mb^2$.

7.2 Eulerian Method for Rigid-Body Dynamics

7.2.1 Euler Equations

The time derivative of the angular momentum $\mathbf{L} = \mathbf{I}\cdot\boldsymbol{\omega}$ in the fixed (LAB) frame is given as

$$\left(\frac{d\mathbf{L}}{dt}\right)_f \;=\; \left(\frac{d\mathbf{L}}{dt}\right)_r \;+\; \boldsymbol{\omega}\times\mathbf{L} \;=\; \mathbf{N},$$

where $\mathbf{N}$ represents the external torque applied to the system and $(d\mathbf{L}/dt)_r$ denotes the rate of change of $\mathbf{L}$ in the rotating frame. By choosing the body frame as the rotating frame, we find

$$\left(\frac{d\mathbf{L}}{dt}\right)_r \;=\; \mathbf{I}\cdot\dot{\boldsymbol{\omega}} \;=\; (I_1\,\dot{\omega}_1)\,\widehat{\mathsf{e}}_1 \;+\; (I_2\,\dot{\omega}_2)\,\widehat{\mathsf{e}}_2 \;+\; (I_3\,\dot{\omega}_3)\,\widehat{\mathsf{e}}_3, \tag{7.23}$$

while

$$\boldsymbol{\omega}\times\mathbf{L} \;=\; -\,\widehat{\mathsf{e}}_1\,\{\,\omega_2\,\omega_3\;(I_2 - I_3)\,\} \;-\; \widehat{\mathsf{e}}_2\,\{\,\omega_3\,\omega_1\;(I_3 - I_1)\,\} \;-\; \widehat{\mathsf{e}}_3\,\{\,\omega_1\,\omega_2\;(I_1 - I_2)\,\}. \tag{7.24}$$

Thus the time evolution of the angular momentum in the body frame of reference is described in terms of

$$\left.\begin{aligned} I_1\,\dot{\omega}_1 \;-\; \omega_2\,\omega_3\;(I_2 - I_3) &= N_1 \\ I_2\,\dot{\omega}_2 \;-\; \omega_3\,\omega_1\;(I_3 - I_1) &= N_2 \\ I_3\,\dot{\omega}_3 \;-\; \omega_1\,\omega_2\;(I_1 - I_2) &= N_3 \end{aligned}\right\}, \tag{7.25}$$

which are known as the Euler equations. Lastly, we note that the rate of change of the rotational kinetic energy (7.7) is expressed as

$$\frac{dK_{rot}}{dt} \;=\; \boldsymbol{\omega}\cdot\mathbf{I}\cdot\dot{\boldsymbol{\omega}} \;=\; \boldsymbol{\omega}\cdot\left(-\,\boldsymbol{\omega}\times\mathbf{L} \;+\; \mathbf{N}\right) \;=\; \mathbf{N}\cdot\boldsymbol{\omega}. \tag{7.26}$$

We note that in the absence of external torque ($\mathbf{N} = 0$), not only is kinetic energy conserved but also $L^2 = \sum_{i=1}^{3} (I_i\omega_i)^2$, as can be verified from Eq. (7.25).

7.2.2 Euler Equations for a Force-Free Symmetric Top

As an application of the Euler equations (7.25) we consider the case of the dynamics of a force-free symmetric top, for which $\mathbf{N} = 0$ and $I_1 = I_2 \neq I_3$. Accordingly, the Euler equations (7.25) become

$$\left.\begin{array}{rcl} I_1\,\dot{\omega}_1 &=& \omega_2\,\omega_3\;(I_1 - I_3) \\ I_1\,\dot{\omega}_2 &=& \omega_3\,\omega_1\;(I_3 - I_1) \\ I_3\,\dot{\omega}_3 &=& 0 \end{array}\right\}, \tag{7.27}$$

The last Euler equation states that if $I_3 \neq 0$, we have $\dot{\omega}_3 = 0$ or that ω_3 is a constant of motion. Next, after defining the precession frequency

$$\omega_p \;=\; \omega_3\left(\frac{I_3}{I_1} - 1\right), \tag{7.28}$$

which may be positive ($I_3 > I_1$) or negative ($I_3 < I_1$), the first two Euler equations yield

$$\dot{\omega}_1(t) \;=\; -\,\omega_p\,\omega_2(t) \quad\text{and}\quad \dot{\omega}_2(t) \;=\; \omega_p\,\omega_1(t). \tag{7.29}$$

The general solutions for $\omega_1(t)$ and $\omega_2(t)$ are

$$\omega_1(t) \;=\; \omega_0\;\cos(\omega_p t + \phi_0) \quad\text{and}\quad \omega_2(t) \;=\; \omega_0\;\sin(\omega_p t + \phi_0), \tag{7.30}$$

where ω_0 is a constant and ϕ_0 is an initial phase associated with initial conditions for $\omega_1(t)$ and $\omega_2(t)$. Since ω_3 and $\omega_0^2 = \omega_1^2(t) + \omega_2^2(t)$ are constant, then the magnitude of the angular velocity $\boldsymbol{\omega}$,

$$\omega \;=\; \sqrt{\omega_1^2 + \omega_2^2 + \omega_3^2},$$

is also a constant. Thus the angle α between $\boldsymbol{\omega}$ and $\hat{\mathsf{e}}_3$ is constant, with

$$\omega_3 \;=\; \omega\,\cos\alpha \quad\text{and}\quad \sqrt{\omega_1^2 + \omega_2^2} \;=\; \omega_0 \;=\; \omega\,\sin\alpha.$$

Since the magnitude of $\boldsymbol{\omega}$ is also constant, the $\boldsymbol{\omega}$-dynamics simply involves a constant rotation with frequency ω_3 and a precession motion of $\boldsymbol{\omega}$ about the $\hat{\mathsf{e}}_3$-axis with a precession frequency ω_p; as a result of precession, the vector $\boldsymbol{\omega}$ spans the *body* cone with $\omega_p > 0$ if $I_3 > I_1$ (for a pancake-shaped or oblate symmetric top) or $\omega_p < 0$ if $I_3 < I_1$ (for a cigar-shaped or prolate symmetric top).

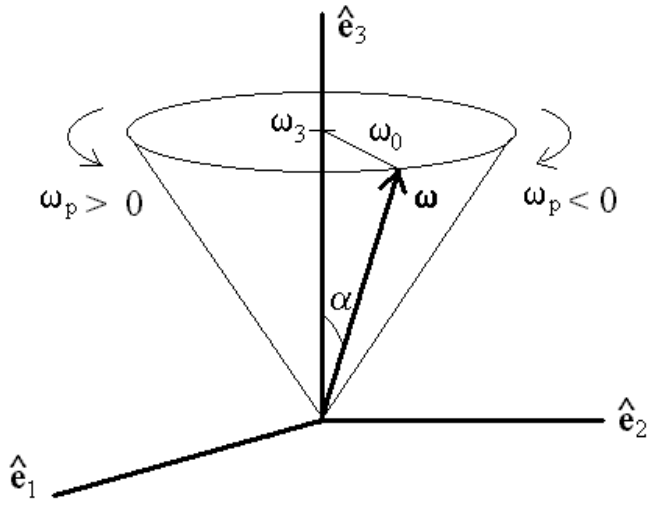

Figure 7.6: Body cone

For example, to a good approximation, Earth is an oblate spheroid with

$$I_1 \;=\; \frac{1}{5}\,M\,\left(a^2+c^2\right) \;=\; I_2 \;\text{ and }\; I_3 \;=\; \frac{2}{5}\,M\,a^2 \;>\; I_1,$$

where $2\,c = 12,714$ km is the Pole-to-Pole distance and $2\,a = 12,756$ km is the equatorial diameter, so that

$$\frac{I_3}{I_1} \;-\; 1 \;=\; \frac{a^2-c^2}{a^2+c^2} \;=\; 0.003298... \;=\; \epsilon.$$

The precession frequency (7.28) of the rotation axis of Earth is, therefore, $\omega_p = \epsilon\,\omega_3$, where $\omega_3 = 2\pi$ rad/day is the rotation frequency of the Earth, so that the precession motion repeats itself every ϵ^{-1} days or 303 days; the actual period is 430 days and the difference is partially due to the non-rigidity of Earth and the fact that the Earth is not a pure oblate spheroid. A slower precession motion of approximately 26,000 years is introduced by the combined gravitational effect of the Sun and the Moon on one hand, and the fact that the Earth's rotation axis is at an angle 23.5^o to the Ecliptic plane (on which most planets move).

The fact that the symmetric top is force-free implies that its rotational kinetic energy is constant [see Eq. (7.26)] and, hence, $\mathbf{L}\cdot\boldsymbol{\omega}$ is constant while $\boldsymbol{\omega}\times\mathbf{L}\cdot\hat{\mathbf{e}}_3 = 0$ according to Eq. (7.24). Since $\mathbf{L}$ itself is constant in magnitude and direction in the LAB (or fixed) frame, we may choose the $\hat{\mathbf{z}}$-axis to be along $\mathbf{L}$ (i.e., $\mathbf{L} = \ell\,\hat{\mathbf{z}}$). If at a given instant, $\omega_1 = 0$, then $\omega_2 = \omega_0 = \omega\,\sin\alpha$ and $\omega_3 = \omega\,\cos\alpha$. Likewise, we may write $L_1 = I_1\,\omega_1 = 0$, and

$$\begin{aligned} L_2 \;&=\; I_2\,\omega_2 \;=\; I_1\,\omega\,\sin\alpha \;=\; \ell\,\sin\theta, \\ L_3 \;&=\; I_3\,\omega_3 \;=\; I_3\,\omega\,\cos\alpha \;=\; \ell\,\cos\theta, \end{aligned}$$

where $\mathbf{L}\cdot\boldsymbol{\omega} = \ell\,\omega\,\cos\theta$, with θ represents the *space*-cone angle. From these equations, we find the relation between the body-cone angle α and the space-cone angle θ to be

$$\tan\theta \;=\; \left(\frac{I_1}{I_3}\right)\,\tan\alpha, \tag{7.31}$$

which shows that $\theta > \alpha$ for $I_3 < I_1$ and $\theta < \alpha$ for $I_3 > I_1$.

7.2.3 Euler Equations for a Force-Free Asymmetric Top

We now consider the general case of an asymmetric top moving under force-free conditions. To facilitate our discussion, we assume that $I_1 > I_2 > I_3$ and thus Euler's equations (7.25) for a force-free asymmetric top are

$$\left.\begin{array}{rcl} I_1\,\dot{\omega}_1 &=& \omega_2\,\omega_3\;(I_2 - I_3) \\ I_2\,\dot{\omega}_2 &=& -\,\omega_3\,\omega_1\;(I_1 - I_3) \\ I_3\,\dot{\omega}_3 &=& \omega_1\,\omega_2\;(I_1 - I_2) \end{array}\right\}. \tag{7.32}$$

As previously mentioned, the Euler equations (7.32) have two constants of the motion: kinetic energy

$$K \;=\; \frac{1}{2}\left(I_1\,\omega_1^2 \;+\; I_2\,\omega_2^2 \;+\; I_3\,\omega_3^2\right), \tag{7.33}$$

and the squared magnitude of the angular momentum

$$L^2 \;=\; I_1^2\,\omega_1^2 \;+\; I_2^2\,\omega_2^2 \;+\; I_3^3\,\omega_3^2. \tag{7.34}$$

Figure 7.7 shows the numerical solution of the Euler equations (7.32) subject to the initial condition $(\omega_{10}, \omega_{20}, \omega_{30}) = (2, 0, 1)$ for different values of the ratios I_1/I_3 and I_2/I_3. Note that in the limit $I_1 = I_2$ (corresponding to a symmetric top), the top evolves solely on the (ω_1, ω_2)-plane at constant ω_3. As I_1 increases from I_2, the asymmetric top exhibits doubly-periodic behavior in the full $(\omega_1, \omega_2, \omega_3)$-space until the motion becomes restricted to the (ω_2, ω_3)-plane in the limit $I_1 \gg I_2$. One also clearly notes the existence of a separatrix which appears as I_1 reaches the critical value

$$I_{1c} \;=\; \frac{I_2}{2} \;+\; \sqrt{\frac{I_2^2}{4} \;+\; I_3\,(I_2 - I_3)\left(\frac{\omega_{30}}{\omega_{10}}\right)^2},$$

at constant I_2 and I_3 and given initial conditions $(\omega_{10}, \omega_{20}, \omega_{30})$.

We note that the existence of two constants of the motion, Eqs. (7.33) and (7.34), for the three Euler equations (7.32) means that we may express the Euler equations in terms of a single equation. For this purpose, we introduce the constants

$$\sigma \;=\; 2\,I_1 K \;-\; L^2 \quad\text{and}\quad \rho \;=\; L^2 \;-\; 2\,I_3 K,$$

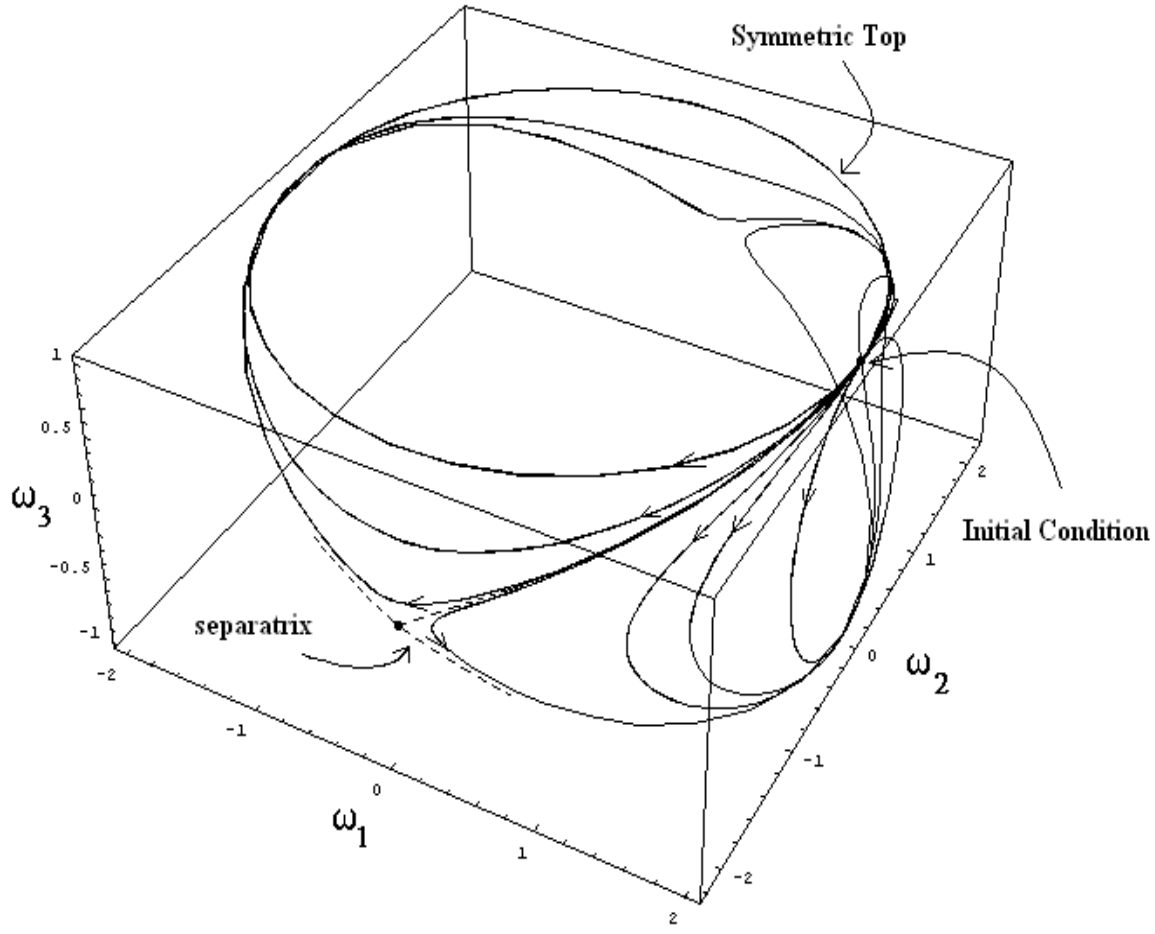

Figure 7.7: Orbits of an asymmetric top with initial condition $(\omega_{10}, \omega_{20}, \omega_{30}) = (2, 0, 1)$ for different values of the ratio I_1/I_3 for a fixed ratio I_2/I_3

from which we obtain expressions for ω_1 (taken here to be negative) and ω_3 in terms of ω_2:

$$\omega_1 \;=\; -\sqrt{\frac{\rho \;-\; I_2(I_2-I_3)\,\omega_2^2}{I_1\,(I_1-I_3)}} \quad \text{and} \quad \omega_3 \;=\; \sqrt{\frac{\sigma \;-\; I_2(I_1-I_2)\,\omega_2^2}{I_3\,(I_1-I_3)}}. \tag{7.35}$$

When we substitute these expressions in the Euler equation for ω_2, we easily obtain

$$\dot{\omega}_2 \;=\; \alpha\,\sqrt{(\Omega_1^2 \;-\; \omega_2^2)\,(\Omega_3^2 \;-\; \omega_2^2)}, \tag{7.36}$$

where α is a positive dimensionless constant defined as

$$\alpha \;=\; \sqrt{\left(1-\frac{I_2}{I_1}\right)\,\left(\frac{I_2}{I_3}-1\right)}, \tag{7.37}$$

while the constant frequencies Ω_1 and Ω_3 are defined as

$$\Omega_1^2 \;=\; \frac{2\;I_1K \;-\; L^2}{I_2(I_1-I_2)} \quad \text{and} \quad \Omega_3^2 \;=\; \frac{L^2 \;-\; 2\;I_3K}{I_2(I_2-I_3)}. \tag{7.38}$$

We immediately note that the evolution of ω_2 is characterized by the two frequencies Ω_1 and Ω_3, which also represent the turning points at which $\dot{\omega}_2$ vanishes. Next, by introducing a dimensionless frequency $\nu \;=\; \omega_2/\Omega_3$ (here, we assume that $\Omega_1 \geq \Omega_3$) and a dimensionless time $\tau = \alpha\Omega_1\;t$, the Euler equation (7.36) becomes

$$\nu'(\tau) \;=\; \sqrt{(1-\nu^2)\;(1-k^2\,\nu^2)},$$

which can now be integrated to yield

$$\tau(\nu) \;=\; \int_0^{\nu} \frac{ds}{\sqrt{(1-s^2)\,(1-k^2\,s^2)}}, \tag{7.39}$$

where $k^2 = \Omega_3^2/\Omega_1^2 \leq 1$ and we assume that $\omega_2(t=0) = 0$; the solution for $\omega_2(\tau) = \Omega_3\;\nu(\tau)$, as well as $\omega_1(\tau)$ and $\omega_3(\tau)$ can be expressed in terms of the Jacobi elliptic functions (as shown in Appendix A). Lastly, we note that the separatrix solution of the force-free asymmetric top (see Figure 7.7) corresponding to $I_1 = I_{1c}$ is associated with $k = 1$ (i.e., $\Omega_1 = \Omega_3$).

7.2.4 Hamiltonian Formulation of Rigid Body Motion

In the absence of external torque, the Euler equations (7.25) can be written as

$$\frac{dL_i}{dt} \;=\; \{L_i,\;K_{rot}\} \;=\; -\,\widehat{i}\cdot\boldsymbol{\omega}\times\mathbf{L} \;=\; -\,\epsilon_{ijk}\;\omega_j\,(I_k\,\omega_k), \tag{7.40}$$

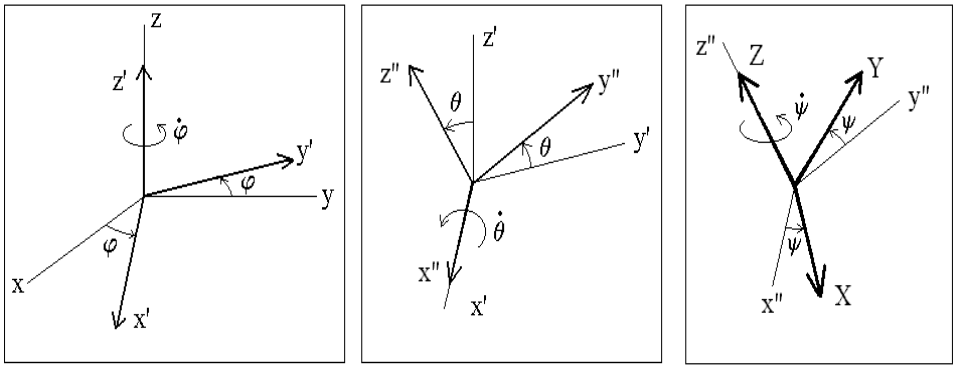

Figure 7.8: Euler angles

where the *Poisson bracket* $\{\ ,\ \}$ is defined in terms of two arbitrary functions $F(\mathbf{L})$ and $G(\mathbf{L})$ as

$$\{F,\ G\}\ =\ -\ \mathbf{L}\cdot\frac{\partial F}{\partial \mathbf{L}}\times\frac{\partial G}{\partial \mathbf{L}}. \tag{7.41}$$

Note that, for a general function $F(\mathbf{L})$ of angular momentum and in the absence of external torque, we find

$$\frac{dF}{dt}\ =\ -\ \mathbf{L}\cdot\frac{\partial F}{\partial \mathbf{L}}\times\frac{\partial K_{rot}}{\partial \mathbf{L}}\ =\ -\ \frac{\partial F}{\partial \mathbf{L}}\cdot\boldsymbol{\omega}\times\mathbf{L},$$

and thus any function of $|\mathbf{L}|$ is a constant of the motion for rigid body dynamics.

7.3 Lagrangian Method for Rigid-Body Dynamics

7.3.1 Eulerian Angles as generalized Lagrangian Coordinates

To describe the physical state of a rotating object with principal moments of inertia (I_1, I_2, I_3), we need the three Eulerian angles (φ, θ, ψ) in the body frame of reference (see Figure 7.8). The Eulerian angle φ is associated with the rotation of the fixed-frame unit vectors $(\hat{\mathsf{x}}, \hat{\mathsf{y}}, \hat{\mathsf{z}})$ about the z-axis. We thus obtain the new unit vectors $(\hat{\mathsf{x}}', \hat{\mathsf{y}}', \hat{\mathsf{z}}')$ defined as

$$\begin{pmatrix} \hat{\mathsf{x}}' \\ \hat{\mathsf{y}}' \\ \hat{\mathsf{z}}' \end{pmatrix}\ =\ \overbrace{\begin{pmatrix} \cos\varphi & \sin\varphi & 0 \\ -\sin\varphi & \cos\varphi & 0 \\ 0 & 0 & 1 \end{pmatrix}}^{=\,\mathsf{R}_3(\varphi)}\cdot\begin{pmatrix} \hat{\mathsf{x}} \\ \hat{\mathsf{y}} \\ \hat{\mathsf{z}} \end{pmatrix} \tag{7.42}$$

The rotation matrix $\mathsf{R}_3(\varphi)$ has the following properties associated with a general rotation matrix $\mathsf{R}_n(\alpha)$, defined in Eq. (7.21), where a rotation of axes about the x^n-axis is performed through an arbitrary angle α. First, the matrix $\mathsf{R}_n(-\alpha)$ is the inverse matrix of $\mathsf{R}_n(\alpha)$, i.e.,

$$\mathsf{R}_n(-\alpha)\cdot\mathsf{R}_n(\alpha)\ =\ \underline{\mathbf{1}}\ =\ \mathsf{R}_n(\alpha)\cdot\mathsf{R}_n(-\alpha).$$

Next, the determinant of $\mathsf{R}_n(\alpha)$ is $+1$ and the eigenvalues of $\mathsf{R}_n(\alpha)$ are $+1$, $e^{i\alpha}$, and $e^{-i\alpha}$ (see Appendix A.2 for further details).

The Eulerian angle θ is associated with the rotation of the unit vectors $(\widehat{\mathsf{x}}', \widehat{\mathsf{y}}', \widehat{\mathsf{z}}')$ about the x'-axis. We thus obtain the new unit vectors $(\widehat{\mathsf{x}}'', \widehat{\mathsf{y}}'', \widehat{\mathsf{z}}'')$ defined as

$$\begin{pmatrix} \widehat{\mathsf{x}}'' \\ \widehat{\mathsf{y}}'' \\ \widehat{\mathsf{z}}'' \end{pmatrix} = \overbrace{\begin{pmatrix} 1 & 0 & 0 \\ 0 & \cos\theta & \sin\theta \\ 0 & -\sin\theta & \cos\theta \end{pmatrix}}^{= \mathsf{R}_1(\theta)} \cdot \begin{pmatrix} \widehat{\mathsf{x}}' \\ \widehat{\mathsf{y}}' \\ \widehat{\mathsf{z}}' \end{pmatrix} \tag{7.43}$$

The Eulerian angle ψ is associated with the rotation of the unit vectors $(\widehat{\mathsf{x}}'', \widehat{\mathsf{y}}'', \widehat{\mathsf{z}}'')$ about the z''-axis. We thus obtain the body-frame unit vectors $(\widehat{\mathsf{e}}_1, \widehat{\mathsf{e}}_2, \widehat{\mathsf{e}}_3)$ defined as

$$\begin{pmatrix} \widehat{\mathsf{e}}_1 \\ \widehat{\mathsf{e}}_2 \\ \widehat{\mathsf{e}}_3 \end{pmatrix} = \overbrace{\begin{pmatrix} \cos\psi & \sin\psi & 0 \\ -\sin\psi & \cos\psi & 0 \\ 0 & 0 & 1 \end{pmatrix}}^{= \mathsf{R}_3(\psi)} \cdot \begin{pmatrix} \widehat{\mathsf{x}}'' \\ \widehat{\mathsf{y}}'' \\ \widehat{\mathsf{z}}'' \end{pmatrix} \tag{7.44}$$

Hence, the relation between the fixed-frame unit vectors $(\widehat{\mathsf{x}}, \widehat{\mathsf{y}}, \widehat{\mathsf{z}})$ and the body-frame unit vectors $(\widehat{\mathsf{e}}_1, \widehat{\mathsf{e}}_2, \widehat{\mathsf{e}}_3)$ involves the matrix $\mathsf{R} = \mathsf{R}_3(\psi) \cdot \mathsf{R}_1(\theta) \cdot \mathsf{R}_3(\varphi)$, such that $\widehat{\mathsf{e}}_i = R_{ij}\, \widehat{\mathsf{x}}^j$, or

$$\left.\begin{aligned} \widehat{\mathsf{e}}_1 &= \cos\psi\, \widehat{\perp} + \sin\psi\,(\cos\theta\, \widehat{\varphi} + \sin\theta\, \widehat{\mathsf{z}}) \\ \widehat{\mathsf{e}}_2 &= -\sin\psi\, \widehat{\perp} + \cos\psi\,(\cos\theta\, \widehat{\varphi} + \sin\theta\, \widehat{\mathsf{z}}) \\ \widehat{\mathsf{e}}_3 &= -\sin\theta\, \widehat{\varphi} + \cos\theta\, \widehat{\mathsf{z}} \end{aligned}\right\}, \tag{7.45}$$

where $\widehat{\varphi} = -\sin\varphi\, \widehat{\mathsf{x}} + \cos\varphi\, \widehat{\mathsf{y}}$ and $\widehat{\perp} = \cos\varphi\, \widehat{\mathsf{x}} + \sin\varphi\, \widehat{\mathsf{y}} = \widehat{\varphi} \times \widehat{\mathsf{z}}$.

7.3.2 Angular Velocity in terms of Eulerian Angles

The angular velocity $\boldsymbol{\omega}$ represented in the three Figures above is expressed as

$$\boldsymbol{\omega} = \dot{\varphi}\, \widehat{\mathsf{z}} + \dot{\theta}\, \widehat{\mathsf{x}}' + \dot{\psi}\, \widehat{\mathsf{e}}_3.$$

The unit vectors $\widehat{\mathsf{z}}$ and $\widehat{\mathsf{x}}'$ are written in terms of the body-frame unit vectors $(\widehat{\mathsf{e}}_1, \widehat{\mathsf{e}}_2, \widehat{\mathsf{e}}_3)$ as

$$\begin{aligned} \widehat{\mathsf{z}} &= \sin\theta\, (\sin\psi\, \widehat{\mathsf{e}}_1 + \cos\psi\, \widehat{\mathsf{e}}_2) + \cos\theta\, \widehat{\mathsf{e}}_3, \\ \widehat{\mathsf{x}}' &= \widehat{\mathsf{x}}'' = \cos\psi\, \widehat{\mathsf{e}}_1 - \sin\psi\, \widehat{\mathsf{e}}_2. \end{aligned}$$

The angular velocity can, therefore, be written exclusively in the body frame of reference in terms of the Euler basis vectors (7.45) as

$$\boldsymbol{\omega} = \omega_1\, \widehat{\mathsf{e}}_1 + \omega_2\, \widehat{\mathsf{e}}_2 + \omega_3\, \widehat{\mathsf{e}}_3, \tag{7.46}$$

where the body-frame angular frequencies are

$$\left.\begin{array}{rcl} \omega_1 &=& \dot{\varphi}\,\sin\theta\,\sin\psi \;+\; \dot{\theta}\,\cos\psi \\ \omega_2 &=& \dot{\varphi}\,\sin\theta\,\cos\psi \;-\; \dot{\theta}\,\sin\psi \\ \omega_3 &=& \dot{\psi} \;+\; \dot{\varphi}\,\cos\theta \end{array}\right\}. \tag{7.47}$$

Note that all three frequencies are independent of φ (i.e., $\partial\omega_i/\partial\varphi = 0$), while derivatives with respect to ψ and $\dot{\psi}$ are

$$\frac{\partial\omega_1}{\partial\psi} \;=\; \omega_2, \quad \frac{\partial\omega_2}{\partial\psi} \;=\; -\,\omega_1, \quad \text{and} \quad \frac{\partial\omega_3}{\partial\psi} \;=\; 0,$$

and

$$\frac{\partial\omega_1}{\partial\dot{\psi}} \;=\; 0 \;=\; \frac{\partial\omega_2}{\partial\dot{\psi}} \quad \text{and} \quad \frac{\partial\omega_3}{\partial\dot{\psi}} \;=\; 1.$$

The relations (7.47) can be inverted to yield

$$\begin{array}{rcl} \dot{\varphi} &=& \csc\theta\,(\sin\psi\,\omega_1 \;+\; \cos\psi\,\omega_2), \\ \dot{\theta} &=& \cos\psi\,\omega_1 \;-\; \sin\psi\,\omega_2, \\ \dot{\psi} &=& \omega_3 \;-\; \cot\theta\,(\sin\psi\,\omega_1 \;+\; \cos\psi\,\omega_2). \end{array}$$

7.3.3 Rotational Kinetic Energy of a Symmetric Top

The rotational kinetic energy (7.7) for a symmetric top can be written as

$$K_{rot} \;=\; \frac{1}{2}\,\left\{\, I_3\,\omega_3^2 \;+\; I_1\left(\omega_1^2 \;+\; \omega_2^2\right)\,\right\},$$

or explicitly in terms of the Eulerian angles (φ,θ,ψ) and their time derivatives $(\dot{\varphi},\dot{\theta},\dot{\psi})$ as

$$K_{rot} \;=\; \frac{1}{2}\,\left\{\, I_3\left(\dot{\psi} \;+\; \dot{\varphi}\,\cos\theta\right)^2 \;+\; I_1\left(\dot{\theta}^2 \;+\; \dot{\varphi}^2\,\sin^2\theta\right)\,\right\}. \tag{7.48}$$

We now briefly return to the case of the force-free symmetric top for which the Lagrangian is simply $L(\theta,\dot{\theta};\;\dot{\varphi},\dot{\psi}) = K_{rot}$. Since φ and ψ are ignorable coordinates, i.e., the force-free Lagrangian (7.48) is independent of φ and ψ, their canonical angular momenta

$$p_\varphi \;=\; \frac{\partial L}{\partial\dot{\varphi}} \;=\; I_3\,(\dot{\psi} + \dot{\varphi}\,\cos\theta)\,\cos\theta \;+\; I_1\,\sin^2\theta\,\dot{\varphi}, \tag{7.49}$$

$$p_\psi \;=\; \frac{\partial L}{\partial\dot{\psi}} \;=\; I_3\,(\dot{\psi} + \dot{\varphi}\,\cos\theta) \;=\; I_3\,\omega_3 \tag{7.50}$$

are constants of the motion. By inverting these relations, we obtain

$$\dot{\varphi} \;=\; \frac{p_\varphi - p_\psi\,\cos\theta}{I_1\,\sin^2\theta} \quad \text{and} \quad \dot{\psi} \;=\; \omega_3 \;-\; \frac{(p_\varphi - p_\psi\,\cos\theta)\,\cos\theta}{I_1\,\sin^2\theta}, \tag{7.51}$$

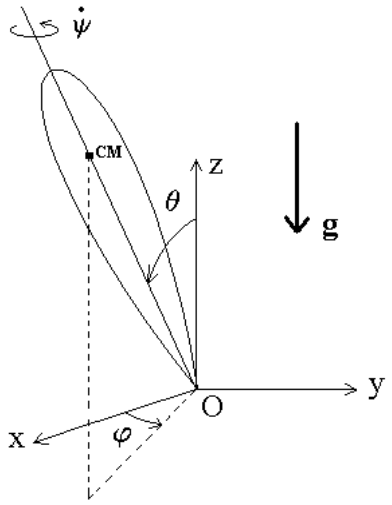

Figure 7.9: Symmetric top with one fixed point

and the rotational kinetic energy (7.48) becomes

$$K_{rot} \;=\; \frac{1}{2}\left\{\; I_1\,\dot\theta^2 \;+\; I_3\,\omega_3^2 \;+\; \frac{(p_\varphi - p_\psi\,\cos\theta)^2}{I_1\,\sin^2\theta}\;\right\}. \tag{7.52}$$

The motion of a force-free symmetric top can now be described in terms of solutions of the Euler-Lagrange equation for the Eulerian angle θ:

$$\begin{aligned}\frac{d}{dt}\left(\frac{\partial L}{\partial\dot\theta}\right) \;=\; I_1\,\ddot\theta \;&=\; \frac{\partial L}{\partial\theta} \;=\; \dot\varphi\,\sin\theta\,(I_1\,\cos\theta\,\dot\varphi \;-\; p_\psi)\\ &=\; -\,\frac{(p_\varphi - p_\psi\,\cos\theta)}{I_1\,\sin\theta}\,\frac{(p_\psi - p_\varphi\,\cos\theta)}{\sin^2\theta}.\end{aligned} \tag{7.53}$$

Once $\theta(t)$ is solved for given values of the principal moments of inertia $I_1 = I_2$ and I_3 and the invariant canonical angular momenta p_φ and p_ψ, the functions $\varphi(t)$ and $\psi(t)$ are determined from the time integration of Eqs. (7.51).

7.3.4 Symmetric Top with One Fixed Point

We now consider the case of a spinning symmetric top of mass M and principal moments of inertia ($I_1 = I_2 \neq I_3$) with one fixed point O moving in a gravitational field with constant acceleration g. The rotational kinetic energy of the symmetric top is given by Eq. (7.48) while the potential energy for the case of a symmetric top with one fixed point is

$$U(\theta) \;=\; Mgh\,\cos\theta, \tag{7.54}$$

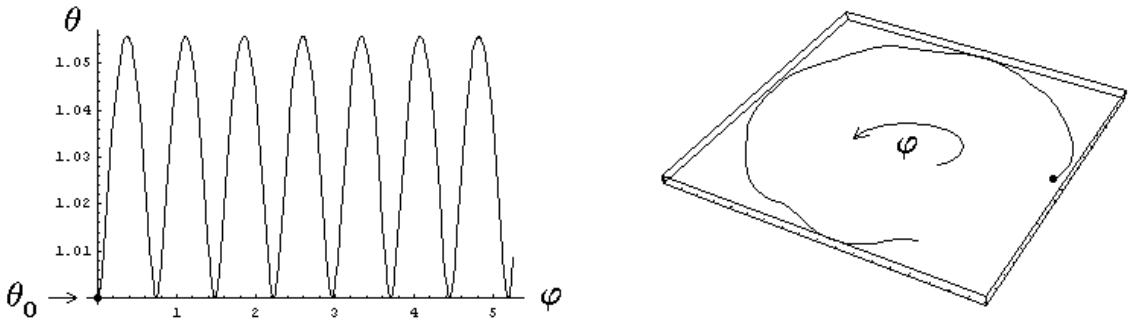

Figure 7.10: Orbits of heavy top – Case I

where h is the distance from the fixed point O and the center of mass (CM) of the symmetric top. The Lagrangian for the symmetric top with one fixed point is

$$L(\theta, \dot\theta;\, \dot\varphi, \dot\psi) \;=\; \frac{1}{2}\,\Big\{\, I_3 \left(\dot\psi \;+\; \dot\varphi\,\cos\theta\right)^2 \;+\; I_1 \left(\dot\theta^2 \;+\; \dot\varphi^2\,\sin^2\theta\right) \Big\} \;-\; Mgh\,\cos\theta. \quad (7.55)$$

A normalized form of the Euler equations for the symmetric top with one fixed point (also known as the *heavy* symmetric top) is expressed as

$$\varphi' \;=\; \frac{(b-\cos\theta)}{\sin^2\theta} \quad \text{and} \quad \theta'' \;=\; a\,\sin\theta \;-\; \frac{(1-b\,\cos\theta)(b-\cos\theta)}{\sin^3\theta}, \qquad (7.56)$$

where time has been rescaled such that $(\cdots)' = (I_1/p_\psi)\,(\cdots)^{\bullet}$ and the two parameters a and b are defined as

$$a \;=\; \frac{Mgh\,I_1}{p_\psi^2} \quad \text{and} \quad b \;=\; \frac{p_\varphi}{p_\psi}.$$

The normalized heavy-top equations (7.56) have been integrated for the initial conditions $(\theta_0, \theta_0';\, \varphi_0) = (1, 0; 0)$. The three Figures shown below correspond to three different cases (I, II, and III) for fixed value of a (here, $a = 0.1$), which exhibit the possibility of azimuthal reversal when φ' changes sign for different values of $b = p_\varphi/p_\psi$; the azimuthal precession motion is called *nutation*.

The Figures on the left show the normalized heavy-top solutions in the (φ, θ)-plane while the Figures on the right show the spherical projection of the normalized heavy-top solutions $(\theta, \varphi) \to (\sin\theta\,\cos\varphi,\ \sin\theta\,\sin\varphi,\ \cos\theta)$, where the initial condition is denoted by a dot ($\bullet$). In Case I ($b > \cos\theta_0$), the azimuthal velocity φ' never changes sign and azimuthal precession occurs monotonically. In Case II ($b = \cos\theta_0$), the azimuthal velocity φ' vanishes at $\theta = \theta_0$ (where θ' also vanishes) and the heavy symmetric top exhibits a *cusp* at $\theta = \theta_0$. In Case III ($b < \cos\theta_0$), the azimuthal velocity φ' vanishes for $\theta > \theta_0$ and the heavy symmetric top exhibits a phase of *retrograde* motion. Since the Lagrangian (7.55) is independent of the Eulerian angles φ and ψ, the canonical angular momenta p_φ and p_ψ,

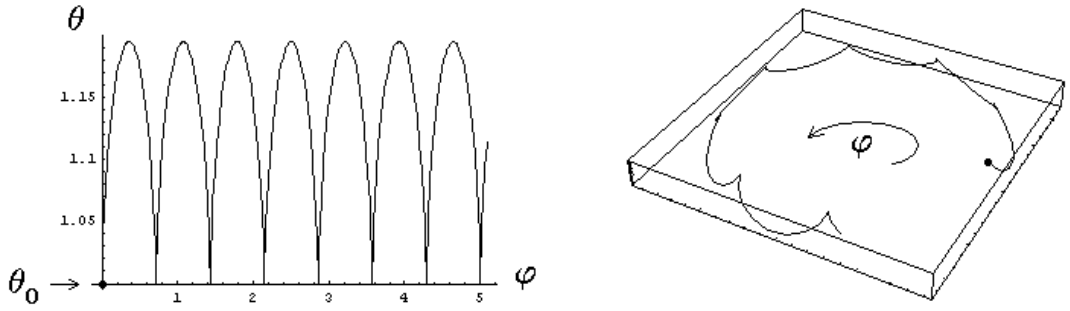

Figure 7.11: Orbits of heavy top – Case II

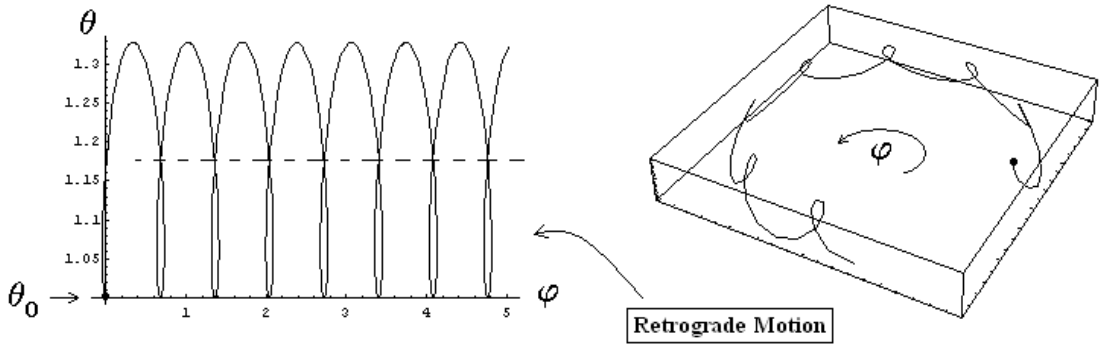

Figure 7.12: Orbits of heavy top – Case III

respectively, are constants of the motion. The solution for $\theta(t)$ is then most easily obtained by considering the energy equation

$$E \;=\; \frac{1}{2}\left\{ I_1\,\dot{\theta}^2 \;+\; I_3\,\omega_3^2 \;+\; \frac{(p_\varphi - p_\psi\,\cos\theta)^2}{I_1\,\sin^2\theta} \right\} \;+\; Mgh\,\cos\theta, \tag{7.57}$$

where p_φ and $p_\psi = I_3\,\omega_3$ are constants of the motion. Since the total energy E is itself a constant of the motion, we may define a new energy constant

$$E' \;=\; E \;-\; \frac{1}{2}\,I_3\,\omega_3^2,$$

and an effective potential energy

$$V(\theta) \;=\; \frac{(p_\varphi - p_\psi\,\cos\theta)^2}{2I_1\,\sin^2\theta} \;+\; Mgh\,\cos\theta, \tag{7.58}$$

so that Eq. (7.57) becomes

$$E' \;=\; \frac{1}{2}\,I_1\,\dot{\theta}^2(t) \;+\; V(\theta), \tag{7.59}$$

which can be *formally solved* as

$$t(\theta) \;=\; \pm \int \frac{d\theta}{\sqrt{(2/I_1)\,[E' - V(\theta)]}}. \tag{7.60}$$

Note that turning points θ_{tp} are again defined as roots of the equation $E' = V(\theta)$.

A simpler formulation for this problem is obtained as follows. First, we define the following quantities

$$\Omega^2 \;=\; \frac{2\,Mgh}{I_1},\;\; \epsilon \;=\; \frac{2\,E'}{I_1\Omega^2} \;=\; \frac{E'}{Mgh},\;\; \alpha \;=\; \frac{p_\varphi}{I_1\Omega},\;\; \text{and}\;\; \beta \;=\; \frac{p_\psi}{I_1\Omega}, \tag{7.61}$$

so that Eq. (7.60) becomes

$$\tau(u) \;=\; \pm \int \frac{du}{\sqrt{(1-u^2)(\epsilon - u) - (\alpha - \beta\,u)^2}} \;=\; \pm \int \frac{du}{\sqrt{(1-u^2)[\epsilon - W(u)]}}, \tag{7.62}$$

where $\tau(u) = \Omega\,t(u)$, $u = \cos\theta$, and the energy equation (7.59) becomes

$$\epsilon \;=\; \frac{1}{(1-u^2)}\left[\left(\frac{du}{d\tau}\right)^2 \;+\; (\alpha \;-\; \beta\,u)^2 \right] \;+\; u \;=\; (1-u^2)^{-1}\,\left(\frac{du}{d\tau}\right)^2 \;+\; W(u), \tag{7.63}$$

where the effective potential is

$$W(u) \;=\; u \;+\; \frac{(\alpha - \beta\,u)^2}{(1-u^2)}.$$

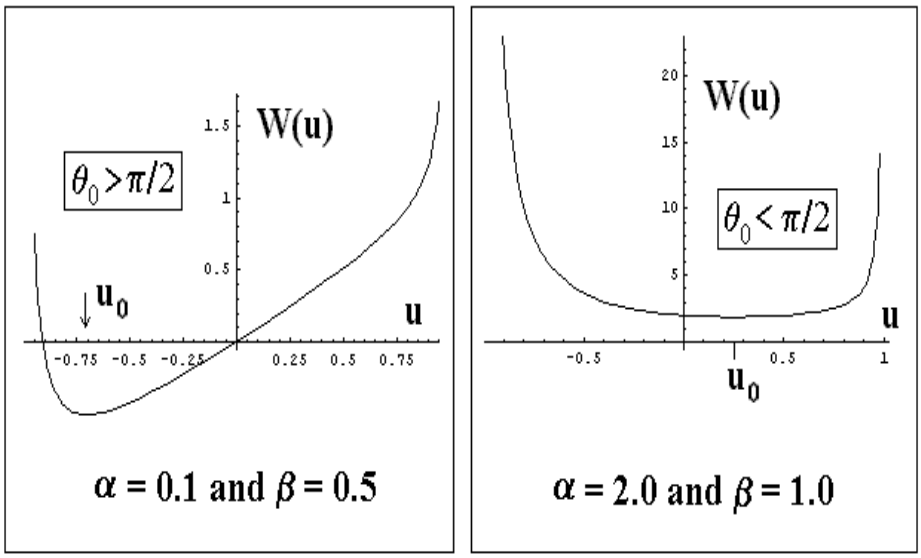

Figure 7.13: Effective potential for the heavy top

We note that the effective potential $W(u)$ is infinite at $u = \pm 1$ and has a single minimum at $u = u_0$ (or $\theta = \theta_0$) defined by the quartic equation

$$W'(u_0) \;=\; 1 \;+\; 2u_0 \left(\frac{\alpha - \beta\, u_0}{1 - u_0^2}\right)^2 \;-\; 2\beta \left(\frac{\alpha - \beta\, u_0}{1 - u_0^2}\right) \;=\; 0. \tag{7.64}$$

This equation has four roots: two roots are complex roots, a third root is always greater than one for $\alpha > 0$ and $\beta > 0$ (which is unphysical since $u = \cos\theta \leq 1$), while the fourth root is less than one for $\alpha > 0$ and $\beta > 0$; hence, this root is the only physical root corresponding to a single minimum for the effective potential $W(u)$ (see Figure 7.13). Note how the linear gravitational-potential term u is apparent at low values of α and β.

We first investigate the motion of the symmetric top at the minimum angle θ_0 for which $\epsilon = W(u_0)$ and $\dot{u}(u_0) = 0$. For this purpose, we note that when the dimensionless azimuthal frequency

$$\frac{d\varphi}{d\tau} \;=\; \frac{\alpha - \beta\, u}{1 - u^2} \;=\; \nu(u)$$

is inserted in Eq. (7.64), we obtain the quadratic equation $1 + 2u_0\,\nu_0^2 - 2\beta\,\nu_0 = 0$, which has two solutions for $\nu_0 = \nu(u_0)$:

$$\nu(u_0) \;=\; \frac{\beta}{2u_0}\left(1 \;\pm\; \sqrt{1 \;-\; \frac{2\,u_0}{\beta^2}}\right).$$

Here, we further note that these solutions require that the radicand be positive, i.e.,

$$\beta^2 \;>\; 2\,u_0 \quad \text{or} \quad I_3\,\omega_3 \geq I_1\Omega\,\sqrt{2\,u_0},$$

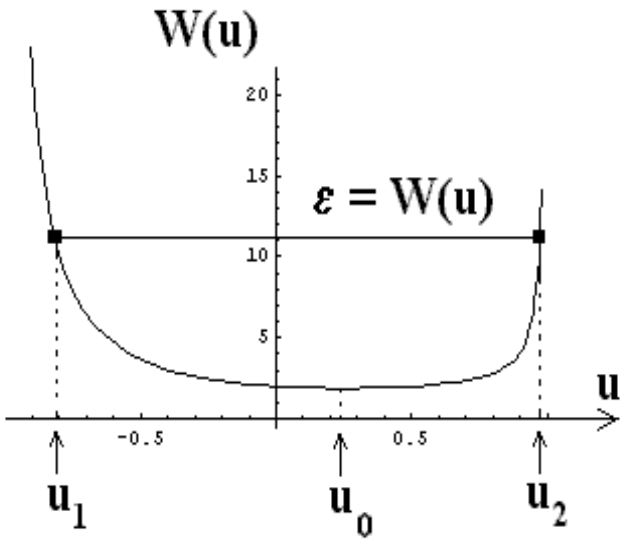

Figure 7.14: Turning-point roots

if $u_0 \geq 0$ (or $\theta_0 \leq \pi/2$); no conditions are applied to ω_3 for the case $u_0 < 0$ (or $\theta_0 > \pi/2$) since the radicand is strictly positive in this case.

Hence, the precession frequency $\dot{\varphi}_0 = \nu(u_0)\,\Omega$ at $\theta = \theta_0$ has a slow component and a fast component

$$(\dot{\varphi}_0)_{slow} \;=\; \frac{I_3\omega_3}{2\,I_1\,\cos\theta_0}\,\left[\,1\;-\;\sqrt{1\;-\;2\left(\frac{I_1\Omega}{I_3\omega_3}\right)^2\cos\theta_0}\,\right],$$

$$(\dot{\varphi}_0)_{fast} \;=\; \frac{I_3\omega_3}{2\,I_1\,\cos\theta_0}\,\left[\,1\;+\;\sqrt{1\;-\;2\left(\frac{I_1\Omega}{I_3\omega_3}\right)^2\cos\theta_0}\,\right].$$

We note that for $\theta_0 < \pi/2$ (or $\cos\theta_0 > 0$) the two precession frequencies $(\dot{\varphi}_0)_{slow}$ and $(\dot{\varphi}_0)_{fast}$ have the same sign while for $\theta_0 > \pi/2$ (or $\cos\theta_0 < 0$) the two precession frequencies have opposite signs $(\dot{\varphi}_0)_{slow} < 0$ and $(\dot{\varphi}_0)_{fast} > 0$.

Next, we investigate the case with two turning points $u_1 < u_0$ and $u_2 > u_1$ (or $\theta_1 > \theta_2$) where $\epsilon = W(u)$ (see Figure 7.14), where the θ-dynamics oscillates between θ_1 and θ_2. The turning points u_1 and u_2 are roots of the function

$$F(u) = (1-u^2)\,[\epsilon - W(u)] \;=\; u^3 \;-\; (\epsilon+\beta^2)\,u^2 \;-\; (1-2\,\alpha\beta)\,u \;+\; (\epsilon-\alpha^2). \qquad (7.65)$$

Although a third root u_3 exists for $F(u) = 0$, it is unphysical since $u_3 > 1$. Since the azimuthal frequencies at the turning points are expressed as

$$\frac{d\varphi_1}{d\tau} \;=\; \frac{\alpha-\beta\,u_1}{1-u_1^2} \quad\text{and}\quad \frac{d\varphi_2}{d\tau} \;=\; \frac{\alpha-\beta\,u_2}{1-u_2^2},$$

where $\alpha - \beta\, u_1 > \alpha - \beta\, u_2$, we can study the three cases for nutation numerically investigated below Eqs. (7.56); here, we assume that both $\alpha = b\,\beta$ and β are positive. In Case I ($\alpha > \beta\, u_2$), the precession frequency $d\varphi/d\tau$ is strictly positive for $u_1 \leq u \leq u_2$ and nutation proceeds monotonically. In Case II ($\alpha = \beta\, u_2$), the precession frequency $d\varphi/d\tau$ is positive for $u_1 \leq u < u_2$ and vanishes at $u = u_2$; nutation in this Case exhibits a cusp at θ_2. In Case III ($\alpha < \beta\, u_2$), the precession frequency $d\varphi/d\tau$ reverses its sign at $u_r = \alpha/\beta = b$ or $\theta_2 < \theta_r = \arccos(b) < \theta_1$.

7.3.5 Stability of the Sleeping Top

Let us consider the case where a symmetric top with one fixed point is launched with initial conditions $\theta_0 \neq 0$ and $\dot{\theta}_0 = \dot{\varphi}_0 = 0$, with $\dot{\psi}_0 \neq 0$. In this case, the invariant canonical momenta are

$$p_\psi \;=\; I_3\, \dot{\psi}_0 \quad \text{and} \quad p_\varphi \;=\; p_\psi\, \cos\theta_0.$$

These initial conditions ($u_0 = \alpha/\beta, \dot{u}_0 = 0$), therefore, imply from Eq. (7.63) that $\epsilon = u_0$ and that the energy equation (7.63) now becomes

$$\left(\frac{du}{d\tau}\right)^2 \;=\; \Big[\, (1-u^2) \;-\; \beta^2\,(u_0 - u)\,\Big]\;(u_0 - u). \tag{7.66}$$

Next, we consider the case of the *sleeping* top for which an additional initial condition is $\theta_0 = 0$ (and $u_0 = 1$). Thus Eq. (7.66) becomes

$$\left(\frac{du}{d\tau}\right)^2 \;=\; \Big(1 \;+\; u \;-\; \beta^2\Big)\;(1-u)^2. \tag{7.67}$$

The sleeping top has the following equilibrium points (where $\dot{u} = 0$): $u_1 = 1$ and $u_2 = \beta^2 - 1$. We now investigate the stability of the equilibrium point $u_1 = 1$ by writing $u = 1 - \delta$ (with $\delta \ll 1$) so that Eq. (7.67) becomes

$$\frac{d\delta}{d\tau} \;=\; \Big(2 - \beta^2\Big)^{\frac{1}{2}}\;\delta.$$

The solution of this equation is exponential (and, therefore, u_1 is unstable) if $\beta^2 < 2$ or oscillatory (and, therefore, u_1 is stable) if $\beta^2 > 2$. Note that in the latter case, the condition $\beta^2 > 2$ implies that the second equilibrium point $u_2 = \beta^2 - 1 > 1$ is unphysical. We, therefore, see that stability of the sleeping top requires a large spinning frequency ω_3; in the presence of friction, the spinning frequency slows down and ultimately the sleeping top becomes unstable.

7.4 Problems

Problem 1

Consider a thin homogeneous rectangular plate of mass M and area ab that lies on the (x, y)-plane.

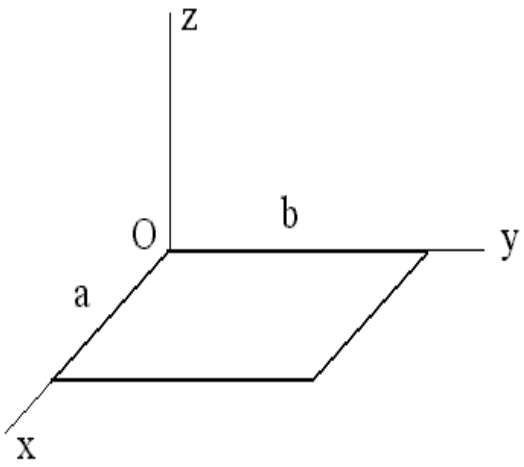

(a) Show that the inertia tensor (calculated in the reference frame with its origin at point O in the Figure above) takes the form

$$\mathbf{I} = \begin{pmatrix} A & -C & 0 \\ -C & B & 0 \\ 0 & 0 & A+B \end{pmatrix},$$

and find suitable expressions for A, B, and C in terms of M, a, and b.

(b) Show that by performing a rotation of the coordinate axes about the z-axis through an angle θ, the new inertia tensor is

$$\mathbf{I}'(\theta) = \mathsf{R}(\theta) \cdot \mathbf{I} \cdot \mathsf{R}^T(\theta) = \begin{pmatrix} A' & -C' & 0 \\ -C' & B' & 0 \\ 0 & 0 & A'+B' \end{pmatrix},$$

where

$$\begin{aligned} A' &= A\cos^2\theta + B\sin^2\theta - C\sin 2\theta \\ B' &= A\sin^2\theta + B\cos^2\theta + C\sin 2\theta \\ C' &= C\cos 2\theta - \frac{1}{2}(B-A)\sin 2\theta. \end{aligned}$$

(c) When

$$\theta \;=\; \frac{1}{2}\,\arctan\left(\frac{2C}{B-A}\right),$$

the off-diagonal component C' vanishes and the $x'-$ and $y'-$axes become principal axes. Calculate expressions for A' and B' in terms of M, a, and b for this particular angle.

(d) Calculate the inertia tensor $\mathbf{I}_{CM}$ in the CM frame by using the Parallel-Axis Theorem and show that

$$I^x_{CM} \;=\; \frac{M\,b^2}{12},\;\; I^y_{CM} \;=\; \frac{M\,a^2}{12},\;\; \text{and}\;\; I^z_{CM} \;=\; \frac{M}{12}\left(b^2 \;+\; a^2\right).$$

Problem 2

(a) The Euler equation for an asymmetric top ($I_1 > I_2 > I_3$) with $L^2 = 2\,I_2 K$ is

$$\dot{\omega}_2 \;=\; \alpha\,\left(\Omega^2 \;-\; \omega_2^2\right),$$

where

$$\Omega^2 \;=\; \frac{2K}{I_2} \quad \text{and} \quad \alpha \;=\; \sqrt{\left(1 \;-\; \frac{I_2}{I_1}\right)\left(\frac{I_2}{I_3} \;-\; 1\right)}$$

Solve for $\omega_2(t)$ with the initial condition $\omega_2(0) = 0$.

(b) Use the solution $\omega_2(t)$ found in Part (a) to find the solutions $\omega_1(t)$ and $\omega_3(t)$ given by Eqs. (7.35).

Problem 3

(a) Consider a circular cone of height H and base radius $R = H\,\tan\alpha$ with uniform mass

density $\rho = 3\,M/(\pi\,HR^2)$.

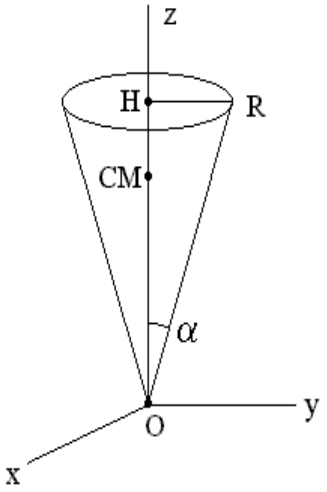

Show that the non-vanishing components of the inertia tensor **I** calculated from the vertex O of the cone are

$$I_{xx} \;=\; I_{yy} \;=\; \frac{3}{5}\,M\left(H^2 \;+\; \frac{R^2}{4}\right) \quad \text{and} \quad I_{zz} \;=\; \frac{3}{10}\,M\,R^2$$

(b) Show that the principal moments of inertia calculated in the CM frame (located at a height $h = 3H/4$ on the symmetry axis) are

$$I_1 \;=\; I_2 \;=\; \frac{3}{20}\,M\left(R^2 \;+\; \frac{H^2}{4}\right) \quad \text{and} \quad I_3 \;=\; \frac{3}{10}\,M\,R^2$$

Problem 4

Show that the Euler basis vectors $(\hat{\mathsf{e}}_1, \hat{\mathsf{e}}_2, \hat{\mathsf{e}}_3)$ are expressed as shown in Eq. (7.45).

Problem 5

Since the Lagrangian (7.55) for the motion of a symmetric top with one fixed point is independent of the Euler angles φ and ψ, derive the Routhian

$$R(\theta, \dot\theta; p_\varphi, p_\psi) \;=\; L \;-\; p_\varphi\,\dot\varphi \;-\; p_\psi\,\dot\psi,$$

and find the corresponding Routh-Euler-Lagrange equation for θ.

Chapter 8

Normal-Mode Analysis

8.1 Stability of Equilibrium Points

A nonlinear force equation $m\,\ddot{x} = f(x)$ has equilibrium points (labeled x_0) when $f(x_0)$ vanishes. The stability of the equilibrium point x_0 is determined by the sign of $f'(x_0)$: the equilibrium point x_0 is stable if $f'(x_0) < 0$ or it is unstable if $f'(x_0) > 0$. Since $f(x)$ is also derived from a potential $V(x)$ as $f(x) = -\,V'(x)$, we say that the equilibrium point x_0 is stable (or unstable) if $V''(x_0)$ is positive (or negative).

8.1.1 Bead on a Rotating Hoop

In Chap. 2, we considered the problem of a bead of mass m sliding freely on a hoop of radius r rotating with angular velocity ω_0 in a constant gravitational field with acceleration g. The Lagrangian for this system is

$$L(\theta,\dot{\theta}) \;=\; \frac{m}{2}\,r^2\dot{\theta}^2 \;+\; \left(\frac{m}{2}\,r^2\omega_0^2\,\sin^2\theta \;+\; mgr\,\cos\theta\right) \;=\; \frac{m}{2}\,r^2\dot{\theta}^2 \;-\; V(\theta),$$

where $V(\theta)$ denotes the effective potential, and the Euler-Lagrange equation for θ is

$$mr^2\,\ddot{\theta} \;=\; -\,V'(\theta) \;=\; -\,mr^2\omega_0^2\,\sin\theta\,(\nu-\cos\theta), \tag{8.1}$$

where $\nu = g/(r\,\omega_0^2)$. The equilibrium points of Eq. (8.1) are $\theta = 0$ (for all values of ν) and $\theta = \arccos(\nu)$ if $\nu < 1$. The stability of the equilibrium point $\theta = \theta_0$ is determined by the sign of

$$V''(\theta_0) \;=\; mr^2\omega_0^2\,\left[\nu\,\cos\theta_0 \;-\; \left(2\,\cos^2\theta_0 - 1\right)\right].$$

Hence,

$$V''(0) \;=\; mr^2\omega_0^2\,(\nu \;-\; 1) \tag{8.2}$$

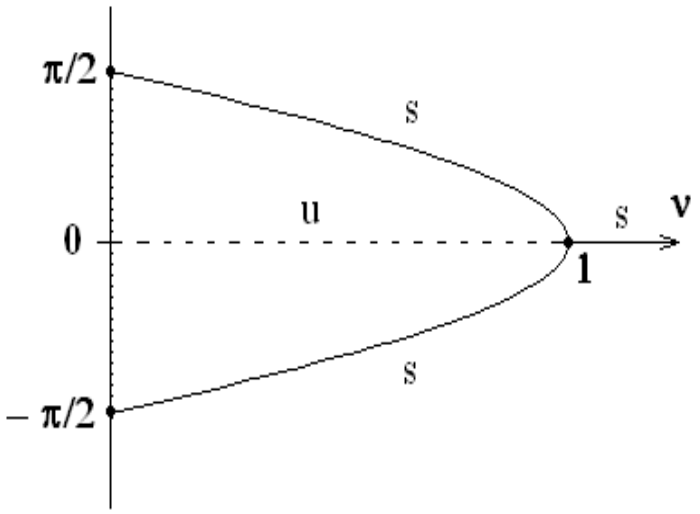

Figure 8.1: Bifurcation tree for the bead on a rotating-hoop problem

is positive (i.e., $\theta = 0$ is stable) if $\nu > 1$ or negative (i.e., $\theta = 0$ is unstable) if $\nu < 1$. In the latter case, when $\nu < 1$ and the second equilibrium point $\theta_0 = \arccos(\nu)$ is possible, we find

$$V''(\theta_0) \;=\; mr^2\omega_0^2 \left[\nu^2 \;-\; \left(2\,\nu^2 - 1\right)\right] \;=\; mr^2\omega_0^2 \left(1 - \nu^2\right) \;>\; 0, \tag{8.3}$$

and thus the equilibrium point $\theta_0 = \arccos(\nu)$ is stable when $\nu < 1$. The stability of the bead on a rotating hoop is displayed on the *bifurcation* diagram (see Figure 7.14) which shows the stable regime bifurcates at $\nu = 1$.

8.1.2 Circular Orbits in Central-Force Fields

The radial force equation

$$\mu\,\ddot{r} \;=\; \frac{\ell^2}{\mu\,r^3} \;-\; k\,r^{n-1} \;=\; -\,V'(r),$$

studied in Chap. 4 for a central-force field $F(r) = -\,k\,r^{n-1}$ (here, μ is the reduced mass of the system, the azimuthal angular momentum ℓ is a constant of the motion, and k is a constant), has the equilibrium point at $r = \rho$ defined by the relation

$$\rho^{n+2} \;=\; \frac{\ell^2}{\mu\,k}. \tag{8.4}$$

The second derivative of the effective potential is

$$V''(r) \;=\; \frac{\ell^2}{\mu\,r^4}\left(3 \;+\; (n-1)\,\frac{k\,\mu}{\ell^2}\,r^{n+2}\right),$$

which becomes

$$V''(\rho) \;=\; \frac{\ell^2}{\mu\,\rho^4}\,(2+n). \tag{8.5}$$

Hence, $V''(\rho)$ is positive if $n > -2$, and, thus, circular orbits are stable in central-force fields $F(r) = -\,k\,r^{n-1}$ if $n > -2$.

8.2 Small Oscillations about Stable Equilibria

Once an equilibrium point x_0 is shown to be stable, i.e., $f'(x_0) < 0$ or $V''(x_0) > 0$, we may expand $x = x_0 + \delta x$ about the equilibrium point (with $\delta x \ll x_0$) to find the *linearized* force equation

$$m\;\delta\ddot{x} \;=\; -\,V''(x_0)\;\delta x, \tag{8.6}$$

which has oscillatory behavior with frequency

$$\omega(x_0) \;=\; \sqrt{\frac{V''(x_0)}{m}}.$$

We first look at the problem of a bead on a rotating hoop, where the frequency of small oscillations $\omega(\theta_0)$ is either given in Eq. (8.2) as

$$\omega(0) \;=\; \sqrt{\frac{V''(0)}{mr^2}} \;=\; \omega_0\,\sqrt{\nu-1}$$

for $\theta_0 = 0$ and $\nu > 1$, or is given in Eq. (8.3) as

$$\omega(\theta_0) \;=\; \sqrt{\frac{V''(\theta_0)}{mr^2}} \;=\; \omega_0\,\sqrt{1-\nu^2}$$

for $\theta_0 = \arccos(\nu)$ and $\nu < 1$.

Next, we look at the frequency of small oscillations about the stable circular orbit in a central-force field $F(r) = -\,k\,r^{-n}$ (with $n < 3$). Here, from Eq. (8.5), we find

$$\omega \;=\; \sqrt{\frac{V''(\rho)}{\mu}} \;=\; \sqrt{\frac{k\,(3-n)}{\mu\,\rho^{n+1}}},$$

where $\ell^2 = \mu\,k\;\rho^{3-n}$ was used. We note that for the Kepler problem ($n = 2$), the period of small oscillations $T = 2\pi/\omega$ is expressed as

$$T^2 \;=\; \frac{(2\pi)^2\,\mu}{k}\;\rho^3,$$

which is precisely the statement of Kepler's Third Law for circular orbits. Hence, a small perturbation of a stable Keplerian circular orbit does not change its orbital period.

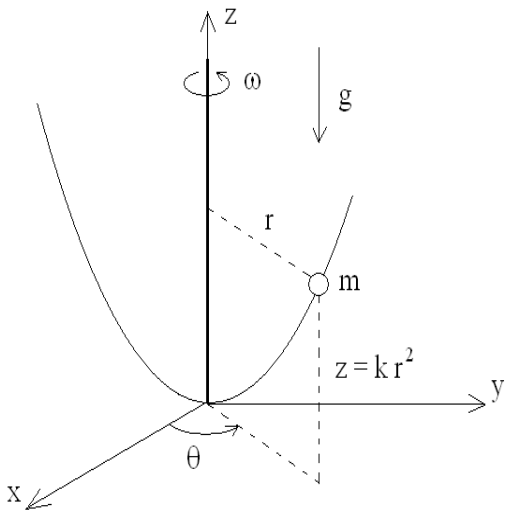

Figure 8.2: Bead on a rotating parabolic wire.

As a last example of linear stability, we consider the case of a time-dependent equilibrium. A rigid parabolic wire having equation $z = k\,r^2$ is fastened to a vertical shaft rotating at constant angular velocity $\dot{\theta} = \omega$. A bead of mass m is free to slide along the wire in the presence of a constant gravitational field with potential $U(z) = mg\,z$ (see Figure 8.2). The Lagrangian for this mechanical system is given as

$$L(r, \dot{r}) \;=\; \frac{m}{2}\left(1 + 4\,k^2 r^2\right)\,\dot{r}^2 \;+\; m\left(\frac{\omega^2}{2} - g\,k\right) r^2,$$

and the Euler-Lagrange equation of motion is easily obtained as

$$\left(1 + 4\,k^2 r^2\right)\ddot{r} \;+\; 4\,k^2 r\,\dot{r}^2 \;=\; \left(\omega^2 - 2\,gk\right)\,r.$$

Note that when $\omega^2 < 2\,gk$ we see that the bead moves in an effective potential represented by an isotropic simple harmonic oscillator with spring constant $\sqrt{m\,(2\,gk - \omega^2)}$ (i.e., the radial position of the bead is bounded), while when $\omega^2 > 2\,gk$, the bead appears to move on the surface of an inverted paraboloid and, thus, the radial position of the bead in this case is unbounded.

We now investigate the stability of the linearized motion $r(t) = r_0 + \delta r(t)$ about an initial radial position r_0. The linearized equation for $\delta r(t)$ is

$$\delta\ddot{r} \;=\; \left(\frac{\omega^2 - 2\,gk}{1 + 4\,k^2 r_0^2}\right)\,\delta r,$$

so that the radial position $r = r_0$ is stable if $\omega^2 < 2\,gk$ and unstable if $\omega^2 > 2\,gk$. In the stable case ($\omega^2 < 2\,gk$), the bead oscillates back and forth with $0 \le r(t) \le r_0$, although the

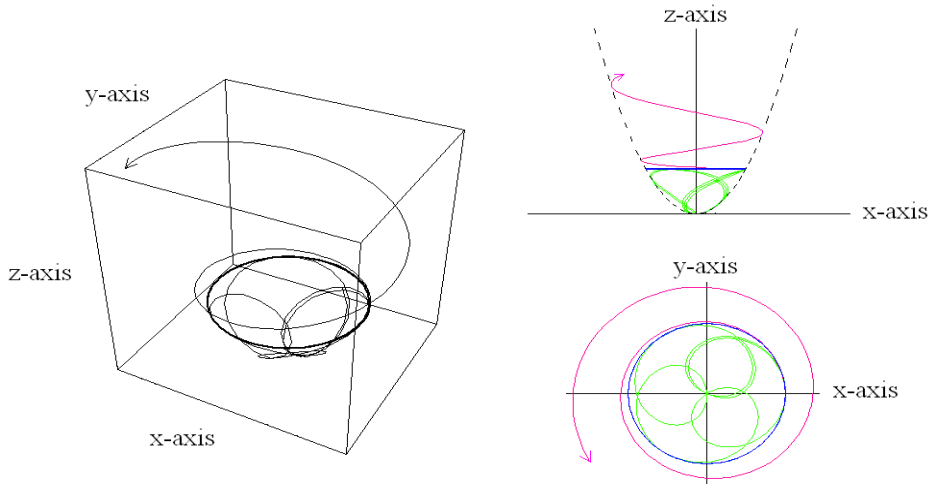

Figure 8.3: Normalized orbits for the nonlinear r-dynamics for the stable case ($\omega^2 < 2\,gk$), the marginal case ($\omega^2 = 2\,gk$), and the unstable case ($\omega^2 > 2\,gk$).

motion can be rather complex (see Figure 8.3 for orbits inside the radius r_0, with initial condition $\dot{r}_0 = 0$). For the special case $\omega^2 = 2\,gk$, the linearized equation $\delta\ddot{r} = 0$ implies that the radial dynamics $r(t) = r_0$ is marginally stable. In the unstable case ($\omega^2 > 2\,gk$), the radial position of the bead increases exponentially as it spirals outward away from the initial radial position r_0.

8.3 Coupled Oscillations and Normal-Mode Analysis

8.3.1 Coupled Simple Harmonic Oscillators

We begin our study of linearily-coupled oscillators by considering the following coupled system comprised of two block-and-spring systems, with identical mass m and identical spring constant k, coupled by means of a spring of constant K (see Figure 8.4). The coupled equations are

$$m\,\ddot{x} \;=\; -\,(k+K)\,x \;+\; K\,y \quad \text{and} \quad m\,\ddot{y} \;=\; -\,(k+K)\,y \;+\; K\,x. \tag{8.7}$$

The solutions for $x(t)$ and $y(t)$ by following a method known as the normal-mode analysis. First, we write $x(t)$ and $y(t)$ in the normal-mode representation

$$x(t) \;=\; \overline{x}\,e^{-\,i\omega t} \quad \text{and} \quad y(t) \;=\; \overline{y}\,e^{-\,i\omega t}, \tag{8.8}$$

where $\overline{x}$ and $\overline{y}$ are constants and the eigenfrequency ω is to be solved in terms of the system parameters (m, k, K). Next, substituting the normal-mode representation into Eq. (8.7),

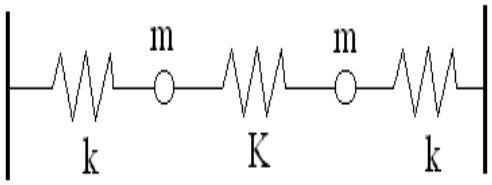

Figure 8.4: Coupled identical masses and springs

we obtain the following normal-mode matrix equation

$$\begin{pmatrix} \omega^2 m - (k+K) & K \\ K & \omega^2 m - (k+K) \end{pmatrix} \begin{pmatrix} \overline{x} \\ \overline{y} \end{pmatrix} = 0. \tag{8.9}$$

To obtain a non-trivial solution $\overline{x}, \overline{y} \neq 0$, the determinant of the matrix in Eq. (8.9) is required to vanish, which yields the characteristic polynomial

$$[\omega^2 m - (k+K)]^2 - K^2 = 0,$$

whose solutions are the eigenfrequencies

$$\omega_\pm^2 = \frac{(k+K)}{m} \pm \frac{K}{m}.$$

If we insert $\omega_+^2 = (k+2K)/m$ into the matrix equation (8.9), we find

$$\begin{pmatrix} K & K \\ K & K \end{pmatrix} \begin{pmatrix} \overline{x} \\ \overline{y} \end{pmatrix} = 0,$$

which implies that $\overline{y} = -\overline{x}$, and thus the *eigenfrequency* ω_+ is associated with an *anti-symmetric* coupled motion. If we insert $\omega_-^2 = k/m$ into the matrix equation (8.9), we find

$$\begin{pmatrix} -K & K \\ K & -K \end{pmatrix} \begin{pmatrix} \overline{x} \\ \overline{y} \end{pmatrix} = 0,$$

which implies that $\overline{y} = \overline{x}$, and thus the eigenfrequency ω_- is associated with a *symmetric* coupled motion.

Figures 8.5 and 8.6 show the normalized solutions of the coupled equations (8.7), where time is normalized as $t \to \sqrt{k/m}\, t$, for the weak coupling ($K < k$) and strong coupling ($K > k$) cases, respectively. Note that the two eigenfrequencies are said to be *commen-surate* if the ratio $\omega_+/\Omega_- = \sqrt{1+2K/k}$ is expressed as a rational number ρ for values of

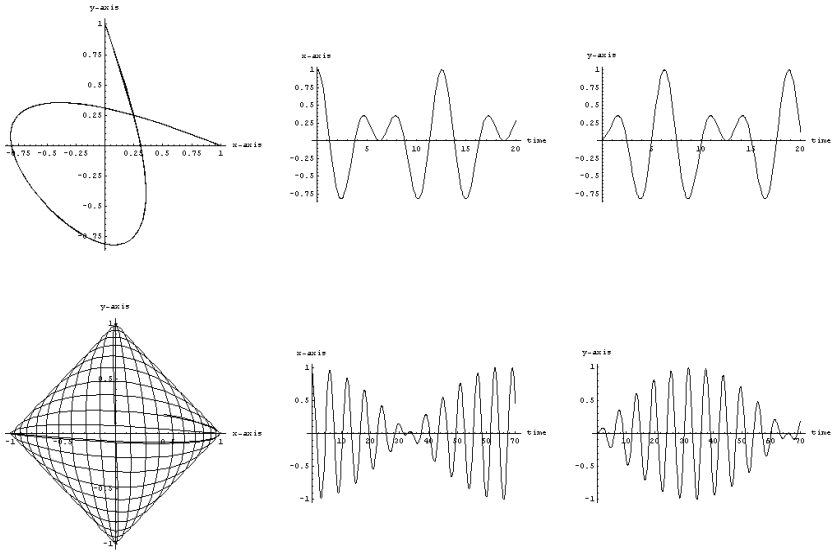

Figure 8.5: Weak-coupling normalized solutions of the coupled equations (8.7) for $K/k = 5/8$ (top graphs) and $K/k = 0.1$ (bottom graphs).

the ratio $K/k = (\rho^2 - 1)/2$ and that for commensurate eigenfrequencies, the graph of the solutions on the (x, y)-plane generates the so-called Lissajou figures. For noncommensurate eigenfrequencies, however, the graph of the solutions on the (x, y)-plane shows more complex behavior.

Lastly, we construct the normal coordinates η_+ and η_-, which satisfy the condition $\ddot{\eta}_\pm = -\,\omega_\pm^2\,\eta_\pm$. From the discussion above, we find

$$\eta_-(t) \;=\; x(t) + y(t) \quad \text{and} \quad \eta_+(t) \;=\; x(t) - y(t). \tag{8.10}$$

Figure 8.7 shows the graphs of the normal coordinates $\eta_\pm(t) = x(t) \mp y(t)$, which clearly displays the single-frequency behavior predicted by the present normal-mode analysis. The solutions $\eta_\pm(t)$ are of the form

$$\eta_\pm \;=\; A_\pm\, \cos(\omega_\pm t + \varphi_\pm),$$

where $A_\pm$ and $\varphi_\pm$ are constants (determined from initial conditions). The general solution of Eqs. (8.7) can, therefore, be written explicitly in terms of the normal coordinates $\eta_\pm$ as follows

$$\begin{pmatrix} x(t) \\ y(t) \end{pmatrix} \;=\; \frac{A_-}{2}\, \cos(\omega_- t + \varphi_-) \;\pm\; \frac{A_+}{2}\, \cos(\omega_+ t + \varphi_+).$$

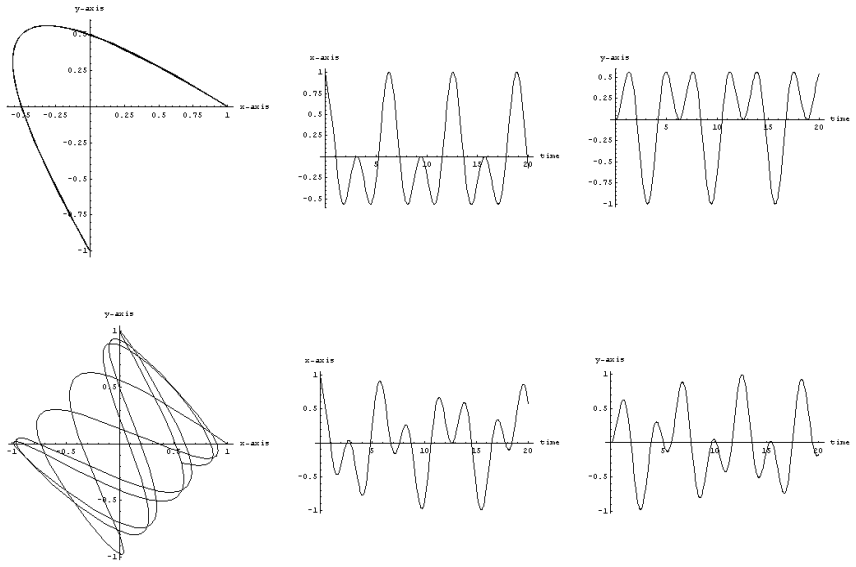

Figure 8.6: Strong-coupling normalized solutions of the coupled equations (8.7) for $K/k = 3/2$ (top graphs) and $K/k = 2$ (bottom graphs).

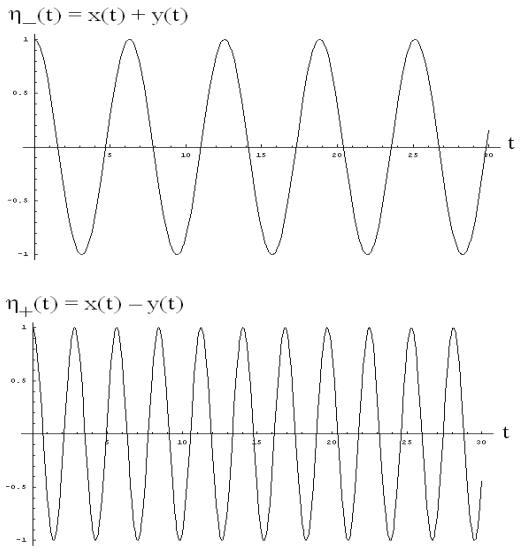

Figure 8.7: Normal coordinates $\eta_-(t)$ and $\eta_+(t)$ as a function of normalized time for the case $K/k = 2$ with normalized frequencies 1 and $\sqrt{5}$, respectively.

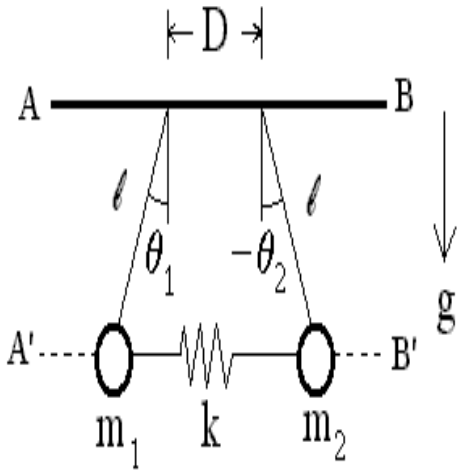

Figure 8.8: Coupled pendula

8.3.2 Nonlinear Coupled Oscillators

We now consider the following system composed of two pendula of identical length ℓ but different masses m_1 and m_2 coupled by means of a spring of constant k in the presence of a gravitational field of constant acceleration g (see Figure 8.8). Here, the distance D between the two points of attach of the pendula is equal to the length of the spring in its relaxed state and we assume, for simplicity, that the masses always stay on the same horizontal line.

Using the generalized coordinates (θ_1, θ_2) defined in Figure 8.8, the Lagrangian for this system is

$$\begin{aligned} L &= \frac{\ell^2}{2}\left(m_1\,\dot\theta_1^2 + m_2\,\dot\theta_2^2\right) - g\ell\,\left[\,m_1\,(1-\cos\theta_1) + m_2\,(1-\cos\theta_2)\,\right] \\ &\quad - \frac{k\ell^2}{2}\,(\sin\theta_1 - \sin\theta_2)^2\,, \end{aligned}$$

and the nonlinear coupled equations of motion are

$$\begin{aligned} m_1\,\ddot\theta_1 &= -\,m_1\,\omega_g^2\,\sin\theta_1 - k\,(\sin\theta_1 - \sin\theta_2)\,\cos\theta_1, \\ m_2\,\ddot\theta_2 &= -\,m_2\,\omega_g^2\,\sin\theta_2 + k\,(\sin\theta_1 - \sin\theta_2)\,\cos\theta_2, \end{aligned}$$

where $\omega_g^2 = g/\ell$.

It is quite clear that the equilibrium point is $\theta_1 = 0 = \theta_2$ and expansion of the coupled equations about this equilibrium yields the coupled linear equations

$$m_1\,\ddot q_1 = -\,m_1\,\omega_g^2\,q_1 - k\,(q_1 - q_2),$$

$$m_2\,\ddot{q}_2 \;=\; -\,m_2\,\omega_g^2\,q_2 \;+\; k\,(q_1 - q_2),$$

where $\theta_1 = q_1 \ll 1$ and $\theta_2 = q_2 \ll 1$. The normal-mode matrix associated with these coupled linear equations is

$$\begin{pmatrix} (\omega^2 - \omega_g^2)\,m_1 - k & k \\ k & (\omega^2 - \omega_g^2)\,m_2 - k \end{pmatrix} \begin{pmatrix} q_1 \\ q_2 \end{pmatrix} \;=\; 0,$$

and the characteristic polynomial is

$$M\,\left[\,(\omega^2 - \omega_g^2)\,\mu \;-\; k\,\right]\,(\omega^2 - \omega_g^2) \;=\; 0,$$

where $\mu = m_1 m_2/M$ is the reduced mass for the system and $M = m_1 + m_2$ is the total mass. The eigenfrequencies are thus

$$\omega_-^2 \;=\; \omega_g^2 \quad\text{and}\quad \omega_+^2 \;=\; \omega_g^2 \;+\; \frac{k}{\mu}.$$

The normal coordinates $\eta_\pm$ are expressed in terms of (q_1, q_2) as $\eta_\pm = a_\pm\,q_1 + b_\pm\,q_2$, where $a_\pm$ and $b_\pm$ are constant coefficients determined from the condition $\ddot{\eta}_\pm = -\,\omega_\pm^2\,\eta_\pm$. From this condition we find

$$\left(\frac{k}{m_1} + \omega_g^2\right) \;-\; \frac{b_\pm}{a_\pm}\,\frac{k}{m_2} \;=\; \omega_\pm^2 \;=\; \left(\frac{k}{m_2} + \omega_g^2\right) \;-\; \frac{a_\pm}{b_\pm}\,\frac{k}{m_1}.$$

For the eigenfrequency $\omega_-^2 = \omega_g^2$, we find $b_-/a_- = m_2/m_1$, and thus we may choose

$$\eta_- \;=\; \frac{m_1}{M}\,q_1 \;+\; \frac{m_2}{M}\,q_2,$$

which represents the center of mass position for the system. For the eigenfrequency $\omega_+^2 = \omega_g + k/\mu$, we find $b_+/a_+ = -\,1$, and thus we may choose

$$\eta_+ \;=\; q_1 \;-\; q_2.$$

Lastly, we may solve for q_1 and q_2 as

$$q_1 \;=\; \eta_- \;+\; \frac{m_2}{M}\,\eta_+ \quad\text{and}\quad q_2 \;=\; \eta_- \;-\; \frac{m_1}{M}\,\eta_+,$$

where $\eta_\pm = A_\pm\,\cos(\omega_\pm\,t + \varphi_\pm)$ are general solutions of the normal-mode equations $\ddot{\eta}_\pm = -\,\omega_\pm^2\,\eta_\pm$.

8.4 Problems

Problem 1

The following compound pendulum is composed of two identical masses m attached by massless rods of identical length ℓ to a ring of mass M, which is allowed to slide up and down along a vertical axis in a gravitational field with constant g. The entire system rotates about the vertical axis with an azimuthal angular frequency ω_φ.

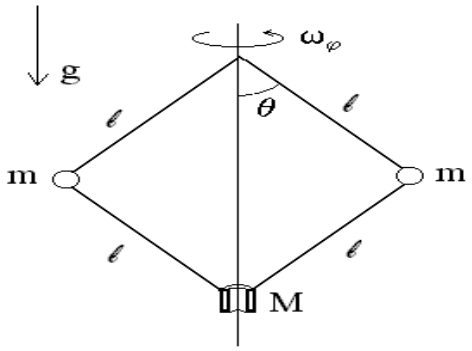

(a) Show that the Lagrangian for the system can be written as

$$L(\theta, \dot{\theta}) \;=\; \ell^2 \dot{\theta}^2 \left(m + 2M \, \sin^2 \theta \right) \;+\; m\ell^2 \, \omega_\varphi^2 \, \sin^2 \theta \;+\; 2\,(m+M) g\ell \, \cos\theta$$

(b) Identify the equilibrium points for the system and investigate their stability.

(c) Determine the frequency of small oscillations about each stable equilibrium point found in Part (b).

Problem 2

Consider the same problem as in Sec. (8.3.1) but now with different masses ($m_1 \neq m_2$).

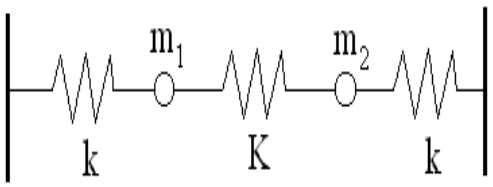

Calculate the eigenfrequencies and eigenvectors (normal coordinates) for this system.

Problem 3

Find the eigenfrequencies associated with small oscillations of the system shown below.

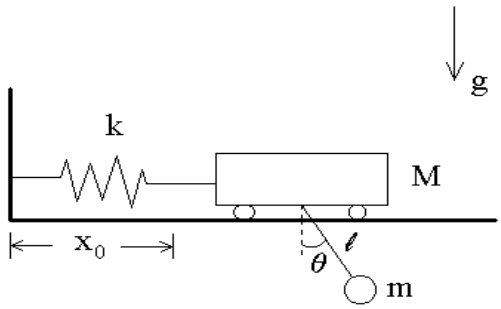

Problem 4

Two blocks of identical mass m are attached by massless springs (with identical spring constant k) as shown in the Figure below.

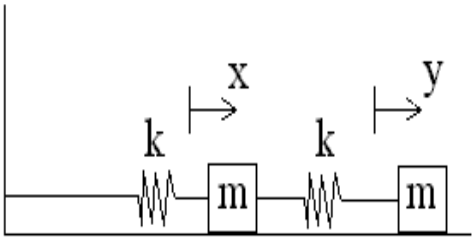

The Lagrangian for this system is

$$L(x, \dot{x};\, y, \dot{y}) \;=\; \frac{m}{2}\left(\dot{x}^2 \;+\; \dot{y}^2\right) \;-\; \frac{k}{2}\left[\, x^2 \;+\; (y-x)^2 \,\right],$$

where x and y denote departures from equilibrium.

(a) Derive the Euler-Lagrange equations for x and y.

(b) Show that the eigenfrequencies for small oscillations for this system are

$$\omega_{\pm}^2 \;=\; \frac{\omega_k^2}{2}\,\left(\,3 \;\pm\; \sqrt{5}\,\right),$$

where $\omega_k^2 = k/m$.

(c) Show that the eigenvectors associated with the eigenfrequencies $\omega_\pm$ are represented by the relations

$$\overline{y}_\pm \;=\; \frac{1}{2}\Big(\,1 \;\mp\; \sqrt{5}\,\Big)\,\overline{x}_\pm$$

where $(\overline{x}_\pm,\ \overline{y}_\pm)$ represent the normal-mode amplitudes.

Problem 5

An infinite sheet with surface mass density σ has a hole of radius R cut into it. A particle of mass m sits (in equilibrium) at the center of the circle. Assuming that the sheet lies on the (x, y)-plane (with the hole centered at the origin) and that the particle is displaced by a small amount $z \ll R$ along the z-axis, calculate the frequency of small oscillations.

Problem 6

Two identical masses are connected by two identical massless springs and are constrained to move on a circle (see Figure below). Of course, the two masses are in equilibrium when they are diametrically opposite points on the circle.

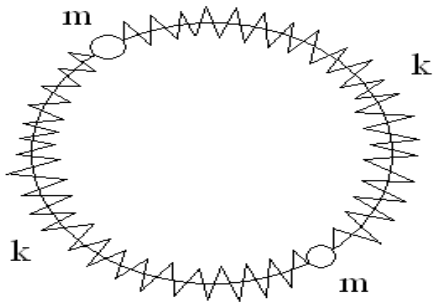

Solve for the normal modes of the system.

Problem 7

Consider a pendulum of mass m attached at a point O with the help of a massless rigid rod on length ℓ. Here, point O is located at a distance $R > \ell$ from a axis of rotation and is rotating at an angular velocity Ω about the axis of rotation (see Figure below).

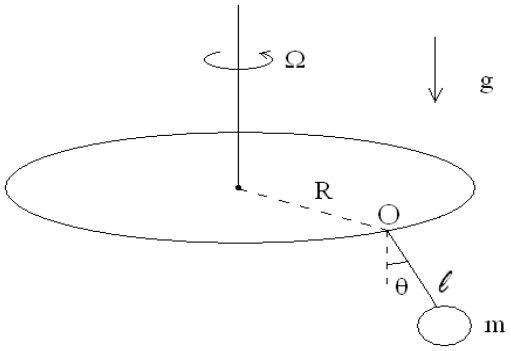

(a) Show that there are two equilibrium configurations to this problem, which are obtained from finding the roots to the transcendental equation

$$(R \, - \, \ell \, \sin\theta) \, \Omega^2 \, \cos\theta \, = \, g \, \sin\theta.$$

(b) Show that one equilibrium configuration is stable while the other is unstable.

Chapter 9

Continuous Lagrangian Systems

9.1 Waves on a Stretched String

9.1.1 Wave Equation

The equation describing waves propagating on a stretched string of constant linear mass density ρ under constant tension T is

$$\rho \, \frac{\partial^2 u(x,t)}{\partial t^2} \;=\; T \, \frac{\partial^2 u(x,t)}{\partial x^2}, \tag{9.1}$$

where $u(x,t)$ denotes the amplitude of the wave at position x along the string at time t. General solutions to this equation involve arbitrary functions $g(x \pm v\,t)$, where $v = \sqrt{T/\rho}$ represents the speed of waves propagating on the string. Indeed, we find

$$\rho \, \partial_t^2 g(x \pm v\,t) \;=\; \rho \, v^2 \; g'' \;=\; T \; g'' \;=\; T \, \partial_x^2 g(x \pm v\,t).$$

The interpretation of the two different signs is that $g(x - v\,t)$ represents a wave propagating to the right while $g(x + v\,t)$ represents a wave propagating to the left. The general solution of the wave equation (9.1) is

$$u(x,t) \;=\; A_- \; g(x - v\,t) \;+\; A_+ \; g(x + v\,t),$$

where $A_\pm$ are arbitrary constants.

9.1.2 Lagrangian Formalism

The question we now ask is whether the wave equation (9.1) can be derived from a variational principle

$$\delta \int \; \mathcal{L}(u, \partial_t u, \partial_x u;\; x, t) \; dx \, dt \;=\; 0, \tag{9.2}$$

where the Lagrangian *density* $\mathcal{L}(u, \partial_t u, \partial_x u;\ x, t)$ is a function of the dynamical variable $u(x,t)$ and its space-time derivatives. Here, the variation of the Lagrangian density $\mathcal{L}$ is expressed as

$$\delta\mathcal{L} \ = \ \delta u \, \frac{\partial \mathcal{L}}{\partial u} \ + \ \partial_t \delta u \, \frac{\partial \mathcal{L}}{\partial(\partial_t u)} \ + \ \partial_x \delta u \, \frac{\partial \mathcal{L}}{\partial(\partial_x u)},$$

where $\delta u(x,t)$ is a general variation of $u(x,t)$ subject to the condition that it vanishes at the integration boundaries in Eq. (9.2). By re-arranging terms, the variation of $\mathcal{L}$ can be written as

$$\begin{aligned} \delta\mathcal{L} \ &= \ \delta u \left\{ \frac{\partial \mathcal{L}}{\partial u} \ - \ \frac{\partial}{\partial t}\left(\frac{\partial \mathcal{L}}{\partial(\partial_t u)} \right) \ - \ \frac{\partial}{\partial x}\left(\frac{\partial \mathcal{L}}{\partial(\partial_x u)} \right) \right\} \\ &\quad + \ \frac{\partial}{\partial t}\left(\delta u \, \frac{\partial \mathcal{L}}{\partial(\partial_t u)} \right) \ + \ \frac{\partial}{\partial x}\left(\delta u \, \frac{\partial \mathcal{L}}{\partial(\partial_x u)} \right). \end{aligned} \tag{9.3}$$

When we insert this expression for $\delta\mathcal{L}$ into the variational principle (9.2), we obtain

$$\int dx\, dt\ \delta u \left\{ \frac{\partial \mathcal{L}}{\partial u} \ - \ \frac{\partial}{\partial t}\left(\frac{\partial \mathcal{L}}{\partial(\partial_t u)} \right) \ - \ \frac{\partial}{\partial x}\left(\frac{\partial \mathcal{L}}{\partial(\partial_x u)} \right) \right\} \ = \ 0, \tag{9.4}$$

where the last two terms in Eq. (9.3) cancel out because δu vanishes on the integration boundaries. Since the variational principle (9.4) is true for general variations δu, we obtain the Euler-Lagrange equation for the dynamical field $u(x,t)$:

$$\frac{\partial}{\partial t}\left(\frac{\partial \mathcal{L}}{\partial(\partial_t u)} \right) \ + \ \frac{\partial}{\partial x}\left(\frac{\partial \mathcal{L}}{\partial(\partial_x u)} \right) \ = \ \frac{\partial \mathcal{L}}{\partial u}. \tag{9.5}$$

9.1.3 Lagrangian Description for Waves on a Stretched String

The question we posed earlier now focuses on deciding what form the Lagrangian density must take. Here, the answer is surprisingly simple: the kinetic energy density of the wave is $\rho\ (\partial_t u)^2/2$, while the potential energy density is $T\ (\partial_x u)^2/2$, and thus the Lagrangian density for waves on a stretched string is

$$\mathcal{L}(u, \partial_t u, \partial_x u;\ x, t) \ = \ \frac{\rho}{2}\left(\frac{\partial u}{\partial t} \right)^2 \ - \ \frac{T}{2}\left(\frac{\partial u}{\partial x} \right)^2. \tag{9.6}$$

Since $\partial\mathcal{L}/\partial u = 0$, we find

$$\begin{aligned} \frac{\partial}{\partial t}\left(\frac{\partial \mathcal{L}}{\partial(\partial_t u)} \right) \ &= \ \frac{\partial}{\partial t}\left(\rho \, \frac{\partial u}{\partial t} \right) \ = \ \rho \, \frac{\partial^2 u}{\partial t^2}, \\ \frac{\partial}{\partial x}\left(\frac{\partial \mathcal{L}}{\partial(\partial_x u)} \right) \ &= \ \frac{\partial}{\partial x}\left(-\, T \, \frac{\partial u}{\partial x} \right) \ = \ -\, T \, \frac{\partial^2 u}{\partial x^2}, \end{aligned}$$

and Eq. (9.1) is indeed represented as an Euler-Lagrange equation (9.5) in terms of the Lagrangian density (9.6).

The energy density $\mathcal{E}$ of a stretched string can also be calculated by using the Legendre transformation

$$\mathcal{E} \equiv \frac{\partial u}{\partial t}\,\frac{\partial \mathcal{L}}{\partial(\partial_t u)} - \mathcal{L} = \frac{\rho}{2}\left(\frac{\partial u}{\partial t}\right)^2 + \frac{T}{2}\left(\frac{\partial u}{\partial x}\right)^2.$$

By using the wave equation (9.1), we readily find that the time derivative of the energy density

$$\frac{\partial \mathcal{E}}{\partial t} = \frac{\partial}{\partial x}\left(T\,\frac{\partial u}{\partial t}\,\frac{\partial u}{\partial x}\right)$$

can be expressed as an energy conservation law $\partial_t \mathcal{E} + \partial \mathcal{S} = 0$, where the energy-density flux is defined as $\mathcal{S} \equiv -\,T\,\partial_x u\,\partial_t u$. The next Section will present the general variational formulation of classical field theory, which will enable to show that the wave equation (9.1) also satisfies the momentum conservation law $\partial_t \mathcal{P} + \partial_x \mathcal{E} = 0$, where the momentum density is $\mathcal{P} \equiv \mathcal{S}/v^2$.

9.2 General Variational Principle for Field Theory*

The simple example of waves on a stretched string allows us to view the Euler-Lagrange equation (9.5) as a generalization of the Euler-Lagrange equations

$$\frac{d}{dt}\left(\frac{\partial L}{\partial \dot{q}^i}\right) = \frac{\partial L}{\partial q^i},$$

in terms of the generalized coordinates q^i. We now spend some time investigating the Lagrangian description of continuous systems, in which the dynamical variables are fields $\psi(\mathbf{x}, t)$ instead of spatial coordinates $\mathbf{x}$.

9.2.1 Action Functional

Classical and quantum field theories rely on variational principles based on the existence of action functionals. The typical action functional is of the form

$$\mathcal{A}[\psi] = \int d^4x\, \mathcal{L}(\psi,\, \partial_\mu \psi), \tag{9.7}$$

where the wave function $\psi(\mathbf{x}, t)$ represents the state of the system at position $\mathbf{x}$ and time t while the entire physical content of the theory is carried by the Lagrangian density $\mathcal{L}$.

The variational principle is based on the stationarity of the action functional

$$\delta\mathcal{A}[\psi] \;=\; \mathcal{A}[\psi+\delta\psi] \;-\; \mathcal{A}[\psi] \;=\; \int\, \delta\mathcal{L}(\psi,\, \partial_\mu\psi)\, d^4x,$$

where $\partial_\mu = (c^{-1}\partial_t,\ \nabla)$ and the metric tensor is defined as $g^{\mu\nu} = \mathrm{diag}(-1,+1,+1,+1)$.[1] Here, the variation of the Lagrangian density is

$$\begin{aligned}\delta\mathcal{L} \;&=\; \frac{\partial\mathcal{L}}{\partial\psi}\,\delta\psi \;+\; \frac{\partial\mathcal{L}}{\partial(\partial_\mu\psi)}\,\partial_\mu\delta\psi \\ &\equiv\; \delta\psi\left[\,\frac{\partial\mathcal{L}}{\partial\psi} \;-\; \frac{\partial}{\partial x^\mu}\left(\frac{\partial\mathcal{L}}{\partial(\partial_\mu\psi)}\right)\,\right] \;+\; \frac{\partial\Lambda^\mu}{\partial x^\mu},\end{aligned} \tag{9.8}$$

where

$$\frac{\partial\mathcal{L}}{\partial(\partial_\mu\psi)}\,\partial_\mu\delta\psi \;=\; \frac{\partial\mathcal{L}}{\partial(\nabla\psi)}\cdot\nabla\delta\psi \;+\; \frac{\partial\mathcal{L}}{\partial(\partial_t\psi)}\,\partial_t\delta\psi,$$

and the exact space-time divergence $\partial_\mu\Lambda^\mu$ is obtained by rearranging terms, with

$$\Lambda^\mu \;=\; \delta\psi\,\frac{\partial\mathcal{L}}{\partial(\partial_\mu\psi)} \quad\text{and}\quad \frac{\partial\Lambda^\mu}{\partial x^\mu} \;=\; \frac{\partial}{\partial t}\left(\delta\psi\,\frac{\partial\mathcal{L}}{\partial(\partial_t\psi)}\right) \;+\; \nabla\cdot\left(\delta\psi\,\frac{\partial\mathcal{L}}{\partial(\nabla\psi)}\right).$$

The variational principle $\delta\mathcal{A}[\psi] = 0$ then yields

$$0 \;=\; \int d^4x\;\delta\psi\left[\,\frac{\partial\mathcal{L}}{\partial\psi} \;-\; \frac{\partial}{\partial x^\mu}\left(\frac{\partial\mathcal{L}}{\partial(\partial_\mu\psi)}\right)\right],$$

where the exact divergence $\partial_\mu\Lambda^\mu$ drops out under the assumption that the variation $\delta\psi$ vanish on the integration boundaries. Following the standard rules of Calculus of Variations, the Euler-Lagrange equation for the wave function ψ is

$$\frac{\partial}{\partial x^\mu}\left(\frac{\partial\mathcal{L}}{\partial(\partial_\mu\psi)}\right) \;=\; \frac{\partial}{\partial t}\left(\frac{\partial\mathcal{L}}{\partial(\partial_t\psi)}\right) \;+\; \nabla\cdot\left(\frac{\partial\mathcal{L}}{\partial(\nabla\psi)}\right) \;=\; \frac{\partial\mathcal{L}}{\partial\psi}. \tag{9.9}$$

9.2.2 Noether Method and Conservation Laws

Since the Euler-Lagrange equations (9.9) hold true for arbitrary field variations $\delta\psi$, the variation of the Lagrangian density $\mathcal{L}$ is now expressed as the Noether equation

$$\delta\mathcal{L} \;\equiv\; \partial_\mu\Lambda^\mu \;=\; \frac{\partial}{\partial x^\mu}\left[\,\delta\psi\,\frac{\partial\mathcal{L}}{\partial(\partial_\mu\psi)}\,\right]. \tag{9.10}$$

which associates symmetries with conservation laws $\partial_\mu\,\mathcal{J}^\mu_a = 0$, where the index a denotes the possibility of conserved four-vector quantities (see below).

[1] For two four-vectors $A^\mu = (A^0, \mathbf{A})$ and $B^\mu = (B^0, \mathbf{B})$, we have $A\cdot B = A_\mu\,B^\mu = \mathbf{A}\cdot\mathbf{B} - A^0\,B^0$, where $A_0 = -\,A^0$.

Energy-Momentum Conservation Law

The conservation of energy-momentum (a four-vector quantity!) involves symmetry of the Lagrangian with respect to constant *space-time* translations ($x^\nu \rightarrow x^\nu + \delta x^\nu$). Here, the variation $\delta\psi$ is no longer arbitrary but is required to be of the form

$$\delta\psi \;=\; -\,\delta x^\nu\,\partial_\nu\psi \tag{9.11}$$

while the variation $\delta\mathcal{L}$ is of the form

$$\delta\mathcal{L} \;=\; -\,\delta x^\nu\left[\;\partial_\nu\mathcal{L} \;-\; (\partial_\nu\mathcal{L})_\psi\;\right], \tag{9.12}$$

where $(\partial_\nu\mathcal{L})_\psi$ denotes a explicit space-time derivative of $\mathcal{L}$ at constant ψ. The Noether equation (9.10) can now be written as

$$\frac{\partial}{\partial x^\mu}\left(\mathcal{L}\;g^\mu{}_\nu \;-\; \frac{\partial\mathcal{L}}{\partial(\partial_\mu\psi)}\,\partial_\nu\psi\right) \;=\; \left(\frac{\partial\mathcal{L}}{\partial x^\nu}\right)_\psi .$$

If the Lagrangian is explicitly independent of the space-time coordinates, i.e., $(\partial_\nu\mathcal{L})_\psi = 0$, the energy-momentum conservation law $\partial_\mu T^\mu{}_\nu = 0$ is written in terms of the energy-momentum tensor

$$T^\mu{}_\nu \;\equiv\; \mathcal{L}\;g^\mu{}_\nu \;-\; \frac{\partial\mathcal{L}}{\partial(\partial_\mu\psi)}\,\partial_\nu\psi. \tag{9.13}$$

We note that the derivation of the energy-momentum conservation law is the same for classical and quantum fields. A similar procedure would lead to the conservation of angular momentum but this derivation is beyond the scope of the present Notes and we move on instead to an important conservation in wave dynamics.

Wave-Action Conservation Law

Waves are known to exist on a great variety of media. When waves are supported by a spatially nonuniform or time-dependent medium, the conservation law of energy or momentum no longer apply and instead energy or momentum is transfered between the medium and the waves. There is however one conservation law which still applies and the quantity being conserved is known as *wave action*.

The derivation of a wave-action conservation law differs for classical fields and quantum fields. The difference is related to the fact that whereas classical fields are generally represented by real-valued wave functions (i.e., $\psi^* = \psi$), the wave functions of quantum field theories are generally complex-valued (i.e., $\psi^* \neq \psi$).

The first step in deriving a wave-action conservation law in classical field theory involves transforming the real-valued wave function ψ into a complex-valued wave function ψ. Next, variations of ψ and its complex conjugate ψ^* are of the form

$$\delta\psi \;\equiv\; i\epsilon\;\psi \;\text{ and }\; \delta\psi^* \;\equiv\; -\,i\epsilon\;\psi^*, \tag{9.14}$$

Lastly, we transform the classical Lagrangian density $\mathcal{L}$ into a real-valued Lagrangian density $\mathcal{L}_R(\psi, \psi^*)$ such that $\delta\mathcal{L}_R \equiv 0$. The wave-action conservation law is, therefore, expressed in the form $\partial_\mu \mathcal{J}^\mu = 0$, where the wave-action four-density is

$$\mathcal{J}^\mu \equiv 2\,\mathrm{Im}\left[\,\psi\,\frac{\partial\mathcal{L}_R}{\partial(\partial_\mu\psi)}\,\right], \tag{9.15}$$

where $\mathrm{Im}[\cdots]$ denotes the imaginary part.

9.3 Variational Principle for Schroedinger Equation*

A simple yet important example for a quantum field theory is provided by the Schroedinger equation for a spinless particle of mass m subjected to a real-valued potential energy function $V(\mathbf{x}, t)$. The Lagrangian density for the Schroedinger equation is given as

$$\mathcal{L}_R = -\frac{\hbar^2}{2m}\,|\nabla\psi|^2 + \frac{i\hbar}{2}\left(\psi^*\,\frac{\partial\psi}{\partial t} - \psi\,\frac{\partial\psi^*}{\partial t}\right) - V\,|\psi|^2. \tag{9.16}$$

The Schroedinger equation for ψ is derived as an Euler-Lagrange equation (9.9) in terms of ψ^*, where

$$\begin{aligned}
\frac{\partial\mathcal{L}_R}{\partial(\partial_t\psi^*)} &= -\frac{i\hbar}{2}\,\psi \;\rightarrow\; \frac{\partial}{\partial t}\left(\frac{\partial\mathcal{L}_R}{\partial(\partial_t\psi^*)}\right) = -\frac{i\hbar}{2}\,\frac{\partial\psi}{\partial t},\\
\frac{\partial\mathcal{L}_R}{\partial(\nabla\psi^*)} &= -\frac{\hbar^2}{2m}\,\nabla\psi \;\rightarrow\; \nabla\cdot\left(\frac{\partial\mathcal{L}_R}{\partial(\nabla\psi^*)}\right) = -\frac{\hbar^2}{2m}\,\nabla^2\psi,\\
\frac{\partial\mathcal{L}_R}{\partial\psi^*} &= \frac{i\hbar}{2}\,\frac{\partial\psi}{\partial t} - V\,\psi,
\end{aligned}$$

so that the Euler-Lagrange equation (9.9) for the Schroedinger Lagrangian (9.16) becomes

$$i\hbar\,\frac{\partial\psi}{\partial t} = -\frac{\hbar^2}{2m}\,\nabla^2\psi + V\,\psi, \tag{9.17}$$

where the Schroedinger equation for ψ^* is as an Euler-Lagrange equation (9.9) in terms of ψ, which yields

$$-i\hbar\,\frac{\partial\psi^*}{\partial t} = -\frac{\hbar^2}{2m}\,\nabla^2\psi^* + V\,\psi^*, \tag{9.18}$$

which is simply the complex-conjugate equation of Eq. (9.17).

The energy-momentum conservation law is now derived by Noether method. Because the potential $V(\mathbf{x}, t)$ is spatially nonuniform and time dependent, the energy-momentum contained in the wave field is not conserved and energy-momentum is exchanged between

the wave field and the potential V. For example, the energy *transfer* equation is of the form

$$\frac{\partial \mathcal{E}}{\partial t} \; + \; \nabla \cdot \mathbf{S} \; = \; |\psi|^2 \, \frac{\partial V}{\partial t}, \tag{9.19}$$

where the energy density $\mathcal{E}$ and energy density flux $\mathbf{S}$ are given explicitly as

$$\begin{aligned} \mathcal{E} \;\; &= \;\; - \, \mathcal{L}_R \; + \; \frac{i\hbar}{2} \left(\psi^* \, \frac{\partial \psi}{\partial t} \; - \; \psi \, \frac{\partial \psi^*}{\partial t} \right) \\ \mathbf{S} \;\; &= \;\; - \, \frac{\hbar^2}{2m} \left(\frac{\partial \psi}{\partial t} \, \nabla \psi^* \; + \; \frac{\partial \psi^*}{\partial t} \, \nabla \psi \right). \end{aligned}$$

The momentum transfer equation, on the other hand, is

$$\frac{\partial \mathbf{P}}{\partial t} \; + \; \nabla \cdot \mathsf{T} \; = \; - \, |\psi|^2 \, \nabla V, \tag{9.20}$$

where the momentum density $\mathbf{P}$ and momentum density tensor T are given explicitly as

$$\begin{aligned} \mathbf{P} \;\; &= \;\; \frac{i\hbar}{2} \, (\psi \, \nabla \psi^* \; - \; \psi^* \, \nabla \psi) \\ \mathsf{T} \;\; &= \;\; \mathcal{L}_R \, \mathsf{I} \; + \; \frac{\hbar^2}{2m} \, (\nabla \psi^* \, \nabla \psi \; + \; \nabla \psi \, \nabla \psi^*) \, . \end{aligned}$$

Note that Eqs. (9.19) and (9.20) are exact equations.

Whereas energy-momentum is transfered between the wave field ψ and potential V, the amount of wave-action contained in the wave field is conserved. Indeed the wave-action conservation law is

$$\frac{\partial \mathcal{J}}{\partial t} \; + \; \nabla \cdot \mathbf{J} = 0, \tag{9.21}$$

where the wave-action density $\mathcal{J}$ and wave-action density flux $\mathbf{J}$ are

$$\mathcal{J} \; = \; \hbar \, |\psi|^2 \quad \text{and} \quad \mathbf{J} \; = \; \frac{i\hbar^2}{2m} \, (\psi \, \nabla \psi^* \; - \; \psi^* \, \nabla \psi) \tag{9.22}$$

Thus wave-action conservation law is none other than the law of conservation of probability associated with the normalization condition

$$\int \, |\psi|^2 \, d^3x \; = \; 1$$

for bounds states or the conservation of the number of quanta in a scattering problem.

Appendix A

Basic Mathematical Methods

Appendix A introduces, first, an explicit derivation of the Frenet-Serret formulas for an arbitrary curve in three-dimensional space used in Chapters 1 and 2. Next, some basic concepts in linear algebra that a student may have acquired before taking this course are summarized. Hopefully, this material will assist the student in following the presentation in Chapters 7 and 8. Lastly, some general integrals involving the trigonometric substitution are also solved explicitly, while the optional Section A.3.2 summarizes the properties of the Jacobi and Weierstrass elliptic functions and integrals involved in solutions of various differential equations throughout the text.

A.1 Frenet-Serret Formulas

Consider a curve

$$\mathbf{r}(t) \;=\; x(t)\,\widehat{\mathsf{x}} \;+\; y(t)\,\widehat{\mathsf{y}} \;+\; z(t)\,\widehat{\mathsf{z}} \tag{A.1}$$

in three-dimensional space parametrized by time t. The infinitesimal length element along the curve $ds(t) = v(t)\,dt$ is also parametrized by time t, with $v(t) \equiv |\dot{\mathbf{r}}|$ denoting the speed along the curve.

The Frenet-Serret formulas associated with the curvature κ and torsion τ of the curve (A.1) are defined in terms of the right-handed set of unit vectors $(\widehat{\mathsf{t}}, \widehat{\mathsf{n}}, \widehat{\mathsf{b}})$, where $\widehat{\mathsf{t}}$ denotes the *tangent* unit vector, $\widehat{\mathsf{n}}$ denotes the *normal* unit vector, and $\widehat{\mathsf{b}}$ denotes the *binormal* unit vector. First, by definition, the tangent unit vector is defined as

$$\widehat{\mathsf{t}} \;\equiv\; \frac{d\mathbf{r}}{ds} \;=\; \frac{\dot{\mathbf{r}}(t)}{v(t)}. \tag{A.2}$$

The definitions of the curvature κ and the normal unit vector $\widehat{\mathsf{n}}$ are defined as

$$\frac{d\widehat{\mathsf{t}}}{ds} \;=\; \frac{\ddot{\mathbf{r}}}{v^2} \;-\; \frac{\dot{v}}{v^2}\,\widehat{\mathsf{t}} \;=\; \frac{\widehat{\mathsf{t}}}{v^2} \times \left(\ddot{\mathbf{r}} \times \widehat{\mathsf{t}}\right) \;=\; \left(\frac{\dot{\mathbf{r}} \times \ddot{\mathbf{r}}}{v^3}\right) \times \widehat{\mathsf{t}} \;=\; \kappa\,\left(\widehat{\mathsf{b}} \times \widehat{\mathsf{t}}\right) \;\equiv\; \kappa\,\widehat{\mathsf{n}}, \tag{A.3}$$

where $\dot{v} \equiv d|\dot{\mathbf{r}}|/dt = \widehat{\mathsf{t}} \cdot \ddot{\mathbf{r}}$, so that the curvature is defined as

$$\kappa \;\equiv\; \frac{|\dot{\mathbf{r}} \times \ddot{\mathbf{r}}|}{v^3}, \tag{A.4}$$

while the normal and binormal unit vectors are defined as

$$\widehat{\mathsf{n}} \;\equiv\; \frac{\dot{\mathbf{r}} \times (\ddot{\mathbf{r}} \times \dot{\mathbf{r}})}{\kappa\, v^4} \;=\; \widehat{\mathsf{t}} \times \left(\frac{\ddot{\mathbf{r}} \times \dot{\mathbf{r}}}{|\ddot{\mathbf{r}} \times \dot{\mathbf{r}}|} \right), \tag{A.5}$$

and

$$\widehat{\mathsf{b}} \;\equiv\; \frac{\dot{\mathbf{r}} \times \ddot{\mathbf{r}}}{|\dot{\mathbf{r}} \times \ddot{\mathbf{r}}|}. \tag{A.6}$$

Hence, the curve (A.1) exhibits curvature if its velocity $\dot{\mathbf{r}}$ and acceleration $\ddot{\mathbf{r}}$ are not colinear.

Next, we obtain the following expression for the derivative of the normal unit vector (A.5):

$$\begin{aligned}
\frac{d\widehat{\mathsf{n}}}{ds} \;&=\; \frac{d\widehat{\mathsf{t}}}{ds} \times \left(\frac{\ddot{\mathbf{r}} \times \dot{\mathbf{r}}}{|\ddot{\mathbf{r}} \times \dot{\mathbf{r}}|} \right) \;+\; \widehat{\mathsf{t}} \times \frac{d}{ds} \left(\frac{\ddot{\mathbf{r}} \times \dot{\mathbf{r}}}{|\ddot{\mathbf{r}} \times \dot{\mathbf{r}}|} \right) \\
&=\; \left[\widehat{\mathsf{t}} \times \left(\frac{\ddot{\mathbf{r}} \times \dot{\mathbf{r}}}{v^3} \right) \right] \times \left(\frac{\ddot{\mathbf{r}} \times \dot{\mathbf{r}}}{|\ddot{\mathbf{r}} \times \dot{\mathbf{r}}|} \right) \;+\; \frac{\widehat{\mathsf{t}}}{v} \times \left[\widehat{\mathsf{b}} \times \left(\frac{\left(\dddot{\mathbf{r}} \times \dot{\mathbf{r}} \right) \times \widehat{\mathsf{b}}}{|\ddot{\mathbf{r}} \times \dot{\mathbf{r}}|} \right) \right] \\
&=\; \kappa \left(\widehat{\mathsf{t}} \times \widehat{\mathsf{b}} \right) \times \widehat{\mathsf{b}} \;+\; \left(\frac{\widehat{\mathsf{t}} \cdot \left[\left(\dddot{\mathbf{r}} \times \dot{\mathbf{r}} \right) \times \widehat{\mathsf{b}} \right]}{v\, |\ddot{\mathbf{r}} \times \dot{\mathbf{r}}|} \right) \widehat{\mathsf{b}} \;\equiv\; -\,\kappa\, \widehat{\mathsf{t}} \;+\; \tau\, \widehat{\mathsf{b}},
\end{aligned} \tag{A.7}$$

where the torsion

$$\tau \;\equiv\; \frac{\widehat{\mathsf{t}} \cdot \left[\left(\dddot{\mathbf{r}} \times \dot{\mathbf{r}} \right) \times \widehat{\mathsf{b}} \right]}{v\, |\ddot{\mathbf{r}} \times \dot{\mathbf{r}}|} \;=\; \frac{\widehat{\mathsf{n}} \cdot \left(\dddot{\mathbf{r}} \times \dot{\mathbf{r}} \right)}{\kappa\, v^4} \;=\; \frac{\dot{\mathbf{r}} \cdot \left(\ddot{\mathbf{r}} \times \dddot{\mathbf{r}} \right)}{\kappa^2\, v^6} \tag{A.8}$$

is defined in terms of the triple product $\dot{\mathbf{r}} \cdot (\ddot{\mathbf{r}} \times \dddot{\mathbf{r}})$. Hence, the torsion requires that the rate of change of acceleration $\dddot{\mathbf{r}} = d\ddot{\mathbf{r}}/dt$ (known as *jerk*) along the curve have a nonvanishing component perpendicular to the plane constructed by the velocity $\dot{\mathbf{r}}$ and the acceleration $\ddot{\mathbf{r}}$.

Lastly, we obtain the expression for the derivative of the normal unit vector (A.6):

$$\frac{d\widehat{\mathsf{b}}}{ds} \;=\; \frac{\widehat{\mathsf{b}} \times \left[\left(\dot{\mathbf{r}} \times \dddot{\mathbf{r}} \right) \times \widehat{\mathsf{b}} \right]}{v\, |\dot{\mathbf{r}} \times \ddot{\mathbf{r}}|} \;=\; \alpha\, \widehat{\mathsf{t}} \;+\; \beta\, \widehat{\mathsf{n}} \;\equiv\; -\,\tau\, \widehat{\mathsf{n}}, \tag{A.9}$$

where

$$\alpha \;\equiv\; \widehat{\mathsf{t}} \cdot \frac{d\widehat{\mathsf{b}}}{ds} \;=\; \frac{\widehat{\mathsf{t}} \cdot \left(\dot{\mathbf{r}} \times \dddot{\mathbf{r}} \right)}{\kappa\, v^4} \;\equiv\; 0,$$

and

$$\beta \equiv \widehat{\mathsf{n}} \cdot \frac{d\widehat{\mathsf{b}}}{ds} = \frac{\widehat{\mathsf{n}} \cdot \left(\dot{\mathbf{r}} \times \dddot{\mathbf{r}} \right)}{\kappa \, v^4} = \left[\frac{\dot{\mathbf{r}} \times (\ddot{\mathbf{r}} \times \dot{\mathbf{r}})}{\kappa^2 \, v^8} \right] \cdot \left(\dot{\mathbf{r}} \times \dddot{\mathbf{r}} \right) = \frac{\ddot{\mathbf{r}} \cdot \left(\dot{\mathbf{r}} \times \dddot{\mathbf{r}} \right)}{\kappa^2 \, v^6} = -\tau.$$

The equations (A.3), (A.7), and (A.9) are refered to as the Frenet-Serret formulas, which describes the evolution of the unit vectors $(\widehat{\mathsf{t}}, \widehat{\mathsf{n}}, \widehat{\mathsf{b}})$ along the curve (A.1) in terms of the curvature (A.4) and the torsion (A.8). Note that by introducing the *Darboux* vector (Gaston Darboux, 1842-1917) $\boldsymbol{\omega} \equiv \tau \, \widehat{\mathsf{t}} + \kappa \, \widehat{\mathsf{b}}$, the Frenet-Serret equations (A.3), (A.7), and (A.9) may be written as

$$\frac{d\widehat{\mathsf{e}}_i}{ds} \equiv \boldsymbol{\omega} \times \widehat{\mathsf{e}}_i, \tag{A.10}$$

where $\widehat{\mathsf{e}}_i = (\widehat{\mathsf{t}}, \widehat{\mathsf{n}}, \widehat{\mathsf{b}})$ denotes a component of the so-called Frenet *frame*. Hence, curvature is a measure of the rotation of the Frenet frame about the binormal unit vector $\widehat{\mathsf{b}}$, while torsion is the measure of the rotation of the Frenet frame about the tangent unit vector $\widehat{\mathsf{t}}$.

We now compute the Frenet-Serret formulas for the helical path

$$\mathbf{r}(\theta) = a \, (\cos\theta \, \widehat{\mathsf{x}} + \sin\theta \, \widehat{\mathsf{y}}) + b \, \theta \, \widehat{\mathsf{z}} \tag{A.11}$$

parametrized by the angle θ. Here, the distance s along the helix is simply given as $s = c\,\theta$, where $c = \sqrt{a^2 + b^2}$. Hence, the tangent unit vector is defined as

$$\widehat{\mathsf{t}} = \frac{d\mathbf{r}}{ds} = \cos\alpha \, (-\sin\theta \, \widehat{\mathsf{x}} + \cos\theta \, \widehat{\mathsf{y}}) + \sin\alpha \, \widehat{\mathsf{z}}, \tag{A.12}$$

where $(a, b) \equiv (c \cos\alpha, c \sin\alpha)$ and $0 \leq \alpha < \pi/2$ denotes the pitch of the helix (e.g., a circle is a helical path with pitch $\alpha = 0$). Next, the derivative of the tangent unit vector yields

$$\frac{d\widehat{\mathsf{t}}}{ds} = -\frac{\cos\alpha}{c} \, (\cos\theta \, \widehat{\mathsf{x}} + \sin\theta \, \widehat{\mathsf{y}}) \equiv \kappa \, \widehat{\mathsf{n}}, \tag{A.13}$$

so that the normal unit vector is

$$\widehat{\mathsf{n}} = -(\cos\theta \, \widehat{\mathsf{x}} + \sin\theta \, \widehat{\mathsf{y}}) \tag{A.14}$$

and the curvature is $\kappa = c^{-1} \cos\alpha$ (i.e., a circle of radius a has a scalar curvature $\kappa = a^{-1}$). Lastly, note that the binormal vector is

$$\widehat{\mathsf{b}} = \widehat{\mathsf{t}} \times \widehat{\mathsf{n}} = \sin\alpha \, (-\sin\theta \, \widehat{\mathsf{x}} + \cos\theta \, \widehat{\mathsf{y}}) + \cos\alpha \, \widehat{\mathsf{z}}, \tag{A.15}$$

so that its derivative yields

$$\frac{d\widehat{\mathsf{b}}}{ds} = \frac{\sin\alpha}{c} \, (\cos\theta \, \widehat{\mathsf{x}} + \sin\theta \, \widehat{\mathsf{y}}) \equiv -\tau \, \widehat{\mathsf{n}}, \tag{A.16}$$

where the torsion is $\tau = c^{-1} \sin\alpha$. We can now easily verify that

$$\frac{d\widehat{\mathsf{n}}}{ds} = \frac{1}{c} (\sin\theta \, \widehat{\mathsf{x}} - \cos\theta \, \widehat{\mathsf{y}}) \equiv -\kappa \, \widehat{\mathsf{t}} + \tau \, \widehat{\mathsf{b}}.$$

We point out that for a two-dimensional curve $\mathbf{r} = x(s)\,\hat{\mathsf{x}} + y(s)\,\hat{\mathsf{y}}$, we find

$$\hat{\mathsf{t}} \;=\; \frac{d\mathbf{r}}{ds} \;=\; x'\,\hat{\mathsf{x}} + y'\,\hat{\mathsf{y}} \;\equiv\; \cos\phi\,\hat{\mathsf{x}} \;+\; \sin\phi\,\hat{\mathsf{y}},$$

where $\phi(s)$ denotes the tangential angle. With this definition, we readily show that the curvature is defined as

$$\kappa \;\equiv\; \left|\frac{d\hat{\mathsf{t}}}{ds}\right| \;=\; \frac{d\phi}{ds}.$$

Exercise: Calculate the Darboux vector $\boldsymbol{\omega} = \tau\,\hat{\mathsf{t}} + \kappa\,\hat{\mathsf{b}}$ for the helical path (A.11).

A.2 Linear Algebra

A fundamental object in linear algebra is the $m \times n$ matrix A with components (labeled A_{ij}) distributed on m rows ($i = 1, 2, ..., m$) and n columns ($j = 1, 2, ..., n$); for simplicity of notation, we write $\mathsf{A}_{(m\times n)}$ when we want to specify the *order* of the matrix A and we say that a matrix is *square* if $m = n$.

A.2.1 Matrix Algebra

We begin with a discussion of general properties of matrices and later focus our attention on square matrices (in particular 2×2 matrices). First, we can add (or subtract) two matrices only if they are of the same order; hence, the matrix $\mathsf{C} = \mathsf{A} \pm \mathsf{B}$ has components $C_{ij} = A_{ij} \pm B_{ij}$. Next, we can multiply a matrix A by a scalar a and obtain the new matrix $\mathsf{B} = a\,\mathsf{A}$ with components $B_{ij} = a\,A_{ij}$. Lastly, we introduce the *transpose* operation (denoted $^\top$): $\mathsf{A} \to \mathsf{A}^\top$ such that $(\mathsf{A}^\top)_{ij} \equiv A_{ji}$, i.e., the transpose of a $m \times n$ matrix is a $n \times m$ matrix. Note that the vector

$$\mathbf{v} \;=\; \begin{pmatrix} v_1 \\ \vdots \\ v_n \end{pmatrix}$$

is a $n \times 1$ matrix while its transpose $\mathbf{v}^\top = (v_1, ..., v_n)$ is a matrix of order $1 \times n$. With this definition, we now introduce the operation of matrix multiplication

$$\mathsf{C}_{(m\times k)} \;=\; \mathsf{A}_{(m\times n)} \;\cdot\; \mathsf{B}_{(n\times k)},$$

where $\mathsf{C}_{(m\times k)}$ is a new matrix of order $m \times k$ with components

$$C_{ij} \;=\; \sum_{\ell=1}^{n} A_{i\ell}\,B_{\ell j}.$$

Note that the matrix multiplication

$$\mathbf{u}^\top \cdot \mathbf{v} = \sum_{i=1}^{n} u_i \, v_i = \mathbf{u} \cdot \mathbf{v}$$

coincides with the standard dot product of two vectors.

The remainder of this Section will now exclusively deal with square matrices. First, we introduce two important operations on square matrices: the determinant $\det(\mathsf{A})$ and the trace $\mathrm{Tr}(\mathsf{A})$ defined, respectively, as

$$\det(\mathsf{A}) \equiv \sum_{i=1}^{n} (-1)^{i+j} \, A_{ij} \, \mathrm{ad}_{ij} \equiv \sum_{j=1}^{n} (-1)^{i+j} \, A_{ij} \, \mathrm{ad}_{ij}, \tag{A.17}$$

$$\mathrm{Tr}(\mathsf{A}) \equiv \sum_{i=1}^{n} A_{ii}, \tag{A.18}$$

where ad_{ij} denotes the determinant of the *reduced* matric obtained by removing the i^{th}-row and j^{th}-column from A. Next, we say that the matrix A is invertible if its determinant $\Delta \equiv \det(\mathsf{A})$ does not vanish and we define the inverse A^{-1} with components

$$(\mathsf{A}^{-1})_{ij} \equiv \frac{(-1)^{i+j}}{\Delta} \, \mathrm{ad}_{ji},$$

which, thus, satisfies the identity relation

$$\mathsf{A} \cdot \mathsf{A}^{-1} = \mathbf{I} = \mathsf{A}^{-1} \cdot \mathsf{A},$$

where I denotes the $n \times n$ identity matrix. Note, here, that the matrix multiplication

$$\mathsf{A} \cdot \mathsf{B} \neq \mathsf{B} \cdot \mathsf{A}$$

of two matrices A and B is generally not commutative.

Lastly, fundamental properties of a square $n \times n$ matrix A are discussed in terms of its eigenvalues $(\lambda_1, ..., \lambda_n)$ and eigenvectors $(\mathbf{e}_1, ..., \mathbf{e}_n)$ which satisfy the eigenvalue equation

$$\mathsf{A} \cdot \mathbf{e}_i = \lambda_i \, \mathbf{e}_i, \tag{A.19}$$

for $i = 1, ..., n$. Here, the determinant and the trace of the $n \times n$ matrix A are expressed in terms of its eigenvalues $(\lambda_1, ..., \lambda_n)$ as

$$\det(\mathsf{A}) = \lambda_1 \times ... \times \lambda_n \quad \text{and} \quad \mathrm{Tr}(\mathsf{A}) = \lambda_1 + ... + \lambda_n.$$

In order to continue our discussion of this important problem, we now focus our attention on 2×2 matrices.

A.2.2 Eigenvalue analysis of a 2×2 matrix

Consider the 2×2 matrix

$$\mathsf{M} \;=\; \begin{pmatrix} a & b \\ c & d \end{pmatrix}, \tag{A.20}$$

where (a, b, c, d) are arbitrary real (or complex) numbers and introduce the following two matrix *invariants*:

$$\Delta \;\equiv\; \det(\mathsf{M}) \;=\; a\,d - b\,c \quad \text{and} \quad \sigma \;\equiv\; \mathrm{Tr}(\mathsf{M}) \;=\; a + d, \tag{A.21}$$

which denote the determinant and the trace of matrix M, respectively.

Eigenvalues of M

The *eigenvalues* λ and *eigenvectors* $\mathbf{e}$ of matrix M are defined by the eigenvalue equation

$$\mathsf{M} \cdot \mathbf{e} \;=\; \lambda\,\mathbf{e}. \tag{A.22}$$

This equation has nontrivial solutions only if the determinant of the matrix $\mathsf{M} - \lambda\,\mathbf{I}$ vanishes (where $\mathbf{I}$ denotes the 2×2 identity matrix), which yields the characteristic quadratic polynomial:

$$\det(\mathsf{M} - \lambda\,\mathbf{I}) \;=\; (a - \lambda)\,(d - \lambda) \;-\; b\,c \;\equiv\; \lambda^2 \;-\; \sigma\,\lambda \;+\; \Delta, \tag{A.23}$$

and the eigenvalues $\lambda_\pm$ are obtained as the roots of this characteristic polynomial:

$$\lambda_\pm \;=\; \frac{\sigma}{2} \;\pm\; \sqrt{\frac{\sigma^2}{4} \;-\; \Delta}. \tag{A.24}$$

Here, we note that the matrix invariants (σ, Δ) are related to the eigenvalues $\lambda_\pm$:

$$\lambda_+ \;+\; \lambda_- \;\equiv\; \sigma \quad \text{and} \quad \lambda_+ \;\cdot\; \lambda_- \;\equiv\; \Delta. \tag{A.25}$$

Lastly, the eigenvalues are said to be *degenerate* if $\lambda_+ = \lambda_- \equiv \sigma/2$, i.e.,

$$\Delta \;=\; \frac{\sigma^2}{4} \quad \text{or} \quad b\,c \;=\; -\left(\frac{a-d}{2}\right)^2.$$

Eigenvectors of M

Next, the eigenvectors $\mathbf{e}_\pm$ associated with the eigenvalues $\lambda_\pm$ are constructed from the eigenvalue equations $\mathsf{M} \cdot \mathbf{e}_\pm = \lambda_\pm\,\mathbf{e}_\pm$, which yield the general solutions

$$\mathbf{e}_\pm \;\equiv\; \begin{pmatrix} 1 \\ \mu_\pm \end{pmatrix} \epsilon_\pm, \tag{A.26}$$

where $\epsilon_\pm$ denotes an arbitrary constant and

$$\mu_\pm \;=\; \frac{\lambda_\pm - a}{b} \;=\; \frac{c}{\lambda_\pm - d}. \tag{A.27}$$

The normalization of the eigenvectors $\mathbf{e}_\pm$ ($|\mathbf{e}_\pm| = 1$), for example, can be achieved by choosing

$$\epsilon_\pm \;=\; \frac{1}{\sqrt{1 + (\mu_\pm)^2}}.$$

We note that the eigenvectors $\mathbf{e}_\pm$ are not automatically orthogonal to each other (i.e., the dot product $\mathbf{e}_+ \cdot \mathbf{e}_-$ may not vanish). Indeed, we find

$$\mathbf{e}_+ \cdot \mathbf{e}_- \;=\; \epsilon_+ \, \epsilon_- \, (1 + \mu_+ \, \mu_-), \tag{A.28}$$

where

$$1 \;+\; \mu_+ \, \mu_- \;=\; 1 \;+\; \frac{1}{b^2} \, (\lambda_+ - a) \, (\lambda_- - a) \;=\; 1 \;+\; \left(\frac{a-d}{2\,b} \right)^2 \;-\; \frac{1}{b^2} \left(\frac{\sigma^2}{4} \;-\; \Delta \right),$$

whose sign is indefinite. By using the Gram-Schmidt orthogonalization procedure, however, we may construct two orthogonal vectors $(\mathbf{e}_1, \mathbf{e}_2)$:

$$\left. \begin{array}{rcl} \mathbf{e}_1 & = & \alpha \, \mathbf{e}_+ \;+\; \beta \, \mathbf{e}_- \\ \mathbf{e}_2 & = & \gamma \, \mathbf{e}_+ \;+\; \delta \, \mathbf{e}_- \end{array} \right\}, \tag{A.29}$$

where the coefficients $(\alpha, \beta, \gamma, \delta)$ are chosen to satisfy the orthogonalization condition $\mathbf{e}_1 \cdot \mathbf{e}_2 \equiv 0$; it is important to note that the vectors $(\mathbf{e}_1, \mathbf{e}_2)$ are not themselves eigenvectors of the matrix M. For example, we may choose $\alpha = 1 = \delta$, $\beta = 0$, and

$$\gamma \;=\; -\left(\frac{\mathbf{e}_+ \cdot \mathbf{e}_-}{|\mathbf{e}_+|^2} \right),$$

which corresponds to choosing $\mathbf{e}_1 = \mathbf{e}_+$ and constructing $\mathbf{e}_2$ as the component of $\mathbf{e}_-$ that is orthogonal to $\mathbf{e}_+$.

Lastly, we point out that any two-dimensional vector $\mathbf{u}$ may be decomposed in terms of the eigenvectors $\mathbf{e}_\pm$:

$$\mathbf{u} \;=\; \sum_{i=\pm} \, u_i \, \mathbf{e}_i \;\equiv\; \sum_{i=\pm} \left(\frac{\mathbf{u} \cdot \mathbf{e}_i}{|\mathbf{e}_i|^2} \right) \mathbf{e}_i, \tag{A.30}$$

where we assumed, here, that the eigenvectors are orthogonal to each other. Furthermore, the *transformation* $\mathsf{M} \cdot \mathbf{u}$ generates a new vector

$$\mathbf{v} \;=\; \mathsf{M} \cdot \mathbf{u} \;=\; \sum_{i=\pm} \, u_i \, \mathsf{M} \cdot \mathbf{e}_i \;\equiv\; \sum_{i=\pm} \, v_i \, \mathbf{e}_i,$$

where the components of $\mathbf{v}$ are $v_i \equiv u_i \, \lambda_i$.

Inverse of matrix M

The matrix (A.20) has an inverse, denoted M^{-1}, if its determinant Δ does not vanish. In this nonsingular case, we easily find

$$\mathsf{M}^{-1} \;=\; \frac{1}{\Delta}\begin{pmatrix} d & -b \\ -c & a \end{pmatrix}, \tag{A.31}$$

so that $\mathsf{M}^{-1}\cdot\mathsf{M} = \mathbf{I} = \mathsf{M}\cdot\mathsf{M}^{-1}$. The determinant of M^{-1}, denoted Δ', is

$$\Delta' \;=\; \frac{d\,a - b\,c}{\Delta^2} \;\equiv\; \frac{1}{\Delta} \;=\; \frac{1}{\lambda_+\,\cdot\,\lambda_-},$$

while its trace, denoted σ', is

$$\sigma' \;=\; \frac{d+a}{\Delta} \;\equiv\; \frac{\sigma}{\Delta} \;=\; \frac{1}{\lambda_+} \;+\; \frac{1}{\lambda_-}.$$

Hence, the eigenvalues of the inverse matrix (A.31) are

$$\lambda'_\pm \;\equiv\; \frac{1}{\lambda_\pm} \;=\; \frac{\lambda_\mp}{\Delta},$$

and its eigenvectors $\overline{\mathbf{e}}_\pm$ are identical to $\mathbf{e}_\pm$ since

$$\mathsf{M}\cdot\mathbf{e}_\pm \;=\; \lambda_\pm\,\mathbf{e}_\pm \quad\rightarrow\quad \mathbf{e}_\pm \;=\; \lambda_\pm\,\mathsf{M}^{-1}\cdot\mathbf{e}_\pm \quad\rightarrow\quad \mathsf{M}^{-1}\cdot\mathbf{e}_\pm \;=\; \lambda_\pm^{-1}\,\mathbf{e}_\pm \;\equiv\; \lambda'_\pm\,\mathbf{e}_\pm.$$

We note that once the inverse M^{-1} of a matrix M is known, then any inhomogeneous linear system of equations of the form $\mathsf{M}\cdot\mathbf{u} = \mathbf{v}$ may be solved as $\mathbf{u} \equiv \mathsf{M}^{-1}\cdot\mathbf{v}$.

Special case I: Real Hermitian Matrix

A real matrix is said to be *Hermitian* if its transpose, denoted $\mathsf{M}^\top$ (i.e., $M^\top_{ij} = M_{ji}$), satisfies the identity $\mathsf{M}^\top = \mathsf{M}$, which requires that $c = b$ in Eq. (A.20). In this case, the eigenvalues are automatically real

$$\lambda_\pm \;=\; \left(\frac{a+d}{2}\right) \;\pm\; \sqrt{\left(\frac{a-d}{2}\right)^2 \;+\; b^2},$$

and the associated eigenvectors (A.26), which are defined with

$$\mu_\pm \;=\; -\;\left(\frac{a-d}{2b}\right) \;\pm\; \sqrt{1 \;+\; \left(\frac{a-d}{2}\right)^2},$$

are automatically orthogonal to each other ($\mathbf{e}_+\cdot\mathbf{e}_- = 0$) since $\mu_+\,\mu_- \equiv -1$.

Special case II: Rotation Matrix

Another special matrix is given by the rotation matrix

$$\mathsf{R} \;=\; \begin{pmatrix} \cos\theta & \sin\theta \\ -\sin\theta & \cos\theta \end{pmatrix}, \tag{A.32}$$

with determinant $\det(\mathsf{R}) = 1$ and trace $\mathrm{Tr}(\mathsf{R}) = 2\cos\theta = e^{i\theta} + e^{-i\theta}$. The rotation matrix (A.32) is said to be *unitary* since its transverse $\mathsf{R}^{\top}$ is equal to its inverse $\mathsf{R}^{-1} = \mathsf{R}^{\top}$ (which is possible only if its determinant is one).

The eigenvalues of the rotation matrix (A.32) are $e^{\pm i\theta}$ and the eigenvectors are

$$\mathsf{e}_{\pm} \;=\; \begin{pmatrix} 1 \\ \pm\, i \end{pmatrix}.$$

Note that the rotation matrix (A.32) can be written as $\mathsf{R} = \exp(i\theta\,\boldsymbol{\sigma})$, where the matrix

$$\boldsymbol{\sigma} \;=\; \begin{pmatrix} 0 & -i \\ i & 0 \end{pmatrix}$$

(also known as the Pauli *spin* matrix $\boldsymbol{\sigma}_2$) satisfies the properties $\boldsymbol{\sigma}^{2n} = \mathbf{I}$ and $\boldsymbol{\sigma}^{2n+1} = \boldsymbol{\sigma}$ and, thus, we find

$$\exp(i\theta\,\boldsymbol{\sigma}) \;=\; \sum_{n=0}^{\infty} \frac{(i\theta)^n}{n!}\,\boldsymbol{\sigma}^n \;=\; \cos\theta\,\mathbf{I} \;+\; i\,\sin\theta\,\boldsymbol{\sigma} \;=\; \mathsf{R}.$$

Note that the time derivative of the rotation matrix (A.32) satisfies the property

$$\mathsf{R}^{-1}\cdot\dot{\mathsf{R}} \;=\; i\,\dot{\theta}\,\boldsymbol{\sigma} \;=\; \begin{pmatrix} 0 & \dot{\theta} \\ -\dot{\theta} & 0 \end{pmatrix}.$$

Lastly, we note that the rotation matrix (A.32) can be used to *diagonalize* a real Hermitian matrix

$$\mathsf{M} \;=\; \begin{pmatrix} a & b \\ b & d \end{pmatrix},$$

by constructing the new matrix

$$\overline{\mathsf{M}} \;=\; \mathsf{R}^{\top}\cdot\mathsf{M}\cdot\mathsf{R} \;=\; \begin{pmatrix} a + (d-a)\,\sin^2\theta - b\,\sin 2\theta & b\,\cos 2\theta - \frac{1}{2}(d-a)\,\sin 2\theta \\ \\ b\,\cos 2\theta - \frac{1}{2}(d-a)\,\sin 2\theta & d - (d-a)\,\sin^2\theta + b\,\sin 2\theta \end{pmatrix}. \tag{A.33}$$

Next, by setting (assuming that $d > a$)

$$\tan 2\theta \;=\; \frac{2b}{d-a} \quad\rightarrow\quad \begin{cases} \cos 2\theta \;=\; (d-a)/\sqrt{\sigma^2 - 4\,\Delta} \\ \\ \sin 2\theta \;=\; 2b/\sqrt{\sigma^2 - 4\,\Delta} \end{cases},$$

where $\sigma = a + d$ and $\Delta = ad - b^2$ denote the trace and determinant of M, respectively, $\overline{\mathsf{M}}$ becomes a diagonal matrix

$$\overline{\mathsf{M}} \;=\; \begin{pmatrix} \lambda_- & 0 \\ 0 & \lambda_+ \end{pmatrix}, \tag{A.34}$$

where the diagonal components are

$$\lambda_\pm \;=\; \frac{\sigma}{2} \;\pm\; \frac{1}{2}\,\sqrt{\sigma^2 - 4\,\Delta}.$$

Note that the trace and determinant of $\overline{\mathsf{M}}$ are the same as that of M, i.e., the trace and determinant of any real Hermitian matrix are invariant under the *congruence* transformation (A.33).

A.3 Important Integrals

The present Section summarizes the integral representation of trigonometric functions, which is used extensively in the integration by quadrature of several dynamical problems, e.g., light-ray propagation in a nonuniform medium, time-independent Hamiltonian systems, and scattering problems. In addition, the basic theory of elliptic functions is introduced, so that the complete solution of some important dynamical problems (e.g., the force-free evolution of an asymmetric top) can be presented.

A.3.1 Trigonometric Functions and Integrals

Trigonometric functions with period τ

Functions that are periodic, with period τ, are all related to trigonometric functions (with period 2π). Indeed, a periodic function $f(t)$ can be represented in terms of a (Fourier) series involving $\cos(2\pi n\, t/\tau)$ and $\sin(2\pi n\, t/\tau)$, where $n = 1, 2, ...$ represents the Fourier harmonic number.

Hence, the study of singly-periodic functions can focus its attention on the trigonometric functions $\sin z$ and $\cos z$, defined in terms of the inverse formulas

$$\begin{aligned} z \;&=\; \int_0^y \frac{dx}{\sqrt{1-x^2}} \;=\; \sin^{-1} y \\ &=\; \int_y^1 \frac{dx}{\sqrt{1-x^2}} \;=\; \cos^{-1} y \end{aligned}$$

Here, the period τ of the trigonometric functions $\sin z$ and $\cos z$ is defined as

$$\frac{1}{4}\,\tau \;\equiv\; \int_0^1 \frac{dx}{\sqrt{1-x^2}} \;=\; \frac{\pi}{2}$$

with the periodicity conditions: $\sin(z + n\,\tau) = \sin z$ and $\cos(z + n\,\tau) = \cos z$.

Trigonometric integrals

Trigonometric functions are often involved in the evaluation of integrals of the form

$$\int_{x_0}^{x} \frac{dy}{\sqrt{a\,y^2+b\,y+c}}, \tag{A.35}$$

where x_0 denotes one of the roots of the quadratic equation $a\,x^2+b\,x+c=0$ and we assume that $a\,x^2+b\,x+c\geq 0$ over the interval between x_0 and x, for a given set of parameters (a,b,c). The solution for integrals of this type depend on the sign of a: $a>0$ (case I) or $a<0$ (case II).

For case I ($a>0$), we choose the parameters $a=1$ and $b=-2$ in Eq. (A.35), so that we need to solve the following integral:

$$\tau(x;x_0) \;=\; \int_{x_0}^{x} \frac{dy}{\sqrt{y^2-2\,y+c}}. \tag{A.36}$$

First, the roots $(1\,\pm\,\sqrt{1-c}\equiv 1\pm\mathsf{e})$ of the quadratic polynomial $x^2-2\,x+c=0$ are both real (if $c<1$) or complex-valued (if $c>1$); for $c<1$, the radicand is positive for $x<1-\mathsf{e}$ and $x>1+\mathsf{e}$. Next, by completing the square $y^2-2\,y+c=(y-1)^2-\mathsf{e}^2$ and using the trigonometric substitution $y=1+\mathsf{e}\,\sec\theta$ in Eq. (A.36), with $\Theta(x)=\sec^{-1}[(x-1)/\mathsf{e}]$ and $\Theta(1+\mathsf{e})=\sec^{-1}(1)=0$, we solve the integral (A.36) as

$$\tau(x;c) \;=\; \int_{1+\mathsf{e}}^{x} \frac{dy}{\sqrt{y^2-2\,y+c}} \;=\; \int_{0}^{\Theta(x)} \sec\theta\;d\theta \;=\; \ln\left[\;\frac{x-1}{\mathsf{e}}\;+\;\frac{1}{\mathsf{e}}\,\sqrt{x^2-2\,x+c}\;\right].$$

By inverting this function, we finally obtain the solution

$$x(\tau;\mathsf{e}) \;=\; 1\;+\;\mathsf{e}\,\cosh\tau \;\equiv\; 1\;+\;\frac{\mathsf{e}}{2}\left(e^{\tau}+e^{-\tau}\right),$$

where the *hyperbolic* cosine function $\cosh\tau\equiv\cos(i\tau)$ is defined in terms of the cosine of an imaginary argument. Hence, this solution is periodic along the imaginary axis (with period $2\pi i$), i.e., $\cosh(\tau+2\pi\,i)=\cosh\tau$.

For case II ($a<0$), we choose the parameters $a=-1$ and $b=2$ in Eq. (A.35), so that we need to solve the following integral:

$$\tau(x;x_0) \;=\; \int_{x_0}^{x} \frac{dy}{\sqrt{c+2\,y-y^2}}. \tag{A.37}$$

First, the roots $(1\;\pm\;\sqrt{1+c}\equiv 1\pm\mathsf{e})$ of the quadratic polynomial $x^2-2\,x-c=0$ are both real (if $c>-1$) or complex-valued (if $c<-1$); for $c>-1$, the radicand is positive for $1-\mathsf{e}<x<1+\mathsf{e}$. Next, by completing the square $c+2\,y-y^2=\mathsf{e}^2-(y-1)^2$ and using the trigonometric substitution $y=1+\mathsf{e}\,\cos\theta$ in Eq. (A.37), with $\Theta(x)=\cos^{-1}[(x-1)/\mathsf{e}]$ and $\Theta(1+\mathsf{e})=\cos^{-1}(1)=0$, we solve the integral (A.37) as

$$\tau(x;c) \;=\; \int_{x}^{1+\mathsf{e}} \frac{dx}{\sqrt{c+2\,y-y^2}} \;=\; \int_{0}^{\Theta(x)} d\theta \;=\; \cos^{-1}\left(\frac{x-1}{\mathsf{e}}\right).$$

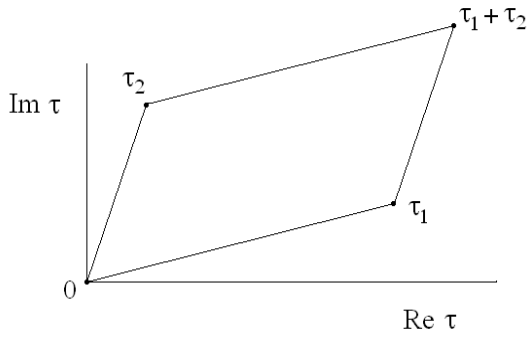

Figure A.1: Unit cell for a doubly-periodic elliptic function with periods τ_1 and τ_2.

By inverting this function, we easily obtain the solution

$$x(\tau; \mathsf{e}) \;=\; 1 \;+\; \mathsf{e}\,\cos\tau,$$

which is periodic along the real axis with period 2π.

A.3.2 Elliptic Functions and Integrals*

A function $f(z)$ is doubly periodic, with periods τ_1 and τ_2 (where the ratio τ_2/τ_1 is complex-valued), if

$$f(z + m\,\tau_1 + n\,\tau_2) \;=\; f(z),$$

for $m, n = 0, \pm 1, \pm 2, ...$ (but not $m = 0 = n$). Figure A.1 shows the *unit cell* with corners at $z = 0, \tau_1, \tau_2$, and $\tau_1 + \tau_2$ in the complex plane. Here, we note that, in the limit $|\tau_2| \to \infty$, the function $f(z)$ becomes singly-periodic with period τ_1.

Elliptic functions (of second order) are doubly-periodic functions with 2 simple zeroes per unit cell and either a second-order pole (Weierstrass elliptic function) or two first-order poles (Jacobi elliptic function). Note that there are no elliptic functions of first order and that there are no multiply-periodic functions with more than two periods. Elliptic functions are defined in terms of integrals of the form

$$\int_{x_0}^{x} \frac{dy}{\sqrt{a_4\,y^4 + a_3\,y^3 + a_2\,y^2 + a_1\,y + a_0}},$$

where x_0 is a real root of the quartic polynomial $a_4\,x^4 + a_3\,x^3 + a_2\,x^2 + a_1\,x + a_0 = 0$ (with $a_0 \neq 0$); Jacobi elliptic functions are defined in terms of quartic polynomials with $a_4 \neq 0$ while Weierstrass elliptic functions are defined in terms of cubic polynomials with $a_4 = 0$.

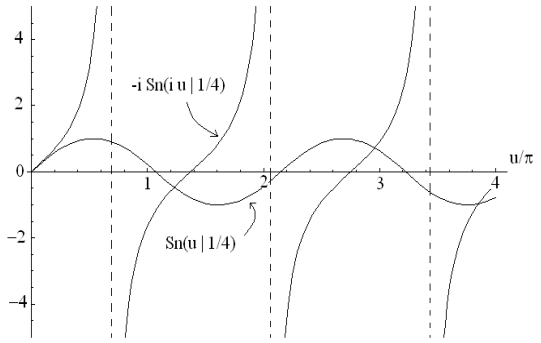

Figure A.2: Plots of $\mathrm{sn}(u|k)$ and $-i\,\mathrm{sn}(iu|k)$ for $k = \frac{1}{4}$.

Jacobi Elliptic Functions

The Jacobi elliptic function $\mathrm{sn}(u\,|\,k)$ is defined in terms of the inverse-function formula

$$u \;=\; \int_0^{\varphi} \frac{d\theta}{\sqrt{1 \;-\; k^2\,\sin^2\theta}} \;=\; \int_0^{\sin\varphi} \frac{dt}{\sqrt{(1-t^2)\,(1-k^2\,t^2)}} \;\equiv\; \mathrm{sn}^{-1}(\sin\varphi\,|\,k), \qquad \text{(A.38)}$$

where $0 \le k \le 1$ and the amplitude φ varies from 0 to 2π so that

$$\mathrm{sn}\,u \;\equiv\; \mathrm{sn}(u|k) \;=\; \sin\varphi.$$

From this definition, we easily check that $\mathrm{sn}^{-1}(\sin\varphi\,|\,0) = \sin^{-1}(\sin\varphi) = \varphi$.[1]

The function $\mathrm{sn}\,u$ has a purely-real period $4\,K$, defined as

$$K \;\equiv\; K(k) \;=\; \int_0^{\pi/2} \frac{d\theta}{\sqrt{1 \;-\; k^2\,\sin^2\theta}}$$

and a purely-imaginary period $4\,iK'$, defined as (with $k'^2 \equiv 1 - k^2$)

$$i\,K' \;\equiv\; i\,K(k') \;=\; i\,\int_0^{\pi/2} \frac{d\theta}{\sqrt{1 \;-\; k'^2\,\sin^2\theta}}.$$

Figure A.2 shows plots of $\mathrm{sn}\,u$ and $-i\,\mathrm{sn}(iu)$ for $k = \frac{1}{4}$, which exhibit both a real period and an imaginary period. Note that, while the Jacobi elliptic function $\mathrm{sn}\,u$ alternates between -1 and $+1$ for real values of u, it also exhibits singularities for imaginary values of u at $(2n+1)\,iK'$ $(n = 0, 1, ...)$. Furthermore, as $k \to 0$ (and $k' \to 1$), we find $K \to \pi/2$ and $|K'| \to \infty$, and $\mathrm{sn}\,u$ becomes singly-periodic. By comparing Figure A.2 with Figure A.3, which shows plots of $\sin x$ and $-i\,\sin(ix) = \sinh x$, we see that as $k \to 0$, the real period $K \to \pi/2$ and the imaginary period $|K'| \to \infty$.

[1] An alternate definition for the Jacobi elliptic function (A.38) replaces k^2 with m: $\mathrm{sn}(u|k) = \mathrm{sn}(u, m)$.

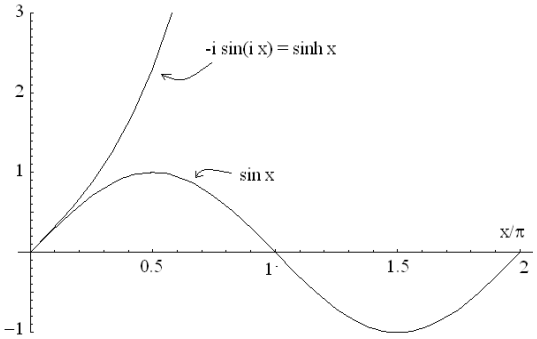

Figure A.3: Plots of $\sin x$ and $-i\,\sin(ix) = \sinh x$ exhibiting a real period 2π and an *infinite* imaginary period.

Additional Jacobi elliptic functions $\mathrm{cn}(u\,|\,k)$ and $\mathrm{dn}(u\,|\,k)$ are defined as

$$u = \int_{\mathrm{cn}(u|k)}^{1} \frac{dt}{\sqrt{(1-t^2)\,(k'^2+k^2\,t^2)}}, \tag{A.39}$$

$$= \int_{\mathrm{dn}(u|k)}^{1} \frac{dt}{\sqrt{(1-t^2)\,(t^2-k'^2)}}, \tag{A.40}$$

with the properties

$$\mathrm{cn}\,u \;\equiv\; \mathrm{cn}(u|k) \;=\; \cos\varphi, \quad \mathrm{dn}\,u \;\equiv\; \mathrm{dn}(u|k) \;=\; \sqrt{1-k^2\,\sin^2\varphi},$$

and $\mathrm{sn}^2u + \mathrm{cn}^2u = 1 = \mathrm{dn}^2u + k^2\,\mathrm{sn}^2u$. The Jacobi elliptic functions $\mathrm{cn}\,u$ and $\mathrm{dn}\,u$ are also doubly-periodic with periods $4\,K$ and $4i\,K'$. The following properties are useful. First, we find the limiting definitions

$$\begin{pmatrix} \mathrm{sn}(u|0) \\ \mathrm{cn}(u|0) \\ \mathrm{dn}(u|0) \end{pmatrix} = \begin{pmatrix} \sin u \\ \cos u \\ 1 \end{pmatrix} \quad \text{and} \quad \begin{pmatrix} \mathrm{sn}(u|1) \\ \mathrm{cn}(u|1) \\ \mathrm{dn}(u|1) \end{pmatrix} = \begin{pmatrix} \tanh u \\ \mathrm{sech}\,u \\ \mathrm{sech}\,u \end{pmatrix}. \tag{A.41}$$

Next, the derivatives with respect to u are

$$\left.\begin{array}{rcl} \mathrm{sn}'(u|k) &=& \mathrm{cn}(u|k)\,\mathrm{dn}(u|k) \\ \mathrm{cn}'(u|k) &=& -\,\mathrm{sn}(u|k)\,\mathrm{dn}(u|k) \\ \mathrm{dn}'(u|k) &=& -\,k^2\,\mathrm{cn}(u|k)\,\mathrm{sn}(u|k) \end{array}\right\}. \tag{A.42}$$

Lastly, if $k > 1$, we use the identities

$$\left.\begin{array}{rcl} \mathrm{sn}(u|k) &=& k^{-1}\,\mathrm{sn}(k\,u|k^{-1}) \\ \mathrm{cn}(u|k) &=& \mathrm{dn}(k\,u|k^{-1}) \\ \mathrm{dn}(u|k) &=& \mathrm{cn}(k\,u|k^{-1}) \end{array}\right\}. \tag{A.43}$$

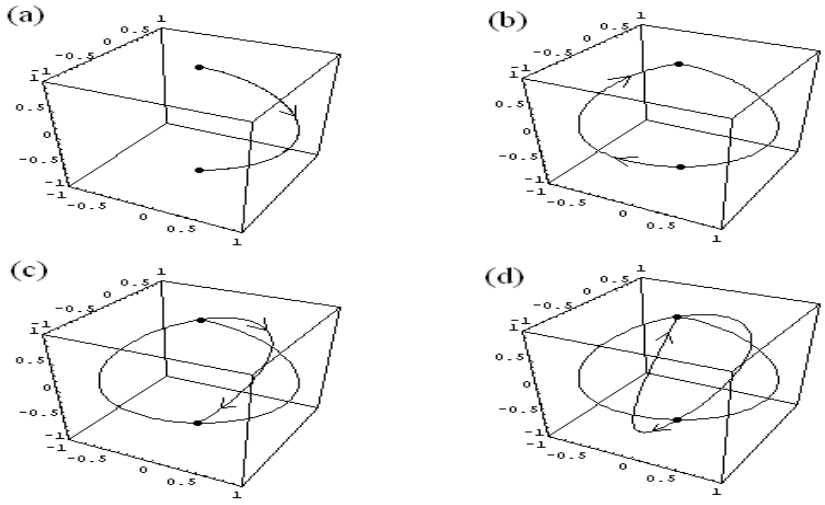

Figure A.4: Seiffert Spherical Spiral: Plot of the unit vector $\widehat{\mathsf{r}}(s) = \mathrm{sn}(s)\,\cos(ks)\,\widehat{\mathsf{x}} + \mathrm{sn}(s)\,\sin(ks)\,\widehat{\mathsf{y}} + \mathrm{cn}(s)\,\widehat{\mathsf{z}}$ for $k = 0.15$ from $s = 0$ to (a) $s = 2K$, (b) $s = 4K$, (c) $s = 6K$, and (d) $s = 8K$.

A simple example that clearly shows the periodicity properties of the Jacobi elliptic functions $\mathrm{sn}\,u$ and $\mathrm{cn}\,u$ is given by the *Seiffert spherical spiral*, defined as a curve on the unit sphere and constructed as follows. First, we use the cylindrical metric $ds^2 = d\rho^2 + \rho^2\,d\theta^2 + dz^2$, with $z = \sqrt{1-\rho^2}$ and the polar angle $\theta(s) \equiv k\,s$ parametrized by the arc length s with $0 < k < 1$ (assuming that the initial point of the curve is $\rho = 0$, $\theta = 0$, and $z = 1$). Hence, we readily find

$$ds^2 \;=\; \frac{d\rho^2}{(1-\rho^2)\,(1-k^2\,\rho^2)} \;\;\rightarrow\;\; s \;=\; \int_0^\rho \frac{dt}{\sqrt{(1-t^2)\,(1-k^2t^2)}} \;\equiv\; \mathrm{sn}^{-1}(\rho|k),$$

and, thus, we obtain the Jacobi elliptic solutions

$$\rho(s) \;=\; \mathrm{sn}(s|k) \quad\text{and}\quad z(s) \;=\; \sqrt{1-\rho^2(s)} \;=\; \mathrm{cn}(s|k).$$

The Seiffert spherical spiral is generated by plotting the path of the unit vector $\widehat{\mathsf{r}}(s) = \mathrm{sn}(s)\,\cos(ks)\,\widehat{\mathsf{x}} + \mathrm{sn}(s)\,\sin(ks)\,\widehat{\mathsf{y}} + \mathrm{cn}(s)\,\widehat{\mathsf{z}}$ as a function of s (see Figure A.4). Note that at each value $4n\,K$ $(n = 1, 2, ...)$, the orbit returns to the initial point.

Our next example looks at orbits in the quartic potential $U(x) = 1 - x^2/2 + x^4/16$ shown in Figure A.5. Here, the turning points x_t for $E \equiv \mathsf{e}^2$ are

$$x_t \;=\; \begin{cases} \pm 2\,\sqrt{1+\mathsf{e}} & (\mathsf{e} > 1) \\ 0,\;\; \pm\sqrt{8} & (\mathsf{e} = 1) \\ \pm 2\,\sqrt{1-\mathsf{e}},\;\; \pm 2\,\sqrt{1+\mathsf{e}} & (\mathsf{e} < 1) \end{cases}$$

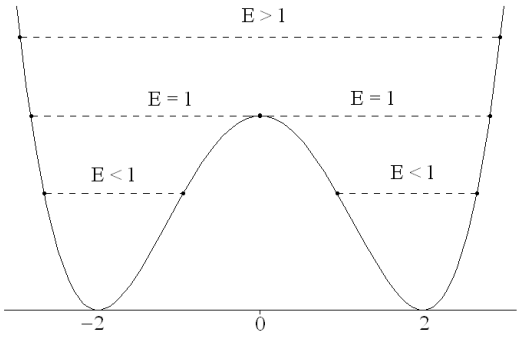

Figure A.5: Quartic potential $U(x) = 1 - x^2/2 + x^4/16$ showing orbits with $E > 1$, $E = 1$ (separatrix) and $E < 1$.

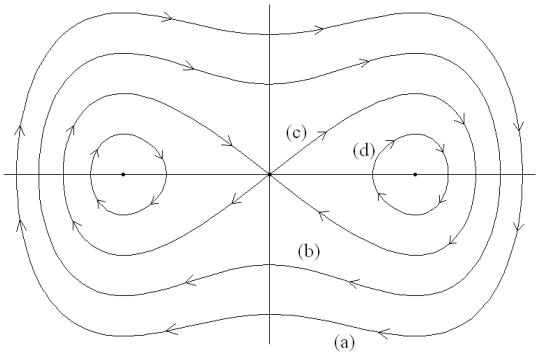

Figure A.6: Phase portait for orbits (A.45)-(A.47) of the quartic potential $U(x) = 1 - x^2/2 + x^4/16$ for (a) $\mathsf{e} = 2$, (b) $\mathsf{e} = 1.5$, (c) $\mathsf{e} = 1$ (separatrix), and (d) $\mathsf{e} = 0.5$.

Each orbit is solved in terms of the integral

$$\begin{aligned} t(x) &= -\int_{2\sqrt{1+\mathsf{e}}}^{x} \frac{ds}{\sqrt{2\,(\mathsf{e}^2-1)\;+\;s^2\,(1-s^2/8)}} \\ &= -\int_{2\sqrt{1+\mathsf{e}}}^{x} \frac{\sqrt{8}\,ds}{\sqrt{[4\,(\mathsf{e}+1)-s^2]\,[s^2+4\,(\mathsf{e}-1)]}} \\ &= \frac{1}{\sqrt{\mathsf{e}}}\int_0^{\Phi(x)} \frac{d\varphi}{\sqrt{1\;-\;k^2\;\sin^2\varphi}}, \end{aligned} \tag{A.44}$$

where $k^2 \equiv (1+\mathsf{e})/2\mathsf{e}$ while we used the trigonometric substitution $s = 2\sqrt{1+\mathsf{e}}\,\cos\varphi$ with $\Phi(x) \equiv \cos^{-1}[x/(2\sqrt{1+\mathsf{e}})]$. For $\mathsf{e} > 1$ ($k = \sqrt{(1+\mathsf{e})/2\mathsf{e}} < 1$), we use Eq. (A.38) to find

$$\sin\Phi(x) \;=\; \mathrm{sn}(\sqrt{\mathsf{e}}\,t|k),$$

which yields the phase-portrait coordinates $(x, \dot{x})$:

$$\left.\begin{aligned} x(t) &= 2\sqrt{1+\mathsf{e}}\;\;\mathrm{cn}(\sqrt{\mathsf{e}}\,t|k) \\ \dot{x}(t) &= -\,2\sqrt{\mathsf{e}\,(1+\mathsf{e})}\;\;\mathrm{sn}(\sqrt{\mathsf{e}}\,t|k)\,\mathrm{dn}(\sqrt{\mathsf{e}}\,t|k) \end{aligned}\right\}, \tag{A.45}$$

where the velocity $\dot{x}(t)$ is derived from Eq. (A.42). For $\mathsf{e} = 1$, these phase-portrait coordinates become

$$\left.\begin{aligned} x(t) &= \sqrt{8}\;\;\mathrm{sech}\,t \\ \dot{x}(t) &= -\sqrt{8}\;\;\mathrm{sech}\,t\;\tanh t \end{aligned}\right\}, \tag{A.46}$$

where the limits (A.41) were used. Lastly, for $\mathsf{e} < 1$ ($k > 1$), we use the relations (A.43) to obtain

$$\left.\begin{aligned} x(t) &= 2\sqrt{1+\mathsf{e}}\;\;\mathrm{dn}(t\,\sqrt{(1+\mathsf{e})/2}\,|k^{-1}) \\ \dot{x}(t) &= -\sqrt{8}\,\mathsf{e}\;\;\mathrm{sn}(t\,\sqrt{(1+\mathsf{e})/2}\,|k^{-1})\,\mathrm{cn}(t\,\sqrt{(1+\mathsf{e})/2}\,|k^{-1}) \end{aligned}\right\}. \tag{A.47}$$

The orbits (A.45)-(A.47) are combined to yield the phase portrait for the quartic potential shown in Figure A.6.

As a first physical example, we now consider the case of the pendulum with a normalized energy $\epsilon\,\omega^2$ expressed as

$$\epsilon\,\omega^2 \;=\; \frac{1}{2}\,\dot{\theta}^2 \;+\; \omega^2\,(1-\cos\theta) \;=\; 2\,\omega^2\;\left(\varphi'^2 \;+\; \sin^2\varphi\right),$$

where $\varphi \equiv \theta/2$ and $\varphi'(\tau) \equiv \omega^{-1}\dot{\varphi}$, with the normalized time $\tau \equiv \omega t$. Hence, we find that ϵ can either be (I) $0 < \epsilon < 2$ or (II) $\epsilon > 2$ and (assuming that $\varphi = 0$ at $\tau = 0$)

$$\tau \;=\; \int_0^{\varphi} \frac{d\phi}{\sqrt{(\epsilon/2) - \sin^2\phi}}.$$

In case (I), where $\epsilon \equiv 2\,\sin^2\alpha$, we set $\sin\phi = \sin\alpha\,\sin\chi$ and obtain (with $k \equiv \sin\alpha$)

$$\tau \;=\; \int_0^{\sin^{-1}(k^{-1}\sin\varphi)} \frac{d\chi}{\sqrt{1\;-\;k^2\,\sin^2\chi}} \;\equiv\; \mathrm{sn}^{-1}(k^{-1}\sin\varphi\,|\,k).$$

Hence, the solution for case (I) is expressed in terms of the Jacobi elliptic function

$$\varphi(\tau) \;=\; \sin^{-1}\left[\;k\;\mathrm{sn}(\tau\,|\,k)\;\right],$$

and in the limit $k \ll 1$, we find the simple harmonic solution $\varphi(\tau) = \alpha\,\sin\tau$, where α denotes the amplitude of simple harmonic motion. In case (II), we have $k^{-2} = 2/\epsilon < 1$ and obtain

$$\tau \;=\; k^{-1}\;\int_0^{\varphi} \frac{d\phi}{\sqrt{1-k^{-2}\,\sin^2\phi}} \;\equiv\; k^{-1}\,\mathrm{sn}^{-1}(\sin\varphi\,|\,k^{-1}).$$

Hence, the solution for case (II) is expressed in terms of the Jacobi elliptic function

$$\varphi(\tau) \;=\; \sin^{-1}\left[\mathrm{sn}(k\tau\,|\,k^{-1})\;\right].$$

Note that, in the limit $k \to 1$, both solutions coincide with the *separatrix* solution (3.30), which is expressed in terms of singly-periodic trigonometric functions.

As a second physical example, we consider the Euler's equations (7.25) for a force-free asymmetric top (with $I_1 > I_2 > I_3$), where conservation laws of kinetic energy (7.33) and angular momentum (7.34) lead to the following expressions

$$\omega_1(\tau) \;=\; -\sqrt{\frac{I_2\,(I_2-I_3)}{I_1\,(I_1-I_3)}}\;\Omega_3\;\sqrt{1-\nu^2(\tau)}, \tag{A.48}$$

$$\omega_2(\tau) \;=\; \Omega_3\;\nu(\tau), \tag{A.49}$$

$$\omega_3(\tau) \;=\; \sqrt{\frac{I_2\,(I_1-I_2)}{I_3\,(I_1-I_3)}}\;\Omega_1\;\sqrt{1-k^2\,\nu^2(\tau)}, \tag{A.50}$$

where Ω_1 and Ω_3 are defined in Eq. (7.38), with $k^2 = \Omega_3^2/\Omega_1^2 \le 1$, and $\tau = \alpha\,\Omega_1\,t$, with α defined in Eq. (7.37). When we substitute these expressions in the Euler equation (7.36) for ω_2, we easily obtain

$$\nu'(\tau) \;=\; \sqrt{(1-\nu^2)\,(1-k^2\,\nu^2)}, \tag{A.51}$$

which can now be integrated to yield

$$\tau \;=\; \int_0^{\nu} \frac{ds}{\sqrt{(1-s^2)\,(1-k^2\,s^2)}} \;\equiv\; \mathrm{sn}^{-1}(\nu\,|\,k), \tag{A.52}$$

or

$$\omega_2(\tau) \;=\; \Omega_3\;\mathrm{sn}(\tau\,|\,k), \tag{A.53}$$

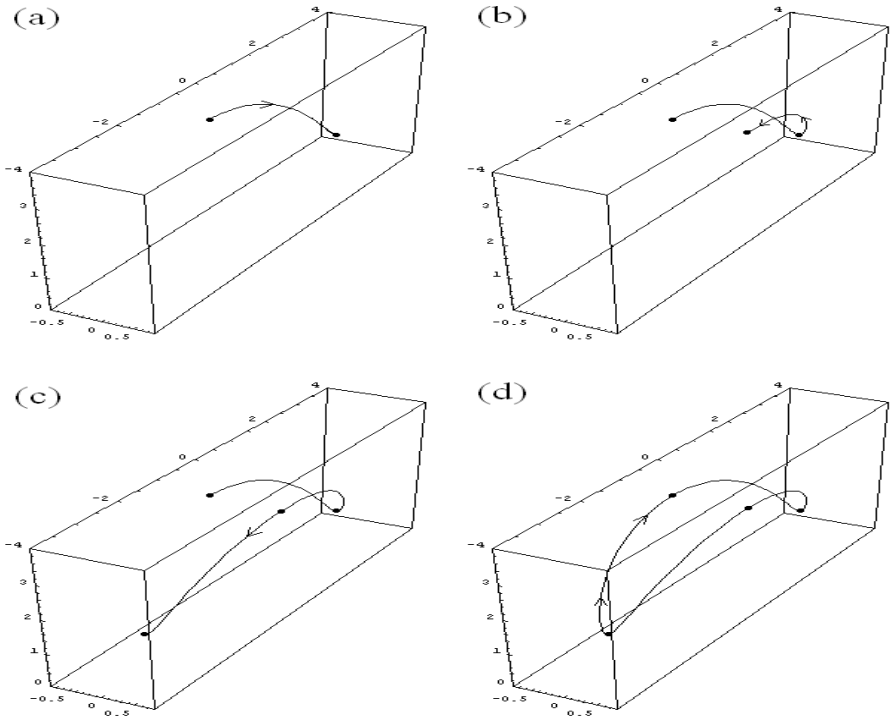

Figure A.7: Plots of $(\omega_1, \omega_2, \omega_3)$ at different times: (a) $\tau = K$, (b) $\tau = 2K$, (c) $\tau = 3K$, and (d) $\tau = 4K$.

while ω_1 and ω_3 are expressed as

$$\omega_1(\tau) \;=\; -\sqrt{\frac{I_2\,(I_2 - I_3)}{I_1\,(I_1 - I_3)}}\;\Omega_3\,\mathrm{cn}(\tau \,|\, k), \tag{A.54}$$

$$\omega_3(\tau) \;=\; \sqrt{\frac{I_2\,(I_1 - I_2)}{I_3\,(I_1 - I_3)}}\;\Omega_1\,\mathrm{dn}(\tau \,|\, k). \tag{A.55}$$

These solutions are shown in Figure A.7, where the $4K$-periodicity is clearly observed.

Weierstrass Elliptic Functions

A different kind of elliptic function is provided by the Weierstrass[2] elliptic function $\mathcal{P}(z; g_2, g_3)$ defined in terms of the differential equation

$$(\sigma')^2 \;=\; 4\,\sigma^3 \;-\; g_2\,\sigma \;-\; g_3 \;\equiv\; 4\,(\sigma - e_1)\,(\sigma - e_2)\,(\sigma - e_3), \tag{A.56}$$

[2]Karl Theodor Wilhelm Weierstrass (1815-1897)

where (e_1, e_2, e_3) denote the roots of the cubic polynomial $4\sigma^3 - g_2\,\sigma - g_3 = 0$ (such that $e_1 + e_2 + e_3 = 0$) and the parameters g_2 and g_3 are defined in terms of the cubic roots as

$$\left.\begin{array}{rcl} g_2 &=& -4\,(e_1\,e_2 + e_2\,e_3 + e_3\,e_1) \;=\; 2\;(e_1^2 + e_2^2 + e_3^2) \\ g_3 &=& 4\;e_1\,e_2\,e_3 \end{array}\right\}. \tag{A.57}$$

Since physical values for the cubic parameters g_2 and g_3 are always real (and $g_2 > 0$), then either all three roots are real (where we assume that $e_3 < e_2 < e_1$ for $g_3 > 0$) or one root e_a is real and we have a conjugate pair of complex roots (e_b, e_b^*) with $\mathrm{Re}(e_b) = -\,e_a/2$. In general, the roots (r_a, r_b, r_c) of the cubic polynomial in Eq. (A.56) are expressed as

$$\left(\begin{array}{c} r_a \\ r_b \\ r_c \end{array}\right) \;=\; \sqrt{\frac{g_2}{12}}\left[\left(\epsilon + \sqrt{\epsilon^2 - 1}\right)^{-1/3}\left(\begin{array}{c} 1 \\ -\,e^{-i\pi/3} \\ -\,e^{i\pi/3} \end{array}\right) \;+\; \left(\epsilon + \sqrt{\epsilon^2 - 1}\right)^{1/3}\left(\begin{array}{c} 1 \\ -\,e^{i\pi/3} \\ -\,e^{-i\pi/3} \end{array}\right)\right],$$

where $\epsilon \equiv (3/g_2)^{3/2}\,g_3$ and $r_a + r_b + r_c = 0$.

When $-1 < \epsilon < 1$, we may set $\epsilon = \cos\phi$, so that $0 < \phi < \pi/2$ for $0 < g_3 < (g_2/3)^{3/2}$ and $\pi/2 < \phi < \pi$ for $-\,(g_2/3)^{3/2} < g_3 < 0$, and the roots are expressed as

$$\left(\begin{array}{c} r_a \\ r_b \\ r_c \end{array}\right) \;=\; \left(\begin{array}{c} e_1 \\ e_2 \\ e_3 \end{array}\right) \;=\; \sqrt{\frac{g_2}{3}}\left(\begin{array}{c} \cos(\phi/3) \\ -\,\cos[(\phi+\pi)/3] \\ -\,\cos[(\phi-\pi)/3] \end{array}\right).$$

Note that $e_2 = 0$ (and $e_3 = -\,e_1$) for $g_3 = 0$ (i.e., $\phi = \pi/2$). Next, when $\epsilon < -1$, we set $\epsilon = -\cosh\psi$ and

$$\left(\begin{array}{c} r_a \\ r_b \\ r_c \end{array}\right) \;=\; \left(\begin{array}{c} e_1 \\ e_2 \\ e_3 \end{array}\right) \;=\; \sqrt{\frac{g_2}{12}}\left(\begin{array}{c} \cosh(\psi/3) - i\,\sqrt{3}\,\sinh(\psi/3) \\ -\,2\,\cosh(\psi/3) \\ \cosh(\psi/3) + i\,\sqrt{3}\,\sinh(\psi/3) \end{array}\right),$$

whereas for $\epsilon > 1$, we set $\epsilon = \cosh\psi$ and

$$\left(\begin{array}{c} r_a \\ r_b \\ r_c \end{array}\right) \;=\; \left(\begin{array}{c} e_2 \\ e_3 \\ e_1 \end{array}\right) \;=\; \sqrt{\frac{g_2}{12}}\left(\begin{array}{c} 2\,\cosh(\psi/3) \\ -\,\cosh(\psi/3) - i\,\sqrt{3}\,\sinh(\psi/3) \\ -\,\cosh(\psi/3) + i\,\sqrt{3}\,\sinh(\psi/3) \end{array}\right),$$

where the root labels have been changed to coincide with standard mathematical definitions (e.g., M. Abramowitz and I. A. Stegun, *Handbook of Mathematical Functions*, Chapter 18). Lastly, we note that when $g_3 < 0$, then

$$\mathcal{P}(z; g_2, g_3) = -\,\mathcal{P}(iz; g_2, -\,g_3), \tag{A.58}$$

as can be derived from the definition (A.56). Note that when $\Delta \equiv g_2^3\;(1 - \epsilon^2) > 0$, all three roots are real and $e_1 > 0 \geq e_2 > e_3$ (for $0 < \epsilon < 1$) while for $\epsilon > 1$, $e_2 > 0$ and $e_1 = -\,\frac{1}{2}\,e_2 + i\,\beta = e_3^*$.

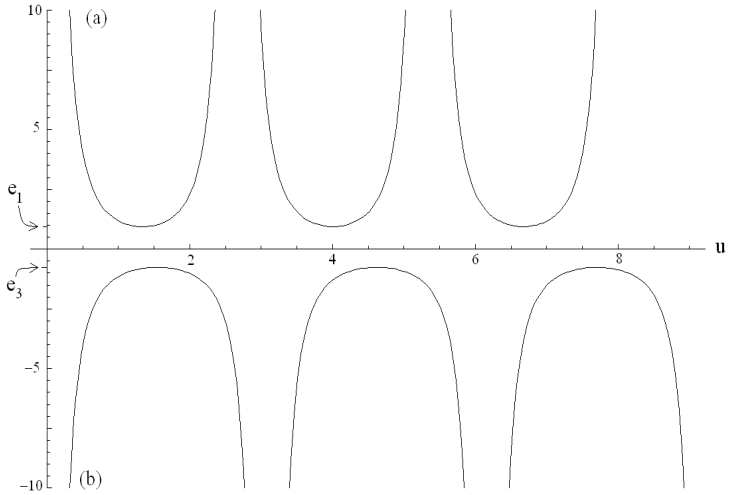

Figure A.8: Plots of (a) $\mathcal{P}(u) > 0$ and (b) $\mathcal{P}(i\,u) < 0$ for $g_2 = 3$ and $g_3 = 0.5$ (with $\epsilon = 0.5$); each plot shows three complete periods.

Figure A.8 shows that, for $0 < \epsilon < 1$, $\mathcal{P}(u)$ has different periods $2\,\omega$ and $2\,\omega'$ along the real and imaginary axes, respectively, where the half-periods ω and ω' are defined as

$$\omega(g_2, g_3) \;=\; \int_{e_1}^{\infty} \frac{dt}{\sqrt{4t^3 - g_2\,t - g_3}} \;\text{ and }\; \omega'(g_2, g_3) \;=\; i \int_{-\infty}^{e_3} \frac{dt}{\sqrt{|4t^3 - g_2\,t - g_3|}}.$$

For $\epsilon > 1$, on the other hand, $\mathcal{P}(u)$ has different periods $2\,\Omega$ and $2\,\Omega'$ along the real and imaginary axes, respectively, where the half-periods Ω and Ω' are defined as

$$\Omega(g_2, g_3) \;=\; \int_{e_2}^{\infty} \frac{dt}{\sqrt{4t^3 - g_2\,t - g_3}} \;\text{ and }\; \Omega'(g_2, g_3) \;=\; i \int_{-\infty}^{e_2} \frac{dt}{\sqrt{|4t^3 - g_2\,t - g_3|}}.$$

Note that, for $0 < \epsilon < 1$, $\mathcal{P}(u)$ is infinite at $\Omega_{m,n} \equiv 2m\,\omega + 2n\,\omega'$ (for $m, n = 0, \pm 1, ...$). By defining the half-periods $\omega_1 = \omega$, $\omega_2 = \omega + \omega'$, and $\omega_3 = \omega'$, we find the identities (for $i = 1, 2, 3$)

$$\left.\begin{array}{rcl} \mathcal{P}(\omega_i) & = & e_i \\ \mathcal{P}(z + \omega_i) & = & e_i \;+\; (e_i - e_j)\,(e_i - e_k)\,[\mathcal{P}(z) - e_i]^{-1} \\ \mathcal{P}(z + 2\,\omega_i) & = & \mathcal{P}(z) \end{array}\right\}, \tag{A.59}$$

where $i \neq j \neq k$ so that $\mathcal{P}(\omega_i + \omega_j) = e_k$. Figure A.9 shows the plots of $\mathcal{P}(u + \omega_2)$ and $\mathcal{P}(u + \omega_3)$ for one complete period from $u = 0$ to $2\,\omega_1$, which clearly satisfies the identities (A.59). For $\epsilon > 1$, the half-periods are $\omega_1 = \Omega'$, $\omega_2 = \Omega$, and $\omega_3 = \Omega + \Omega'$.

As a first example, we return to the one-dimensional problem with a cubic potential $U(x) = x - x^3/3$ described in Figure 3.1. Here, the (dimensionless) energy equation is

$$E \;=\; \frac{\dot{x}^2}{2} \;+\; x \;-\; \frac{x^3}{3}, \tag{A.60}$$

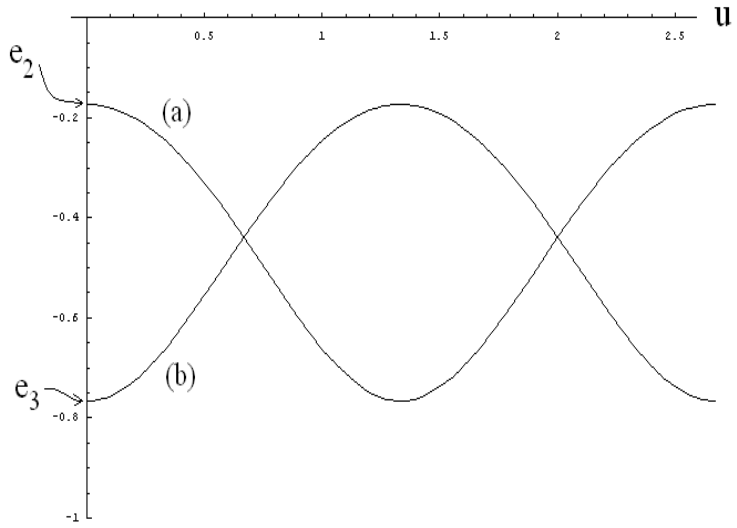

Figure A.9: Plots of (a) $\mathcal{P}(u+\omega_2)$ and (b) $\mathcal{P}(u+\omega_3)$ for $g_2 = 3$ and $g_3 = 0.5$ (with $\epsilon = 0.5$) over one complete period from 0 to $2\,\omega_1$. Note that $\mathcal{P}(\omega_j) = e_j$ for $j = 2$ or 3 and $\mathcal{P}(\omega_i + \omega_j) = e_k$, for $i = 1$ and $(j,k) = (2,3)$ or $(j,k) = (3,2)$.

and the turning points (x_1, x_2, x_3) are shown in Figure A.10.

By writing $x(t) = 6\,\sigma(t)$, Eq. (A.60) becomes the standard Weierstrass elliptic equation $\dot{\sigma}^2 = 4\,\sigma^3 - g_2\,\sigma - g_3$, where

$$g_2 \;=\; \frac{1}{3}, \quad g_3 \;=\; -\,\frac{E}{18}, \quad \text{and} \quad \Delta \;=\; \frac{1}{27}\left(1 \;-\; \frac{9}{4}\,E^2\right).$$

Note that bounded orbits exist only for $-\frac{2}{3} < E < \frac{2}{3}$ (i.e., $\Delta > 0$). The solution for $x(t) = 6\,\sigma(t)$ is $x(t) = 6\,\mathcal{P}(t+\gamma)$, where the constant γ is determined from the initial condition $x(0)$. Figure A.11 shows the plots of $(x, \dot{x})$ for various values of energy E, where $\Delta < 0$ and ϕ is imaginary for cases (a)-(b) while $\Delta > 0$ and ϕ is real for cases (c)-(d); compare this Figure with the numerical integration of $\ddot{x} = -1 + x^2$ shown in Figure 3.2.

Here, in cases (a) and (b), where $E > 2/3$, one root e_1 is positive while the roots $e_2 = e_3^*$ are complex-valued; the half-period ω_1 is imaginary while ω_2 and ω_3 are complex-valued; and $\mathcal{P}(\omega_i) = -\,e_i$. Next, in case (c), where $0 < E < 2/3$, all roots are real $e_3 < e_2 < 0 < e_1$; the half-period ω_1 is imaginary, ω_3 is real, and ω_2 is complex-valued; and $\mathcal{P}(\omega_i) = -\,e_i$. Lastly, in case (d), where $-2/3 < E < 0$, all roots are real $e_3 < e_2 < 0 < e_1$; the half-period ω_1 is real, ω_3 is imaginary, and ω_2 is complex-valued; and $\mathcal{P}(\omega_i) = e_i$.

The motion of a symmetric top with one fixed point was discussed in Section 7.3.4 and its solution was expressed in terms of the differential equation

$$(u')^2 \;=\; (1-u^2)(\epsilon - u) - (\alpha - \beta\,u)^2, \tag{A.61}$$

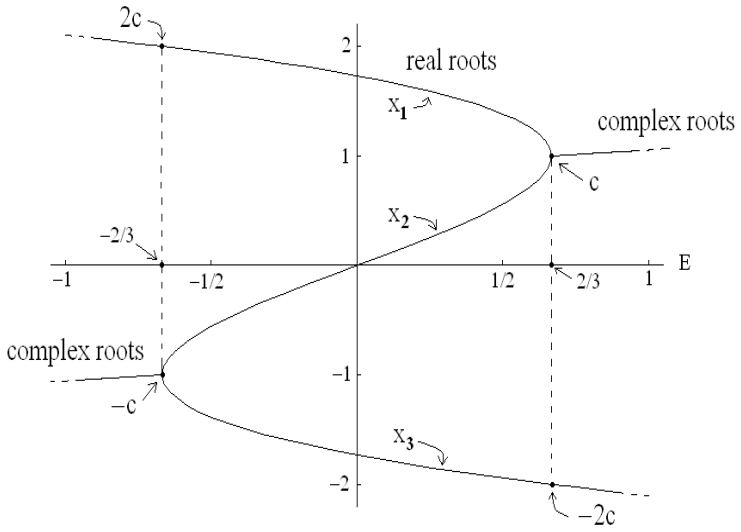

Figure A.10: Roots x_i $(i = 1, 2, 3)$ of the cubic polynomial $E = x - x^3/3$. When $|E| < 2/3$, the three roots are real, with $x_1 > x_2 > x_3$ and $x_1 + x_2 + x_3 = 0$, whereas when $|E| > 2/3$, one root x_a is real and the other two roots (x_b, x_b^*) form a complex-conjugate pair, with $x_b = -\frac{1}{2}\, x_a + i\, \mathrm{Im}(x_b)$. When $|E| = 2/3$, the three roots are $x_1 = 2c$, $x_2 = -c = x_3$ (stable equilibrium at $E = -\,2/3$) and $x_1 = c = x_2$, $x_3 = -\,2c$ (separatrix at $E = 2/3$).

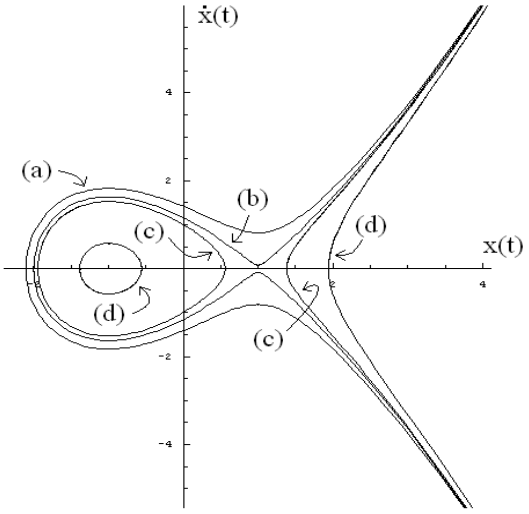

Figure A.11: Plots of $\dot{x}(t) = 6\,\mathcal{P}'(t + \gamma)$ versus $x(t) = 6\,\mathcal{P}(t + \gamma)$ for (a) $E > 2/3$ with $\gamma = \omega_1$ (unbounded orbit), (b) $E = 2/3^+$ with $\gamma = \omega_1$ (separatrix orbit), (c) $0 < E < 2/3$ with $\gamma = \omega_1$ (bounded orbit) or $\gamma = \omega_3$ (unbounded orbit), and (d) $-2/3 < E < 0$ with $\gamma = \omega_2$ (bounded orbit) or $\gamma = \omega_1$ (unbounded orbit).

where the constants $(\epsilon, \alpha, \beta)$ were defined in Section 7.3.4. By using the change of integration variable $u = 4\,\sigma + \gamma$, where $\gamma = (\epsilon + \beta^2)/3$, the differential equation (A.61) becomes the standard differential equation (A.56) for the Weierstrass elliptic function, with

$$\begin{aligned} g_2 &= \frac{1}{4}\left[\,(1\,-\,2\,\alpha\beta)\,+\,3\,\gamma^2\,\right], \\ g_3 &= \frac{1}{16}\left[\,\alpha^2 - \epsilon\,+\,\gamma\,(1\,-\,2\,\alpha\beta)\,+\,2\,\gamma^3\,\right]. \end{aligned}$$

Hence, the solution is expressed in terms of the Weierstrass elliptic function as

$$u(\tau) \;=\; 4\,\mathcal{P}(\tau + \delta)\;+\;\gamma,$$

where δ is determined initial conditions, and we denote the three roots $e_1 > e_2 > e_3$ of the cubic polynomial $4\,\sigma^3 - g_2\,\sigma - g_3 = 0$. Assuming that $4\,e_1 + \gamma > 1$, then at $\tau = 0$, we choose $u(0) = u_1 = 4\,e_3 + \gamma$ so that $\delta \equiv \omega_3$ and, hence, at $\tau = \omega_1$, we find

$$u(\omega_1) \;=\; 4\,\mathcal{P}(\omega_1 + \omega_3)\;+\;\gamma \;=\; 4\,e_2 + \gamma \;=\; u_2.$$

Appendix B

Notes on Feynman's Quantum Mechanics

B.1 Feynman postulates and quantum wave function

Feynman[1] makes use of the Principle of Least Action to derive the Schroedinger equation (9.17) by, first, introducing the following postulates.

Postulate I: Consider the initial and final states a and b of a quantum system and the set $\mathcal{M}$ of all paths connecting the two states. The conditional probability amplitude $K(b|a)$ of finding the system in the final state b if the system was initially in state a is expressed as

$$K(b|a) \equiv \sum_{\mathcal{M}} \phi[X], \tag{B.1}$$

where the summation is over all paths $X(t)$ from a to b and the partial conditional probability amplitude associated with path $X(t)$ is

$$\phi[X] \propto \exp\left(\frac{i}{\hbar} S[X]\right), \tag{B.2}$$

with

$$S[X] = \int_{t_a}^{t_b} L(X, \dot{X}; t)\, dt$$

corresponding to the *classical* action for this path for a particle moving in a time-dependent potential $U(x,t)$. If we take the two states to be infinitesimally close to each other, i.e., whenever the points $a \equiv x_a$ (at time t_a) and $b \equiv x_a + \Delta x$ (at time $t_a + \Delta t$) are infinitesimally

[1]The material presented in this Appendix is adapted from the book *Quantum Mechanics and Path Integrals* by R.P. Feynman and A.R. Hibbs (McGraw-Hill, New York, 1965).

close, Eqs. (B.1)-(B.2) yield

$$K(x_a + \Delta x, t_a + \Delta t | x_a, t_a) \;=\; \frac{1}{A} \exp \frac{i}{\hbar} \left[\frac{m(\Delta x)^2}{2\,\Delta t} \;-\; \Delta t\; U\left(x_a + \frac{\Delta x}{2}, t_a + \frac{\Delta t}{2} \right) \right], \quad \text{(B.3)}$$

where A is a normalization constant and the classical action integral

$$S[x] \;=\; \int_{t_a}^{t_a + \Delta t} \left[\frac{m}{2} \left(\frac{dx}{dt} \right)^2 \;-\; U(x,t) \right] dt \;=\; \frac{m(\Delta x)^2}{2\,\Delta t} \;-\; U\left(x_a + \frac{\Delta x}{2}, t_a + \frac{\Delta t}{2} \right) \Delta t$$

is a function of Δx and Δt as well as the initial space-time point (x_a, t_a); here, the potential energy U is evaluated at the mid-point between x_a and x_b at a time $t_a + \Delta t/2$.

Postulate I provides the appropriate explanation for the mystery behind the Principle of Least Action ("*act locally, think globally*"). Indeed, in the classical limit ($\hbar \to 0$), we find that the variations δX around the paths $X(t)$ which are far away from the physical path $x(t)$ yield changes δS for which $\delta S/\hbar$ is large. Consequently, such contributions tend to average out to zero because of the corresponding wild oscillations in $\phi[X]$. On the other hand, for variations δX near the physical path $x(t)$, we get $\delta S \sim 0$ (to first order) and, consequently, paths $X(t)$ for which $S[X]$ is within $\hbar$ of S_{cl} will contribute strongly. The resulting effect is that only paths in the neighborhood of the physical path $x(t)$ have a nonvanishing probability amplitude. In the strict limit $\hbar \to 0$, the only such path with a nonvanishing probability amplitude is the physical path.

Postulate II: The quantum wave function $\psi(x,t)$ is defined as the probability amplitude for the particle to be at the location x at time t, i.e., $\psi(x,t) \equiv K(x,t|\bullet)$, where we are not interested in the previous history of the particle (its previous location is denoted by $\bullet$) but only on its future time evolution. The Second Postulate states that the integral equation relating the wave function $\psi(x_2, t_2)$ to the wave function $\psi(x_1, t_1)$ is given as

$$\psi(x_2, t_2) \;\equiv\; \int_{-\infty}^{\infty} dx_1\; K(x_2, t_2 | x_1, t_1)\; \psi(x_1, t_1). \quad \text{(B.4)}$$

If we set in Eq. (B.4): $t_1 = t$ and $t_2 = t + \epsilon$, $x_2 = x$ and $x_1 = x + \eta$, then for small enough values of ϵ, the conditional probability amplitude (B.3) can be used in (B.4) to yield

$$\begin{aligned} \psi(x, t+\epsilon) \;&\equiv\; \int_{-\infty}^{\infty} d\eta\; K(x, t+\epsilon | x+\eta, t)\; \psi(x+\eta, t) \quad \text{(B.5)} \\ &=\; \int_{-\infty}^{\infty} \frac{d\eta}{A}\; \exp \left[\frac{i}{\hbar} \left(\frac{m\eta^2}{2\epsilon} \;-\; \epsilon\, U(x + \eta/2,\; t + \epsilon/2) \right) \right] \psi(x+\eta, t), \end{aligned}$$

where a time-dependent potential $U(x,t)$ is considered.

B.2 Derivation of the Schroedinger equation

We will now derive the Schroedinger equation by expanding both sides of Eq. (B.5), up to first order in ϵ (and neglect all higher powers). First, on the left side of Eq. (B.5), we have

$$\psi(x, t+\epsilon) \;=\; \psi(x,t) \;+\; \epsilon\, \frac{\partial \psi(x,t)}{\partial t}. \tag{B.6}$$

Next, on the right side of Eq. (B.5), we note that the exponential

$$\exp\left[\; \left(\frac{im}{2\hbar}\right) \frac{\eta^2}{\epsilon} \;\right]$$

oscillates wildly as $\epsilon \to 0$ for all values of η except those for which $m\eta^2/(2\hbar\epsilon) \sim 1$. We, therefore, conclude that the contribution from the integral in Eq. (B.5) will come from values $\eta = \mathcal{O}(\epsilon^{1/2})$ and, consequently, we may expand the remaining functions appearing on the right side of Eq. (B.5) up to η^2. Thus, we may write

$$\psi(x+\eta, t) \;=\; \psi(x,t) \;+\; \eta\, \frac{\partial \psi(x,t)}{\partial x} \;+\; \frac{\eta^2}{2}\, \frac{\partial^2 \psi(x,t)}{\partial x^2},$$

while

$$\exp\left[\; -\,\frac{i\epsilon}{\hbar}\, U(x+\eta/2,\, t+\epsilon/2) \;\right] \;=\; 1 \;-\; \frac{i\epsilon}{\hbar}\, U(x,t).$$

Expanding the right side of Eq. (B.5) to first order in ϵ, therefore, yields

$$\left[1 \;-\; \frac{i\epsilon}{\hbar}\, U(x,t)\right] \psi(x,t) \;+\; \left(\frac{I_1}{I_0}\right) \frac{\partial \psi(x,t)}{\partial x} \;+\; \left(\frac{I_2}{2\, I_0}\right)\, \frac{\partial^2 \psi(x,t)}{\partial x^2}, \tag{B.7}$$

where $A = I_0$ and

$$I_n \;\equiv\; \int_{-\infty}^{\infty} d\eta\; \eta^n\; e^{-a\eta^2}, \quad a \equiv \frac{m}{2i\hbar\epsilon}$$

with $I_0 = \sqrt{\pi/a}$, $I_1 = 0$, and $I_2 = 1/2a = (i\hbar/m)\,\epsilon$.

Lastly, we find that the terms of first order in ϵ in Eqs. (B.6) and (B.7) must be equal, and we obtain

$$\frac{\partial \psi(x,t)}{\partial t} \;=\; -\,\frac{i}{\hbar}\, U(x,t)\, \psi(x,t) \;+\; \frac{i\hbar}{2m}\, \frac{\partial^2 \psi(x,t)}{\partial x^2},$$

or

$$i\hbar\, \frac{\partial \psi(x,t)}{\partial t} \;=\; -\,\frac{\hbar^2}{2m}\, \frac{\partial^2 \psi(x,t)}{\partial x^2} \;+\; U(x,t)\, \psi(x,t). \tag{B.8}$$

This equation is known as the Schroedinger equation and it describes the time evolution of the wave function $\psi(x,t)$.